UNIVERSITEIT VAN PRETORIA
UNIVERSITY OF PRETORIA
YUNIBESITHI YA PRETORIA

Structural characterisation, anticandidal activity and mode of action of a tryptophan end-tagged tick-derived peptide

By

Court Kudakwashe Chiramba

13328507

Supervisor: Prof Anabella R. M. Gaspar

Co-supervisor: Prof Megan J. Bester

Submitted in fulfilment of the requirements for the degree:

Doctor of Philosophy in Biochemistry

in the Faculty of Natural and Agricultural Sciences

University of Pretoria

15 July 2024

DECLARATION OF ORIGINALITY UNIVERSITY OF PRETORIA

Full names of student: Court Kudakwashe Chiramba

Student number: 13328507

Topic of work: Structural characterisation, anticandidal activity and mode of action of a tryptophan end-tagged tick-derived peptide.

1. I understand what plagiarism is and am aware of the University's policy in this regard.
2. I declare that this thesis is my own original work. Where other people's work has been used (either from a printed source, Internet, or any other source), this has been properly acknowledged and referenced in accordance with departmental requirements.
3. I have not used work previously produced by another student or any other person to hand in as my own.
4. I have not allowed and will not allow anyone to copy my work with the intention of passing it off as his or her own work.

SIGNATURE: 

Summary

The WHO has identified several *Candida* species including *C. albicans* as critical priority fungal pathogens due to greater infection prevalence and formation of recalcitrant biofilms. Resistance to antifungal drugs and increased rates of infection highlight an urgent need for novel antifungal agents. Antimicrobial peptides (AMPs) are a potential alternative to antifungal drugs due to their novel modes of action and broad-spectrum activity. However, further therapeutic development of many AMPs is halted by inactivation in physiological concentrations of salts, serum, and plasma. Tryptophan end-tagging was identified as a structural modification that increases the activity of AMPs in these physiological environments. In this study, Os-C was tagged with tryptophan residues to form Os-C(W_5) and the effect of tryptophan end-tagging on the structural characteristics, anticandidal activity and mode of action of Os-C was investigated.

Mechanistic insight into the structural characteristics of Os-C(W_5) compared with Os-C is provided by circular dichroism (CD) spectroscopy and molecular dynamics (MD) simulations. Steady state analysis using CD spectroscopy shows that tryptophan end-tagging alters the secondary structure in Tris buffer and sodium dodecyl sulfate. *In silico*, MD simulations of peptides were performed with a *C. albicans* model membrane consisting of the lipids 1-palmitoyl-2-oleoyl-*sn*-glycero-3-phosphocholine (POPC), 1-palmitoyl-2-oleoyl-*sn*-glycero-3-phosphoethanolamine (POPE), 1-palmitoyl-2-oleoyl-*sn*-glycero-3-phosphoinositol (POPI), 1-palmitoyl-2-oleoyl-*sn*-glycero-3-phospho-L-serine (POPS) and ergosterol. Like the CD data, MD simulation data reveals changes in the secondary structure of Os-C after end-tagging. Furthermore, MD simulations show that tryptophan end-tagging reduces interactions with and insertion into a model *C. albicans* membrane and promotes peptide aggregation at its surface.

Antiplanktonic assays indicate that tryptophan end-tagging enhances the activity of Os-C which decreases the growth and viability of *C. albicans*. More in-depth mode of action studies reveal that Os-C(W_5) does not cause membrane permeabilisation. Instead, the antifungal activity correlates with the induction of reactive oxygen species and changes in cell morphology.

Further antibiofilm studies show that Os-C(W_5) prevents biofilm formation and eradicates preformed biofilms. Reduced cell adhesion and viability contribute to reduced biofilm extracellular matrix formation. Although reduced, Os-C(W_5) retains some antibiofilm activity in RPMI-1640 supplemented with 50% foetal bovine serum and in a synthetic wound medium.

In conclusion, this study demonstrates that tryptophan end-tagging is a simple modification that transforms a salt-sensitive AMP (Os-C) into a peptide (Os-C(W_5)) with antifungal activity in physiologically relevant environments.

Acknowledgements

Firstly, I would like to thank God for giving me the wisdom and the ability to do this PhD and surrounding me with the following people who were essential for the completion of this PhD:

- My supervisors Prof Gaspar and Prof Bester for their support and insight. I would also like to thank Dr Helena Taute for her input concerning this project.
- Prof James Mason, Prof Christian Lorenz, and Dr Philip Ferguson from King's College London for their assistance with running and analysing molecular dynamics simulation data.
- Prof Yasien Sayed and Keiran Mcinnes from the Protein Structure-Function Research Unit at the University of the Witwatersrand for their assistance with circular dichroism experiments.
- The staff of the Laboratory for Microscopy and Microanalysis at the University of Pretoria for their assistance with the scanning electron microscope.
- Ms Sandra van Wyngaardt and Ms Sonỳa September for their technical assistance.
- My colleagues in the Biotherapeutics Research Group for their support. Special thanks to my fellow PhD colleagues Dalton Möller, Mandelie van der Walt and Rosalind van Wyk for their assistance with the molecular dynamics simulations.
- My family and my friends for their unwavering support throughout this degree.

Finally, I want to acknowledge the National Research Foundation and the University of Pretoria for their financial support. This study was also made possible through capacity built and supported by the SA UK Newton Fund Antibiotic Accelerator (MR/T029552/1) administered by the UK Medical Research Council (UKMRC) and the South African Medical Research Council (SAMRC). I would like to extend my thanks to the UK Materials and Molecular Modelling Hub, which is partially funded by EPSRC (EP/P020194/1 and EP/T022213/1), and the UK HPC Materials Chemistry Consortium, which is also funded by EPSRC (EP/R029431), for providing access to computational resources. This work also benefited from access to the King's Computational Research, Engineering and Technology Environment (CREATE) at King's College London.

Table of Contents

Summary ..... **ii**
Acknowledgements ..... **iii**
List of Tables ..... **vii**
List of Figures ..... **viii**
List of Abbreviations ..... **x**
Chapter 1: Introduction **1**
1.1 Outputs 4
Chapter 2: Literature Review **5**
2.1 *Candida* fungal infections 5
2.1.1 Candida albicans 5
2.1.2 *Candida albicans* biofilm development 6
2.2 Antifungal drugs 7
2.3 Antifungal drug resistance mechanisms in *Candida* 11
2.4 Antimicrobial peptides 13
2.5 Mode of action of antifungal peptides 16
2.5.1 Interaction with the fungal cell wall 16
2.5.2 Interaction with the cell membrane 17
2.5.3 Intracellular effects 19
2.6 Limitations of using antimicrobial peptides and possible solutions 21
2.7 Antifungal peptides under clinical investigation 23
2.8 Background to the study and rationale 25
2.9 References 26
Chapter 3: Characterisation of the structural properties and membrane interactions of Os-C and the tryptophan end-tagged analogue, Os-C(W_5) **47**
3.1 Introduction 47
3.2 Materials and Methods 49
3.2.1 Peptides 49
3.2.2 Circular dichroism spectroscopy 49
3.2.3 Molecular dynamics simulations 50
3.3 Results and Discussion 52
3.3.1 Physicochemical properties of Os-C and Os-C(W_5) 52
3.3.2 Steady state secondary structure analysis 53
3.3.3 Effect of tryptophan end-tagging on peptide secondary structure 55
3.3.4 Effect of tryptophan end-tagging on peptide-membrane interactions and peptide aggregation 57
3.4 Conclusion 66

3.5 References 66
Chapter 4: Antifungal activity and mode of action of Os-C(W_5) against planktonic *C. albicans* .71
4.1 Introduction 71
4.2 Materials and Methods 73
4.2.1 Antifungal agents 73
4.2.2 Preparation of cells for antiplanktonic assays 73
4.2.3 Antifungal susceptibility testing 73
4.2.4 CellTiter Blue cell viability assay 74
4.2.5 SYTOX Green uptake assay 74
4.2.6 Measurement of reactive oxygen species production 75
4.2.7 Scanning electron microscopy 76
4.2.8 Data analysis 77
4.3 Results and Discussion 78
4.3.1 Antifungal activity 78
4.3.2 Mode of action studies 79
4.4 Conclusion 87
4.5 References 88
Chapter 5: The antibiofilm activity of Os-C(W_5) and its associated mode of action 94
5.1 Introduction 94
5.2 Materials and Methods 96
5.2.1 Antifungal agents 96
5.2.2 Preparation of cells for antibiofilm assays 96
5.2.3 Screening for biofilm preventing activity 96
5.2.4 Adhesion assay 97
5.2.5 Morphological transition 97
5.2.6 Biochemical analysis of extracellular material 98
5.2.7 Screening for biofilm eradicating activity 99
5.2.8 Activity in serum containing media 99
5.2.9 Data analysis 100
5.3 Results and Discussion 101
5.3.1 Biofilm preventing activity 101
5.3.2 Interference with cell adhesion 106
5.3.3 Morphological transition 108
5.3.4 Production of extracellular material 109
5.3.5 Biofilm eradication activity 111
5.3.6 Antifungal activity in serum containing environments 114

5.4 Conclusion....117
5.5 References....118
Chapter 6: Concluding Discussion....126
6.1 Limitations and future perspectives....131
6.2 References....138
Appendix A: Reverse-phase high performance liquid chromatography data for Os-C and Os-C(W_5)....153
Appendix B: Mass spectrometry data for Os-C and Os-C(W_5)....155

List of Tables

Page

Table 2.1: Estimated burden of *Candida* infections. 5

Table 2.2: Examples of antifungal peptides, their sources, and modes of action. 16

Table 2.3: Selected antifungal peptides in clinical trials or approved for use. 24

Table 2.4: Primary sequences of OsDef2, Os and Os-C. 25

Table 3.1: Physicochemical properties of melittin, Os-C and Os-C(W_5). 51

Table 3.2: Secondary structure analysis of melittin, Os-C and Os-C(W_5) in sodium dodecyl sulfate. 54

Table 4.1: Antiplanktonic activity of amphotericin B, Os-C and Os-C(W_5). 77

Table 5.1: Biofilm preventing activity of amphotericin B. 100

Table 5.2: Biofilm preventing activity of Os-C and Os-C(W_5). 102

Table 5.3: Biofilm eradicating activity of amphotericin B and Os-C(W_5). 111

Table 6.1: Antifungal activities of amphotericin B, Os-C and Os-C(W_5). 128

List of Figures

Page

Figure 2.1: Overview of biofilm development in *Candida albicans*. 7

Figure 2.2: Structure of 5-flucytosine. 8

Figure 2.3: Structures of terbinafine and naftifine. 8

Figure 2.4: Structure of amphotericin B. 9

Figure 2.5: Structures of fluconazole and voriconazole. 9

Figure 2.6: Structures of micafungin, anidulafungin and caspofungin. 10

Figure 2.7: Structural diversity of antifungal peptides. 15

Figure 2.8: *Candida albicans* cell wall structure. 17

Figure 2.9: Membrane and intracellular targets of antifungal peptides. 19

Figure 3.1: Circular dichroism spectra of melittin, Os-C and Os-C(W_5). 53

Figure 3.2: Secondary structure analysis of Os-C and Os-C(W_5). 55

Figure 3.3: Secondary structures of Os-C and Os-C(W_5) at 1 μs. 56

Figure 3.4: Hydrogen bonding between Os-C and Os-C(W_5) and the model membrane. 57

Figure 3.5: Insertion of Os-C and Os-C(W_5) into a model *C. albicans* membrane. 58

Figure 3.6: Insertion of Os-C into the lipid bilayer at 250 ns, 500 ns, 750 ns, and 1 μs. 59

Figure 3.7: Insertion of Os-C(W_5) into the lipid bilayer at 250 ns, 500 ns, 750 ns, and 1 μs. 60

Figure 3.8: Contact between peptide residues. 62

Figure 3.9: Aggregation of Os-C at 850 ns and Os-C(W_5) at 1 μs. 63

Figure 4.1: Reduction of resazurin to resorufin in the CellTiter Blue cell viability assay. 73

Figure 4.2: 2',7'-Dichlorodihydrofluorescein diacetate assay principle. 75

Figure 4.3: Effect of amphotericin B and Os-C(W_5) on cell growth and viability. 78

Figure 4.4: Effect of amphotericin B, Os-C and Os-C(W_5) on planktonic cell viability after three hours. 79

Figure 4.5: Effect of AMB and Os-C(W_5) on membrane permeability. 80

Figure 4.6: Reactive oxygen species production by Os-C(W_5). 82

Figure 4.7: Effect of reactive oxygen species production on the antifungal activity of Os-C(W_5). 83

Figure 4.8: Effect of Os-C(W_5) on the morphology of planktonic *C. albicans* cells. 85

Figure 5.1: Structure of crystal violet. 96

Figure 5.2: Biofilm preventing activity of amphotericin B. 101

Figure 5.3: Microscopy images of cells exposed to amphotericin B for 6 hours and 24 hours. 102

Figure 5.4: Biofilm preventing activity of Os-C and Os-C(W_5) after 6 hours and 24 hours. 103

Figure 5.5: Microscopy images of cells exposed to Os-C and Os-C(W_5) for 6 hours and 24 hours. 104

Figure 5.6: Effect of amphotericin B and Os-C(W_5) on *Candida albicans* adhesion. 106

Figure 5.7: Effect of amphotericin B and Os-C(W_5) on the yeast-to-hypha transition. 108

Figure 5.8: Effect of amphotericin B and Os-C(W_5) on the production of the extracellular matrix. 109

Figure 5.9: Biofilm eradicating activity of amphotericin B and Os-C(W_5). 112

Figure 5.10: Biofilm preventing activity of amphotericin B and Os-C(W_5) in serum containing media. 114

Figure 5.11: Biofilm eradicating activity of amphotericin B and Os-C(W_5) in serum containing media. 115

List of Abbreviations

A. fumigatus	*Aspergillus fumigatus*
AMB	Amphotericin B
AMP	Antimicrobial peptide
ANOVA	Analysis of variance
APD	Antimicrobial Peptide Database
ATP	Adenosine triphosphate
BaAMPs	Biofilm active antimicrobial peptides
B. subtilis	*Bacillus subtilis*
BCA	Bicinchoninic acid
BEC	Lowest concentration of an antifungal agent that reduced cell viability or biomass of a preformed biofilm by 50%
BIC	Lowest concentration of an antifungal agent that reduced cell viability or biomass by 50%
C. albicans	*Candida albicans*
C. auris	*Candida auris*
C. elegans	*Caenorhabditis elegans*
C. glabrata	*Candida glabrata*
C. neoformans	*Cryptococcus neoformans*
C. parapsilosis	*Candida parapsilosis*
C. tropicalis	*Candida tropicalis*
Ca^{2+}	Calcium ion
cAMP-PKA	Cyclic adenosine monophosphate-protein kinase A
CD	Circular dichroism
CRAMP	Cathelicidin-related antimicrobial peptide
CTB	CellTiter Blue
CV	Crystal violet
DAPI	6-Diamidino-2-phenylindole
DCF	2’,7’-Dichlorofluorescein
DCFH	2’,7’-Dichlorodihydrofluorescein
DCFH-DA	2’,7’-Dichlorodihydrofluorescein diacetate
dddH_2O	Double distilled deionised water
DDS	Drug delivery system

DMSO	Dimethyl sulfoxide
DsS3(1-16)	Dermaseptin s3
E. coli	*Escherichia coli*
ECM	Extracellular matrix
ER	Endoplasmic reticulum
FBS	Foetal bovine serum
G. mellonella	*Galleria mellonella*
K^+	Potassium ion
LB	Luria-Bertani
MD	Molecular dynamics
Mg^{2+}	Magnesium ion
MFC	Minimum fungicidal concentration
MIC	Minimum inhibitory concentration
NaP	Sodium phosphate
NET	Neutrophil extracellular trap
NMR	Nuclear magnetic resonance
O. savignyi	*Ornithodoros savignyi*
OD	Optical density
P. aeruginosa	*Pseudomonas aeruginosa*
PA	Phosphatidic acid
PBS	Phosphate buffered saline
PE	Phosphatidylethanolamine
PI	Phosphatidylinositol
$PI(4,5)P_2$	Phosphatidylinositol-(4,5)-bisphosphate
POPC	1-palmitoyl-2-oleoyl-*sn*-glycero-3-phosphocholine
POPE	1-palmitoyl-2-oleoyl-*sn*-glycero-3-phosphoethanolamine
POPI	1-palmitoyl-2-oleoyl-*sn*-glycero-3-phosphoinositol
POPS	1-palmitoyl-2-oleoyl-*sn*-glycero-3-phospho-L-serine
PS	Phosphatidylserine
ROS	Reactive oxygen species
RPMI-1640	Roswell Park Memorial Institute 1640
RPMI-1640-50% FBS	RPMI-1640 supplemented with 50% FBS
S. aureus	*Staphylococcus aureus*
S. cerevisiae	*Saccharomyces cerevisiae*
SDS	Sodium dodecyl sulfate

SEM	Standard error of the mean
SWM	Synthetic wound medium
TEM	Transmission electron microscopy
TUNEL	Terminal deoxynucleotidyl transferase dUTP nick end labelling
VMD	Visual molecular dynamics
WHO	World Health Organization
WHO FPPL	World Health Organization Fungal Priority Pathogens List
YPD	Yeast peptone dextrose

Chapter 1: Introduction

Approximately 1.2 billion people globally are affected by fungal infections. Furthermore, it is estimated that fungal infections claim the lives of approximately 1.5 million individuals annually (1). The COVID-19 pandemic was associated with a rise in the incidence of comorbid invasive fungal infections such as aspergillosis, mucormycosis and candidaemia (2). Despite their growing threat to public health, little attention and resources have been directed towards fungal infections (3). Therefore, it is difficult to diagnose fungal pathogens, obtain surveillance data and estimate the burden of fungal infections. In response to increasing fungal infections, the World Health Organization (WHO) developed the fungal priority pathogens list (WHO FPPL) which sought to drive further research and policy interventions to strengthen the global response to fungal infections and antifungal drug resistance (2).

Individuals at risk of contracting fungal infections tend to have underlying health problems and weak immune systems. People with chronic lung disease, prior tuberculosis, diabetes mellitus, HIV, cancer, recipients of organ transplants, and individuals undergoing immunosuppressant therapy are more predisposed to fungal infections (4). In addition, new groups of people at risk of contracting fungal infections have been identified and include individuals suffering from viral respiratory tract infections, liver and kidney disease, and chronic obstructive pulmonary disease.

To combat the growing number of fungal infections, polyene, azole, echinocandin, and pyrimidine antifungal drugs are currently used in clinical practice and several other drugs are being developed (5, 6). However, an inability to access high-quality treatment and diagnostics in some regions, a limited repertoire of antifungal drugs, and the development of antifungal resistance has led to a global health issue that mainly impacts vulnerable populations (1, 7). Antifungal resistance is linked to longer therapy times and hospital stays and a greater need for second-line antifungal drugs that are more effective, but highly toxic. These second-line drugs are expensive and sometimes unavailable in low- and middle-income countries (8). In their global antimicrobial resistance survey, the WHO reported that resistance to fluconazole, the first-line treatment against oral *Candida* infections, in South Africa was approximately 49% (9). Epidemiological studies of treatment centres in Africa have shown that resistance to all three classes of antifungal drugs is prevalent (10-12). The development of antifungal resistance is due to the prevalence of several resistance mechanisms developed by fungi. Furthermore,

fungi can form biofilms that are difficult to treat and require higher doses of antifungal drugs, which may lead to toxic side effects (13). Therefore, novel antifungal agents are required to halt the increasing incidence of antifungal drug resistance.

The WHO FPPL identified *Cryptococcus neoformans* (*C. neoformans*), *Candida auris* (*C. auris*), *Aspergillus fumigatus* (*A. fumigatus*) and *Candida albicans* (*C. albicans*) as critical priority pathogens. *C. albicans* is especially problematic since it is responsible for 70% of fungal infections and a mortality rate of 20% to 50% (2). Although antifungal treatments are available, *C. albicans* can survive exposure to antifungal drugs through gene mutations that alter antifungal drug targets and confer antifungal drug resistance (14). Antifungal therapy is further complicated by *C. albicans* biofilms that can be formed within the body on mucosal surfaces or on implanted medical devices (15). Biofilms are difficult to treat because the extracellular matrix (ECM) limits the access of antifungal drugs to biofilm-associated cells. The ECM associated proteins, carbohydrates and extracellular nucleic acids can interact with antifungal drugs and prevent them from reaching cells within the biofilm (16).

Cationic antimicrobial peptides (AMPs) present a potential solution to antifungal drug resistance. These molecules are short (12 – 50 amino acids), positively charged, and amphipathic. Studies have shown that AMPs are active against bacteria, fungi, viruses and parasites (17). Antimicrobial peptides kill microorganisms via multiple modes of action which reduces the likelihood of resistance development (18). In addition, AMPs can potentially be used in combination therapy with antifungal drugs, meaning a lower dosage of antifungal drugs will be required. Therefore, the cost of treatment, emergence of side effects and antifungal drug resistance could be reduced (19, 20). To date, some AMPs are under investigation in clinical trials or are currently used in clinical settings for the treatment of fungal infections. Novexatin, Pac-113 and CZEN-002 have completed phase II clinical trials for the treatment of onychomycosis, oral candidiasis, and vulvovaginal candidiasis, respectively (21). The echinocandins caspofungin, anidulafungin and micafungin are cyclic lipopeptides that are used clinically to treat *Candida* related infections (22). Another echinocandin, rezafungin, recently received FDA approval in March 2023 for the treatment of candidaemia and invasive candidiasis (23).

Several studies have investigated the antibacterial (24-26) and antifungal (27) activity of a synthetic peptide Os-C, a derivative of a defensin OsDef2 which was identified in the midgut of the soft tick *Ornithodoros savignyi* (*O. savignyi*). Although Os-C possessed antiplanktonic

activity against bacteria and *C. albicans*, its activity could only be determined in 0.01 M sodium phosphate (NaP) buffer, pH 7.4. Under these conditions, anticandidal mode of action studies revealed that Os-C interacted with the cell wall polysaccharides mannan and laminarin. Confocal microscopy images showed that Os-C entered the cytoplasm via an energy-dependent mechanism and induced reactive oxygen species (ROS) production rather than membrane permeabilisation, a common AMP mode of action (27). Further development of Os-C for clinical application is limited due to its reduced antifungal activity in physiologically relevant environments. Consequently, further modification of Os-C was required. Tryptophan end-tagging is a strategy that has been successfully used to increase the activity of AMPs in physiologically complex environments (28, 29). In this study, Os-C was modified by tagging the C-terminus with five tryptophan residues to create the analogue Os-C(W_5).

This study aimed to investigate the effect of tryptophan end-tagging on the structural characteristics, anticandidal activity and mode of action of the modified analogue, Os-C(W_5).

The research objectives were to:

1. Characterise the secondary structures and peptide-membrane interactions of Os-C and Os-C(W_5) using CD spectroscopy and MD simulations (**Chapter 3**).
2. Investigate the effect of tryptophan end-tagging on the antiplanktonic activity of Os-C and identify the mode of action (**Chapter 4**).
3. Evaluate the effect of tryptophan end-tagging on the antibiofilm activity of Os-C and further identify the mode of action (**Chapter 5**).

1.1 Outputs

A manuscript for the results of this study was submitted to *ACS Omega* and accepted for publication:

Chiramba, C. K., Möller, D. S., Lorenz, C. D., Chirombo, R. R., Mason, J. A., Bester, M. J., and Gaspar, A. R. M. (2024) **Tryptophan end-tagging confers antifungal activity on a tick-derived peptide by triggering reactive oxygen species production**. *ACS Omega* **9**, 15556-15572. 10.1021/acsomega.4c00478

The results of this study were presented at the following events:

1. Department of Biochemistry, Genetics and Microbiology seminar. 9 May 2022. Topic: **Anticandidal activity and mode of action of tryptophan end-tagged tick-derived peptide**.
2. Inter-institutional Biofilm Research Meeting. 11 September 2023. Topic: **Structural characterisation, anticandidal activity and mode of action of tryptophan end-tagged tick-derived peptide**.
3. Department of Biochemistry, Genetics and Microbiology symposium. 1 December 2023. Topic: **Structural characterisation, anticandidal activity and mode of action of tryptophan end-tagged tick-derived peptide**.

Chapter 2: Literature Review

2.1 *Candida* fungal infections

Candida is a yeast that is part of the normal skin and gut microbiota and is present in up to 60% of healthy individuals (30). However, when the host immune system is compromised, *Candida* can overgrow and cause invasive disease. At least 15 *Candida* species can cause infections, but *C. albicans*, *C. glabrata*, *C. tropicalis*, *C. parapsilosis* and *C. krusei* are responsible for most infections. Recently, *C. auris* has emerged as a threat in clinical settings (31).

Candida infections (candidiasis) affect the skin, mucosa and organs and can affect individuals of any age. Invasive candidiasis is more dangerous and includes bloodstream infections (candidaemia) and deep-seated infections such as peritonitis, intra-abdominal abscess, and osteomyelitis (32). *Candida* species are ranked highly regarding bloodstream infections in healthcare settings. Approximately half of candidaemia cases occur in intensive care units due to a myriad of risk factors such as the use of indwelling catheters, exposure to broad-spectrum antibiotics, recent surgery, and prolonged stay in an intensive care unit (33).

The burden of *Candida* infections, and fungal infections in general, is difficult to quantify due to a lack of surveillance programs in some countries so it is nearly impossible to establish the impact of *Candida* infections in regional and global settings. The approximate global burden of *Candida* related infections is indicated in **Table 2.1**. Although the numbers shown are estimates, *Candida* is a public health threat and must be dealt with accordingly. *C. albicans* is the most common fungal pathogen in clinical settings, but non-*albicans Candida* species account for almost half of the bloodstream isolates in certain regions (3).

Table 2.1: Estimated global burden of *Candida* infections. Adapted from Bongomin *et al.* (3).

Fungal infection	Annual incidence	Global burden
Oral candidiasis	~ 2 000 000	-
Oesophageal candidiasis	~ 1 300 000	-
Recurrent vulvovaginal candidiasis	-	~ 134 000 000
Invasive candidiasis	~ 750 000	-

2.1.1 Candida albicans

In the recently published WHO FPPL, *C. albicans* was ranked in the critical priority group (2). Globally, *C. albicans* accounts for almost 70% of fungal infections and is a common cause of

mucosal and systemic infections (34). Candidiasis caused by *C. albicans* has a mortality rate between 20 and 50% despite the availability of antifungal drugs. Patients affected by infections can stay in hospitals for two to eight weeks depending on the presence of underlying conditions and up to 4% of cases develop secondary growths which can prolong hospital stays and complicate treatment (2).

In the normal microbiota, *C. albicans* exists in the yeast form. However, when host immunity is compromised, *C. albicans* becomes an opportunistic organism. Infection is made possible by several virulence traits. First, *C. albicans* can undergo a morphological transition from the unicellular yeast form to the multicellular pseudohyphal and hyphal forms (35) which contribute to its virulence. Second, the secretion of aspartyl proteases and phospholipases facilitate tissue invasion and organ damage (36) by producing candidalysin, a 31-amino acid, α-helical amphipathic peptide. Candidalysin is thought to damage the epithelial membrane by intercalation, permeabilisation and pore formation (37). Finally, *C. albicans* can enter the bloodstream by adhering to and invading endothelial and epithelial cells (38). The ability to adhere to surfaces also enables *C. albicans* to form biofilms which are a source of long-term candidaemia (39).

2.1.2 *Candida albicans* biofilm development

Fungal biofilms protect cells from the external environment (40) and are found in aquatic environments, artificial structures, biomaterials as well as plant and mammalian tissue (15). Most *C. albicans* infections are linked to biofilm formation which leads to high morbidity and mortality (41). The transition from the yeast to the hyphal form is a crucial part of *C. albicans* pathogenesis and biofilm formation results in the formation of a complex structure that contains *C. albicans* cells in the yeast, pseudohyphal and hyphal forms (42).

Biofilm development occurs sequentially in four steps: adherence, initiation, maturation, and dispersal (**Figure 2.1**). Initially, yeast cells adhere to a surface through weak van der Waals forces then cells begin to grow and divide on the surface which forms a basal layer that will anchor the biofilm to the surface. When the basal layer is formed, yeast cells will transition to the hyphal form. Further growth of hyphae and the production of the ECM occurs at the maturation stage (15). Finally, yeast cells will disperse from the biofilm to other tissues, organs, or surfaces to form new biofilms (43).

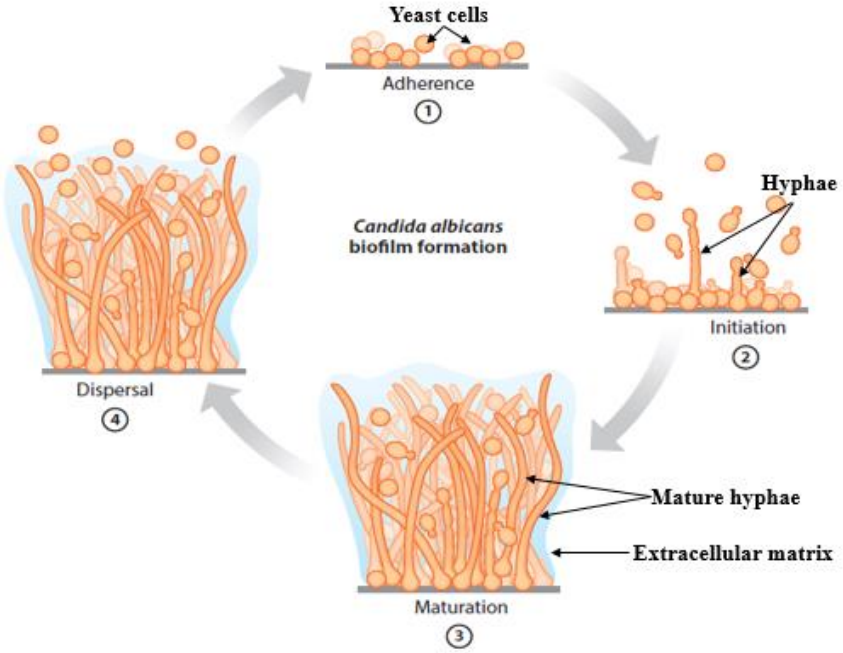

Figure 2.1: Overview of biofilm development in *Candida albicans*. Initially, 1) yeast cells will adhere to a substrate. Once the adherence stage is complete, cells begin to grow and 2) develop pseudohyphae and hyphae in the initiation stage. In the 3) maturation stage, further hyphal growth and ECM production occurs. Finally, when the biofilm is mature, yeast cells will 4) disperse to form new biofilms. Adapted from Nobile and Johnson (15). Permission to use the image was granted.

The ECM of *C. albicans* biofilms is made up of carbohydrates, proteins, lipids, and extracellular DNA which play different roles in maintaining the biofilm and establishing resistance to antifungal drugs (15). Since biofilms present a major challenge to the treatment of *C. albicans* infections, the structure of biofilms and their role in antifungal drug resistance will be discussed in detail in Section 2.3.

2.2 Antifungal drugs

Although there are many groups of antifungal drugs, the five most important groups for the treatment of infections are fluorinated pyrimidine analogues, allylamines, azoles, polyenes and echinocandins (44). Fluorinated pyrimidine analogues are comprised of a single drug, 5-flucytosine (**Figure 2.2**), that interferes with DNA replication or translation, leading to a fungistatic effect. The replication of DNA is prevented when 5-flucytosine enters the cell via cytosine permease then inhibits thymidylate synthase, an enzyme involved in DNA replication and repair. Translation is prevented when 5-flucytosine is converted to 5-fluorouracil which can be phosphorylated to form 5-fluorodeoxyuridine monophosphate which is incorporated into RNA during translation (45). Flucytosine is normally used in combination with

amphotericin B (AMB) in clinical settings due to toxic side effects such as hepatotoxicity, disruption of bone marrow function and rapid onset of resistance (13).

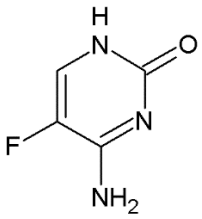

Figure 2.2: Structure of 5-flucytosine. 5-flucytosine is a pyrimidine analogue that interferes with DNA and RNA synthesis. The structure was drawn using ChemSketch (ACD/Labs).

Allylamines, such as terbinafine and naftifine (**Figure 2.3**), are currently used for the topical treatment of superficial fungal infections (46). These drugs inhibit the synthesis of ergosterol, a component of fungal cell membranes, by inhibiting the enzyme squalene epoxidase which converts squalene to lanosterol. As a result, squalene accumulates within the cell, toxic products accumulate, and the cell membrane ruptures (44).

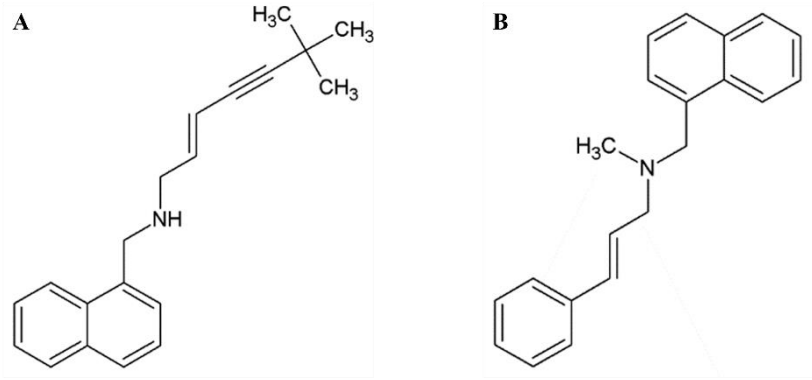

Figure 2.3: Structures of (A) terbinafine and (B) naftifine. Terbinafine and naftifine are allylamine antifungal drugs which inhibit ergosterol synthesis by inhibiting the enzyme squalene epoxidase. Structures were drawn using ChemSketch (ACD/Labs).

Polyene antifungal drugs were first discovered in the 1950s and the first drug to be introduced to the market was AMB deoxycholate (**Figure 2.4**) in 1958 (47). Polyenes have the widest spectrum of antifungal activity of all available antifungal agents and can alter membrane function by binding to ergosterol. Consequently, cell permeability increases, cytoplasmic contents leak out of the cell and eventually, cell death occurs (48). Amphotericin B is administered intravenously, and due to its nephrotoxicity, lipid formulations were developed and are preferred over AMB deoxycholate due to their efficacy and lower risk of toxicity (49).

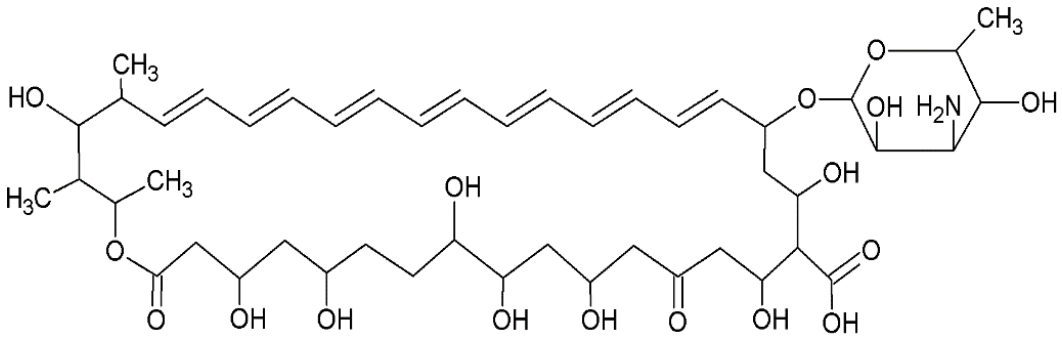

Figure 2.4: Structure of amphotericin B. Amphotericin B is a member of the polyene antifungal drug class and kills fungi by binding to ergosterol which leads to cell leakage and cell death. Structures were drawn using ChemSketch (ACD/Labs).

Voriconazole and fluconazole (**Figure 2.5**) are azole drugs that inhibit the enzyme lanosterol 14-α-demethylase in the ergosterol biosynthesis pathway (13). As a result, the conversion of lanosterol to ergosterol is prevented and leads to the accumulation of 14-α-methyl-3,6-diol. Since less ergosterol is produced, the integrity of the cell membrane is disrupted, and cell growth is prevented (14). Fluconazole is commonly used in clinical settings since it is active against a range of *Candida* species and can be administered orally or intravenously (50). Some limitations of using azoles include hepatotoxicity and emergence of resistance (51). In some cases, azoles can act as substrates or inhibitors of cytochrome P450 enzymes (13). Since the introduction of echinocandins in 2003, fluconazole is now used as a second-line drug, however, it is used as a first-line therapy in regions where there is limited availability of antifungal drugs or there is low azole resistance.

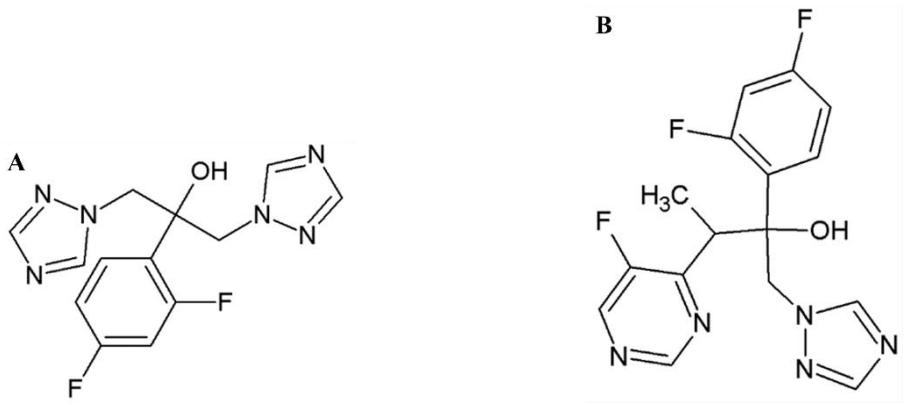

Figure 2.5: Structures of (A) fluconazole and (B) voriconazole. Fluconazole and voriconazole are members of the azole class of antifungal drugs. Azoles kill fungi by inhibiting the enzyme 14α-lanosterol demethylase in the ergosterol biosynthesis pathway. Structures were drawn using ChemSketch (ACD/Labs).

The echinocandins are the most recently discovered class of antifungal drugs and have broad-spectrum fungicidal activity against *Candida* species (52). This class is composed of the drugs anidulafungin, caspofungin and micafungin (**Figure 2.6**).

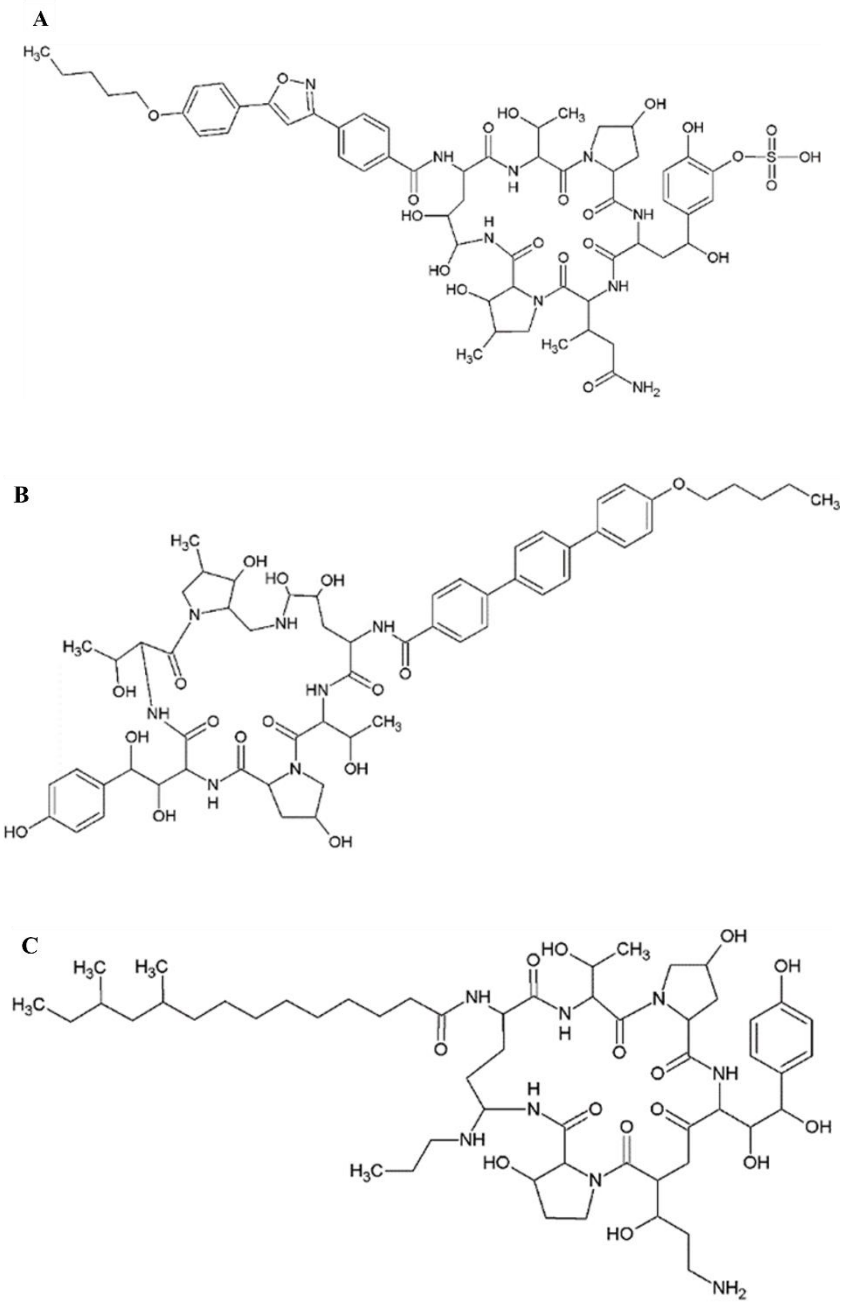

Figure 2.6: Structures of the echinocandin drugs (A) micafungin, (B) anidulafungin and (C) caspofungin. Echinocandins are semisynthetic lipopeptides that inhibit cell wall biosynthesis by inhibiting the enzyme 1,3-β-D-glucan synthase. Structures of micafungin, anidulafungin and caspofungin were drawn using ChemSketch (ACD/Labs).

Echinocandins inhibit 1,3-β-D-glucan synthase, an enzyme that catalyses the production of 1,3-β-D-glucan, a component of the fungal cell wall. Inhibiting 1,3-β-D-glucan synthase disrupts

the integrity of the growing cell wall which leads to osmotic instability and cell death. In clinical settings, echinocandins are used as a first-line therapy due to the lower risk of side effects since mammalian cells lack a cell wall. Due to their poor oral bioavailability, echinocandins are administered intravenously (53). Despite their inclusion in the essential medicines list in 2021, echinocandins are still unavailable in many countries (2).

Although many antifungal drugs have been developed, no drug has all the attributes needed for the ideal antifungal agent (54). Notable shortcomings of antifungal drugs are fungistatic activity, high toxicity, low bioavailability, harmful side effects, and a narrow spectrum of activity (55, 56). Due to these limitations, the emergence of drug resistance and pathogenicity of clinical *Candida* isolates, there is an urgent need for novel antifungal agents that have different modes of action, are more effective and have fewer side effects.

2.3 Antifungal drug resistance mechanisms in *Candida*

Antifungal resistance is an emerging problem worldwide, and this further complicates the selection of antifungal therapy. *Candida* strains resistant to echinocandins and azoles are increasingly being identified and their occurrence usually correlates with high azole or echinocandin use in hospitals (32). Resistance in *Candida* species can either be intrinsic (found in all isolates within a species) or acquired (found in an isolate from a species that is normally susceptible). Studies have shown an increase in the number of azole-resistant isolates, and the use of azoles in agriculture also contributes to the growing rates of resistance (57-59). *Candida* species can overcome the action of antifungal drugs by using several mechanisms in response to different drug classes. The main function of resistance mechanisms is to reduce the concentration of the drug within the cell, reduce affinity for the drug target and counter the effects of the drug (60).

Resistance to polyene drugs is not very common and is achieved by either replacing ergosterol with a precursor molecule or reducing the amount of ergosterol in the cell membrane. Mutations of the genes *ERG2* (encodes C-8 sterol isomerase) and *ERG3* (encodes $\Delta_{5,6}$-desaturase), two enzymes involved in ergosterol biosynthesis, reduce the ergosterol content of the cell membrane. Mutation of the *ERG3* gene results in the conversion of fecosterol to episterol which has a low affinity for AMB (61). Another likely mechanism of resistance to AMB is enhanced catalase activity which serves to reduce oxidative damage caused by ROS (62).

Resistance to azole drugs involves modification of the target enzyme, lanosterol 14α-demethylase which is coded by the *ERG11* gene. A mutation in this gene prevents azoles from binding to the target site (63) and the fungistatic effects of azoles are lost (14). Efflux pumps reduce intracellular concentrations of azole drugs thereby increasing resistance while expression of the active transporters Cdr1, Cdr2 and Mdr1 prevents the accumulation of azole drugs in the intracellular compartment (62).

Resistance to echinocandins has been linked to point mutations in specific regions of genes encoding the *FKS* subunits of 1,3-β-D-glucan synthase. These mutations increase resistance and lower 1,3-β-D-glucan synthase sensitivity to echinocandins (64). In other cases, increased production of a cell wall component can compensate for decreased production of another component. One example is the production of greater concentrations of chitin in response to decreased 1,3-β-D-glucan production (65).

Biofilms possess characteristics that make cells within biofilms up to 1000 times more resistant to antifungal drugs than their planktonic counterparts (66). Cells become resistant to antifungal agents due to the limited availability of nutrients. In conditions of limited glucose and iron, *C. albicans* biofilms exhibited resistance to AMB (67). Biofilms also contain persister cells which are phenotypic variants of wild-type fungal cells that are less susceptible to antifungal drugs due to their metabolically dormant state that can withstand high concentrations of antifungal drugs (68, 69).

The ECM serves as a barrier that covers cells within the biofilm and maintains cell-cell and cell-surface interactions and interactions with the surrounding environment (16). Extracellular matrix formation occurs when *Candida* cells produce extracellular vesicles of macromolecules that are released into the extracellular space where the cargo is incorporated into the growing matrix (70). In *Candida* species, the ECM contains carbohydrates, proteins, lipids, and extracellular DNA (71). Some ECM components play a role in the long-term colonisation of living or non-living substrates by facilitating adhesive and cohesive interactions which provide structural stability to the biofilm (16). These components regulate the dispersion of cells from the biofilm and even break down molecules to provide nutrients for biofilm-associated cells.

Besides enabling adhesion and structural integrity of the biofilm, the ECM allows cells to tolerate high concentrations of antifungals. Access to the cells is limited by the polysaccharides in the ECM, namely β-1,3-glucan, β-1,6-glucan, and α-1,2-branched α-1,6 mannan. Several

studies observed that matrix polysaccharides will interact to create a complex that sequesters antifungal drugs and prevents them from reaching the cells (72, 73).

Cells encased within the ECM can evade host immune defences by covering cell wall-associated epitopes which prevents recognition of *Candida* species by host cells. The biofilm matrix can also suppress the production of ROS which are signalling molecules for the formation of neutrophil extracellular traps (NETs) (74-76).

Candida species can form mixed biofilms with bacteria or other *Candida* species. In this setting, the ECM produced by one microorganism may protect other microorganisms in the biofilm. The bacterium *Staphylococcus aureus* (*S. aureus)* in a polymicrobial biofilm with *C. albicans* was more resistant to vancomycin than *S. aureus* in a monomicrobial biofilm (77). Resistance was due to the failure of vancomycin to penetrate the ECM produced by *C. albicans* which covers both microorganisms (78). Moreover, bacterial polysaccharides can enhance antifungal resistance. In a study by Kim *et al.*, α-glucan produced by *Streptococcus mutans* enhanced the resistance of *C. albicans* to fluconazole (79).

Changes in the global distribution of *Candida* species will lead to changes in the administration of antifungal therapy, due to the susceptibility of the various *Candida* species to antifungal drugs. Currently, there is a need for novel antifungal agents with broad-spectrum antifungal activity against planktonic and biofilm forms of fungi and new modes of action to overcome the emergence of resistant *Candida* species. Antimicrobial peptides can potentially address the need for new antifungal drugs and their diversity, structures, modes of action, and potential as antifungal drugs will be reviewed in detail in the following sections.

2.4 Antimicrobial peptides

Antimicrobial peptides are natural antibiotics that are produced by almost all organisms and are part of their innate immune system. These peptides serve as the first line of defence against pathogens (80). To date, the Antimicrobial Peptide Database (APD, https://aps.unmc.edu) contains 3940 AMPs (81-83). Most AMPs are short (12 – 50 amino acids) and cationic at physiological pH (21). Up to half of the AMP sequence consists of hydrophobic residues, which makes them amphipathic and improves their interaction with target membranes (84).

Antimicrobial peptides exhibit sequence and structural diversity (**Figure 2.7**). The β-sheet peptides consist of an antiparallel β-sheet that is held in place by disulfide bonds. The tachyplesins are β-sheet AMPs isolated from the Japanese horseshoe crab, *Tachypleus*

tridentatus (85). The α-helix peptides have α-helical conformations and usually have a minor curvature in the middle of the structure due to the presence of a proline or glycine residue. The magainins, isolated from the skin of the African clawed frog *Xenopus laevis* possess an α-helical conformation (86). Extended AMPs do not have a secondary structure but have a high proportion of a particular residue such as arginine, tryptophan, or proline in their sequences. An example of an extended AMP is indolicidin which was isolated from cytoplasmic granules of bovine neutrophils. Indolicidin is a 13-amino acid long tryptophan-rich peptide amidated at its C-terminus (87). Loop AMPs are characterised by a loop due to a disulfide, amide or isopeptide bond. Thanatin, a 21-amino acid AMP from the spined soldier bug *Podisus maculiventris*, is a loop AMP that contains an antiparallel β-sheet stabilised by a single disulfide bond (88).

In some cases, AMPs consist of a combination of secondary structures. These peptides can have a prominent α-helix and a triple-stranded antiparallel β-sheet that is stabilised by disulfide bonds (89, 90). This structure is commonly seen in plant defensins such as MsDef1 from alfalfa seeds (91). The depsipeptide class of AMPs consists of peptides whose backbone structure is made up of amide and ester bonds (92). Aureobasidin A, which is produced by the fungus *Aureobasidium pullulans*, is a cyclic 8-amino acid depsipeptide containing an α-hydroxyacid (93). Some peptides possess a cyclic structure with multiple variations. Gramicidin S, produced by *Bacillus brevis*, is a cyclic peptide with broad-spectrum activity against Gram-positive bacteria, Gram-negative bacteria and fungi (94). The iturin peptides are cyclic lipopetpides that are produced by *Bacillus subtilis* and are made up of D- and L-amino acids that are linked to a fatty acid chain (95).

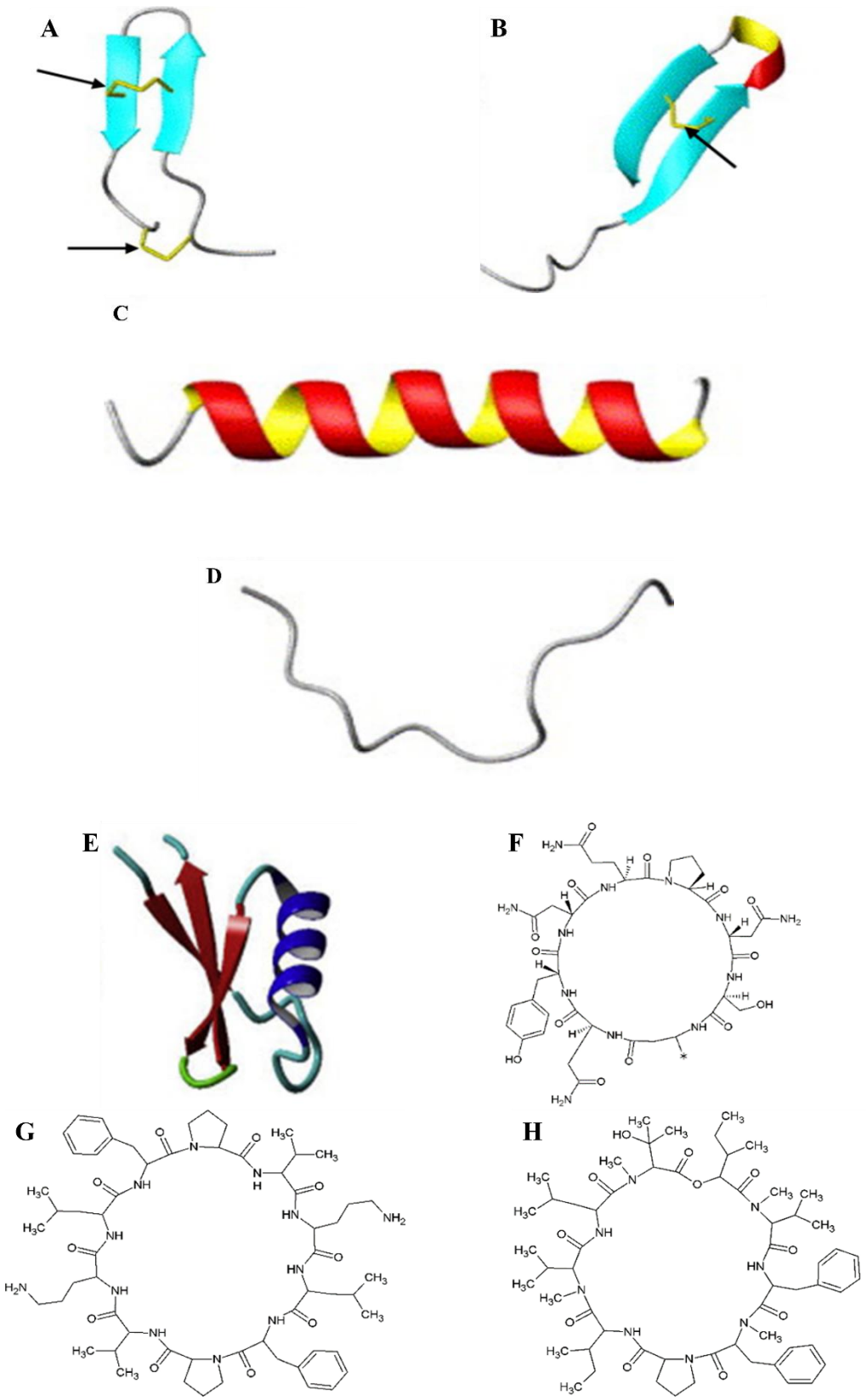

Figure 2.7: Structural diversity of antifungal peptides. (A) β-sheet, (B) loop, (C) α-helix, (D) extended, (E) combined α-helix and β-sheet, (F) cyclic lipopeptide (* represents the fatty acid chain), (G) cyclic peptide and (H) depsipeptide. Structures A-D were adapted from Powers and Hancock (96). Arrows indicate disulfide bonds. Structure E was adapted from Rautenbach *et al*. (97). Structures F-H were drawn using ChemSketch (ACD/Labs). Permission to use the images of peptide structures was granted.

2.5 Mode of action of antifungal peptides

Previously, it was believed that all AMPs kill target cells by interacting with the membrane and inducing pore formation. However, numerous studies have shown that many AMPs have a more complex mechanism of action. Antifungal peptides exert their activity on cells by targeting extracellular and intracellular components (98). As a result, cell growth is affected, leading to fungistatic or fungicidal activity. Antifungal peptide targets include the cell wall, cell membrane and intracellular targets. Examples of antifungal peptides and some of their modes of action are shown in **Table 2.2**.

Table 2.2: Examples of antifungal peptides, their sources, and modes of action.

Peptide	Source	Mode(s) of action	Reference(s)
DmAMP1	*Dahlia merckii*	Membrane permeabilisation Ca^{2+} influx and K^{+} efflux	(99, 100)
Histatin 5	Human saliva	Cell wall interaction ROS production ATP and K^{+} efflux	(101-103)
ETD151	Heliomicin analogue	Mitochondrial dysfunction	(104)
Psd1	*Pisum sativum*	Cell cycle disruption	(105)
HsAFP1	*Heuchera sanguinea*	Membrane permeabilisation ROS production Mitochondrial dysfunction Cell autophagy	(106-108)
RsAFP2	*Raphanus sativus*	Membrane permeabilisation ROS production Cell wall stress Apoptosis	(109, 110)
Scolopendin	*Scolopendra subspinipes mutilans*	ROS production Mitochondrial dysfunction Ca^{2+} influx Apoptosis	(111)

2.5.1 Interaction with the fungal cell wall

Before interacting with the cell membrane, some AMPs interact with cell wall components such as mannans, β-glucans, chitin, and cell wall proteins (**Figure 2.8**). Fungal mannoproteins include proteins involved in cell adhesion (112), cell wall stability (113) and enzymes involved in cell wall remodelling (114) and synthesis (115). Histatin 5, a 24 amino acid human salivary

peptide, was found to interact with the *Candida* cell wall protein Ssa1/2p. After binding to Ssa1/2p, histatin 5 moves to an intracellular compartment, where further candidacidal effects occur (116).

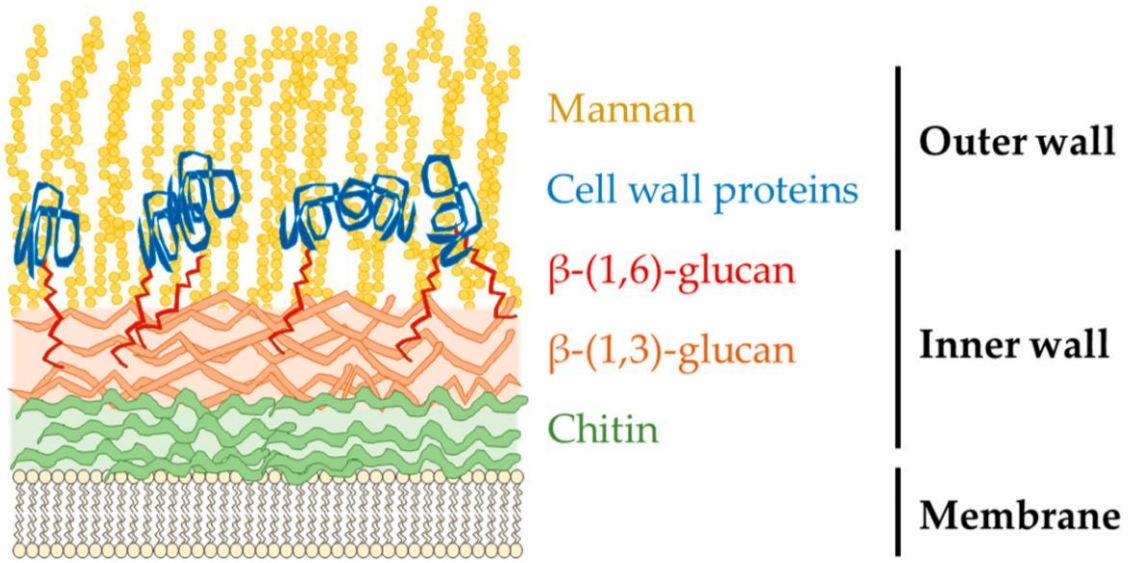

Figure 2.8: *Candida albicans* cell wall structure. The cell wall of *C. albicans* is a complex structure consisting of mannan, glucans, chitin, and cell wall-associated proteins while the cell membrane consists of glycerosphingolipids, sphingolipids and sterols. The image was obtained from Yoo *et al*. (117). Permission to use the image was granted.

Chitin is a 1,4-β-N-acetylglucosamine polymer that is anchored to the glucan network and is necessary for preserving structural integrity (118). *In vitro* experiments showed that the peptides AFP (a 51-amino acid peptide secreted by *Aspergillus giganteus*) and arasin 1 (a proline-rich AMP from the spider crab *Hyas araneus*) bind to chitin. Further assays revealed that AFP inhibits chitin synthase in sensitive fungi (119, 120).

The β-glucans such as 1,3-β-glucan and 1,6-β-glucan make up the polysaccharide network of the cell wall of fungi (121). The echinocandins were found to inhibit 1,3-β-D-glucan synthesis in the cell wall (122). Initially, the lipid tail of the echinocandin inserts into the cell membrane close to the target enzyme 1,3-β-D-glucan synthase (123). Afterwards, 1,3-β-D-glucan synthase is non-competitively inhibited by the echinocandin, leading to reduced 1,3-β-D-glucan synthesis, a weaker cell wall structure and loss of fungal viability (122).

2.5.2 Interaction with the cell membrane

The cell membrane is the most common target of antifungal peptides. Disturbing the integrity of the cell membrane results in the formation of pores, leakage of ions and other molecules

from the cell and culminates in the loss of membrane function. Several mechanisms of pore formation including the barrel-stave, toroidal pore and carpet models have been described. These mechanisms involve peptides forming a bundle with a central lumen through the membrane, accumulating on the membrane surface or inserting into the membrane and causing the lipids to bend through the pore forming a central lumen composed of lipids and peptides (124, 125).

For AMPs to form pores, they must interact with components of the cell membrane such as glycerophospholipids, sphingolipids and sterols. Cecropin B from the *Cecropia* moth permeabilises fungal membranes by binding to anionic glycerophospholipids such as phosphatidylinositol (PI), phosphatidic acid (PA), and phosphatidylserine (PS) (126). The tomato defensin TPP3 binds to phosphatidylinositol-(4,5)-bisphosphate ($PI(4,5)P_2$) which is critical for membrane permeabilisation and leads to lipid disorder (127). Cools *et al*. showed that HsAFP1 interacted with PA and histidine at position 32 and arginine at position 52 played key roles in the interaction (128). Selective targeting and disruption of membranes containing phosphatidylethanolamine was linked to the membrane disruptive activity of the cyclotide, cycloviolacin O2 (129).

Some antifungal peptides target glycosphingolipids. RsAFP2, a defensin produced by the radish plant *Raphanus sativus*, targets glucosylceramide which is a glycosphingolipid that plays a key role in fungal virulence (130) and mycelial growth (131). As a result, fungal membranes are permeabilised in a biphasic manner (99). Syringomycin E, a cyclic lipodepsipeptide produced by strains of *Pseudomonas syringae* (132), acts on fungal cells by targeting the glycosphingolipid mannosyldiinositolphosphorylceramide (133).

Antifungal peptides are also capable of interacting with sterols and proteins located in the fungal membrane. The antifungal drug AMB and *Ps*d1 from *Pisum sativum* interact with ergosterol (134). The tyrocidines, a group of cyclic decapeptides from *Brevibacillus parabrevis*, bound more selectively to model phosphatidylcholine membranes that contained ergosterol rather than cholesterol (97). Therefore, greater affinity for ergosterol containing membranes revealed that tyrocidines interact with lipid rafts containing glucosylceramide and ergosterol without causing membrane permeabilisation. However, this binding can lead to the presence of non-viable hyperbranched hyphae observed in spores that survived and were able to germinate at low peptide concentrations (135). Human lactoferrin targets the membrane protein Pmap H^+-ATPase, which interferes with cation homeostasis (136).

2.5.3 Intracellular effects

Some antifungal peptides kill fungal cells by targeting intracellular components as described in **Figure 2.9**. After interacting with the membrane, peptides are internalised without disrupting the membrane. Internalisation is not necessary for inducing intracellular activity as observed for RsAFP2 which does not enter the cell yet induces ROS production and apoptosis (109, 110).

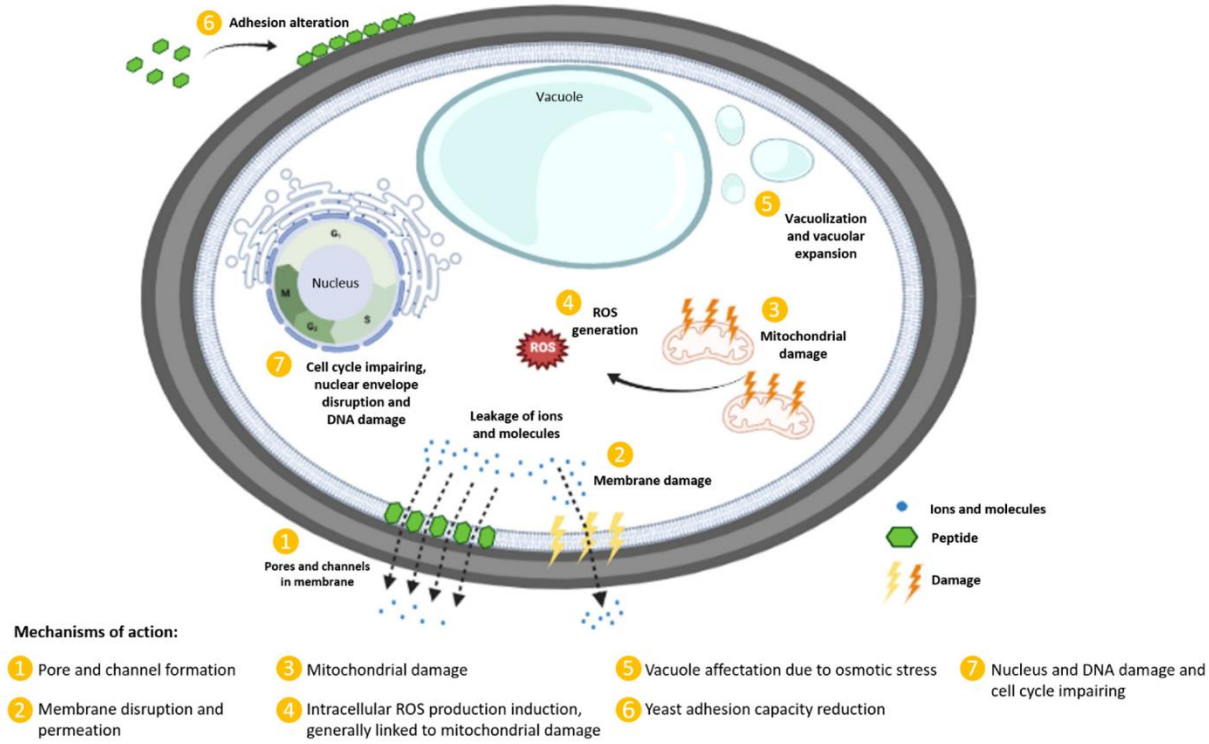

Figure 2.9: Membrane and intracellular targets of antifungal peptides. Some antifungal peptides can enter the cell and target intracellular components. Image obtained from Perez-Rodriguez *et al*. (137). Permission to use the image was granted.

Peptides can enter the cell by direct penetration of the membrane, endocytosis or via transport proteins. Direct penetration involves an initial interaction between the cationic AMP and the negatively charged membrane. This interaction alters the membrane potential and leads to pore formation which results in increased peptide entry (138). Pep-1 is a 21-residue peptide that crosses the cell membrane by forming pore-like structures (139). Endocytosis is an energy-dependent process where molecules are transported into the cytosol in vacuoles or vesicles which are formed from invaginations in the membrane (140). The peptides K28, NaD1, and Os-C were found to enter the cell via endocytosis (27, 141, 142). In yeast cells, membrane-

bound transport proteins play a crucial role in the uptake of peptides, amino acids, and sugars. Some of the transport proteins characterised in *C. albicans* include polyamine, peptide, and oligopeptide transporters (143).

Polyamine transporters facilitate the uptake of polycationic molecules such as spermidine, putrescine and spermine which are required for nucleic acid and protein synthesis (144). In *C. albicans*, the polyamine transporters Dur3 and Dur31 are essential for the uptake and toxicity of histatin 5 (143). Peptide and oligopeptide transporters are essential for uptake of nutrients in *C. albicans*. Peptide transporters are involved in the transport of dipeptides and tripeptides while oligopeptide transporters are involved in the transport of tetrapeptides and pentapeptides (145, 146).

Many antifungal peptides induce ROS production. Excessive ROS production leads to oxidative damage to proteins, lipids, nucleic acids, organelles, and membranes (147). Peptides such as scolopendin (111), HsAFP1 (106) and human lactoferrin (148) are known to induce ROS production. Oxidative damage due to ROS production can lead to the activation of apoptosis in which apoptotic bodies are formed without spillage of cellular content while intracellular content is broken down in a programmed manner (98). Apoptosis is indicated by many hallmarks including chromatin condensation, PS externalisation, metacaspase activation, cytochrome *c* release, disrupted mitochondrial membrane potential and DNA and nuclear fragmentation (147, 149). Melittin, a peptide from the venom of the honeybee *Apis mellifera*, induced PS externalisation, and DNA and nuclear fragmentation in *C. albicans*. The plant defensin ApDef1 induced chromatin condensation which led to cell death via a metacaspase-dependent pathway (150).

Exposure to some peptides has a detrimental effect on mitochondria which leads to mitochondrial dysfunction. ETD151 is an analogue of the insect defensin heliomicin which disrupts the mitochondrial membrane, leading to mitochondrial dysfunction (104). HsAFP1 treatment of *C. albicans* in the presence of sodium azide, which inhibits complex IV of the electron transport chain, led to reduced antifungal activity. This finding indicated that a functional respiratory chain was critical for the antifungal activity of HsAFP1 (106). Adenosine triphosphate (ATP) efflux involves the release of ATP from target cells. The antifungal activities of histatin 5, hBD-2 and hBD-3 involved ATP release, but minimal membrane disruption occurred upon ATP efflux (103, 116).

Antifungal peptides can also target the cell cycle. Psd1 from *Pisum sativum* enters the nucleus and interacts with cyclin F, a protein that plays a role in cell cycle control. As a result, the cell cycle is hindered (105). K28, a toxin produced by *Saccharomyces cerevisiae* (*S. cerevisiae*), is endocytosed and transferred into the cytoplasm using a retrograde transport pathway. Once in the cytoplasm, K28 blocks the cell cycle via inhibition of DNA synthesis (141).

Cation homeostasis is crucial for normal cell function. Calcium ions (Ca^{2+}) are involved in signal transduction pathways and are stored in the endoplasmic reticulum (ER) and the mitochondria (151), whereas potassium ions (K^{+}) control the ionic strength of the cytoplasm (101). Upon interaction with fungal cells, DmAMP1 and cecropin A induced K^{+} efflux and Ca^{2+} influx (100, 152), scolopendin and MtDef4 induced Ca^{2+} influx, and human lactoferrin and histatin 5 induced K^{+} efflux (111, 153).

In response to treatment with some antifungal peptides, cells will undergo autophagy, a protective process where intracellular material is digested in the vacuole (154). High levels of autophagy have been associated with cell death (155). Exposure to moderate concentrations of HsAFP1 led to autophagy in *S. cerevisiae* cells (108). Since functional vacuoles are important for autophagy induction (156), the vacuole may play a role in antifungal tolerance to HsAFP1. Further experiments showed that higher concentrations of HsAFP1 increased the pH of the vacuole, which may affect autophagy and lead to cell death (157). Treatment with the plant defensin NbD6 led to the fusion of vacuoles in *S. cerevisiae* and *Fusarium graminearum* into a single large vacuole. On the other hand, cells treated with the peptide SBI6 contained multiple fragmented vacuoles, indicating vacuolar disruption. Deletion of vacuole-related genes led to increased resistance to NbD6 and SBI6 indicating that antifungal activity is dependent on a properly functioning vacuole (157). The diversity of AMPs and the different modes of action provide a source of antifungal agents that can be further developed for therapeutic applications.

2.6 Limitations of using antimicrobial peptides and possible solutions

Despite the potential shown by AMPs as alternatives to conventional antifungal drugs, there are several issues concerning their use. The lack of safety profiles is concerning since few toxicity profiles are available, meaning the toxic effects of most peptides are unknown. Data on toxicity has been limited to effects on cell lines, erythrocytes and animal models (158).

Production of AMPs can be a costly process, therefore, more cost-effective methods of producing AMPs must be developed. One approach is recombinant production, but this process

involves an initial optimisation stage which is time-consuming and expensive. Furthermore, only natural amino acids can be used to synthesise the peptide of interest. An example of a recombinantly produced peptide used in therapeutic applications is plectasin from *Pseudoplectania nigrella* (159). One approach to reduce the cost of peptide synthesis is to decrease the peptides to the shortest possible sequence that has equal or greater antifungal activity. If the target site is known, *in silico* peptide design and modelling is attempted to identify whether the peptide is active before *in vitro* studies are carried out.

Proteolytic degradation limits the use of peptides in systemic applications. Oral and intravenous administration of peptides is difficult due to degradation by proteolytic enzymes in the gastrointestinal tract (160). The poor stability of AMPs makes them susceptible to degradation by proteases such as pepsin, trypsin and chymotrypsin (161). Therefore, most peptides are ideal for topical administration in the form of creams and gels (162).

Peptides can be modified to avoid proteolytic degradation. D-enantiomers of the peptide can be used since interactions between target membranes and peptides are not dependent on the stereochemistry of the peptide (163). Besides greater proteolytic stability, the use of non-natural D-enantiomer peptides was reported to increase the activity of some peptides. In addition to retaining activity after exposure to trypsin, the D-enantiomer of the synthetic peptide KK14 was more active against fungi than its L-enantiomer (164).

Blocking the N- and C-termini of peptides also increases resistance to proteolytic degradation. Modifications such as adding pyroglutamate (165), adding an acetyl group to the N-terminus and adding an amide group to the C-terminus have been found to diminish the sensitivity to proteolytic enzymes (166). Cyclisation of peptides renders the peptide insensitive to the action of some proteolytic enzymes, increases activity and reduces cytotoxicity (167). Peptide cyclisation can be done in multiple ways such as by connecting the N-terminus and C-terminus amino acids using an amide bond (head-to-tail cyclisation) or by connecting two side chains of individual amino acids (side chain cyclisation). Another strategy to create cyclic peptides is by creating linkages between specific amino acids. For example, cyclisation can be achieved by forming disulfide bridges between two cysteine residues (disulfide cyclisation) or by forming lactam bridges between lysine and either glutamic acid or aspartic acid residues (168).

A consequence of proteolytic degradation is the inability of the peptide to reach the target site, therefore a drug delivery system (DDS) can be used to ensure the peptide reaches its desired target. Other advantages of using DDSs include improved bioavailability and enhanced

transport across mucosal, endothelial, and epithelial barriers (169). The use of perfluorocarbon nanoemulsion particles loaded with melittin enabled the targeting of tumour cells whilst simultaneously inhibiting the haemolytic activity of melittin (170). Other examples of DDSs include microparticles, self-emulsifying DDSs, liposomes, DNA cages, carbon nanotubes, dendritic polymers, and solid core nanoparticles (171, 172).

Many peptides lose their activity when exposed to physiological salt concentrations which hinders their potential for systemic use (158). For example, P-113, LL-37 and several human β-defensins have been found to lose activity in physiological salt concentrations (116, 173, 174). Inactivity in high salt environments is a common issue for highly charged and hydrophilic peptides due to the presence of cations which can hinder interactions of the peptide with the membrane. Peptides with a high content of hydrophobic residues are not affected by high salt environments, but tend to be less selective and can lyse both human and microbial cells (124). Therefore, it is necessary to modify peptides in a manner that confers greater hydrophobicity, potency and selectivity while reducing toxic effects.

One solution involves the incorporation of hydrophobic unnatural amino acids such as β-naphtylalanine and β-(4,4'-biphenyl)alanine (173). Alternatively, the termini of peptides can be tagged with hydrophobic natural amino acids such as tryptophan and phenylalanine. Studies by Schmidtchen *et al.* and Pasupuleti *et al.* showed that tryptophan end-tagging led to better activity against bacteria and fungi, better selectivity for liposomes containing bacterial and fungal membrane components, and improved activity in the presence of physiological concentrations of sodium chloride and plasma (28, 175-177).

2.7 Antifungal peptides under clinical investigation

Despite the limitations described in the previous section, many AMPs are undergoing clinical trials for a variety of indications. Using AMPs in clinical applications could be beneficial since the degradation products of most AMPs would consist of natural amino acids. The short half-life of AMPs means that minimal concentrations of peptide would accumulate in tissues and the environment (160). Several antifungal peptides displayed promising activity which has made them ideal candidates for therapeutic applications (**Table 2.3**). The lipopeptide rezafungin, another member of the echinocandin family, was effective in treating candidiasis and aspergillosis and received FDA approval in March 2023 for the treatment of candidaemia and invasive candidiasis (23).

Three AMPs in phase II of clinical trials are novexatin, CZEN-002 and Pac-113. Novexatin is a cyclic heptamer peptide based on arginine and has shown promise as a treatment for onychomycosis (178). CZEN-002 is a peptide dimer that was derived from α-melanocyte stimulating hormone and acts by inducing accumulation of cyclic adenosine monophosphate and disrupting related signalling pathways. Furthermore, CZEN-002 is under investigation for topical treatment of vaginal candidiasis (179). Pac-113, a derivative of histatin 5, possesses potent antifungal activity against *C. albicans* and is being tested for the treatment of oral *Candida* infections in HIV seropositive patients (180).

Table 2.3: Selected antifungal peptides in clinical trials or approved for use. Adapted from Mookherjee *et al.* (21).

Peptide	Origin	Indication	Clinical trial phase	Company
Topical application				
Novexatin	Cyclic arginine-based heptamer	Fungal nail infections	IIb (complete)	NovaBiotics
Pac-113	Histatin 5 derivative	Oral candidiasis	IIb (complete)	Demegen, Pacgen Biopharmaceuticals Corporation
CZEN-002	Derivative of α-melanocyte stimulating hormone	Vulvovaginal candidiasis	II (complete)	Zengen, Abiogen Pharma
HXP124	Plant defensin	Fungal nail infections	IIa (complete)	Hexima
Intravenous application				
Rezafungin	Semisynthetic lipopeptide	Candidaemia and invasive candidiasis	Approved (March 2023)	Cidara Therapeutics
hLF1-11	Derivative of human lactoferrin	Candidaemia	I/II (withdrawn)	AM-Pharma
Novamycin	Synthetic peptide	Invasive fungal disease	Preclinical	NovaBiotics

The synthetic peptide novamycin consists of 14 arginine residues and possesses potent activity against invasive *Aspergillus* and *Candida* infections. Novamycin is in the preclinical stage of clinical trials for the treatment of invasive fungal disease and *Candida* infections occurring in the mouth and throat (181). HXP124 is a novel plant defensin with a cysteine-stabilised αβ-motif structure. This peptide displayed antifungal activity against clinically relevant human pathogens, including *Candida* species, *Cryptococcus* species, dermatophytes, and other moulds. HXP124 was active in an *ex vivo* model of nail infection and penetrated human nails.

In preclinical testing, HXP124 demonstrated a favourable safety profile (182). The peptide hLF1-11 consists of the first 11 amino acids of human lactoferrin. Despite poor activity *in vitro* under physiological conditions, hLF1-11 displayed potent antibacterial and antifungal activity *in vivo* (183). Despite reaching phase II trials for life-threatening bacterial and fungal infections, hlF1-11 was withdrawn from further trials due to the unavailability of the patient population (184). The limited number of antifungal peptides in clinical trials highlights the need for further research to discover new peptides.

2.8 Background to the study and rationale

Previous research showed that Os, a peptide derived from a tick defensin (OsDef2) and its cysteine-free analogue Os-C (**Table 2.4**) possessed antibacterial and antifungal activity in the low micromolar range in 0.01 M NaP buffer (pH 7.4), without cytotoxicity (25, 27). However, the salt-sensitive Os and Os-C were inactive against Gram-positive (*B. subtilis* and *S. aureus*) and Gram-negative (*Escherichia coli* (*E. coli*) and *Pseudomonas aeruginosa* (*P. aeruginosa*)) bacteria when tested in Luria-Bertani (LB) broth (25).

Investigations into the bactericidal modes of action of Os and Os-C in a low salt environment revealed that both peptides could translocate into the cytosol of bacteria (26). Both peptides also possessed antioxidant, anti-endotoxin, and anti-inflammatory properties (25, 185). Antifungal activity assays performed in 0.01 M NaP buffer showed that Os-C was less active against planktonic *C. albicans* with a minimum fungicidal concentration (MFC) of 28 µM compared with Os which had an MFC of 6 µM (27). For Os-C, the identified antifungal mode of action was ROS formation with limited membrane permeabilisation that probably occurs because of ROS production (27). Further development of Os-C is thus limited due to its reduced activity in a more physiological environment such as Roswell Park Memorial Institute (RPMI)-1640 medium.

Table 2.4: Primary sequences of OsDef2, Os and Os-C.

Peptide	Sequence
OsDef2	GYGCPFNQYQCHSHC**KGIRGYKGGYCKGAFKQTCKCY**
Os	**KGIRGYKGGYCKGAFKQTCKCY**
Os-C	**KGIRGYKGGY _KGAFKQT _K_Y**

Note: Omitted cysteine residues are replaced with underscores.

In this study, Os-C was selected because it is shorter than Os, and the absence of cysteine residues limits complications due to disulfide bond formation between cysteine residues. To overcome inactivity in the presence of high salt concentrations and subsequently boost the antifungal activity, Os-C was tagged with five tryptophan residues at the C-terminus to create the peptide Os-C(W_5). Tryptophan end-tagging was reported to improve antimicrobial activity in high salt environments and led to greater selectivity for liposomes representative of bacterial and fungal membranes. Furthermore, antimicrobial activity was retained in the presence of salts, serum, and plasma (28, 29, 175-177, 186).

Therefore, this study aimed to investigate the effect of tryptophan end-tagging on the structural characteristics, anticandidal activity and mode of action of the modified analogue, Os-C(W_5).

2.9 References

1. Brown, G. D., Denning, D. W., Gow, N. A., Levitz, S. M., Netea, M. G., and White, T. C. (2012) Hidden killers: human fungal infections. *Science Translational Medicine* **4**, 165rv113-165rv116. 10.1126/scitranslmed.3004404
2. World Health Organization. (2022) WHO fungal priority pathogens list to guide research, development and public health action., https://www.who.int/publications/i/item/9789240060241
3. Bongomin, F., Gago, S., Oladele, R. O., and Denning, D. W. (2017) Global and multi-national prevalence of fungal diseases-estimate precision. *Journal of Fungi (Basel)* **3**, 1-17. 10.3390/jof3040057
4. Fox, E. P., and Nobile, C. J. (2013) The role of *Candida albicans* biofilms in human disease. In *Candida albicans*: symptoms, causes and treatment options, Nova Science Publishers, 1-24.
5. Hoenigl, M., Sprute, R., Egger, M., Arastehfar, A., Cornely, O. A., Krause, R., Lass-Florl, C., Prattes, J., Spec, A., Thompson III, G. R., Wiederhold, N., and Jenks, J. D. (2021) The antifungal pipeline: fosmanogepix, ibrexafungerp, olorofim, opelconazole, and rezafungin. *Drugs* **81**, 1703-1729. 10.1007/s40265-021-01611-0
6. Perfect, J. R. (2017) The antifungal pipeline: a reality check. *Nature Reviews Drug Discovery* **16**, 603-616. 10.1038/nrd.2017.46
7. Denning, D. W. (2021) Antifungal drug resistance: an update. *European Journal of Hospital Pharmacy* **29**, 109-112. 10.1136/ejhpharm-2020-002604

8. Pfaller, M. A. (2012) Antifungal drug resistance: mechanisms, epidemiology, and consequences for treatment. *The American Journal of Medicine* **125**, S3-S13. 10.1016/j.amjmed.2011.11.001
9. World Health Organization. (2015) Global action plan on antimicrobial resistance., https://www.who.int/publications/i/item/9789241509763
10. Dos Santos Abrantes, P. M., McArthur, C. P., and Africa, C. W. (2014) Multi-drug resistant oral *Candida* species isolated from HIV-positive patients in South Africa and Cameroon. *Diagnostic Microbiology and Infectious Disease* **79**, 222-227. 10.1016/j.diagmicrobio.2013.09.016
11. Mnge, P., Okeleye, B. I., Vasaikar, S. D., and Apalata, T. (2017) Species distribution and antifungal susceptibility patterns of *Candida* isolates from a public tertiary teaching hospital in the Eastern Cape Province, South Africa. *Brazilian Journal of Medical and Biological Research* **50**, e5797-e5803. 10.1590/1414-431X20175797
12. Mulu, A., Kassu, A., Anagaw, B., Moges, B., Gelaw, A., Alemayehu, M., Belyhun, Y., Biadglegne, F., Hurissa, Z., Moges, F., and Isogai, E. (2013) Frequent detection of 'azole' resistant *Candida* species among late presenting AIDS patients in northwest Ethiopia. *BMC Infectious Diseases* **13**, 1-10. 10.1186/1471-2334-13-82
13. Nett, J. E., and Andes, D. R. (2016) Antifungal agents: spectrum of activity, pharmacology, and clinical indications. *Infectious Disease Clinics of North America* **30**, 51-83. 10.1016/j.idc.2015.10.012
14. Sanguinetti, M., Posteraro, B., and Lass-Florl, C. (2015) Antifungal drug resistance among *Candida* species: mechanisms and clinical impact. *Mycoses* **58**, 2-13. 10.1111/myc.12330
15. Nobile, C. J., and Johnson, A. D. (2015) *Candida albicans* biofilms and human disease. *Annual Reviews of Microbiology* **69**, 71-92. 10.1146/annurev-micro-091014-104330
16. Mitchell, K. F., Zarnowski, R., and Andes, D. R. (2016) Fungal super glue: the biofilm matrix and its composition, assembly, and functions. *PLoS Pathogens* **12**, e1005828-e1005833. 10.1371/journal.ppat.1005828
17. Brandenburg, L., Merres, J., Albrecht, L., Varoga, D., and Pufe, T. (2012) Antimicrobial peptides: multifunctional drugs for different applications. *Polymers* **4**, 539-560. 10.3390/polym4010539
18. Zasloff, M. (2002) Antimicrobial peptides of multicellular organisms. *Nature* **415**, 389-395. 10.1038/415389a

19. Harris, M. R., and Coote, P. J. (2010) Combination of caspofungin or anidulafungin with antimicrobial peptides results in potent synergistic killing of *Candida albicans* and *Candida glabrata in vitro*. *International Journal of Antimicrobial Agents* **35**, 347-356. 10.1016/j.ijantimicag.2009.11.021

20. Vriens, K., Cools, T. L., Harvey, P. J., Craik, D. J., Braem, A., Vleugels, J., De Coninck, B., Cammue, B. P. A., and Thevissen, K. (2016) The radish defensins RsAFP1 and RsAFP2 act synergistically with caspofungin against *Candida albicans* biofilms. *Peptides* **75**, 71-79. 10.1016/j.peptides.2015.11.001

21. Mookherjee, N., Anderson, M. A., Haagsman, H. P., and Davidson, D. J. (2020) Antimicrobial host defence peptides: functions and clinical potential. *Nature Reviews Drug Discovery* **19**, 311-332. 10.1038/s41573-019-0058-8

22. Grover, N. D. (2010) Echinocandins: a ray of hope in antifungal drug therapy. *Indian Journal of Pharmacology* **42**, 9-11. 10.4103/0253-7613.62396

23. Thompson, G. R., Soriano, A., Skoutelis, A., Vazquez, J. A., Honore, P. M., Horcajada, J. P., Spapen, H., Bassetti, M., Ostrosky-Zeichner, L., Das, A. F., Viani, R. M., Sandison, T., and Pappas, P. G. (2021) Rezafungin versus caspofungin in a phase 2, randomized, double-blind study for the treatment of candidemia and invasive candidiasis: the STRIVE trial. *Clinical Infectious Diseases* **73**, e3647-e3655. 10.1093/cid/ciaa1380

24. Ismail, N. O., Odendaal, C., Serem, J. C., Strömstedt, A. A., Bester, M. J., Sayed, Y., Neitz, A. W.H., and Gaspar, A. R.M. (2019) Antimicrobial function of short amidated peptide fragments from the tick-derived OsDef2 defensin. *Journal of Peptide Science* **25**, e3223-e3231. 10.1002/psc.3223

25. Prinsloo, L., Naidoo, A., Serem, J. C., Taute, H., Sayed, Y., Bester, M. J., Neitz, A. W. H., and Gaspar, A. R. M. (2013) Structural and functional characterization of peptides derived from the carboxy-terminal region of a defensin from the tick *Ornithodoros savignyi*. *Journal of Peptide Science* **19**, 325-332. 10.1002/psc.2505

26. Taute, H., Bester, M. J., Neitz, A. W. H., and Gaspar, A. R. M. (2015) Investigation into the mechanism of action of the antimicrobial peptides Os and Os-C derived from a tick defensin. *Peptides* **71**, 179-187. 10.1016/j.peptides.2015.07.017

27. Mbuayama, K. R., Taute, H., Strömstedt, A. A., Bester, M. J., and Gaspar, A. R. M. (2021) Antifungal activity and mode of action of synthetic peptides derived from the tick OsDef2 defensin. *Journal of Peptide Science* **28**, e3383-e3394. 10.1002/psc.3383

28. Schmidtchen, A., Pasupuleti, M., Morgelin, M., Davoudi, M., Alenfall, J., Chalupka, A., and Malmsten, M. (2009) Boosting antimicrobial peptides by hydrophobic oligopeptide end tags. *Journal of Biological Chemistry* **284**, 17584-17594. 10.1074/jbc.M109.011650

29. Sonesson, A., Nordahl, E. A., Malmsten, M., and Schmidtchen, A. (2011) Antifungal activities of peptides derived from domain 5 of high-molecular-weight kininogen. *International Journal of Peptides* **2011**, 761037-761047. 10.1155/2011/761037

30. McCarty, T. P., and Pappas, P. G. (2016) Invasive Candidiasis. *Infectious Disease Clinics of North America* **30**, 103-124. 10.1016/j.idc.2015.10.013

31. Chowdhary, A., Sharma, C., and Meis, J. F. (2017) *Candida auris*: a rapidly emerging cause of hospital-acquired multidrug-resistant fungal infections globally. *PLoS Pathogens* **13**, e1006290-e1006299. 10.1371/journal.ppat.1006290

32. Pappas, P. G., Lionakis, M. S., Arendrup, M. C., Ostrosky-Zeichner, L., and Kullberg, B. J. (2018) Invasive candidiasis. *Nature Reviews Disease Primers* **4**, 18026-18045. 10.1038/nrdp.2018.26

33. Playford, E. G., Lipman, J., Kabir, M., McBryde, E. S., Nimmo, G. R., Lau, A., and Sorrell, T. C. (2009) Assessment of clinical risk predictive rules for invasive candidiasis in a prospective multicentre cohort of ICU patients. *Intensive Care Medicine* **35**, 2141-2145. 10.1007/s00134-009-1619-9

34. Morad, H. O. J., Wild, A. M., Wiehr, S., Davies, G., Maurer, A., Pichler, B. J., and Thornton, C. R. (2018) Pre-clinical imaging of invasive candidiasis using immunoPET/MR. *Frontiers in Microbiology* **9**, 1996-2010. 10.3389/fmicb.2018.01996

35. Lo, H. J., Kohler, J. R., DiDomenico, B., Loebenberg, D., Cacciapuoti, A., and Fink, G., R. (1997) Nonfilamentous *C. albicans* mutants are avirulent. *Cell* **90**, 939-949. 10.1016/S0092-8674(00)80358-X

36. Felk, A., Kretschmar, M., Albrecht, A., Schaller, M., Beinhauer, S.,, Nichterlein, T., Sanglard, D., Korting, H. C., Schafer, W., and Hube, B. (2002) *Candida albicans* hyphal formation and the expression of the Efg1-regulated proteinases Sap4 to Sap6 are required for the invasion of parenchymal organs. *Infection and Immunity* **70**, 3689-3700. 10.1128/IAI.70.7.3689-3700.2002

37. Kasper, L., Konig, A., Koenig, P. A., Gresnigt, M. S., Westman, J., Drummond, R. A., Lionakis, M. S., Gross, O., Ruland, J., Naglik, J. R., and Hube, B. (2018) The fungal peptide toxin candidalysin activates the NLRP3 inflammasome and causes cytolysis in

mononuclear phagocytes. *Nature Communications* **9**, 4260-4279. 10.1038/s41467-018-06607-1

38. Phan, Q. T., Myers, C. L., Fu, Y., Sheppard, D. C., Yeaman, M. R., Welch, W. H., Ibrahim, A. S., Edwards Jr, J. E., and Filler, S. G. (2007) Als3 is a *Candida albicans* invasin that binds to cadherins and induces endocytosis by host cells. *PLoS Biology* **5**, e64-e78. 10.1371/journal.pbio.0050064
39. Desai, J. V., Mitchell, A. P., and Andes, D. R. (2014) Fungal biofilms, drug resistance, and recurrent infection. *Cold Spring Harbor Perspectives in Medicine* **4**, a019729-a019746. 10.1101/cshperspect.a019729
40. Harriott, M. M., and Noverr, M. C. (2011) Importance of *Candida*-bacterial polymicrobial biofilms in disease. *Trends in Microbiology* **19**, 557-563. 10.1016/j.tim.2011.07.004
41. Tsui, C., Kong, E. F., and Jabra-Rizk, M. A. (2016) Pathogenesis of *Candida albicans* biofilm. *Pathogens and Disease* **74**, 1-13. 10.1093/femspd/ftw018
42. Priya, A., and Pandian, S. K. (2020) Piperine impedes biofilm formation and hyphal morphogenesis of *Candida albicans*. *Frontiers in Microbiology* **11**, 756-773. 10.3389/fmicb.2020.00756
43. Park, S. C., Park, Y., and Hahm, K. S. (2011) The role of antimicrobial peptides in preventing multidrug-resistant bacterial infections and biofilm formation. *International Journal of Molecular Sciences* **12**, 5971-5992. 10.3390/ijms12095971
44. Bondaryk, M., Staniszewska, M., Zielinska, P., and Urbanczyk-Lipkowska, Z. (2017) Natural antimicrobial peptides as inspiration for design of a new generation antifungal compounds. *Journal of Fungi (Basel)* **3**, 1-36. 10.3390/jof3030046
45. Maubon, D., Garnaud, C., Calandra, T., Sanglard, D., and Cornet, M. (2014) Resistance of *Candida* spp. to antifungal drugs in the ICU: where are we now? *Intensive Care Medicine* **40**, 1241-1255. 10.1007/s00134-014-3404-7
46. Jessup, C. J., Ryder, N. S., and Ghannoum, M. A. (2000) An evaluation of the *in vitro* activity of terbinafine. *Medical Mycology* **38**, 155-159. 10.1080/mmy.38.2.155.159
47. Mesa-Arango, A. C., Scorzoni, L., and Zaragoza, O. (2012) It only takes one to do many jobs: amphotericin B as antifungal and immunomodulatory drug. *Frontiers in Microbiology* **3**, 286-295. 10.3389/fmicb.2012.00286
48. Odds, F. C., Brown, A. J., and Gow, N. A. (2003) Antifungal agents: mechanisms of action. *Trends in Microbiology* **11**, 272-279. 10.1016/s0966-842x(03)00117-3

49. Kuse, E. R., Chetchotisakd, P., da Cunha, C. A., Ruhnke, M., Barrios, C., Raghunadharao, D., Sekhon, J. S., Freire, A., Ramasubramanian, V., Demeyer, I., Nucci, M., Leelarasamee, A., Jacobs, F., Decruyenaere, J., Pittet, D., Ullmann, A. J., Ostrosky-Zeichner, L., Lortholary, O., Koblinger, S., Diekmann-Berndt, H., and Cornely, O. A. (2007) Micafungin versus liposomal amphotericin B for candidaemia and invasive candidosis: a phase III randomised double-blind trial. *The Lancet* **369**, 1519-1527. 10.1016/S0140-6736(07)60605-9

50. Kullberg, B. J., Sobel, J. D., Ruhnke, M., Pappas, P. G., Viscoli, C., Rex, J. H., Cleary, J. D., Rubinstein, E., Church, L. W., Brown, J. M., Schlamm, H. T., Oborska, I. T., Hilton, F., and Hodges, M. R. (2005) Voriconazole versus a regimen of amphotericin B followed by fluconazole for candidaemia in non-neutropenic patients: a randomised non-inferiority trial. *The Lancet* **366**, 1435-1442. 10.1016/S0140-6736(05)67490-9

51. Carrillo-Munoz, A. J., Giusiano, G., Ezkurra, P. A., and Quindos, G. (2006) Antifungal agents: mode of action in yeast cells. *Spanish Society of Chemotherapy* **19**, 130-139.,

52. Park, S., Kelly, R., Kahn, J. N., Robles, J., Hsu, M. J., Register, E., Li, W., Vyas, V., Fan, H., Abruzzo, G., Flattery, A., Gill, C., Chrebet, G., Parent, S. A., Kurtz, M., Teppler, H., Douglas, C. M., and Perlin, D. S. (2005) Specific substitutions in the echinocandin target Fks1p account for reduced susceptibility of rare laboratory and clinical *Candida* sp. isolates. *Antimicrobial Agents and Chemotherapy* **49**, 3264-3273. 10.1128/AAC.49.8.3264-3273.2005

53. Pappas, P. G., Rotstein, C. M., Betts, R. F., Nucci, M., Talwar, D., De Waele, J. J., Vazquez, J. A., Dupont, B. F., Horn, D. L., Ostrosky-Zeichner, L., Reboli, A. C., Suh, B., Digumarti, R., Wu, C., Kovanda, L. L., Arnold, L. J., and Buell, D. N. (2007) Micafungin versus caspofungin for treatment of candidemia and other forms of invasive candidiasis. *Clinical Infectious Diseases* **45**, 883-893. 10.1086/520980

54. Wong, S. S. W., Samaranayake, L. P., and Seneviratne, C. J. (2014) In pursuit of the ideal antifungal agent for *Candida* infections: high-throughput screening of small molecules *Drug Discovery Today* **19**, 1721-1730. 10.1016/j.drudis.2014.06.009

55. Bayhan, G. I., Garipardic, M., Karaman, K., and Akbayram, S. (2016) Voriconazole-associated visual disturbances and hallucinations. *Cutaneous and Ocular Toxicology* **35**, 80-82. 10.3109/15569527.2015.1020544

56. Safdar, A., Ma, J., Saliba, F., Dupont, B., Wingard, J. R., Hachem, R. Y., Mattiuzzi, G. N., Chandrasekar, P. H., Kontoyiannis, D. P., Rolston, K. V., Walsh, T. J., Champlin, R. E., and Raad, I. I. (2010) Drug-induced nephrotoxicity caused by amphotericin B

lipid complex and liposomal amphotericin B: a review and meta-analysis. *Medicine (Baltimore)* **89**, 236-244. 10.1097/MD.0b013e3181e9441b

57. Fisher, M. C., Hawkins, N. J., Sanglard, D., and Gurr, S. J. (2018) Worldwide emergence of resistance to antifungal drugs challenges human health and food security. *Science* **360**, 739-742. 10.1126/science.aap7999
58. Fisher, M. C., Alastruey-Izquierdo, A., Berman, J., Bicanic, T., Bignell, E. M., Bowyer, P., Bromley, M., Bruggemann, R., Garber, G., Cornely, O. A., Gurr, S. J., Harrison, T. S., Kuijper, E., Rhodes, J., Sheppard, D. C., Warris, A., White, P. L., Xu, J., Zwaan, B., and Verweij, P. E. (2022) Tackling the emerging threat of antifungal resistance to human health. *Nature Reviews Microbiology* **20**, 557-571. 10.1038/s41579-022-00720-1
59. Riera, F., Caeiro, J. P., and Sotomayor, C. E. (2019) Antifungal stewardship in low-and middle-income countries. *Current Treatment Options in Infectious Diseases* **11**, 292-299. 10.1007/s40506-019-00197-2
60. Spampinato, C., and Leonardi, D. (2013) *Candida* infections, causes, targets, and resistance mechanisms: traditional and alternative antifungal agents. *Biomed Research International* **2013**, 204237-204249. 10.1155/2013/204237
61. Sheikh, N., Jahagirdar, V., Kothadia, S., and Nagoba, B. (2013) Antifungal drug resistance in *Candida* species. *European Journal of General Medicine* **10**, 254-258.,
62. Kanafani, Z. A., and Perfect, J. R. (2008) Antimicrobial resistance: resistance to antifungal agents: mechanisms and clinical impact. *Clinical Infectious Diseases* **46**, 120-128. 10.1086/524071
63. Flowers, S. A., Colon, B., Whaley, S. G., Schuler, M. A., and Rogers, P. D. (2015) Contribution of clinically derived mutations in *ERG11* to azole resistance in *Candida albicans. Antimicrobial Agents and Chemotherapy* **59**, 450-460. 10.1128/AAC.03470-14
64. Beyda, N. D., Lewis, R. E., and Garey, K. W. (2012) Echinocandin resistance in *Candida* species: mechanisms of reduced susceptibility and therapeutic approaches. *Annals of Pharmacotherapy* **46**, 1086-1096. 10.1345/aph.1R020
65. Walker, L. A., Munro, C. A., de Bruijn, I., Lenardon, M. D., McKinnon, A., and Gow, N. A. (2008) Stimulation of chitin synthesis rescues *Candida albicans* from echinocandins. *PLoS Pathogens* **4**, e1000040-e1000051. 10.1371/journal.ppat.1000040

66. Sun, F., Qu, F., Ling, Y., Mao, P., Xia, P., Chen, H., Zhou, D. (2013) Biofilm-associated infections: antibiotic resistance and novel therapeutic strategies. *Future Microbiology* **8**, 877-886. 10.2217/fmb.13.58

67. Baillie, G. S., and Douglas, L. J. (1998) Iron-limited biofilms of *Candida albicans* and their susceptibility to amphotericin B. *Antimicrobial Agents and Chemotherapy* **42**, 2146-2149. 10.1128/AAC.42.8.2146

68. LaFleur, M. D., Kumamoto, C. A., and Lewis, K. (2006) *Candida albicans* biofilms produce antifungal-tolerant persister cells. *Antimicrobial Agents and Chemotherapy* **50**, 3839-3846. 10.1128/AAC.00684-06

69. Galdiero, E., de Alteriis, E., De Natale, A., D'Alterio, A., Siciliano, A., Guida, M. *et al.* (2020) Eradication of Candida albicans persister cell biofilm by the membranotropic peptide gH625 Sci Rep **10**, 5780 10.1038/s41598-020-62746-w

70. Zarnowski, R., Sanchez, H., Covelli, A. S., Dominguez, E., Jaromin, A., Bernhardt, J., Mitchell, K. F., Heiss, C., Azadi, P., Mitchell, A., and Andes, D. R. (2018) *Candida albicans* biofilm-induced vesicles confer drug resistance through matrix biogenesis. *PLoS Biology* **16**, e2006872-e2006889. 10.1371/journal.pbio.2006872

71. Zarnowski, R., Westler, W. M., Lacmbouh, G. A., Marita, J. M., Bothe, J. R., Bernhardt, J., Lounes-Hadj Sahraoui, A., Fontaine, J., Sanchez, H., Hatfield, R. D., Ntambi, J. M., Nett, J. E., Mitchell, A. P., and Andes, D. R. (2014) Novel entries in a fungal biofilm matrix encyclopedia. *mBio* **5**, e01333-01314. 10.1128/mBio.01333-14

72. Taff, H. T., Nett, J. E., Zarnowski, R., Ross, K. M., Sanchez, H., Cain, M. T., Hamaker, J., Mitchell, A. P., and Andes, D. R. (2012) A *Candida* biofilm-induced pathway for matrix glucan delivery: implications for drug resistance. *PLoS Pathogens* **8**, e1002848-e1002860. 10.1371/journal.ppat.1002848

73. Nett, J. E., Crawford, K., Marchillo, K., and Andes, D. R. (2010) Role of Fks1p and matrix glucan in *Candida albicans* biofilm resistance to an echinocandin, pyrimidine, and polyene. *Antimicrobial Agents and Chemotherapy* **54**, 3505-3508. 10.1128/AAC.00227-10

74. Johnson, C. J., Cabezas-Olcoz, J., Kernien, J. F., Wang, S. X., Beebe, D. J., Huttenlocher, A., Ansari, H., and Nett, J. E. (2016) The extracellular matrix of *Candida albicans* biofilms impairs formation of neutrophil extracellular traps. *PLoS Pathogens* **12**, e1005884-e1005906. 10.1371/journal.ppat.1005884

75. Fuchs, T. A., Abed, U., Goosmann, C., Hurwitz, R., Schulze, I., Wahn, V. *et al.* (2007) Novel cell death program leads to neutrophil extracellular traps Journal of Cell Biology **176**, 231-241 10.1083/jcb.200606027

76. Xie, Z., Thompson, A., Sobue, T., Kashleva, H., Xu, H., Vasilakos, J., and Dongari-Bagtzoglou, A. (2012) *Candida albicans* biofilms do not trigger reactive oxygen species and evade neutrophil killing. *Journal of Infectious Diseases* **206**, 1936-1945. 10.1093/infdis/jis607

77. Harriott, M. M., and Noverr, M. C. (2009) *Candida albicans* and *Staphylococcus aureus* form polymicrobial biofilms: effects on antimicrobial resistance. *Antimicrobial Agents and Chemotherapy* **53**, 3914-3922. 10.1128/AAC.00657-09

78. Kong, E. F., Tsui, C., Kucharikova, S., Andes, D., Van Dijck, P., and Jabra-Rizk, M. A. (2016) Commensal protection of *Staphylococcus aureus* against antimicrobials by *Candida albicans* biofilm matrix. *mBio* **7**, 1-12. 10.1128/mBio.01365-16

79. Kim, D., Liu, Y., Benhamou, R. I., Sanchez, H., Simon-Soro, A., Li, Y., Hwang, G., Fridman, M., Andes, D. R., and Koo, H. (2018) Bacterial-derived exopolysaccharides enhance antifungal drug tolerance in a cross-kingdom oral biofilm. *The ISME Journal* **12**, 1427-1442. 10.1038/s41396-018-0113-1

80. Jenssen, H., Hamill, P., and Hancock, R. E. (2006) Peptide antimicrobial agents. *Clinical Microbiology Reviews* **19**, 491-511. 10.1128/CMR.00056-05

81. Wang, Z., and Wang, G. (2004) APD: the Antimicrobial Peptide Database. *Nucleic Acids Research* **32**, D590-D592. 10.1093/nar/gkh025

82. Wang, G., Li, X., and Wang, Z. (2009) APD2: the updated antimicrobial peptide database and its application in peptide design. *Nucleic Acids Research* **37**, D933-D937. 10.1093/nar/gkn823

83. Wang, G., Li, X., and Wang, Z. (2016) APD3: the antimicrobial peptide database as a tool for research and education. *Nucleic Acids Research* **44**, D1087-D1093. 10.1093/nar/gkv1278

84. Gomes, B., Augusto, M. T., Felicio, M. R., Hollmann, A., Franco, O. L., Goncalves, S., and Santos, N. C. (2018) Designing improved active peptides for therapeutic approaches against infectious diseases. *Biotechnology Advances* **36**, 415-429. 10.1016/j.biotechadv.2018.01.004

85. Nakamura, T., Furunaka, H., Miyata, T., Tokunaga, F., Muta, T., Iwanaga, S., Niwa, M., Takao, T., and Shimonishi, Y. (1988) Tachyplesin, a class of antimicrobial peptide from the hemocytes of the horseshoe crab (*Tachypleus tridentatus)*. Isolation and

chemical structure. *Journal of Biological Chemistry* **263**, 16709-16713. 10.1016/s0021-9258(18)37448-9

86. Zasloff, M. (1987) Magainins, a class of antimicrobial peptides from *Xenopus* skin: isolation, characterization of two active forms, and partial cDNA sequence of a precursor. *Proceedings of the National Academy of Science* **84**, 5449-5453. 10.1073/pnas.84.15.5449
87. Selsted, M. E., Novotny, M. J., Morris, W. L., Tang, Y. Q., Smith, W., and Cullor, J. S. (1992) Indolicidin, a novel bactericidal tridecapeptide amide from neutrophils. *Journal of Biological Chemistry* **267**, 4292-4295. 10.1016/s0021-9258(18)42830-x
88. Fehlbaum, P., Bulet, P., Chernysh, S. Briand, J., Roussel, J., Letellier, L., Hetru, C., and Hoffmann, J. A. (1996) Structure-activity analysis of thanatin, a 21-residue inducible insect defense peptide with sequence homology to frog skin antimicrobial peptides. *Proceedings of the National Academy of Science* **93**, 1221-1225. 10.1073/pnas.93.3.1221
89. Fant, F., Vranken, W., Broekaert, W., and Borremans, F. (1998) Determination of the three-dimensional solution structure of *Raphanus sativus* antifungal protein 1 by 1H NMR. *Journal of Molecular Biology* **279**, 257-270. 10.1006/jmbi.1998.1767
90. Bruix, M., Gonzalez, C., Santoro, J., Soriano, F., Rocher, A., Mendez, E., and Rico, M. (1995) 1H-NMR studies on the structure of a new thionin from barley endosperm. *Biopolymers* **36**, 751-763. 10.1002/bip.360360608
91. Gao, A., Hakimi, S., Mittanck, C. A., Wu, Y., Woerner, B. M., Stark, D. M., Shah, D. M., Liang, J., and Rommens, C. M. T. (2000) Fungal pathogen protection in potato by expression of a plant defensin peptide. *Nature Biotechnology* **18**, 1307-1310. 10.1038/82436
92. Davies, J. S. (2003) The cyclization of peptides and depsipeptides. *Journal of Peptide Science* **9**, 471-501. 10.1002/psc.491
93. Takesako, K., Ikai, K., Haruna, F., Endo, M., Shimanaka, K., Sono, E., Nakamura, T., Kato, I., and Yamaguchi, H. (1991) Aureobasidins, new antifungal antibiotics taxonomy, fermentation, isolation, and properties. *The Journal of Antibiotics* **44**, 919-924. 10.7164/antibiotics.44.919
94. Meena, K. R., and Kanwar, S. S. (2015) Lipopeptides as the antifungal and antibacterial agents: applications in food safety and therapeutics. *Biomed Research International* **2015**, 473050-473058. 10.1155/2015/473050

95. Besson, F., and Michel, G. (1984) Action of the antibiotics of the iturin group on artificial membranes. *The Journal of Antibiotics* **37**, 646-651 10.7164/antibiotics.37.646

96. Powers, J. P., and Hancock, R. E. (2003) The relationship between peptide structure and antibacterial activity. *Peptides* **24**, 1681-1691. 10.1016/j.peptides.2003.08.023

97. Rautenbach, M., Troskie, A. M., and Vosloo, J. A. (2016) Antifungal peptides: to be or not to be membrane active. *Biochimie* **130**, 132-145. 10.1016/j.biochi.2016.05.013

98. Struyfs, C., Cammue, B. P. A., and Thevissen, K. (2021) Membrane-interacting antifungal peptides. *Frontiers in Cell and Developmental Biology* **9**, 649875-649891. 10.3389/fcell.2021.649875

99. Thevissen, K., Terras, F. R. G., and Broekaert, W. F. (1999) Permeabilization of fungal membranes by plant defensins inhibits fungal growth. *Applied and Environmental Microbiology* **65**, 5451-5458. 10.1128/AEM.65.12.5451-5458.1999

100. Thevissen, K., Francois, I. E., Takemoto, J. Y., Ferket, K. K., Meert, E. M., and Cammue, B. P. A. (2003) DmAMP1, an antifungal plant defensin from dahlia (*Dahlia merckii*), interacts with sphingolipids from *Saccharomyces cerevisiae*. *FEMS Microbiology Letters* **226**, 169-173. 10.1016/S0378-1097(03)00590-1

101. Baev, D., Rivetta, A., Vylkova, S., Sun, J. N., Zeng, G. F., Slayman, C. L., and Edgerton, M. (2004) The TRK1 potassium transporter is the critical effector for killing of *Candida albicans* by the cationic protein, histatin 5. *Journal of Biological Chemistry* **279**, 55060-55072. 10.1074/jbc.M411031200

102. Kavanagh, K., and Dowd, S. (2004) Histatins: antimicrobial peptides with therapeutic potential. *Journal of Pharmacy and Pharmacology* **56**, 285-289. 10.1211/0022357022971

103. Koshlukova, S. E., Lloyd, T. L., Araujo, M. W., and Edgerton, M. (1999) Salivary histatin 5 induces non-lytic release of ATP from *Candida albicans* leading to cell death. *Journal of Biological Chemistry* **274**, 18872-18879. 10.1074/jbc.274.27.18872

104. Aumer, T., Voisin, S. N., Knobloch, T., Landon, C., and Bulet, P. (2020) Impact of an antifungal insect defensin on the proteome of the phytopathogenic fungus *Botrytis cinerea*. *Journal of Proteome Research* **19**, 1131-1146. 10.1021/acs.jproteome.9b00638

105. Lobo, D. S., Pereira, J. B., Fragel-Madeira, L., Medeiros, L. N., Cabral, L., M., Faria, J., Bellio, M., Campos, R. C., Linden, R., and Kurtenbach, E. (2007) Antifungal *Pisum*

sativum defensin 1 interacts with *Neurospora crassa* cyclin F related to the cell cycle. *Biochemistry* **46**, 987-996. 10.1021/bi061441j

106. Aerts, A. M., Bammens, L., Govaert, G., Carmona-Gutierrez, D., Madeo, F., Cammue, B. P. A., and Thevissen, K. (2011) The antifungal plant defensin HsAFP1 from *Heuchera sanguinea* induces apoptosis in *Candida albicans*. *Frontiers in Microbiology* **2**, 47-55. 10.3389/fmicb.2011.00047

107. Cools, T. L., Vriens, K., Struyfs, C., Verbandt, S., Ramada, M. H. S., Brand, G. D., Bloch, C., Jr., Koch, B., Traven, A., Drijfhout, J. W., Demuyser, L., Kucharikova, S., Van Dijck, P., Spasic, D., Lammertyn, J., Cammue, B. P. A., and Thevissen, K. (2017) The antifungal plant defensin HsAFP1 is a phosphatidic acid-interacting peptide inducing membrane permeabilization. *Frontiers in Microbiology* **8**, 2295-2307. 10.3389/fmicb.2017.02295

108. Struyfs, C., Cools, T. L., De Cremer, K., Sampaio-Marques, B., Ludovico, P., Wasko, B. M., Kaeberlein, M., Cammue, B. P. A., and Thevissen, K. (2020) The antifungal plant defensin HsAFP1 induces autophagy, vacuolar dysfunction and cell cycle impairment in yeast. *Biochimica et Biophysica Acta - Biomembranes* **1862**, 183255-183266. 10.1016/j.bbamem.2020.183255

109. Aerts, A. M., Francois, I. E. J. A, Meert, M. K. E, Li, Q., Cammue, B. P. A., and Thevissen, K. T. (2007) The antifungal activity of RsAFP2, a plant defensin from *Raphanus sativus*, involves the induction of reactive oxygen species in *Candida albicans*. *Journal of Molecular Microbiology and Biotechnology* **13**, 243-247. 10.1159/000104753

110. Thevissen, K., de Mello Tavares, P., Xu, D., Blankenship, J., Vandenbosch, D., Idkowiak-Baldys, J., Govaert, G., Bink, A., Rozental, S., de Groot, P. W., Davis, T. R., Kumamoto, C. A., Vargas, G., Nimrichter, L., Coenye, T., Mitchell, A., Roemer, T., Hannun, Y. A., and Cammue, B. P. A. (2012) The plant defensin RsAFP2 induces cell wall stress, septin mislocalization and accumulation of ceramides in *Candida albicans*. *Molecular Microbiology* **84**, 166-180. 10.1111/j.1365-2958.2012.08017.x

111. Lee, H., Hwang, J. S., and Lee, D. G. (2017) Scolopendin, an antimicrobial peptide from centipede, attenuates mitochondrial functions and triggers apoptosis in *Candida albicans*. *Biochemical Journal* **474**, 635-645. 10.1042/BCJ20161039

112. Dranginis, A. M., Rauceo, J. M., Coronado, J. E., and Lipke, P. N. (2007) A biochemical guide to yeast adhesins: glycoproteins for social and antisocial occasions. *Microbiology and Molecular Biology Reviews* **71**, 282-294. 10.1128/MMBR.00037-06

113. Ragni, E., Sipiczki, M., and Strahl, S. (2007) Characterization of Ccw12p, a major key player in cell wall stability of *Saccharomyces cerevisiae*. *Yeast* **24**, 309-319. 10.1002/yea.1465

114. Cabib, E., Blanco, N., Grau, C., Rodriguez-Pena, J. M., and Arroyo, J. (2007) Crh1p and Crh2p are required for the cross-linking of chitin to beta(1-6)glucan in the *Saccharomyces cerevisiae* cell wall. *Molecular Microbiology* **63**, 921-935. 10.1111/j.1365-2958.2006.05565.x

115. Mouyna, I., Fontaine, T., Vai, M., Monod, M., Fonzi, W. A., Diaquin, M., Popolo, L., Hartland, R. P., and Latge, J. P. (2000) Glycosylphosphatidylinositol-anchored glucanosyltransferases play an active role in the biosynthesis of the fungal cell wall. *Journal of Biological Chemistry* **275**, 14882-14889. 10.1074/jbc.275.20.14882

116. Vylkova, S., Nayyar, N., Li, W., and Edgerton, M. (2007) Human beta-defensins kill *Candida albicans* in an energy-dependent and salt-sensitive manner without causing membrane disruption. *Antimicrobial Agents and Chemotherapy* **51**, 154-161. 10.1128/AAC.00478-06

117. Yoo, Y. J., Kim, A. R., Perinpanayagam, H., Han, S. H., and Kum, K. Y. (2020) *Candida albicans* virulence factors and pathogenicity for endodontic infections. *Microorganisms* **8**, 1-18. 10.3390/microorganisms8091300

118. Cabib, E. (2009) Two novel techniques for determination of polysaccharide cross-links show that Crh1p and Crh2p attach chitin to both beta(1-6)- and beta(1-3)glucan in the *Saccharomyces cerevisiae* cell wall. *Eukaryotic Cell* **8**, 1626-1636. 10.1128/EC.00228-09

119. Paulsen, V. S., Blencke, H. M., Benincasa, M., Haug, T., Eksteen, J. J., Styrvold, O. B., Scocchi, M., and Stensvag, K. (2013) Structure-activity relationships of the antimicrobial peptide arasin 1 - and mode of action studies of the N-terminal, proline-rich region. *PLoS One* **8**, e53326-e53336. 10.1371/journal.pone.0053326

120. Hagen, S., Marx, F., Ram, A. F., and Meyer, V. (2007) The antifungal protein AFP from *Aspergillus giganteus* inhibits chitin synthesis in sensitive fungi. *Applied and Environmental Microbiology* **73**, 2128-2134. 10.1128/AEM.02497-06

121. Bowman, S. M., and Free, S. J. (2006) The structure and synthesis of the fungal cell wall. *Bioessays* **28**, 799-808. 10.1002/bies.20441

122. Sawistowska-Schroder, E. T., Kerridge, D., and Perry, H. (1984) Echinocandin inhibition of 1,3-beta-D-glucan synthase from *Candida albicans*. *FEBS Letters* **173**, 134-138. 10.1016/0014-5793(84)81032-7

123. Denning, D. W. (2003) Echinocandin antifungal drugs. *The Lancet* **362**, 1142-1151. 10.1016/S0140-6736(03)14472-8

124. Brogden, K. A. (2005) Antimicrobial peptides: pore formers or metabolic inhibitors in bacteria? *Nature Reviews Microbiology* **3**, 238-250. 10.1038/nrmicro1098

125. Lazzaro, B. P., Zasloff, M., and Rolff, J. (2020) Antimicrobial peptides: application informed by evolution. *Science* **368**, 1-8. 10.1126/science.aau5480

126. De Lucca, A. J., Bland, J. M., Jacks, T., J., Grimm, C., and Walsh, T. J. (1998) Fungicidal and binding properties of the natural peptides cecropin B and dermaseptin. *Medical Mycology* **36**, 291-298.,

127. Baxter, A. A., Richter, V., Lay, F. T., Poon, I. K., Adda, C. G., Veneer, P. K., Phan, T. K., Bleackley, M. R., Anderson, M. A., Kvansakul, M., and Hulett, M. D. (2015) The tomato defensin TPP3 binds phosphatidylinositol (4,5)-bisphosphate via a conserved dimeric cationic grip conformation to mediate cell lysis. *Molecular and Cell Biology* **35**, 1964-1978. 10.1128/MCB.00282-15

128. Cools, T. L., Struyfs, C., Drijfhout, J. W., Kucharikova, S., Lobo Romero, C., Van Dijck, P., Ramada, M. H. S., Bloch, C., Jr., Cammue, B. P. A., and Thevissen, K. (2017) A linear 19-mer plant defensin-derived peptide acts synergistically with caspofungin against *Candida albicans* biofilms. *Frontiers in Microbiology* **8**, 2051-2064. 10.3389/fmicb.2017.02051

129. Burman, R., Stromstedt, A. A., Malmsten, M., and Goransson, U. (2011) Cyclotide-membrane interactions: defining factors of membrane binding, depletion and disruption. *Biochimica et Biophysica Acta* **1808**, 2665-2673. 10.1016/j.bbamem.2011.07.004

130. Rittershaus, P. C., Kechichian, T. B., Allegood, J. C., Merrill Jr, A. H., Hennig, M., Luberto, C., and Del Poeta, M. (2006) Glucosylceramide synthase is an essential regulator of pathogenicity of *Cryptococcus neoformans*. *The Journal of Clinical Investigation* **116**, 1651-1659. 10.1172/JCI27890

131. Zhu, C., Wang, M., Wang, W., Ruan, R., Ma, H., Mao, C., and Li, H. (2014) Glucosylceramides are required for mycelial growth and full virulence in *Penicillium digitatum*. *Biochemical and Biophysical Research Communications* **455**, 165-171. 10.1016/j.bbrc.2014.10.142

132. Bender, C. L., Alarcon-Chaidez, F., and Gross, D. C. (1999) *Pseudomonas syringae* phytotoxins: mode of action, regulation, and biosynthesis by peptide and polyketide

synthetases. *Microbiology and Molecular Biology Reviews* **63**, 266-292. 10.1128/MMBR.63.2.266-292.1999

133. Kaulin, Y. A., Takemoto, J. Y., Schagina, L. V., Ostroumova, O. S., Wangspa, R., Teeter, J. H., and Brand, J. G. (2005) Sphingolipids influence the sensitivity of lipid bilayers to fungicide, syringomycin E. *Journal of Bioenergetics and Biomembranes* **37**, 339-348. 10.1007/s10863-005-8645-2
134. de Medeiros, L. N., Domitrovic, T., de Andrade, P. C., Faria, J., Bergter, E. B., Weissmuller, G., and Kurtenbach, E. (2014) Psd1 binding affinity toward fungal membrane components as assessed by SPR: the role of glucosylceramide in fungal recognition and entry. *Biopolymers* **102**, 456-464. 10.1002/bip.22570
135. Troskie, A. M., de Beer, A., Vosloo, J. A., Jacobs, K., and Rautenbach, M. (2014) Inhibition of agronomically relevant fungal phytopathogens by tyrocidines, cyclic antimicrobial peptides isolated from *Bacillus aneurinolyticus*. *Microbiology (Reading)* **160**, 2089-2101. 10.1099/mic.0.078840-0
136. Andres, M. T., Acosta-Zaldivar, M., and Fierro, J. F. (2016) Antifungal mechanism of action of lactoferrin: identification of H+-ATPase (P3A-Type) as a new apoptotic-cell membrane receptor. *Antimicrobial Agents and Chemotherapy* **60**, 4206-4216. 10.1128/AAC.03130-15
137. Perez-Rodriguez, A., Eraso, E., Quindos, G., and Mateo, E. (2022) Antimicrobial peptides with anti-*Candida* activity. *International Journal of Molecular Sciences* **23**, 1-27. 10.3390/ijms23169264
138. Lace, I., Cotroneo, E. R., Hesselbarth, N., and Simeth, N. A. (2022) Artificial peptides to induce membrane denaturation and disruption and modulate membrane composition and fusion. *Journal of Peptide Science* **29**, e3466-e3495. 10.1002/psc.3466
139. Deshayes, S., Morris, M., Heitz, F., and Divita, G. (2008) Delivery of proteins and nucleic acids using a non-covalent peptide-based strategy. *Advanced Drug Delivery Reviews* **60**, 537-547. 10.1016/j.addr.2007.09.005
140. Doherty, G. J., and McMahon, H. T. (2009) Mechanisms of endocytosis. *Annual Review of Biochemistry* **78**, 857-902. 10.1146/annurev.biochem.78.081307.110540
141. Eisfeld, K., Riffer, F., Mentges, J., and Schmitt, M. J. (2000) Endocytotic uptake and retrograde transport of a virally encoded killer toxin in yeast. *Molecular Microbiology* **37**, 926-940. 10.1046/j.1365-2958.2000.02063.x

142. Hayes, B. M. E., Bleackley, M. R., Anderson, M. A., and van der Weerden, N. L. (2018) The plant defensin NaD1 enters the cytoplasm of *Candida albicans* via endocytosis. *Journal of Fungi (Basel)* **4**, 1-15. 10.3390/jof4010020

143. Kumar, R., Chadha, S., Saraswat, D., Bajwa, J. S., Li, R. A., Conti, H. R., and Edgerton, M. (2011) Histatin 5 uptake by *Candida albicans* utilizes polyamine transporters Dur3 and Dur31 proteins. *Journal of Biological Chemistry* **286**, 43748-43758. 10.1074/jbc.M111.311175

144. Igarashi, K., and Kashiwagi, K. (1999) Polyamine transport in bacteria and yeast. *Biochemical Journal* **15**, 633-642.,

145. Dunkel, N., Hertlein, T., Franz, R., Reuss, O., Sasse, C., Schafer, T., Ohlsen, K., and Morschhauser, J. (2013) Roles of different peptide transporters in nutrient acquisition in *Candida albicans*. *Eukaryotic Cell* **12**, 520-528. 10.1128/EC.00008-13

146. Reuss, O., and Morschhauser, J. (2006) A family of oligopeptide transporters is required for growth of *Candida albicans* on proteins. *Molecular Microbiology* **60**, 795-812. 10.1111/j.1365-2958.2006.05136.x

147. Redza-Dutordoir, M., and Averill-Bates, D. A. (2016) Activation of apoptosis signalling pathways by reactive oxygen species. *Biochimica et Biophysica Acta* **1863**, 2977-2992. 10.1016/j.bbamcr.2016.09.012

148. Andres, M. T., Viejo-Diaz, M., and Fierro, J. F. (2008) Human lactoferrin induces apoptosis-like cell death in *Candida albicans*: critical role of K+-channel-mediated K+ efflux. *Antimicrobial Agents and Chemotherapy* **52**, 4081-4088. 10.1128/AAC.01597-07

149. Carmona-Gutierrez, D., Eisenberg, T., Buttner, S., Meisinger, C., Kroemer, G., and Madeo, F. (2010) Apoptosis in yeast: triggers, pathways, subroutines. *Cell Death and Differentiation* **17**, 763-773. 10.1038/cdd.2009.219

150. Soares, J. R., José Tenório de Melo, E., da Cunha, M., Fernandes, K. V. S., Taveira, G. B., da Silva Pereira, L., Pimenta, S., Trindade, F. G., Regente, M., Pinedo, M., de la Canal, L., Gomes, V. M., and de Oliveira Carvalho, A. (2017) Interaction between the plant ApDef1 defensin and *Saccharomyces cerevisiae* results in yeast death through a cell cycle- and caspase-dependent process occurring via uncontrolled oxidative stress. *Biochimica et Biophysica Acta (BBA) - General Subjects* **1861**, 3429-3443. 10.1016/j.bbagen.2016.09.005

151. Kinjo, T. G., and Schnetkamp, P. P. M. (2005) Ca^{2+} chemistry, storage and transport in biologic systems. In Voltage-Gated Calcium Channels., Zamponi GW, ed. Springer US, Boston, MA 1-11.

152. Yun, J., and Lee, D. G. (2016) Cecropin A-induced apoptosis is regulated by ion balance and glutathione antioxidant system in *Candida albicans*. *IUBMB Life* **68**, 652-662. 10.1002/iub.1527

153. Munoz, A., Chu, M., Marris, P. I., Sagaram, U. S., Kaur, J., Shah, D. M., and Read, N. D. (2014) Specific domains of plant defensins differentially disrupt colony initiation, cell fusion and calcium homeostasis in *Neurospora crassa*. *Molecular Microbiology* **92**, 1357-1374. 10.1111/mmi.12634

154. Carmona-Gutierrez, D., Bauer, M. A., Zimmermann, A., Aguilera, A., Austriaco, N., Ayscough, K., Balzan, R., Bar-Nun, S., Barrientos, A., Belenky, P., Blondel, M., Braun, R. J., Breitenbach, M., Burhans, W. C., Buttner, S., Cavalieri, D., Chang, M., Cooper, K. F., Corte-Real, M., Costa, V., Cullin, C., Dawes, I., Dengjel, J., Dickman, M. B., Eisenberg, T., Fahrenkrog, B., Fasel, N., Frohlich, K. U., Gargouri, A., Giannattasio, S., Goffrini, P., Gourlay, C. W., Grant, C. M., Greenwood, M. T., Guaragnella, N., Heger, T., Heinisch, J., Herker, E., Herrmann, J. M., Hofer, S., Jimenez-Ruiz, A., Jungwirth, H., Kainz, K., Kontoyiannis, D. P., Ludovico, P., Manon, S., Martegani, E., Mazzoni, C., Megeney, L. A., Meisinger, C., Nielsen, J., Nystrom, T., Osiewacz, H. D., Outeiro, T. F., Park, H. O., Pendl, T., Petranovic, D., Picot, S., Polcic, P., Powers, T., Ramsdale, M., Rinnerthaler, M., Rockenfeller, P., Ruckenstuhl, C., Schaffrath, R., Segovia, M., Severin, F. F., Sharon, A., Sigrist, S. J., Sommer-Ruck, C., Sousa, M. J., Thevelein, J. M., Thevissen, K., Titorenko, V., Toledano, M. B., Tuite, M., Vogtle, F. N., Westermann, B., Winderickx, J., Wissing, S., Wolfl, S., Zhang, Z. J., Zhao, R. Y., Zhou, B., Galluzzi, L., Kroemer, G., and, Madeo, F. (2018) Guidelines and recommendations on yeast cell death nomenclature. *Microbial Cell* **5**, 4-31. 10.15698/mic2018.01.607

155. Liu, Y., and Levine, B. (2015) Autosis and autophagic cell death: the dark side of autophagy. *Cell Death and Differentiation* **22**, 367-376. 10.1038/cdd.2014.143

156. Sampaio-Marques, B., Burhans, W. C., and Ludovico, P. (2019) Yeast at the forefront of research on ageing and age-related diseases. In Yeasts in biotechnology and human health: physiological genomic approaches., Sá-Correia I, ed. Springer International Publishing, Cham 217-242

157. Parisi, K., Doyle, S. R., Lee, E., Lowe, R. G. T., van der Weerden, N. L., Anderson, M. A., and Bleackley, M. R. (2019) Screening the *Saccharomyces cerevisiae* nonessential gene deletion library reveals diverse mechanisms of action for antifungal plant defensins. *Antimicrobial Agents and Chemotherapy* **63**, 1-17. 10.1128/AAC.01097-19.

158. Marr, A. K., Gooderham, W. J., and Hancock, R. E. W. (2006) Antibacterial peptides for therapeutic use: obstacles and realistic outlook. *Current Opinion in Pharmacology* **6**, 468-472. 10.1016/j.coph.2006.04.006

159. Mygind, P. H., Fischer, R. L., Schnorr, K. M., Hansen, M. T., Sonksen, C. P., Ludvigsen, S., Raventos, D., Buskov, S., Christensen, B., De Maria, L., Taboureau, O., Yaver, D., Elvig, S. G., Sorensen, M. V., Christensen, B. E., Kjaerulff, S., Frimoldt-Moller, N., Lehrer, R. I., Zasloff, M., and Kristensen, H. (2005) Plectasin is a peptide antibiotic with therapeutic potential from a saprophytic fungus. *Nature* **437**, 975-980 10.1038/nature04051

160. Vlieghe, P., Lisowski, V., Martinez, J., and Khrestchatisky, M. (2010) Synthetic therapeutic peptides: science and market. *Drug Discovery Today* **15**, 40-56. 10.1016/j.drudis.2009.10.009

161. Eckert, R. (2011) Road to clinical efficacy: challenges and novel strategies for antimicrobial peptide development. *Future Microbiology* **6**, 635-651. 10.2217/fmb.11.27

162. Mahlapuu, M., Hakansson, J., Ringstad, L., and Bjorn, C. (2016) Antimicrobial peptides: an emerging category of therapeutic agents. *Frontiers in Cell and Infection Microbiology* **6**, 194-209. 10.3389/fcimb.2016.00194

163. Haney, E. F., and Hancock, R. E. (2013) Peptide design for antimicrobial and immunomodulatory applications. *Biopolymers* **100**, 572-583. 10.1002/bip.22250

164. Thery, T., Shwaiki, L. N., O'Callaghan, Y. C., O'Brien, N. M., and Arendt, E. K. (2019) Antifungal activity of a *de novo* synthetic peptide and derivatives against fungal food contaminants. *Journal of Peptide Science* **25**, e3137-e3148. 10.1002/psc.3137

165. Rink, R., Arkema-Meter, A., Baudoin, I., Post, E., Kuipers, A., Nelemans, S. A., Akanbi, M. H., and Moll, G. N. (2010) To protect peptide pharmaceuticals against peptidases. *Journal of Pharmacological and Toxicological Methods* **61**, 210-218. 10.1016/j.vascn.2010.02.010

166. Brinckerhoff, L. H., Kalashnikov, V. V., Thompson, L. W., Yamshchikov, G. V., Pierce, R. A., Galavotti, H. S., Engelhard, V. H., and Slingluff, C. L. (1999) Terminal modifications inhibit proteolytic degradation of an immunogenic MART-127-35

peptide: implications for peptide vaccines. *International Journal of Cancer* **83**, 326-334. 10.1002/(sici)1097-0215(19991029)83:3<326::Aid-ijc7>3.0.Co;2-x

167. Akkam, Y. (2016) A review of antifungal peptides: basis to new era of antifungal drugs. *Jordan Journal of Pharmaceutical Sciences* **9**, 1-25.,
168. Li, P., and Roller, P. P. (2002) Cyclization strategies in peptide derived drug design. *Current Topics in Medicinal Chemistry* **2**, 325-341. 10.2174/1568026023394209
169. Malhaire, H., Gimel, J. C., Roger, E., Benoit, J. P., and Lagarce, F. (2016) How to design the surface of peptide-loaded nanoparticles for efficient oral bioavailability? *Advanced Drug Delivery Reviews* **106**, 320-336. 10.1016/j.addr.2016.03.011
170. Soman, N. R., Baldwin, S. L., Hu, G., Marsh, J. N., Lanza, G. M., Heuser, J. E., Arbeit, J. M., Wickline, S. A., and Schlesinger, P. H. (2009) Molecularly targeted nanocarriers deliver the cytolytic peptide melittin specifically to tumor cells in mice, reducing tumor growth. *Journal of Clinical Investigation* **119**, 2830-2842. 10.1172/JCI38842
171. Urban, P., Valle-Delgado, J. J., Moles, E., Marques, J., Diez, C., and Fernandez-Busquets, X. (2012) Nanotools for the delivery of antimicrobial peptides. *Current Drug Targets* **13**, 1158-1172. 10.2174/138945012802002302
172. Deshayes, C., Arafath, M. N., Apaire-Marchais, V., Roger, E. (2021) Drug delivery systems for the oral administration of antimicrobial peptides: promising tools to treat infectious diseases. *Frontiers in Medical Technology* **3**, 778645-778657. 10.3389/fmedt.2021.778645
173. Yu, H. Y., Tu, C. H., Yip, B. S., Chen, H. L., Cheng, H. T., Huang, K. C., Lo, H. J., and Cheng, J. W. (2011) Easy strategy to increase salt resistance of antimicrobial peptides. *Antimicrobial Agents and Chemotherapy* **55**, 4918-4921. 10.1128/AAC.00202-11
174. Bowdish, D. M. E., Davidson, D. J., Lau, Y. E., Lee, K., Scott, M. G, and Hancock, R. E. W. (2005) Impact of LL-37 on anti-infective immunity. *Journal of Leukocyte Biology* **77**, 451-459. 10.1189/jlb.0704380
175. Pasupuleti, M., Schmidtchen, A., Chalupka, A., Ringstad, L., and Malmsten, M. (2009) End-tagging of ultra-short antimicrobial peptides by W/F stretches to facilitate bacterial killing. *PLoS One* **4**, e5285-e5294. 10.1371/journal.pone.0005285
176. Pasupuleti, M., Chalupka, A., Morgelin, M., Schmidtchen, A., and Malmsten, M. (2009) Tryptophan end-tagging of antimicrobial peptides for increased potency against *Pseudomonas aeruginosa*. *Biochimica et Biophysica Acta* **1790**, 800-808. 10.1016/j.bbagen.2009.03.029

177. Schmidtchen, A., Ringstad, L., Kasetty, G., Mizuno, H., Rutland, M. W., and Malmsten, M. (2011) Membrane selectivity by W-tagging of antimicrobial peptides. *Biochimica et Biophysica Acta* **1808**, 1081-1091. 10.1016/j.bbamem.2010.12.020

178. Mercer, D. K., Robertson, J. C., Miller, L., Stewart, C. S., and O'Neil, D. A. (2020) NP213 (Novexatin(R)): a unique therapy candidate for onychomycosis with a differentiated safety and efficacy profile. *Medical Mycology* **58**, 1064-1072. 10.1093/mmy/myaa015

179. Fjell, C. D., Hiss, J. A., Hancock, R. E., and Schneider, G. (2011) Designing antimicrobial peptides: form follows function. *Nature Reviews Drug Discovery* **11**, 37-51. 10.1038/nrd3591

180. Yip, B. S., Chen, H. T.Cheng, H. T., Wu, J. M., and Cheng, J. W. (2009) Solution structure and model membrane interactions of P-113, a clinically active antimicrobial peptide derived from human saliva. *Journal of The Chinese Chemical Society* **56**, 961-966. 10.3390/molecules23040800

181. Felicio, M. R., Silva, O. N., Goncalves, S., Santos, N. C., and Franco, O. L. (2017) Peptides with dual antimicrobial and anticancer activities. *Frontiers in Chemistry* **5**, 5-13 10.3389/fchem.2017.00005

182. van der Weerden, N. L., Hayes, B., McKenna, J., Bleackley, M., McCorkelle, Weaver, S., Turner, R., Brown, M., Baker, M., Harvey, P., Craik, D., and Anderson, M. (2018) The plant defensin HXP124 has the potential to be a safe and effective topical treatment for onychomycosis. 20th ISHAM Congress. Amsterdam, Netherlands: The International Society for Human and Animal Mycology.

183. Stallmann, H. P., Faber, C., Bronckers, A. L., J. J. de Blieck-Hogervorst, J. M. A., Brouwer, C. P. J. M., van Amerongen, A. V., and Wuisman, P. I. (2005) Histatin and lactoferrin derived peptides: antimicrobial properties and effects on mammalian cells. *Peptides* **26**, 2355-2359 10.1016/j.peptides.2005.05.014

184. Velden, W. J., van Iersel, T. M., Blijlevens, N. M., and Donnelly, J. P. (2009) Safety and tolerability of the antimicrobial peptide human lactoferrin 1-11 (hLF1-11). *BMC Medicine* **7**, 44-51. 10.1186/1741-7015-7-44

185. Malan, M., Serem, J. C., Bester, M. J., Neitz, A. W. H., and Gaspar, A. R. M. (2016) Anti-inflammatory and anti-endotoxin properties of peptides derived from the carboxy-terminal region of a defensin from the tick *Ornithodoros savignyi*. *Journal of Peptide Science* **22**, 43-51. 10.1002/psc.2838

186. Strömstedt, A. A., Pasupuleti, M., Schmidtchen, A., and Malmsten, M. (2009) Oligotryptophan-tagged antimicrobial peptides and the role of the cationic sequence. *Biochimica et Biophysica Acta (BBA) - Biomembranes* **1788**, 1916-1923. 10.1016/j.bbamem.2009.06.001

Chapter 3: Characterisation of the structural properties and membrane interactions of Os-C and the tryptophan end-tagged analogue, Os-C(W_5)

3.1 Introduction

Molecular dynamics (MD) simulations can provide information about interactions between AMPs and membranes at the atomic level that is difficult to obtain using conventional experimental approaches (1). Over the last couple of decades, research on AMPs using MD simulations has increased due to the wealth of data that can be obtained. This data is especially valuable during the lead optimisation stage of rational drug design where changes can be made to enhance the efficacy or other properties of the peptide (2). Since AMPs tend to target the membrane, many simulations are focused on the dynamic interactions between peptides and a lipid bilayer. Binding of peptides to the membrane can affect the dynamics of a membrane which depends on the lipid composition of the membrane (3).

Using MD simulations, the forces exerted on each atom by other atoms within the system can be calculated. Over time, the forces on each atom can be determined which can be used to evaluate the position and velocity of each atom at a particular timepoint. This allows a trajectory describing the configuration of atoms within the system at each point of the simulated time interval can be created. Using the trajectory data, it is possible to determine the secondary structure adopted by the peptide when in contact with the membrane, how far the peptide inserts into the membrane, and interactions between peptides and the membrane (4).

Despite the advances in computational power and accessibility to MD simulation software, it should be noted that simulations do not represent all the possible configurations that a system can undergo since each configuration is a picture of the conformational space in which a dynamic system evolves. Consequently, the results of MD simulations should be confirmed *in vitro* using techniques such as patch clamp electrophysiology experiments, electron microscopy, nuclear magnetic resonance (NMR) spectroscopy, and circular dichroism (CD) spectroscopy (3).

Circular dichroism spectroscopy is an essential technique used to characterise the secondary structure of AMPs due to the unequal absorption of left-handed and right-handed circularly polarised light (5). From the absorption of light, data is generated and is used to create a

spectrum which contains elements that are associated with specific secondary structures (α-helix, β-sheet and disordered) depending on the peptide's environment. In aqueous solutions such as water or Tris buffer, most peptides adopt a disordered secondary structure. However, in the presence of a membrane mimicking environment such as sodium dodecyl sulfate (SDS) or phospholipid liposomes, peptides may adopt predominantly α-helical, β-sheet or disordered structures (6). Therefore, CD can be used to investigate how altering the primary sequence of an AMP can influence its secondary structure.

Prinsloo *et al*. found that Os-C had a predominantly disordered secondary structure in water and SDS (7) while Mbuayama *et al*. observed that Os-C induced minimal permeabilisation of *S. cerevisiae* liposomes (8). In this chapter, interactions between a lipid bilayer consisting of phospholipids commonly found in the membrane of *C. albicans* and the peptides Os-C and Os-C(W_5) were evaluated using MD simulations. Using the data from these simulations, the effect of tryptophan end-tagging was evaluated by comparing characteristics such as secondary structure, membrane insertion, peptide-membrane hydrogen bond interactions and peptide aggregation. Furthermore, CD was used to determine the effect of tryptophan end-tagging on the secondary structure of Os-C.

3.2 Materials and Methods

3.2.1 Peptides

Os-C, Os-C(W_5) and melittin (AMP control) were synthesised by GenScript (Piscataway, New Jersey, USA). The purity (>95%) and molecular mass of the peptides were determined by the vendor using reverse-phase high-performance liquid chromatography (**Appendix A**) and mass spectrometry (**Appendix B**), respectively. The peptide concentration was determined using the formula:

$$c = \frac{A_{280} \times df \times MW}{n_{Tyr}(\varepsilon_{Tyr}) + n_{Trp}(\varepsilon_{Trp})}$$

where c is the concentration in mg/mL, A_{280} is the absorbance at 280 nm, df is the dilution factor, MW is the molecular weight in mg/mmol, and $n_{Tyr/Trp}(\varepsilon_{Tyr}/\varepsilon_{Trp})$ is the number of tyrosine or tryptophan residues and their corresponding extinction coefficients (tyrosine = 1200 AU/mmol/mL; tryptophan = 5560 AU/mmol/mL). Peptide stocks were prepared in double distilled deionised water (dddH_2O) and aliquots were stored at -20°C.

3.2.2 Circular dichroism spectroscopy

The secondary structure of peptides was analysed using CD spectroscopy. Melittin (25 µM), Os-C (50 µM) and Os-C(W_5) (50 µM) were dissolved in 5 mM Tris (Sigma-Aldrich, St Louis, Missouri, USA) or 50 mM sodium dodecyl sulfate (SDS; Sigma-Aldrich, St Louis, Missouri, USA). Secondary structures were analysed using a Jasco J-1500 CD spectrophotometer (Jasco; Easton, Maryland, USA) and scans were carried out at 20°C over the 180 – 260 nm range with a path length of 0.2 cm, a scan speed of 100 nm/min, using a data pitch of 0.5 nm, and a bandwidth of 2 nm. High tension voltage values above 600 volts were excluded. Samples were scanned ten times and then corrected for solvent effects. Signals were converted to mean residue ellipticity ([θ]) using the following equation:

$$[\theta] = \frac{\theta}{10 \times c \times n \times l}$$

Where θ is the measured ellipticity in millidegrees, c is the concentration (M), n is the number of amino acids and l is the path length (cm).

3.2.3 Molecular dynamics simulations

Simulations were carried out using GROMACS (9). The CHARMM36m all-atom force-field was used in all simulations (10, 11) and the initial bilayer configuration was designed in a water box measuring 90 nm × 90 nm × 110 nm using CHARMM-GUI (12). Membranes contained 256 lipids, composed of 1-palmitoyl-2-oleoyl-*sn*-glycero-3-phosphocholine (POPC), 1-palmitoyl-2-oleoyl-*sn*-glycero-3-phosphoethanolamine (POPE), 1-palmitoyl-2-oleoyl-*sn*-glycero-3-phospho-L-serine (POPS), and 1-palmitoyl-2-oleoyl-*sn*-glycero-3-phosphoinositol (POPI) and ergosterol (in a 59:21:3:4:13 ratio) to reflect the composition of a *C. albicans* membrane (13, 14).

Peptides were designed using Avogadro software and then the starting structures were obtained by running a simulation of the peptides in water for 1 ns. To investigate the collective behaviour of these AMPs, three peptides were inserted 9.7 Å above the lipid bilayer in random positions and orientations at least 5 Å apart from each other to identify possible peptide-peptide interactions. The system was solvated with TIP3P water and neutralised by sodium and chloride ions. Energy minimisation was carried out using the steepest descent algorithm until the maximum force was less than 1000 kJ/mL/nm. Equilibration was run using the NVT ensemble for 250 ps with a target temperature of 310 K and then the NPT ensemble for 1625 ps with a target temperature and pressure of 310 K and 1 bar, respectively, with position restraints on the peptides at a temperature of 310 K and a pressure of 1 bar. Production simulations were run for 1 µs using a semi-isotropic NPT ensemble using 2 fs timesteps. All production simulations were performed at a temperature of 310 K which was controlled by a Nose-Hoover thermostat and a pressure of 1 bar, which was controlled by a Parrinello-Rahman barostat.

The conformation of the peptides was quantified by measuring torsion angles which are circular quantities, and the circular mean of psi or phi angles was calculated as follows:

$$\bar{\psi} = \text{atan2}\left(\frac{1}{n}\sum_{j=1}^{n}\sin\psi_j, \frac{1}{n}\sum_{j=1}^{n}\cos\psi_j\right)$$

Circular variance is calculated as the spread of angles across all peptides and timesteps for each residue and was determined using the equation:

$$Var(\psi) = 1 - R_{av}$$

With R being given by:

$$R^2 = \left(\sum_{i=1}^{n} \cos \psi_i\right)^2 + \left(\sum_{i=1}^{n} \sin \psi_i\right)^2$$

The average psi and phi dihedral angles were used to create a Ramachandran contour plot with contours representing all the dihedral angles for the first and last 20 ns of the simulation.

Hydrogen bond analysis measured the number of hydrogen bonds formed between all hydrogen bond donors and acceptors between each residue and membrane lipids. The distance and angle cutoff values for identifying hydrogen bonds were 3 Å and 150°, respectively. Peptide insertion into the lipid bilayer was determined by *z*-position analysis which measured the *z*-position of the central carbon atom of each residue relative to the average *z*-position of the phosphate group plane in the upper leaflet of the lipid bilayer. A negative value indicated insertion of a residue into the membrane. Peptide aggregation was evaluated by a cluster analysis which measured the number of peptide oligomers formed during the simulation and an aggregation matrix which investigated interactions between individual residues. If the peptides were within 6 Å of each other, they were considered to be in the same oligomer.

3.3 Results and Discussion

3.3.1 Physicochemical properties of Os-C and Os-C(W_5)

The physiochemical characteristics of the peptides used in this study are presented in **Table 3.1**. Melittin (control peptide) is a cationic and amphipathic peptide found in honeybee venom. This peptide has a highly hydrophobic region with a stretch of hydrophilic residues at the C-terminus. The high hydrophobic content of melittin (**Table 3.1**) makes it a cytolytic peptide that targets bacterial and eukaryotic cells with little selectivity (15).

Os-C and Os-C(W_5) have the same cationic net charge of 6 and a pI of 10.8 (**Table 3.1**). One approach to improve peptide-mediated adsorption, membrane rupture and antimicrobial activity is to increase the charge of the peptide. However, this effect is neutralised by electrostatic screening in conditions of high ionic strength which inactivates highly charged and hydrophilic peptides (16). An alternative approach is to increase the hydrophobicity of peptides which can overcome sensitivity in these conditions. Adding five tryptophan residues at the C-terminus increases the hydrophobicity of Os-C from 15.8% to 33.3% (**Table 3.1**). Several quantitative structure-activity relationship studies have shown that hydrophobicity is crucial for the antimicrobial effect but should be tuned carefully to enhance AMP potency without losing selectivity (17-19).

Table 3.1: Physicochemical properties of melittin, Os-C and Os-C(W_5).

Peptide	Sequence	Molecular weight[a] (g/mol)	Length (a.a.)	Charge[a]	pI[a]	Hydrophobicity[b] (%)
Melittin	GIGAVLKVLTTGLPALISWIKRKRQQ-NH_2	2846.48	26	+5	12.6	50
Os-C	KGIRGYKGGYKGAFKQTKY	2150.49	19	+6	10.8	15.8
Os-C(W_5)	KGIRGYKGGYKGAFKQTKY**WWWWW**	3081.55	24	+6	10.8	33.3

[a] Calculated using GenScript peptide molecular weight calculator. https://www.genscript.com/tools/peptide-molecular-weight-calculator
a.a. = amino acids
[b] Calculated using peptide 2.0. https://www.peptide2.com/N_peptide_hydrophobicity_hydrophilicity.php

Sequence-specific point substitutions where individual residues are replaced by a hydrophobic residue are commonly used to enhance the activity of AMPs, but this approach has several drawbacks. First, the analogue may be less active than the original peptide. Second, sequence-specific point mutations may affect the chemical and enzymatic stability of AMPs. Finally, point substitutions may negatively affect non-membrane targeting effects such as coagulation, complement production and cytokine production (16). On the other hand, hydrophobic end-tagging does not involve the removal of residues in the original AMP sequence. Therefore, the

chemical and enzymatic properties of the peptide are retained. End-tagging also means that high but selective AMP activity can be achieved (20). In the context of antifungal activity, the bulky and polarisable nature of AMPs means that they are sensitive to the identity of sterols present in eukaryotic cell membranes. Schmidtchen *et al*. demonstrated that the peptide GRR10W4N was active against *C. albicans* and *C. parapsilosis*, and was non-haemolytic and non-toxic towards epithelial cells (21). One study has shown that Os-C(W_5) is not haemolytic towards human erythrocytes (R. Chirombo, MSc dissertation, 2023) indicating potential for systemic application.

3.3.2 Steady state secondary structure analysis

Antimicrobial peptides are known to adopt different secondary structures when in solution or in contact with a membrane. Therefore, CD spectroscopy was performed to compare the secondary structures of Os-C and Os-C(W_5) in Tris buffer and in SDS which creates a membrane-mimicking environment. Spectra of melittin, Os-C and Os-C(W_5) are shown in **Figure 3.1**.

For melittin, a disordered structure is observed in Tris buffer while a predominantly α-helical structure is adopted in the presence of SDS (**Figure 3.1A**). In Tris buffer, Os-C adopts a predominantly disordered structure (**Figure 3.1B**). The CD spectra of Os-C in Tris buffer and SDS are similar to those obtained by Prinsloo *et al.* where a disordered secondary structure was observed in water and a change in the secondary structure was observed in the presence of SDS (7).

For Os-C(W_5), the spectrum generated in Tris buffer has a negative band at 200 nm and 224 nm (**Figure 3.1C**). In the presence of SDS, the negative bands are less prominent with the second band shifting from 224 nm to 226.5 nm and the mean residue ellipticity increasing by 64% (**Figure 3.1C**). Strömstedt *et al.* observed similar changes in the spectra of the C-terminus tryptophan end-tagged peptides KNK7W5, K7W5 and R7W5 which displayed identical CD spectra in Tris buffer with a negative band observed at 225 nm. In the presence of *E. coli* liposomes, the negative bands of the peptides K7W5 and R7W5 shifted from 225 nm to 229 nm (22). Schmidtchen *et al*. observed a similar effect where a negative band was observed between 220 nm and 230 nm for GRR10W4N (GRRPRPRPRPWWWW-NH_2) in Tris buffer (21).

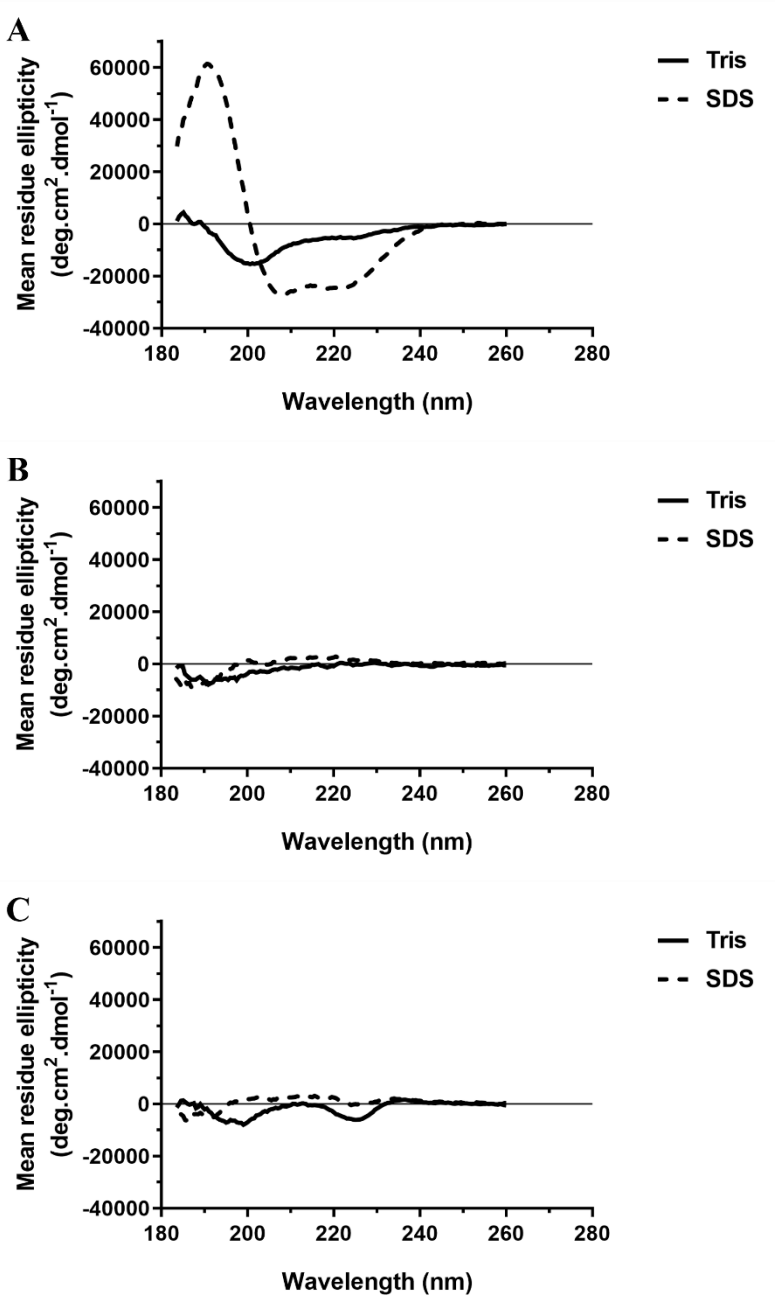

Figure 3.1: Circular dichroism spectra of (A) melittin, (B) Os-C and (C) Os-C(W_5). CD spectra were determined in either Tris buffer or sodium dodecyl sulfate. Mean residue ellipticity values of melittin, Os-C, and Os-C(W_5) were determined between 180 and 260 nm.

Clustering of tryptophan residues in the sequence of Os-C(W_5) may hinder the accurate determination of the secondary structure (23). Therefore, the CD spectra of melittin, Os-C and Os-C(W_5) were analysed using K2D3, an online secondary structure estimation tool (24). Melittin adopts a predominantly α-helical secondary structure while Os-C and Os-C(W_5) are predominantly disordered with Os-C(W_5) having 13.5% more β-strand content than Os-C (**Table 3.2**). Prinsloo *et al*. analysed the spectra of Os-C using PSIPRED, a secondary structure

prediction tool. In that analysis, the authors observed a β-strand content of 21% (7), which is similar to the β-strand content of 19.3%.

Table 3.2: Secondary structure analysis of melittin, Os-C and Os-C(W_5) in sodium dodecyl sulfate.

Peptide	Secondary structure constituent (%)		
	α-helix	β-strand	Disordered
Melittin	95.2	0	4.8
Os-C	0	19.3	81.7
Os-C(W_5)	0.6	32.8	66.6

The presence of tryptophan residues in peptide sequences complicates the assignment of a particular secondary structure to Os-C(W_5) in Tris buffer and SDS. However, differences in the respective CD spectra of Os-C and Os-C(W_5) indicate that interactions between the tryptophan end-tag and the template sequence fundamentally alter the environment around the indole side chains and subsequently change the CD spectra. Previous work demonstrated that amino acids with aromatic side chains (phenylalanine, tryptophan and tyrosine) have large enough electric or magnetic dipole transition moments that can make significant contributions to CD spectra (25). Overall, tryptophan end-tagging induces changes in the CD spectrum in Tris buffer and SDS.

3.3.3 Effect of tryptophan end-tagging on peptide secondary structure

Molecular dynamics simulations showed changes to the secondary structure of Os-C following tryptophan end-tagging. Ramachandran plots indicate that some Os-C residues had a high-density contour in the type II β-turn region (phi = -75°, psi = +150°) (**Figure 3.2A**). This observation is further confirmed by the snapshot of Os-C at the end of the simulation where the peptides have disordered regions along with β-turn regions (**Figure 3.3A**).

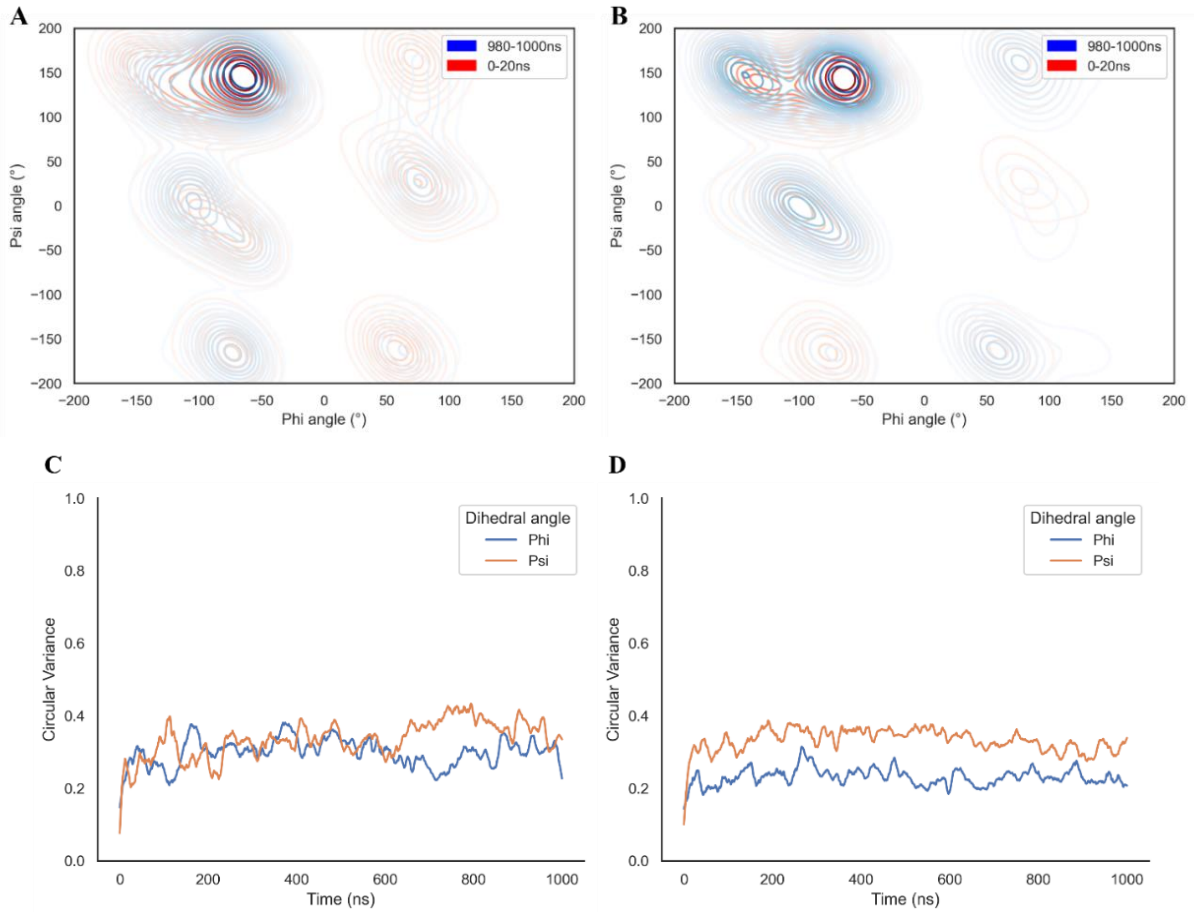

Figure 3.2: Secondary structure analysis of (A and C) Os-C and (B and D) Os-C(W_5). (A and B) Ramachandran contour plots were constructed for the first and last 20 ns of the simulation. (C and D) Circular variance of psi and phi angles for individual peptide residues were averaged for three peptides and plotted as a function of time.

Os-C(W_5) has contours in the β-turn and polyproline II regions along with a contour in the β-sheet region (phi = -139°, psi = +135°) (**Figure 3.2B**). A snapshot of the simulation at 1 μs confirms that tryptophan end-tagging has an effect on the secondary structure as Os-C(W_5) had β-turn and disordered regions along with short β-bridge regions (**Figure 3.3B**) which are short fragments that have similar binding patterns to β-sheet structures (26). The presence of the β-sheet region in the Ramachandran plot of Os-C(W_5) is supported by the K2D3 secondary structure estimation which showed increased β-strand content (**Table 3.2**) indicating that tryptophan end tagging leads to changes in peptide conformation.

The circular variance of Os-C and Os-C(W_5) was measured throughout the simulation. Circular variance is a measure of the conformational flexibility of a peptide that ranges from 0 to 1 with a low value indicating low conformational flexibility and vice versa. Similarities in the circular variance of Os-C and Os-C(W_5) reveal that tryptophan end-tagging does not alter the conformational flexibility of Os-C (**Figures 3.2C and 3.2D**).

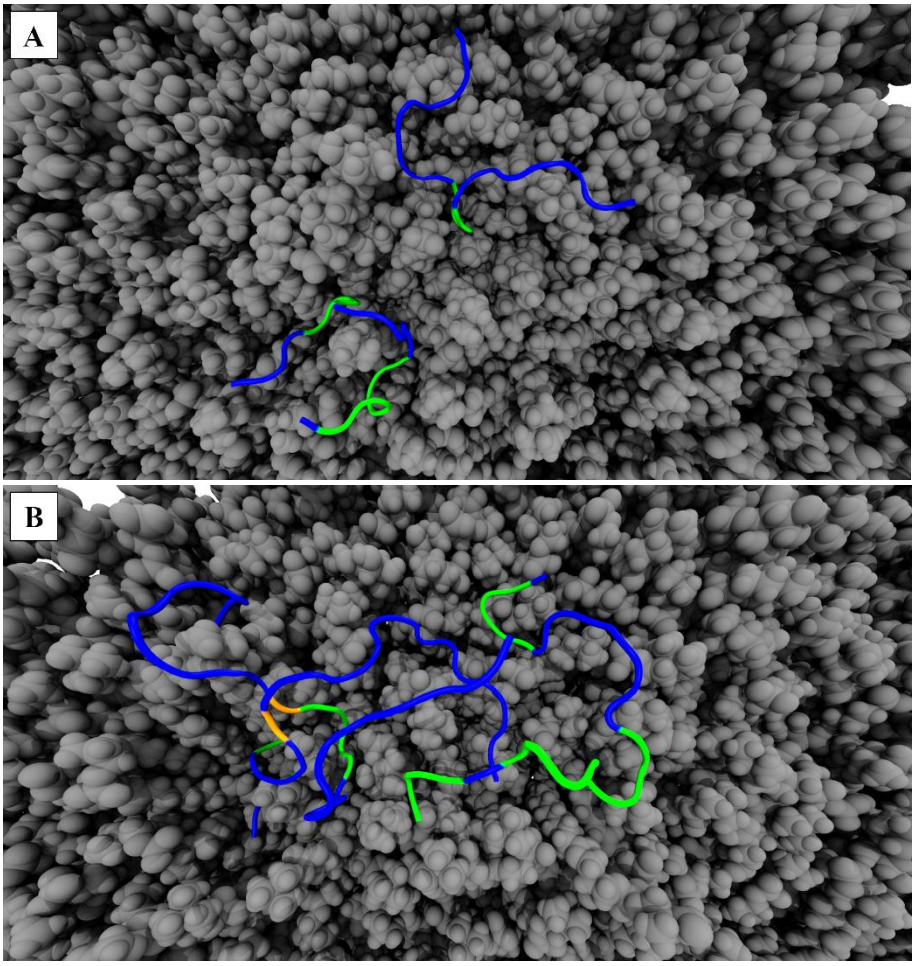

Figure 3.3: Secondary structures of (A) Os-C and (B) Os-C(W_5) at 1 µs. β-bridge regions are shown in orange, β-turn regions are shown in green and disordered regions are shown in blue. Images were created using VMD (University of Illinois Urbana-Champaign).

3.3.4 Effect of tryptophan end-tagging on peptide-membrane interactions and peptide aggregation

Molecular dynamics simulations were also used to characterise hydrogen bond interactions of Os-C and Os-C(W_5) with the model *C. albicans* membrane. For Os-C, hydrogen bonding contributions are seen for Lys1, Arg4, Lys7 and Lys11 with some contributions from Tyr6, Tyr10 and Lys15 (**Figure 3.4A**).

For Os-C(W_5), there are more contributions by Lys1, Arg4 and Lys18 during the second half of the simulation and some hydrogen bonding by Trp24 is observed. Reduced hydrogen bond contributions from Tyr6, Lys7 and Gln16 are also present (**Figure 3.4B**). Tryptophan residues do not show many hydrogen bond contributions with Trp24 interacting with the membrane at approximately 250 ns and 700 ns (**Figure 3.4B**). Reduced interactions by other residues can be attributed to the presence of tryptophan residues which enhanced peptide aggregation.

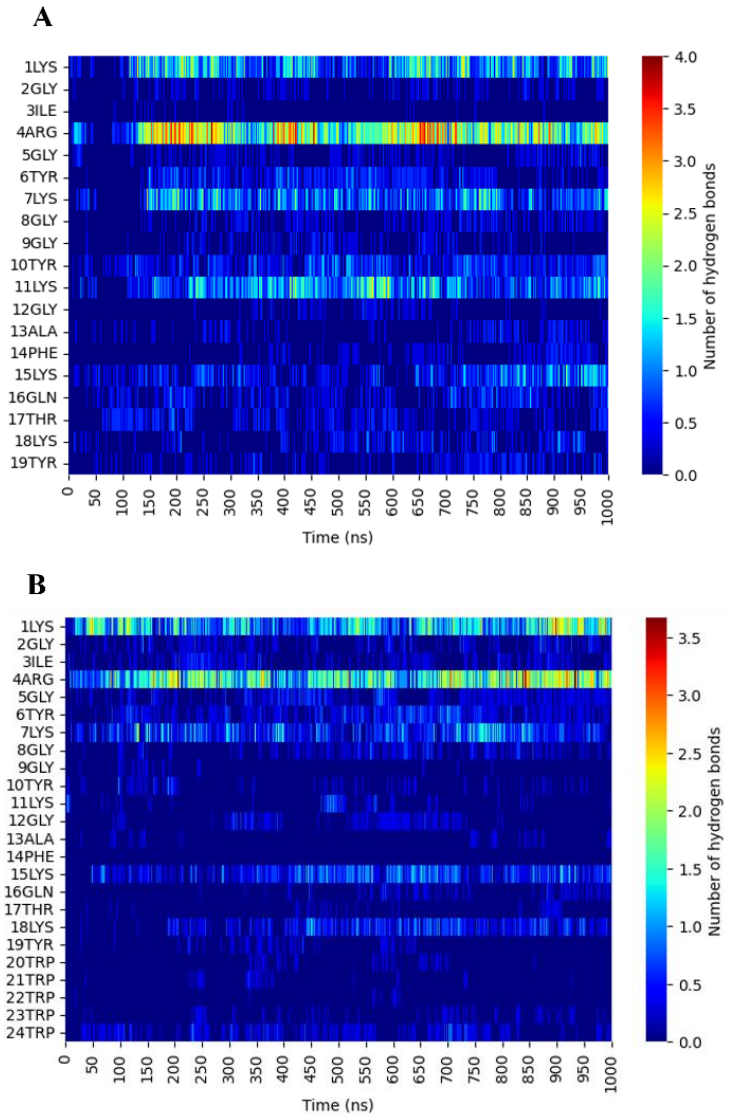

Figure 3.4: Hydrogen bonding between (A) Os-C and (B) Os-C(W_5) and the model membrane. Peptide-lipid hydrogen bonds are shown as a function of time for three peptides. Colour scales on the right-hand side of each figure differ slightly.

Tryptophan forms electrostatic, dipolar, hydrophobic and hydrogen bond interactions with lipid headgroups and other molecules within the environment. The NH group in the indole side chain can serve as a hydrogen bond donor while the aromatic ring acts as a hydrogen bond acceptor (27).

Previous research showed that tryptophan residues prefer to form hydrogen bond interactions with lipid carbonyl groups, especially with the lipids POPC and POPE (28). Therefore, the hydrogen bond contributions at approximately 250 ns and 700 ns could be between Trp24 and one of these lipids. Overall, tryptophan end-tagging does not lead to increased hydrogen bond interactions.

Peptide insertion was measured by determining the depth of insertion of the central carbon atom of each residue. For both peptides, insertion starts at approximately 100 ns and is initiated by residues at the N-terminus. Os-C residues interact with the membrane up to a depth of approximately 0.25 nm up to Phe14 and no insertion is observed from Lys15 to Tyr19 (**Figure 3.5A**). By the end of the simulation, Phe14 is approximately 0.25 nm below the upper leaflet.

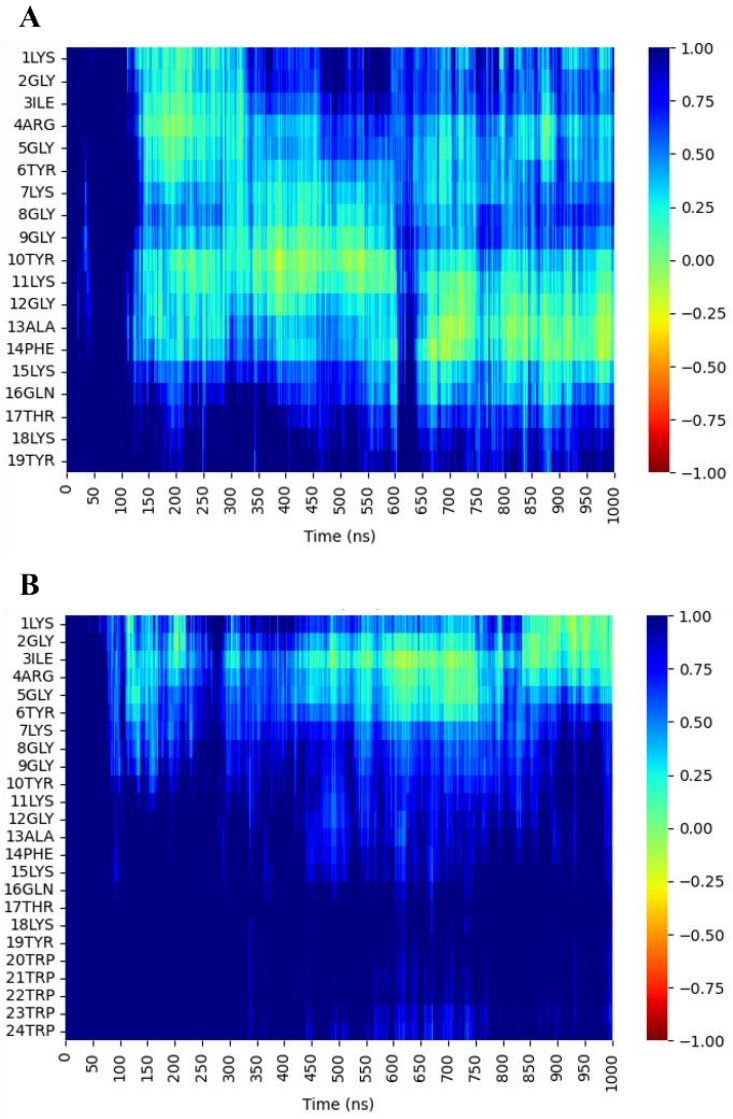

Figure 3.5: Insertion of (A) Os-C and (B) Os-C(W_5) into a model *C. albicans* membrane. The depth of insertion (in nanometres) of the central carbon atom of each residue is calculated and averaged for all three peptides, relative to the phosphate group plane in the upper leaflet. Positive and negative values indicate the peptides are above or below the phosphate group of the upper leaflet of the membrane, respectively.

Snapshots of the simulation at different time points confirm what is seen in **Figure 3.5A**. For Os-C, Ile3 and Tyr6 insert below the phospholipid layer after 250 ns (**Figure 3.6A**). After 500 ns, Tyr10 and Phe14 are inserted below the upper leaflet while Tyr6 is in the same plane as the upper leaflet (**Figure 3.6B**). Minimal insertion is seen after 750 ns where Tyr10 inserts slightly

below the plane of the upper leaflet (**Figure 3.6C**). At 1 μs, only Tyr10 inserts below the upper leaflet and Phe14 is in the same plane as the upper leaflet (**Figure 3.6D**).

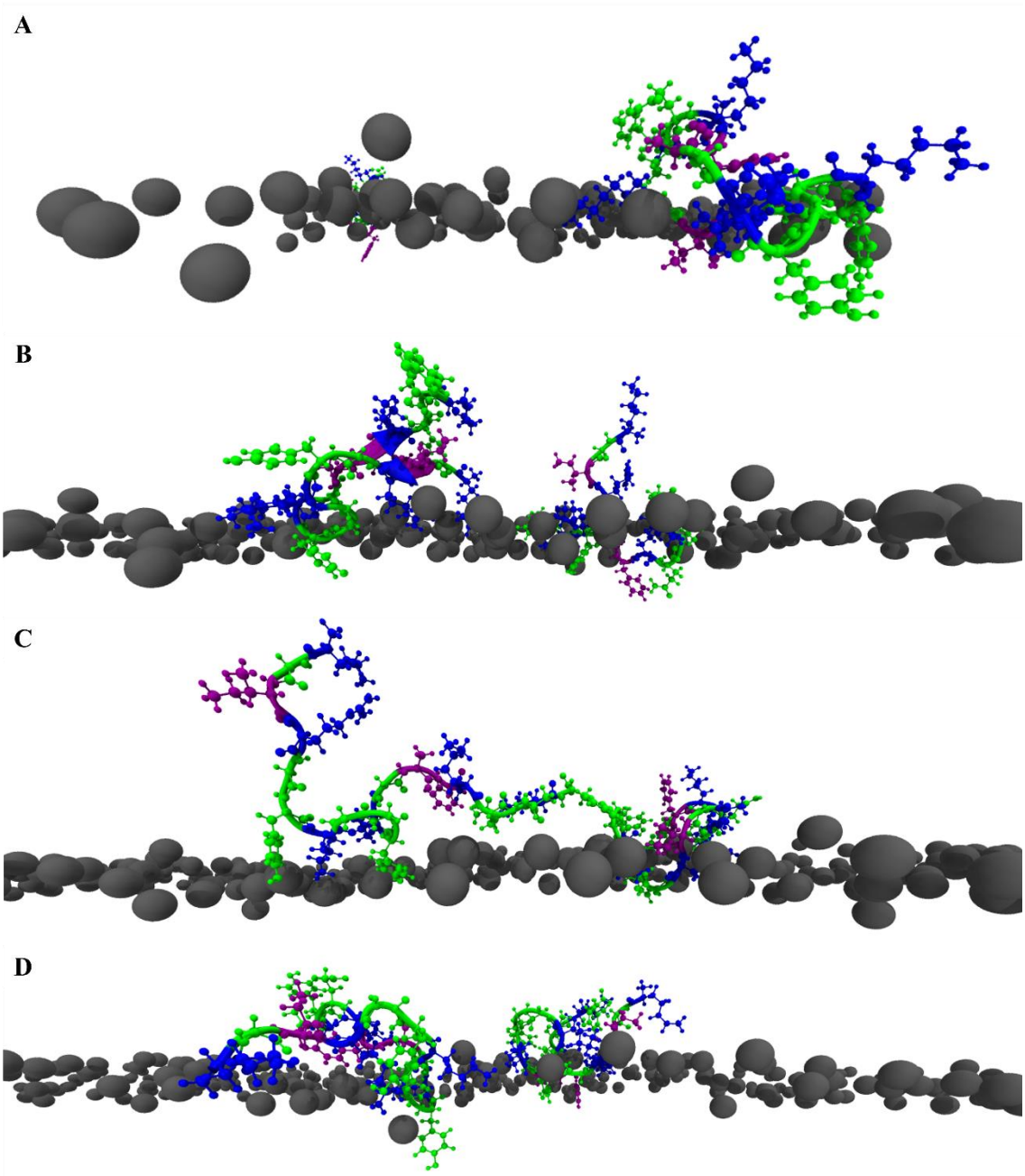

Figure 3.6: Insertion of Os-C into the lipid bilayer at (A) 250 ns (B) 500 ns (C)750 ns, and (D) 1 μs. Basic residues are shown in blue, nonpolar residues are shown in purple, polar residues are shown in green and grey spheres represent the phosphorus atom in the phosphate head group of the lipids in the upper leaflet of the bilayer. Images were created using VMD (University of Illinois Urbana-Champaign).

Os-C(W_5) inserts into the bilayer with a maximum of six residues (Lys1 to Tyr6) inserting approximately 0.25 nm below the upper leaflet and only Lys1, Gly2, Ile3 and Arg4 insert below the upper leaflet at the end of the simulation (**Figure 3.5B**). None of the tryptophan residues

insert into the membrane but are located between 0.5 nm and 1 nm above the bilayer during the simulation.

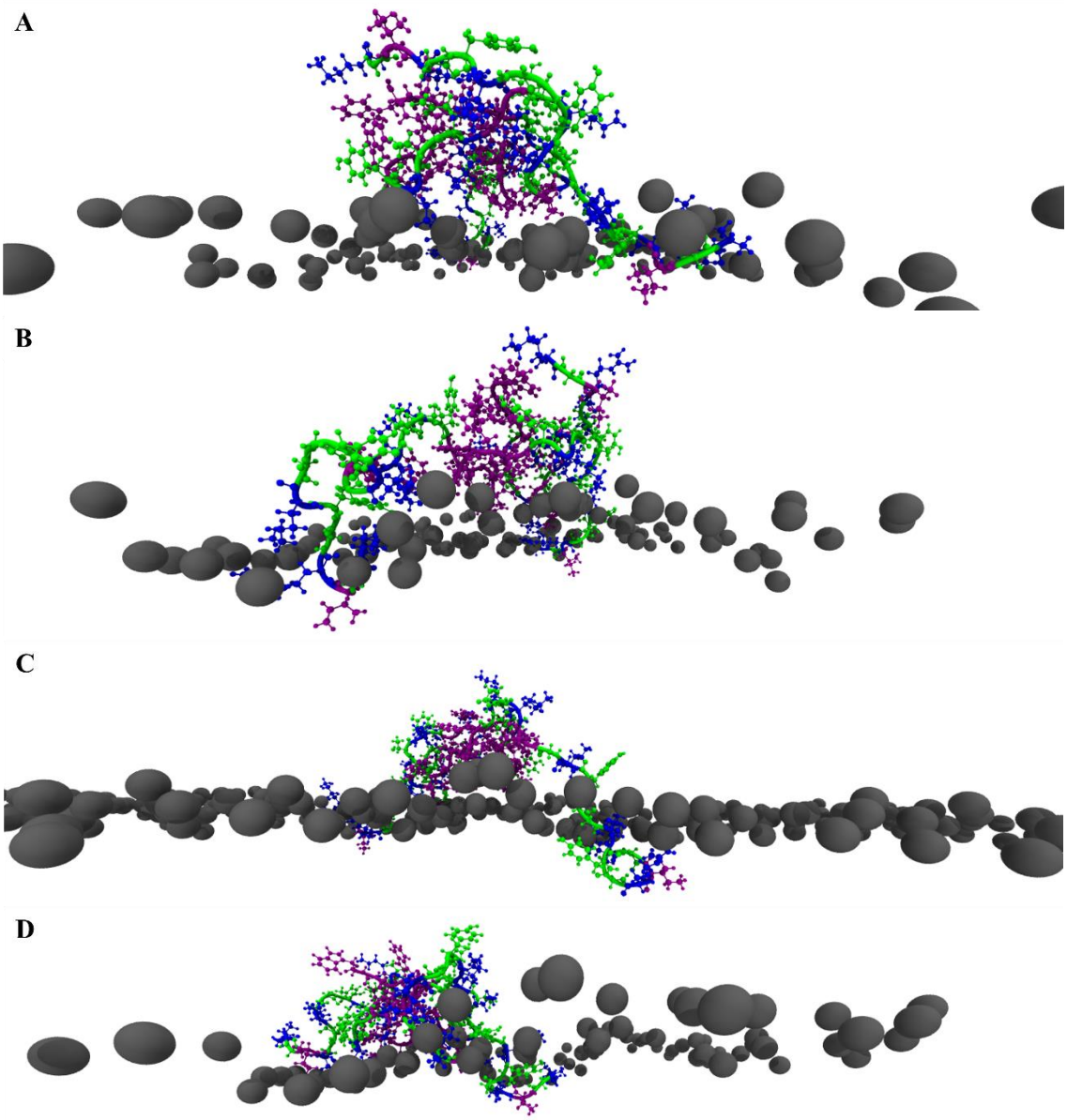

Figure 3.7: Insertion of Os-C(W_5) into the lipid bilayer at (A) 250 ns (B) 500 ns (C)750 ns, and (D) 1 µs. Basic residues are shown in blue, nonpolar residues are shown in purple, polar residues are shown in green and grey spheres represent the phosphorus atom in the phosphate head group of the lipids in the upper leaflet of the bilayer. Images were created using VMD (University of Illinois Urbana-Champaign).

Snapshots of the simulation at various time points reveal that Lys1, Gly2, Arg4 and Gly5 are in the same plane as the upper leaflet while minimal insertion is observed for Ile3 (**Figure 3.7A**) which is the only residue below the upper leaflet after 500 ns (**Figure 3.7B**). Insertion up to Tyr6 is observed after 750 ns (**Figure 3.7C**). After 1 µs, Ile3 is still below the upper leaflet along with Gly2 and Arg3 while Lys1 is in the same plane as the upper leaflet. By the

end of the simulation, only one of the peptides has residues below the plane of the upper leaflet while most residues are above the upper leaflet (**Figure 3.7D**).

Manzo *et al*. observed that the initial insertion of temporin B and pleurocidin into model Gram-negative and Gram-positive bacterial membranes proceeded via the N-terminus (29, 30). Limited peptide insertion could be due to the electrostatic interactions between lysine residues and the anionic lipid headgroups. When the frog peptide temporin B (LLPIVGNLLKSLL) was modified by adding two lysine residues to its N-terminus to form temporin B KKG6A (KKLLPIVANLLKSLL), insertion of temporin B KKG6A into Gram-positive bilayers was restricted to the lysine residues only whereas deeper insertion by temporin B was achieved up to Gly6 (29). Therefore, it is likely that electrostatic interactions between positively charged side chains and anionic lipid headgroups could hinder further insertion of peptides into the membrane.

Insertion of the large and bulky indole sidechain of tryptophan into lipid bilayers is an energetically unfavourable process since the presence of the indole side chain interferes with more favourable and cohesive hydrophobic interactions of the lipid acyl chains. Therefore, the interfacial region of lipid bilayers provides a more favourable environment for tryptophan (31). It is also possible that tryptophan residues favour aggregation rather than inserting into the membrane (32). Hence, the effect of tryptophan end-tagging on aggregation was investigated.

Self-association between peptides is critical and may either promote or hinder their activity (33). Aggregate formation by Os-C and Os-C(W_5) is shown in **Figure 3.8**. Os-C forms transient aggregates but reverts to monomers for the majority of the simulation (**Figure 3.8A**). Since Os-C does not form an aggregate at the end of the simulation, an aggregation matrix was created from interactions at the 850 ns time point. Minimal contacts between Os-C peptides are mediated by Lys11 and Phe14 (**Figure 3.8B**). A snapshot of the simulation shows that Os-C residues do not form close contacts with one dimer formed at 850 ns showing Tyr19 (green) and Lys7 (blue) in close contact (**Figure 3.9A, yellow oval**).

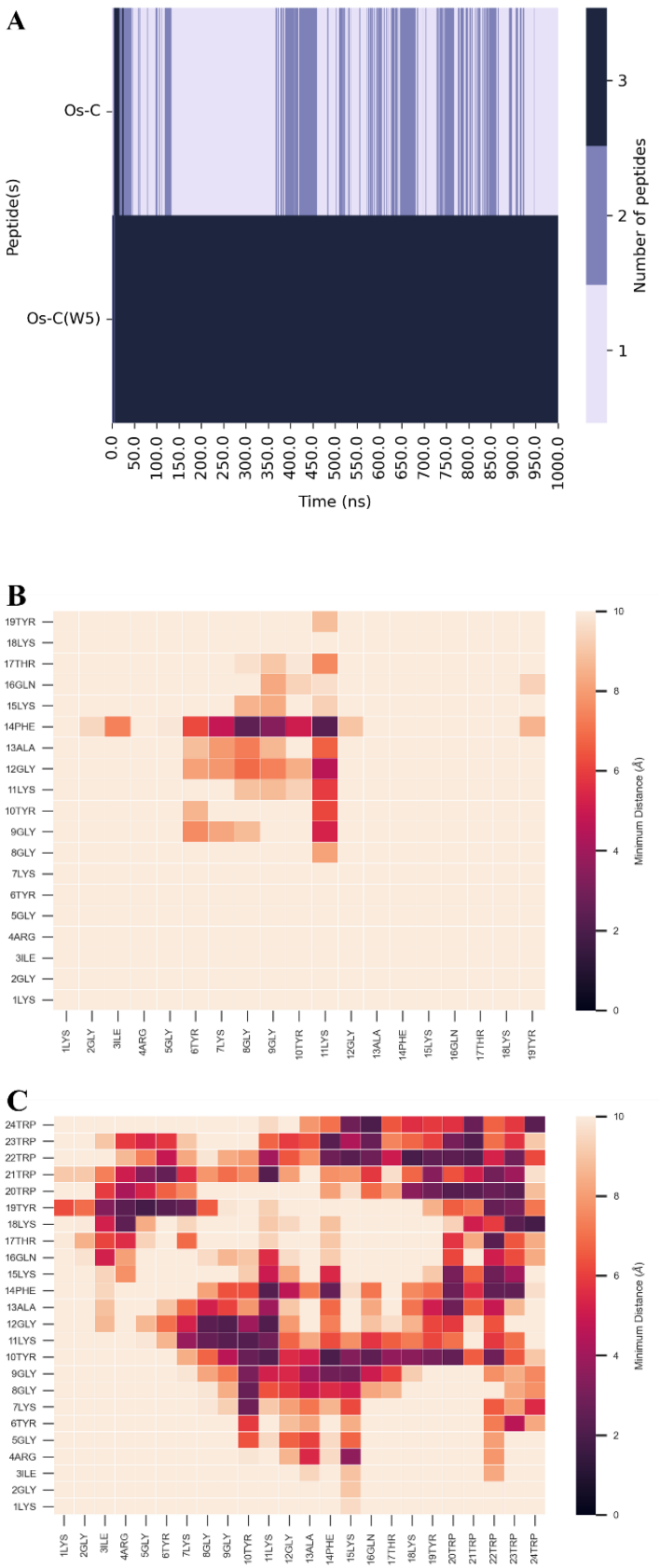

Figure 3.8: Contact between peptide residues. (A) The formation of peptide oligomers was recorded for the duration of the simulation. Aggregation matrix shows distances between (B) Os-C and (C) Os-C(W_5) residues.

Tryptophan end-tagging leads to the formation of a stable trimer throughout the simulation (**Figure 3.8A**) and increased contact between residues. Interactions between the head (Lys1 to Lys7) and tail regions (Tyr19 to Trp24) and between tryptophan residues are present following end-tagging (**Figure 3.8C**). A snapshot of aggregation after 1 µs indicates that tryptophan residues are responsible for greater peptide aggregation (**Figure 3.9B**). Head-to-tail interactions do not affect peptide-lipid hydrogen bonds mediated by Lys1 and Arg4 (**Figure 3.4B**) and membrane insertion (**Figure 3.5B**) of the head region. However, more interactions are mediated by residues 10 – 14 (**Figure 3.8C**) which insert into the membrane in the absence of the end-tag (**Figure 3.5A**). In the presence of the tryptophan end-tag, these residues do not insert into the membrane (**Figure 3.5B**) and Lys11 has a reduced hydrogen bond contribution (**Figure 3.4B**). These results show that tryptophan end-tagging enhances peptide aggregation which inhibits membrane insertion and peptide-lipid hydrogen bonding.

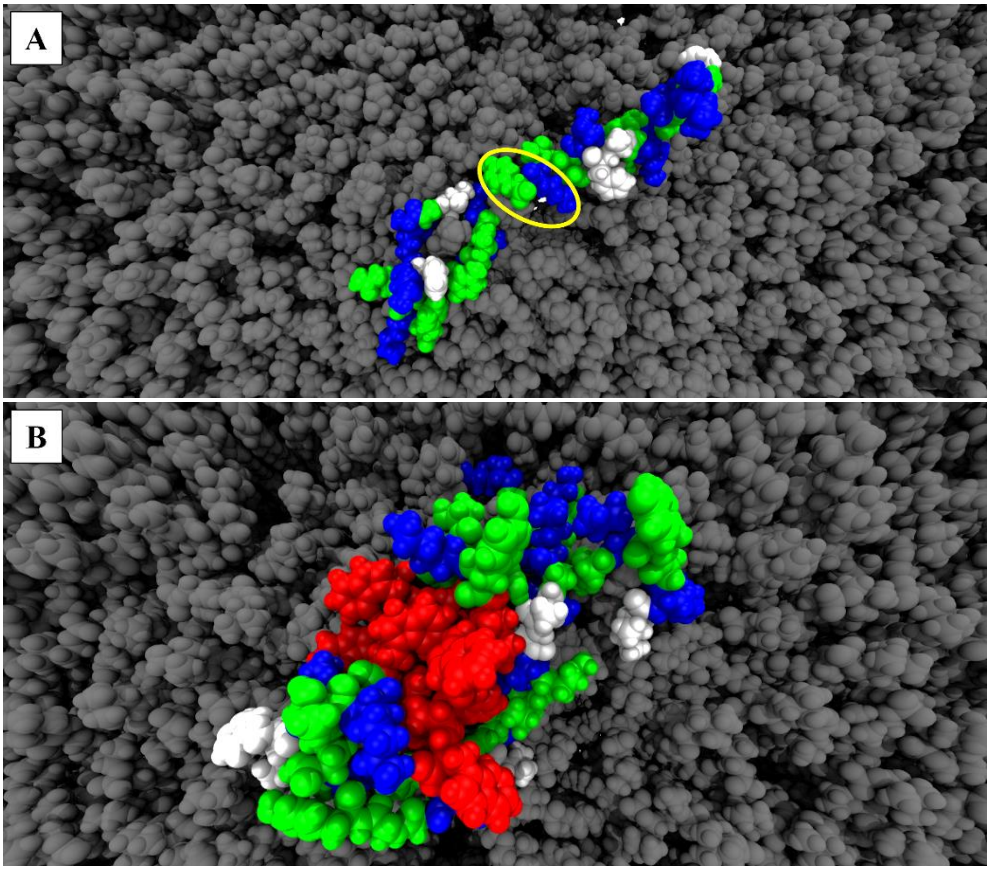

Figure 3.9: Aggregation of (A) Os-C at 850 ns and (B and C) Os-C(W_5) at 1 µs. Basic residues are shown in blue, nonpolar residues are shown in white, and polar residues are shown in green. Aggregation caused by tryptophan residues is shown in red. The yellow oval highlights the interaction between Tyr19 (green) and Lys7 (blue). Images were created using VMD (University of Illinois Urbana-Champaign).

In the present study, the addition of tryptophan residues results in stronger contacts between peptides, especially at the C-terminus. A similar observation was made by Zai *et al*. who

investigated the effect of modifying the frog peptide temporin-PF (FLPLIAGLFGKIF-NH_2) by removing Phe1 and replacing Phe9 and Phe13 with L- or D-enantiomers of tryptophan. Simulations indicated that closer contacts were observed between tryptophan residues at the C-terminus. Furthermore, TPF and its analogues formed dimers within 20 ns and one of the tryptophan containing analogues formed a stable tetramer (32).

Greater aggregation may lead to decreased antimicrobial activity since inter-peptide interactions may prevent attachment to the cell membrane and render the peptide inactive (33). However, aggregation is crucial for membrane permeabilisation, disruption and translocation (34). Peptide aggregation may enhance peptide activity by ensuring that a high local concentration of peptide is available on the membrane surface before pore formation (33). Simulations of melittin in a zwitterionic bilayer by Sengupta *et al*. noted that melittin-induced pore formation did not take place unless a cluster of at least three peptides was present (35). In the case of membrane translocation, the peptides can aggregate before or during adsorption to the membrane surface. If the peptide is hydrophobic enough, it can cross the bilayer without inducing leakage and cell death (35).

Interactions between tryptophan and other aromatic amino acids such as tyrosine, phenylalanine and histidine are established by π-π stacking interactions between the respective side chains (36). In this study, several interactions between tyrosine and other aromatic residues were observed. Contact between tryptophan and residues with positively charged side chains of lysine and arginine residues tends to occur via cation-π interactions due to the π-conjugated electron cloud of the indole side chain that confers an apparent localised negative charge to the aromatic side chain (37). Tryptophan-arginine interactions are more favourable since the guanidinium side chain of arginine is more accessible to the indole side chain than the butylammonium side chain of lysine. Consequently, the guanidinium side chain can form hydrogen bonds with other molecules (38). The tryptophan-arginine pairing was reported to be crucial for better activity and bioavailability in temporin and aurein peptides. Interactions between tryptophan and arginine promote the formation of higher order structures and enhance interactions with lipid bilayers which leads to greater antimicrobial activity (39). Further *in vitro* studies are important to determine if aggregation of Os-C(W_5) leads to membrane permeabilisation.

3.4 Conclusion

Molecular dynamics simulations in combination with CD spectroscopy indicate that tryptophan end-tagging does alter the secondary structure of Os-C with changes in peptide aggregation and amino acid residue interactions. Secondary structure prediction tools and snapshots from MD simulations showed that tryptophan end-tagging leads to an increase in β-strand content. A reduction in peptide-membrane hydrogen bonding and membrane insertion following tryptophan end-tagging may be linked to the preference of tryptophan residues to form oligomers rather than penetrating the membrane. Enhanced aggregation may be beneficial for increasing the local concentration of peptides on the membrane surface which may lead to greater antifungal activity.

3.5 References

1. Martinez-Seara, H., and Rog, T. (2012) Molecular dynamics simulations of lipid bilayers: simple recipe of how to do it. In Biomolecular Simulations, Humana-Press, ed. 407-429.
2. Sliwoski, G., Kothiwale, S., Meiler, J., and Lowe, E. W. (2014) Computational methods in drug discovery. *Pharmacological Reviews* **66**, 334-395. 10.1124/pr.112.007336
3. Palmer, N., Maasch, J. R. M. A, Torres, M. D. T., and de La Fuente-Nunez, C. (2021) Molecular dynamics for antimicrobial peptide discovery. *Infection and Immunity* **89**, 1-10. 10.1128/IAI.00703-20
4. Hollingsworth, S. A., and Dror, R. O. (2018) Molecular dynamics simulation for all. *Neuron* **99**, 1129-1143. 10.1016/j.neuron.2018.08.011
5. Greenfield, N. J. (2006) Using circular dichroism spectra to estimate protein secondary structure. *Nature Protocols* **1**, 2876-2890. 10.1038/nprot.2006.202
6. Rodger, A., and Marshall, D. (2021) Beginners guide to circular dichroism. *The Biochemist* **43**, 58-64. 10.1042/bio_2020_105
7. Prinsloo, L., Naidoo, A., Serem, J. C., Taute, H., Sayed, Y., Bester, M. J., Neitz, A. W. H., and Gaspar, A. R. M. (2013) Structural and functional characterization of peptides derived from the carboxy-terminal region of a defensin from the tick *Ornithodoros savignyi*. *Journal of Peptide Science* **19**, 325-332. 10.1002/psc.2505
8. Mbuayama, K. R., Taute, H., Strömstedt, A. A., Bester, M. J., and Gaspar, A. R. M. (2021) Antifungal activity and mode of action of synthetic peptides derived from the tick OsDef2 defensin. *Journal of Peptide Science* **28**, e3383-e3394. 10.1002/psc.3383

9. Abraham, M. J., Murtola, T., Schulz, R., Páll, S., Smith, J. C., Hess, B., and Lindahl, E. (2015) GROMACS: high performance molecular simulations through multi-level parallelism from laptops to supercomputers. *SoftwareX* **1-2**, 19-25. 10.1016/j.softx.2015.06.001

10. Best, R. B., Zhu, X., Shim, J., Lopes, P. E., Mittal, J., Feig, M., and Mackerell Jr, A. D. (2012) Optimization of the additive CHARMM all-atom protein force field targeting improved sampling of the backbone phi, psi and side-chain χ_1 and χ_2 dihedral angles. *Journal of Chemical Theory and Computation* **8**, 3257-3273. 10.1021/ct300400x

11. Huang, J., and MacKerell Jr, A. D. (2013.) CHARMM36 all-atom additive protein force field: validation based on comparison to NMR data. *Journal of Chemical Theory and Computation* **34**, 2135-2145. 10.1002/jcc.23354

12. Lee, J., Cheng, X., Swails, J. M., Yeom, M. S., Eastman, P. K., Lemkul, J. A., Wei, S., Buckner, J., Jeong, J. C., Qi, Y., Jo, S., Pande, V. S., Case, D. A., Brooks, C. L., MacKerell Jr, A. D., Klauda, J. B., and Im, W. (2016) CHARMM-GUI input generator for NAMD, GROMACS, AMBER, OpenMM, and CHARMM/OpenMM simulations using the CHARMM36 additive force field. *Journal of Chemical Theory and Computation* **12**, 405-413. 10.1021/acs.jctc.5b00935

13. Aguiar, F. L. L., Santos, N. C., de Paula Cavalcante, C. S., Andreu, D., Baptista, G. R., Goncalves, S. (2020) Antibiofilm activity on *Candida albicans* and mechanism of action on biomembrane models of the antimicrobial peptide Ctn[15-34]. *International Journal of Molecular Sciences* **21**, 1-15. 10.3390/ijms21218339

14. Warschawski, D. E., Arnold, A. A., Beaugrand, M., Gravel, A., Chartrand, E., and Marcotte, I. (2011) Choosing membrane mimetics for NMR structural studies of transmembrane proteins. *Biochimica et Biophysica Acta* **1808**, 1957-1974. 10.1016/j.bbamem.2011.03.016

15. Park, C., and Lee, D. G. (2010) Melittin induces apoptotic features in *Candida albicans*. *Biochemical and Biophysical Research Communications* **394**, 170-172. 10.1016/j.bbrc.2010.02.138

16. Schmidtchen, A., Pasupuleti, M., and Malmsten, M. (2014) Effect of hydrophobic modifications in antimicrobial peptides. *Advances in Colloid and Interface Science* **205**, 265-274. 10.1016/j.cis.2013.06.009

17. Brogden, K. A. (2005) Antimicrobial peptides: pore formers or metabolic inhibitors in bacteria? *Nature Reviews Microbiology* **3**, 238-250. 10.1038/nrmicro1098

18. Pasupuleti, M., Walse, B., Svensson, B., Malmsten, M., and Schmidtchen, A. (2008) Rational design of antimicrobial C3a analogues with enhanced effects against staphylococci using an integrated structure and function-based approach. *Biochemistry* **47**, 9057-9070. 10.1021/bi800991e

19. Pasupuleti, M., Schmidtchen, A., and Malmsten, M. (2012) Antimicrobial peptides: key components of the innate immune system. *Critical Reviews in Biotechnology* **32**, 143-171. 10.3109/07388551.2011.594423

20. Schmidtchen, A., Pasupuleti, M., Morgelin, M., Davoudi, M., Alenfall, J., Chalupka, A., and Malmsten, M. (2009) Boosting antimicrobial peptides by hydrophobic oligopeptide end tags. *Journal of Biological Chemistry* **284**, 17584-17594. 10.1074/jbc.M109.011650

21. Schmidtchen, A., Ringstad, L., Kasetty, G., Mizuno, H., Rutland, M. W., and Malmsten, M. (2011) Membrane selectivity by W-tagging of antimicrobial peptides. *Biochimica et Biophysica Acta* **1808**, 1081-1091. 10.1016/j.bbamem.2010.12.020

22. Strömstedt, A. A., Pasupuleti, M., Schmidtchen, A., and Malmsten, M. (2009) Oligotryptophan-tagged antimicrobial peptides and the role of the cationic sequence. *Biochimica et Biophysica Acta (BBA) - Biomembranes* **1788**, 1916-1923. 10.1016/j.bbamem.2009.06.001

23. Freskgard, P. O., Martensson, L. G., Jonasson, P., Jonsson, B. H., and Carlsson, U. (1994) Assignment of the contribution of the tryptophan residues to the circular dichroism spectrum of human carbonic anhydrase II. *Biochemistry* **33**, 14281-14288. 10.1021/bi00251a041

24. Louis-Jeune, C., Andrade-Navarro, M. A., and Perez-Iratxeta, C. (2012) Prediction of protein secondary structure from circular dichroism using theoretically derived spectra. *Proteins* **80**, 374-381. 10.1002/prot.23188

25. Woody, R. W. (1994) Contributions of tryptophan side chains to the far-ultraviolet circular dichroism of proteins. *European Biophysics Journal* **23**, 253-262. 10.1007/BF00213575

26. Reeb, J., and Rost, B. (2019) Secondary structure prediction. *Encyclopedia of Bioinformatics and Computational Biology* **2**, 488-496. 10.1016/B978-0-12-809633-8.20267-7

27. Johnston, A. J., Zhang, Y. R., Busch, S., Pardo, L. C., Imberti, S., and McLain, S. E. (2015) Amphipathic solvation of indole: implications for the role of tryptophan in

membrane proteins. *The Journal of Physical Chemistry* **119**, 5979-5987. 10.1021/acs.jpcb.5b02476

28. de Jesus, A. J., and Allen, T. W. (2013) The role of tryptophan side chains in membrane protein anchoring and hydrophobic mismatch. *Biochimica et Biophysica Acta* **1828**, 864-876. 10.1016/j.bbamem.2012.09.009
29. Manzo, G., Ferguson, P. M., Gustilo, V. B., Hind, C. K., Clifford, M., Bui, T. T., Drake, A. F., Atkinson, R. A., Sutton, J. M., Batoni, G., Lorenz, C. D., Phoenix, D. A., and Mason, A. J. (2019) Minor sequence modifications in temporin B cause drastic changes in antibacterial potency and selectivity by fundamentally altering membrane activity. *Scientific Reports* **9**, 1385-1400. 10.1038/s41598-018-37630-3
30. Manzo, G., Hind, C. K., Ferguson, P. M., Amison, R. T., Hodgson-Casson, A. C., Ciazynska, K. A., Weller, B. J., Clarke, M., Lam, C., Man, R. C. H., Shaughnessy, B. G. O. Clifford, M., Bui, T. T., Drake, A. F., Atkinson, R. A., Lam, J. K. W., Pitchford, S. C., Page, C. P., Phoenix, D. A., Lorenz, C. D., Sutton, J. M., and Mason, A. J. (2020) A pleurocidin analogue with greater conformational flexibility, enhanced antimicrobial potency and *in vivo* therapeutic efficacy. *Communications Biology* **3**, 697-712. 10.1038/s42003-020-01420-3
31. Yau, W. M., Wimley, W. C., Gawrisch, K. , and White, S. H. (1998) The preference of tryptophan for membrane interfaces. *Biochemistry* **37**, 14713-14718. 10.1021/bi980809c
32. Zai, Y., Xi, X., Ye, Z., Ma, C., Zhou, M., Chen, X., Siu, S. W. I., Chen, T., Wang, L., and Kwok, H. F. (2021) Aggregation and its influence on the bioactivities of a novel antimicrobial peptide, temporin-PF, and its analogues. *International Journal of Molecular Sciences* **22**, 1-18. 10.3390/ijms22094509
33. Sarig, H., Rotem, S., Ziserman, L., Danino, D., and Mor, A. (2008) Impact of self-assembly properties on antibacterial activity of short acyl-lysine oligomers. *Antimicrobial Agents and Chemotherapy* **52**, 4308-4314. 10.1128/AAC.00656-08
34. Lace, I., Cotroneo, E. R., Hesselbarth, N., and Simeth, N. A. (2022) Artificial peptides to induce membrane denaturation and disruption and modulate membrane composition and fusion. *Journal of Peptide Science* **29**, e3466-e3495. 10.1002/psc.3466
35. Sengupta, D., Leontiadou, H., Mark, A. E., and Marrink, S. J. (2008) Toroidal pores formed by antimicrobial peptides show significant disorder. *Biochimica et Biophysica Acta* **1778**, 2308-2317. 10.1016/j.bbamem.2008.06.007

36. Khemaissa, S., Walrant, A., and Sagan, S. (2022) Tryptophan, more than just an interfacial amino acid in the membrane activity of cationic cell-penetrating and antimicrobial peptides. *Quarterly Reviews of Biophysics* **55**, e10-e21. 10.1017/S0033583522000105

37. Frontera, A., Gamez, P., Mascal, M., Mooibroek, T. J., and Reedijk, J. (2011) Putting anion-pi interactions into perspective. *Angewandte Chemie International Edition* **50**, 9564-9583. 10.1002/anie.201100208

38. Flocco, M. M., and Mowbray, S. L. (1994) Planar stacking interactions of arginine and aromatic side-chains in proteins. *Journal of Molecular Biology* **235**, 709-717. 10.1006/jmbi.1994.1022

39. Bhattacharjya, S., and Straus, S. K. (2020) Design, engineering and discovery of novel alpha-helical and beta-boomerang antimicrobial peptides against drug resistant bacteria. *International Journal of Molecular Sciences* **21**, 1-21. 10.3390/ijms21165773

Chapter 4: Antifungal activity and mode of action of Os-C(W_5) against planktonic *C. albicans*

4.1 Introduction

Many AMPs have been shown to lose activity in the presence of complex fluids such as broth and serum (1, 2) while other reports have shown that the presence of salts can reduce the activity of AMPs. Cations present in salts can interact with negatively charged phospholipids on the membrane surface and prevent peptide-membrane interactions which render the peptide biologically inactive (3).

Os-C was active when antibacterial activity was evaluated in NaP buffer (0.01 M, pH 7.4) (4). In this milieu, mode of action studies revealed that Os-C interacted with fungal cell wall components, induced 30% permeabilisation of *S. cerevisiae* liposomes but ROS production was identified as the main antifungal mode of action. Further findings were that Os-C crosses the membrane of *C. albicans* via an energy-dependent mechanism (5). However, in LB broth, the antibacterial activity of Os-C against Gram-negative and Gram-positive bacteria was lost with minimum inhibitory concentration (MIC) values greater than the highest test concentration (120 μg/mL). As a result, further therapeutic development of this AMP was limited (4).

To overcome this limitation, AMPs can be end-tagged with hydrophobic stretches of amino acids such as β-naphtylalanine (6) or tryptophan (7). End-tagging with tryptophan led to enhanced antibacterial (8-12) and antifungal (13) activity in Tris buffer supplemented with 0.15 M sodium chloride. Antibacterial assays performed in Mueller-Hinton broth showed that tryptophan end-tagged peptides had lower MIC values compared with their analogues without end-tags (9, 11). Liposome disruption experiments indicated increased selectivity with greater peptide-induced permeabilisation of bacterial and fungal liposomes with lower selectivity for cholesterol containing liposomes. This finding was important since mammalian cell membranes contain cholesterol and are thus less likely to be targeted by tryptophan-tagged peptides (9-13).

A further advantage of tryptophan end-tagging when compared with sequence-specific point substitutions is that amino acid substitutions could lead to a loss of activity while end-tagging does not alter the original peptide sequence. Therefore, antimicrobial activity is enhanced and

the original properties of the peptide are retained (14). Tryptophan end-tagged peptides have increased selectivity between different eukaryotic cells. The bulky and polarisable nature of tryptophan means that it is sensitive to sterol identity. Schmidtchen *et al*. demonstrated that the AMP, GRR10W4N was active against *C. albicans* and *C. parapsilosis* with low haemolytic activity and no toxicity towards epithelial cells (11). In a recent study, Os-C(W_5) did not cause the haemolysis of human erythrocytes when evaluated at 0 – 100 µM (R. Chirombo, MSc dissertation, 2023).

In the previous chapter, MD simulations showed that tryptophan end-tagging led to changes in the secondary structure of Os-C which was predominantly disordered with some β-strand content. Furthermore, tryptophan end-tagging led to reduced membrane insertion, fewer peptide-membrane interactions, and enhanced peptide-peptide aggregation. Circular dichroism identified the secondary structure of Os-C(W_5) as predominantly disordered with more β-strand content than Os-C. Although MD simulations provided information about the structure and potential activity of Os-C(W_5), it was necessary to investigate the activity *in vitro*.

The aim of the research presented in this chapter was to determine if tryptophan end-tagging of Os-C increases activity in more complex physiological environments, represented by RPMI-1640 media, a complex nutrient rich mixture of amino acids, vitamins, and salts (15). Furthermore, mode of action studies sought to identify whether tryptophan end-tagging induces membrane permeabilisation and/or ROS production which leads to cellular damage and eventually cell death.

4.2 Materials and Methods

4.2.1 Antifungal agents

Peptides were synthesised, prepared, and stored as described in Chapter 3 (section 3.2.1). Amphotericin B was purchased from Sigma-Aldrich (St Louis, Missouri, USA) and stocks were prepared in dimethyl sulfoxide (DMSO) and stored at -80°C.

4.2.2 Preparation of cells for antiplanktonic assays

C. albicans ATCC 90028 cells were prepared as described in the EUCAST Definitive Document EDef 7.1 (15). Briefly, cells were streaked on a yeast peptone dextrose (YPD) agar plate and incubated for 18 – 24 hours at 37°C. Single colonies were suspended and diluted in $dddH_2O$ to the required cell density. To ensure that cells were not affected by osmotic swelling, plates were inoculated within 30 minutes of preparing the inoculum suspension.

4.2.3 Antifungal susceptibility testing

Antiplanktonic activity was investigated using the microbroth dilution assay. The method was performed according to the EUCAST Definitive Document EDef 7.1 (15). Double-strength RPMI-1640 medium with L-glutamine and phenol red and without sodium bicarbonate (Sigma-Aldrich, St Louis, Missouri, USA) supplemented with 2% glucose (2× RPMI-1640 2% G, final pH = 7.0), was used. Supplementing RPMI-1640 with glucose has been shown to result in better growth of yeast isolates (15). Os-C and Os-C(W_5) were prepared by diluting stock solutions with 2× RPMI-1640 2% G in 96-well polypropylene plates (Greiner Bio-One, Kremsmünster, Austria) and AMB was prepared in 2× RPMI-1640 2% G supplemented with 1% DMSO.

The cell inoculum was prepared by suspending single colonies in $dddH_2O$ to prepare a yeast suspension. Afterwards, the inoculum was suspended by vortexing and the optical density (OD) of the suspension was measured at 530 nm using a spectrophotometer (VWR, Radnor, Pennsylvania, USA). The suspension was diluted in $dddH_2O$ to an OD_{530} between 0.12 and 0.15 which represents a cell density between 1×10^6 CFU/mL and 5×10^6 CFU/mL, respectively (15). The working suspension was prepared by making a 1/10 dilution in $dddH_2O$ to give a cell concentration of $1 – 5 \times 10^5$ CFU/mL.

The cell suspension (50 µL) was added to equal volumes (50 µL) of AMB (0.009 – 2.5 µM) or Os-C and Os-C(W_5) (0.78 – 200 µM). The final concentration range of AMB was 0.004 – 1.25 µM and that of Os-C and Os-C(W_5) was 0.39 – 100 µM. For the growth control, 50 µL of the

yeast suspension was added to 50 µL of 2× RPMI-1640 2% G. Cells were incubated for 24 hours at 37°C without shaking. Growth inhibition was determined by measuring the OD_{530} using a SpectraMax Paradigm Multi-Mode Microplate Reader (Molecular Devices, Sunnyvale, California, USA). Prior to measurement, plates were agitated for 5 seconds. The MIC was defined as the lowest concentration of antifungal that inhibited fungal growth by at least 90% (15).

4.2.4 CellTiter Blue cell viability assay

Cell viability was determined using the CellTiter Blue (CTB) cell viability assay (Promega, Madison, Wisconsin, USA) which uses the dye resazurin to measure the metabolic capacity of cells. In viable cells, non-fluorescent resazurin (dark blue) is reduced by redox enzymes in the mitochondria and cytosol to form resorufin, a pink, fluorescent compound. The fluorescence is measured at an excitation wavelength of 535 nm and an emission wavelength of 590 nm and is directly proportional to metabolic activity (16). The reduction of resazurin to resorufin is shown in **Figure 4.1**.

The inoculum and antifungal agents were prepared as described in Section 4.2.3. Cells were incubated with AMB and Os-C(W_5) for 24 hours at 37°C without shaking. After 24 hours, 11 µL of CTB was added to each well followed by incubation for one hour at 37°C. Cell viability was quantified by measuring the fluorescence at excitation and emission wavelengths of 535 nm and 590 nm, respectively, using a plate reader.

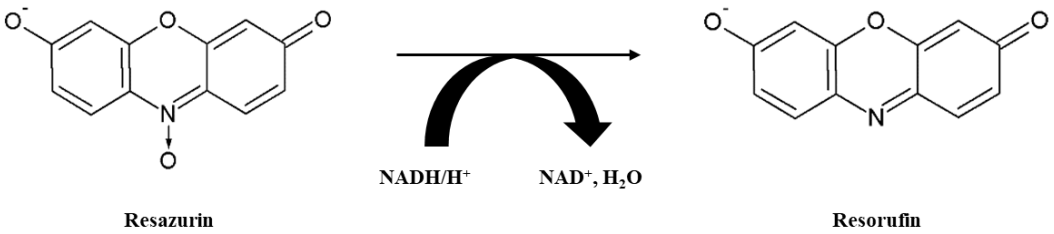

Figure 4.1: Reduction of resazurin to resorufin in the CellTiter Blue cell viability assay. In viable cells, the non-fluorescent dye resazurin is reduced by redox enzymes to form the fluorescent product resorufin. Structures of resazurin and resorufin were drawn using ChemSketch (ACD/Labs). Adapted from the Promega technical document (16).

4.2.5 SYTOX Green uptake assay

Membrane permeabilisation was determined using the DNA-binding dye SYTOX Green. When the cell membrane is intact, SYTOX Green cannot enter the cell. However, when

membrane integrity is compromised, the dye can enter the cell and bind to DNA leading to an increased fluorescent signal.

The assay was conducted as described by Merlino *et al.* (17), with some modifications. *C. albicans* cells were prepared as described in Section 4.2.3 to a density of 1×10^7 CFU/mL. An equal volume of SYTOX Green (Invitrogen; Waltham, Massachusetts, USA) prepared in 0.02 M NaP buffer (pH 7.4) was added to the cell suspension to give a cell density of 5×10^6 CFU/mL and a SYTOX Green concentration of 1 µM. The mixture was incubated in the dark for 50 minutes at 30°C with shaking at 150 rpm to allow for dye equilibration.

Amphotericin B (0.625 – 1.25 µM) was prepared in 2× RPMI-1640 2% G with 1% DMSO while Os-C(W_5) (6.25 – 100 µM) was prepared in 2× RPMI-1640 2% G then 50 µL was added to the wells of a black 96-well plate (Nunc, Roskilde, Denmark). The cell suspension (50 µL) was added to make final concentrations of 0.312 – 0.625 µM for AMB and 3.12 – 50 µM for Os-C(W_5). Fluorescence was measured using a plate reader after three hours at excitation and emission wavelengths of 485 and 535 nm, respectively. Isopropanol (6.25%) was used as a positive control.

4.2.6 Measurement of reactive oxygen species production

Induction of ROS production was determined using the cell-permeable, non-fluorescent dye 2′,7′-dichlorodihydrofluorescin diacetate (DCFH-DA). When DCFH-DA enters the cell, its carboxyl groups are removed by esterase enzymes within the cell to form dichlorodihydrofluorescin (DCFH). In the presence of ROS such as superoxide, peroxynitrite and hydroxyl radicals, DCFH is oxidised to form the fluorescent compound dichlorofluorescin (DCF) (**Figure 4.2**).

Cells were prepared as described in Section 4.2.3 to a density of 1×10^7 CFU/mL. DCFH-DA (40 µM; Sigma-Aldrich, St Louis, Missouri, USA) was prepared in 0.02 M NaP buffer (pH 7.4) and then added to the cell suspension to give a cell density of 5×10^6 CFU/mL and a DCFH-DA concentration of 20 µM. The mixture was incubated in the dark for 30 minutes at 37°C with shaking at 150 rpm. Thereafter, 50 µL of the cell suspension was added to 50 µL of Os-C(W_5) (final concentrations = 3.12 – 25 µM) in a black 96-well plate. Fluorescence was measured using a plate reader every hour for three hours at excitation and emission wavelengths of 485 nm and 535 nm, respectively. Hydrogen peroxide (2 mM) was used as a positive control.

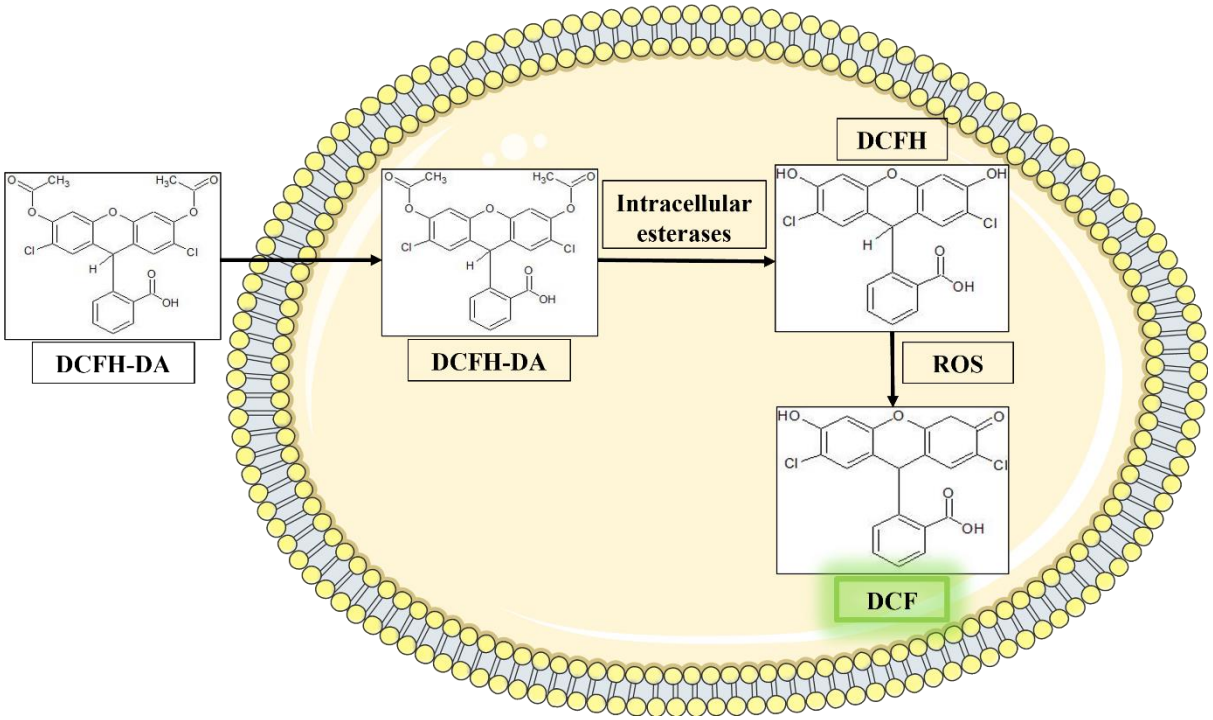

Figure 4.2: 2',7'-Dichlorodihydrofluorescein diacetate assay principle. The non-fluorescent dye 2',7'-dichlorodihydrofluorescein diacetate (DCFH-DA) can enter cells by diffusing through the cell membrane where it is converted to 2',7'-dichlorofihydrofluorescein (DCFH) by intracellular esterases. In the event of oxidative stress, reactive oxygen species (ROS) are generated which in turn react with DCFH to form fluorescent, 2',7'-dichlorofluoresein (DCF). Structures of DCFH-DA, DCFH and DCF were drawn using ChemSketch (ACD/Labs).

To determine whether ROS production was linked to antifungal activity, cells were exposed to Os-C(W_5) (final concentration = 3.12 – 25 µM) for three hours in the absence and presence of 10 mM ascorbic acid (Sigma-Aldrich, St Louis, Missouri, USA). Cell viability was determined by adding 11 µL of CTB for an hour after treatment followed by fluorescence measurements at excitation and emission wavelengths of 535 nm and 590 nm, respectively.

4.2.7 Scanning electron microscopy

Cells (2.5×10^6 CFU/mL) were treated with 6.25 µM and 12.5 µM Os-C(W_5) for three hours as described in Section 4.2.3 then transferred to poly-L-lysine coated coverslips. Samples were washed with 0.075 M NaP buffer (pH 7.4) then fixed with a 2.5% glutaraldehyde/formaldehyde solution for an hour. After primary fixing, samples were rinsed three times with NaP buffer for 10 minutes. Secondary fixation was performed by adding 1% osmium tetroxide to cells for 30 minutes and samples were rinsed three times with NaP buffer for 10 minutes. Dehydration was carried out using 30%, 50%, 70%, 90% and 100% ethanol followed by overnight drying of the samples in hexamethyldisilane. Samples were mounted with carbon tape onto aluminium stubs,

carbon coated and viewed with an Ultra plus field emission gun scanning electron microscope (Zeiss; Oberkochen, Germany).

4.2.8 Data analysis

Statistical analysis of experiments was conducted using GraphPad Prism 7 (GraphPad Software; San Diego, California, USA). Growth inhibition and cell viability were determined using the following formulas:

$$Growth\ inhibition\ (\%) = 100 - (100 \times \frac{Average\ absorbance\ of\ test\ wells - blank}{Average\ absorbance\ of\ untreated\ wells - blank})$$

$$Cell\ viability\ (\%) = 100 \times \frac{Average\ fluorescence\ of\ test\ wells - blank}{Average\ fluorescence\ of\ untreated\ wells - blank}$$

Three biological repeats were performed in triplicate for all assays and results were expressed as the mean ± standard error of the mean (SEM). Statistical analysis was performed using GraphPad Prism 7 (San Diego, California, USA). Analysis of variance (ANOVA) was performed followed by a post-hoc multiple comparisons test. A p-value of < 0.05 was used to indicate significance: *$p < 0.05$; **$p < 0.01$; ***$p < 0.001$; ****$p < 0.0001$.

4.3 Results and Discussion

4.3.1 Antifungal activity

The effect of Os-C and Os-C(W_5) on *C. albicans* cell growth was determined using the microbroth dilution assay. All three antifungals inhibit the growth of planktonic cells in a dose-dependent manner (**Figures 4.3A and 4.3B**). For AMB, the MIC is 0.625 µM (**Table 4.1**). Os-C shows maximal antifungal activity of 45% at 100 µM while Os-C(W_5) has a MIC of 50 µM (**Table 4.1**). A significant difference in antifungal activity between Os-C and Os-C(W_5) is observed between 25 – 100 µM (**Figure 4.3B**). Thus, these results indicate that tryptophan end-tagging significantly increases the antiplanktonic activity of Os-C in 2× RPMI-1640 2% G, a nutrient-rich medium containing amino acids, vitamins, and salts.

Table 4.1: Antiplanktonic activity of amphotericin B, Os-C and Os-C(W_5).

	MIC (growth inhibition)[a] (µM)	MIC (viability)[b] (µM)
Amphotericin B	0.625	0.50 ± 0.13[c]
Os-C	>100	ND[d]
Os-C(W_5)	50	68.4 ± 13.5

[a] Lowest concentration of antifungal agent that leads to an inhibition of growth of ≥90% of the untreated control.
[b] Lowest concentration of antifungal agent that reduced planktonic cell viability by 90%.
[c] Data represents the mean ± SEM of three independent experiments.
[d] Not determined.

Many peptides have been reported to inhibit the growth of *C. albicans*. ApoEdpL-W, a peptide derived from human apolipoprotein had a MIC value of 7.5 µM against *C. albicans* SC5314 (18) which was almost seven times lower than that of Os-C(W_5). Lum *et al*. tested the peptides KABT-AMP, uperin 3.6 and their analogues against several *Candida* strains. Against *C. albicans* ATCC 90028, KABT-AMP and its analogues had MIC values ranging between 6.87 – 27.2 µM. Uperin 3.6 and its analogues had MIC values ranging between 34.5 – 70.1 µM (19). The peptide lycosin-I, derived from the venom of the spider *Lycosa singoriensis* had a similar MIC (46.8 µM) to Os-C(W_5) when tested against a fluconazole-susceptible strain of *C. albicans*. When tested against a fluconazole-resistant strain, the MIC of lycosin-I increased to 93.7 µM (20).

The antifungal activity of Os-C(W_5) was also evaluated in terms of its effect on C. *albicans* cell viability using the CTB cell viability assay. Amphotericin B and Os-C(W_5) reduce cell viability in a dose-dependent manner (**Figures 4.3C and 4.3D**). A 100% reduction in viability

is observed following treatment with 0.625 µM and 1.25 µM AMB (**Figure 4.3C**). For Os-C(W_5), a 100% reduction in viability is observed after treatment with 100 µM (**Figure 4.3D**).

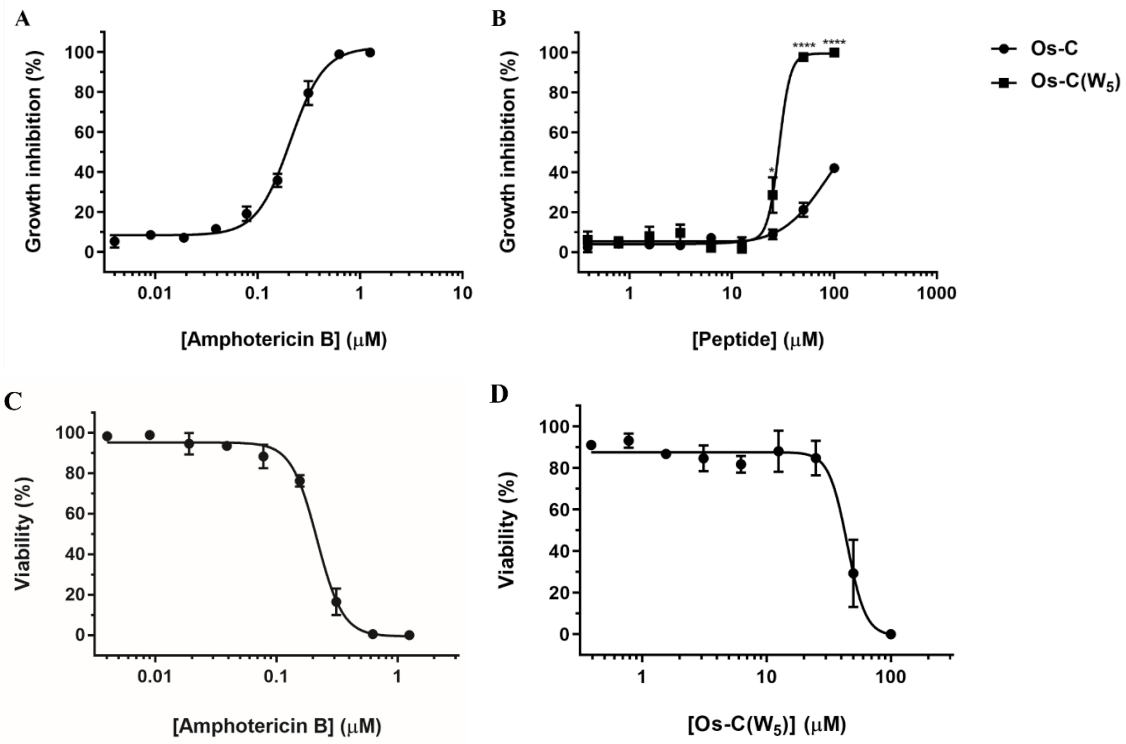

Figure 4.3: Effect of amphotericin B and Os-C(W_5) on cell growth and viability. (A and B) Planktonic *C. albicans* cells were exposed to concentrations of amphotericin B (0.004 – 1.25 µM), Os-C and Os-C(W_5) (both 0.39 – 100 µM) for 24 hours and antifungal activity was quantified by measuring the optical density at 530 nm. Asterisks indicate significant differences between the same concentrations of Os-C and Os-C(W_5). Data represent the mean ± SEM of three independent experiments. A two-way ANOVA was performed followed by a post-hoc Tukey's multiple comparisons test. Asterisks (*p < 0.05; ****p < 0.0001) represent a significant difference between the same concentrations of Os-C and Os-C(W_5). (C and D) Planktonic *C. albicans* cells were exposed to concentrations of amphotericin B (0.004 – 1.25 µM) and Os-C(W_5) (0.39 – 100 µM) for 24 hours then viability was measured using the CellTiter Blue cell viability assay. Data represent the mean ± SEM of three independent experiments. Some error bars are not visible due to small differences.

From the viability dose-response curves, MIC values of 0.50 ± 0.13 µM and 68.4 ± 13.5 µM were determined for AMB and Os-C(W_5), respectively (**Table 4.1**). These values are similar to the MIC values obtained for growth inhibition assays indicating that reduced cell growth is linked to reduced cell viability. A similar dose-dependent effect was reported by D'Auria *et al.* who evaluated the effect of the peptide temporin G on *C. albicans* viability using methylene blue dye (21).

4.3.2 Mode of action studies

For further mode of action studies of Os-C(W_5) against planktonic *C. albicans*, the number of cells used was increased from 1.5 x 10^5 CFU/mL to 2.5 × 10^6 CFU/mL and the incubation time

was reduced from 24 hours to 3 hours. This was to enable a direct comparison between results, irrespective of the assay used. This necessitated the re-evaluation of the effect of AMB and the peptides on cell viability at the higher cell density and shorter incubation time (**Figure 4.4**).

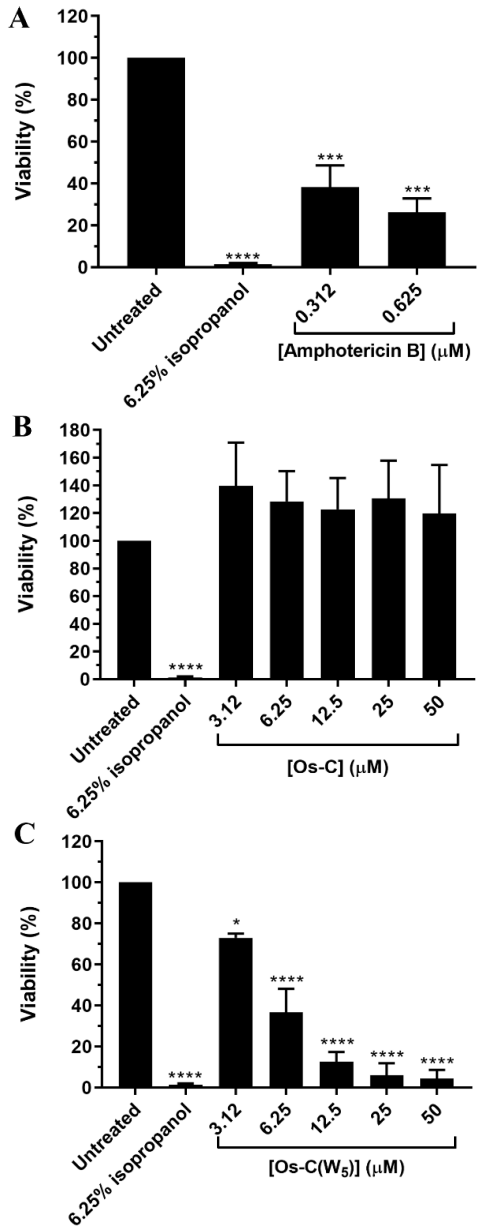

Figure 4.4: Effect of (A) amphotericin B, (B) Os-C and (C) Os-C(W_5) on planktonic cell viability after three hours. Planktonic *C. albicans* cells were exposed to concentrations of amphotericin B (0.312 – 0.625 μM) or Os-C and Os-C(W_5) (3.12 – 50 μM) for three hours and cell viability was quantified using the CellTiter Blue cell viability assay. A one-way ANOVA was performed followed by a post-hoc Dunnett's multiple comparisons test. Data represent the mean ± SEM of three independent experiments. Asterisks (*p < 0.05; ***p < 0.001; ****p < 0.0001) represent a significant difference compared with the untreated control.

Under these conditions, isopropanol (6.25%), which was later used as a positive control for membrane permeabilisation, significantly reduces cell viability to 1.3%. At the higher cell density, 0.625 μM AMB reduces cell viability to 26 ± 6.6% (**Figure 4.4A**), whereas Os-C was

inactive (**Figure 4.4B**). However, 3.12 – 50 µM Os-C(W_5) significantly reduces the viability of *C. albicans* compared with the untreated control. At the highest concentration, 50 µM, cell viability is reduced to 4.3 ± 4.3% (**Figure 4.4C**). Since Os-C was inactive, further mode of action studies focused on Os-C(W_5).

4.3.2.1 Membrane permeabilisation

Many AMPs kill cells by targeting and forming pores in the cell membrane. Therefore, it was necessary to investigate whether tryptophan end-tagging enhances the membrane permeabilising activity of Os-C using the dye SYTOX Green. Isopropanol induces membrane permeabilisation with a significant increase in fluorescence compared with the untreated control (**Figure 4.5**).

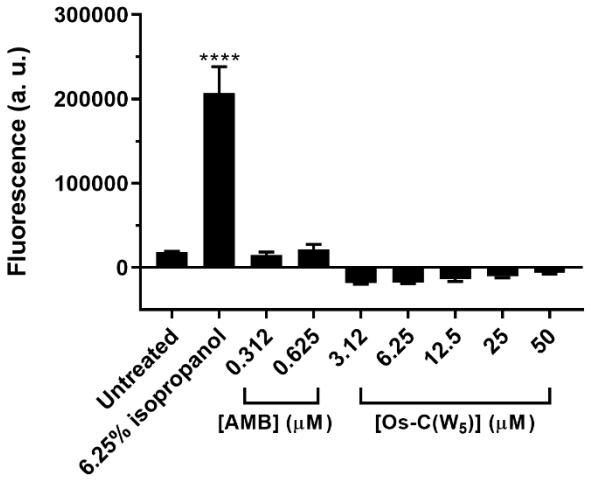

Figure 4.5: Effect of AMB and Os-C(W_5) on membrane permeability. Cells were incubated with SYTOX Green for 50 minutes and exposed to isopropanol, amphotericin B and Os-C(W_5) then fluorescence was measured after three hours. Data represent the mean ± SEM of three independent experiments. A one-way ANOVA was performed followed by a post-hoc Dunnett's multiple comparisons test. Asterisks (****$p < 0.0001$) represent a significant difference compared with the untreated control.

Amphotericin B has similar fluorescence values compared with the untreated control indicating that no permeabilisation occurred (**Figure 4.5**). This is expected since AMB is known to kill fungal cells by sequestering ergosterol from the cell membrane which leads to the efflux of intracellular components and eventually cell death (22). However, another study (21) reported AMB-induced permeabilisation at concentrations much higher than the MIC over 24 hours. Os-C(W_5) does not induce membrane permeabilisation at any of the relevant concentrations (**Figure 4.5**).

In contrast, end-tagging KNK10 (KNKGKKNGKH) with five tryptophan residues induced greater leakage of anionic liposomes containing DOPE and DOPG lipids. Without the tag, 1 µM KNK10 caused no leakage while the same concentration of the tagged peptide KNK10-WWWWW induced approximately 60% leakage within 30 minutes (8). Another study by the same group observed similar results where 10 µM KNK7 (KNKGKKNGKH) and R7 (RRRRRRR) induced 0% and 55% leakage of anionic liposomes, respectively. Tagging the peptides with five tryptophan residues increased leakage to 60% and 80%, respectively (12).

The lack of permeabilisation by Os-C(W_5) supports MD simulation data where minimal membrane insertion is observed for Os-C(W_5). It is likely that aggregation due to tryptophan end-tagging prevents the insertion of Os-C(W_5). Molecular dynamics simulations data combined with membrane permeabilisation data indicate that Os-C(W_5) does not cause membrane permeabilisation.

4.3.2.2 Production of reactive oxygen species

Reactive oxygen species are mainly produced by mitochondria as a consequence of cell metabolism and are generally present in moderate amounts (23). When ROS production exceeds the antioxidant capacity of the cell, oxidative stress occurs which leads to oxidative damage of lipids, DNA, proteins, and cell components such as the cell membrane. Several AMPs are known to induce ROS production which was found to be a key mediator of the antifungal effect (24-29).

Kinetic measurements of ROS production over three hours show that the positive control, hydrogen peroxide, induces ROS production in a time-dependent manner. Likewise, Os-C(W_5) induces ROS production in a dose- and time-dependent manner. Significant ROS production is observed after two hours following exposure to 12.5 µM and 25 µM Os-C(W_5) (**Figure 4.6A**). Under these conditions, increased fluorescence over time suggests that the antifungal activity of Os-C(W_5) may be linked to ROS production similar to the mode of action identified by Mbuayama *et al*. for Os-C although the latter activity was measured in NaP buffer supplemented with 1% YPD broth (5).

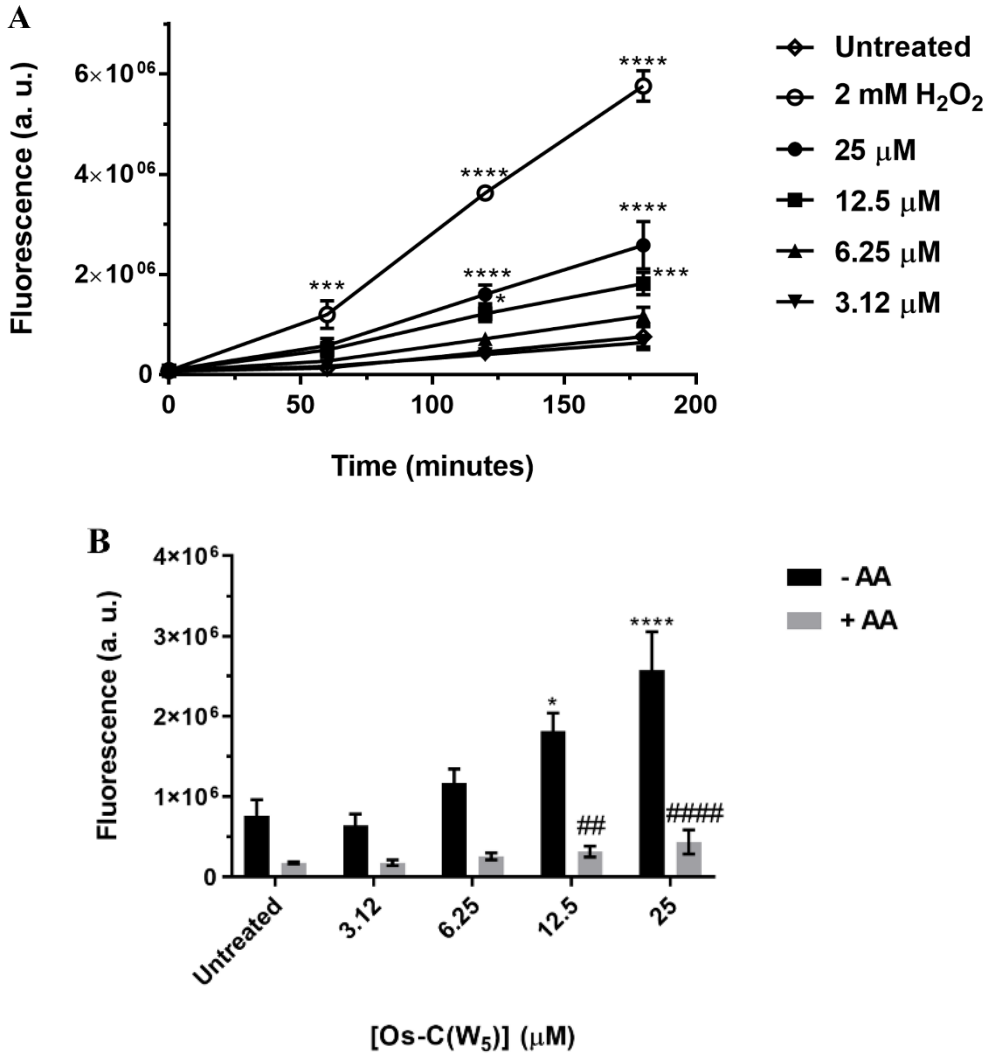

Figure 4.6: Reactive oxygen species production by Os-C(W_5). (A) Cells were treated with Os-C(W_5) (3.12 – 25 μM) and the production of reactive oxygen species was determined by measuring fluorescence every hour for three hours. Hydrogen peroxide (H_2O_2, 2 mM) was used as the positive control. Data represent the mean ± SEM of three independent experiments. A two-way ANOVA was performed followed by a post-hoc Dunnett's multiple comparisons test. Asterisks (*$p < 0.05$; ***$p < 0.001$; ****$p < 0.0001$) represent a significant difference compared with the untreated control. (B) Cells were treated with Os-C(W_5) (3.12 – 25 μM) then the production of reactive oxygen species was determined by measuring fluorescence after three hours. Data represent the mean ± SEM of three independent experiments. A two-way ANOVA was performed followed by a post-hoc Tukey's multiple comparisons test. Asterisks (*$p < 0.01$; ****$p < 0.0001$) represent a significant difference compared with the untreated control and hash symbols ($^{\#\#}p < 0.01$; $^{\#\#\#\#}p < 0.0001$) represent a significant difference between the same concentrations of Os-C(W_5) in the absence and presence of ascorbic acid.

The production of ROS in *C. albicans* by Os-C(W_5) was evaluated in the absence and presence of 10 mM ascorbic acid. In the absence of ascorbic acid, Os-C(W_5) induces ROS production in a dose-dependent manner with significant ROS production occurring after treatment with 12.5 μM and 25 μM. In the presence of ascorbic acid, a significant decrease in ROS production is observed at these concentrations due to ascorbic acid scavenging superoxide, hydroxyl and lipid hydroperoxide radicals (30) (**Figure 4.6B**).

To determine whether ROS production is linked to the antifungal activity of Os-C(W_5), experiments were conducted in the presence and absence of 10 mM ascorbic acid then viability was quantified using CTB. In the absence of ascorbic acid, there is a significant dose-dependent decrease in viability at all the relevant concentrations compared with the untreated control (**Figure 4.4C**). A significant increase in viability compared with the untreated control is observed following exposure to all concentrations of Os-C(W_5) in the presence of ascorbic acid. Increased growth of treated cells in the presence of ascorbic acid could be due to the ROS scavenging effect of ascorbic acid which creates an environment free of oxidants. Therefore, better cell growth is observed. The results reveal that ascorbic acid protects *C. albicans* from the antifungal activity of Os-C(W_5) (**Figure 4.7**). Therefore, it is likely that ROS accumulation takes place in response to Os-C(W_5) rather than changes in the external environment. Similar findings were reported in a recent study on the peptide AMP-17 where the MIC was increased in the presence of 5 mM and 50 mM ascorbic acid by 4- and 8-fold, respectively (31).

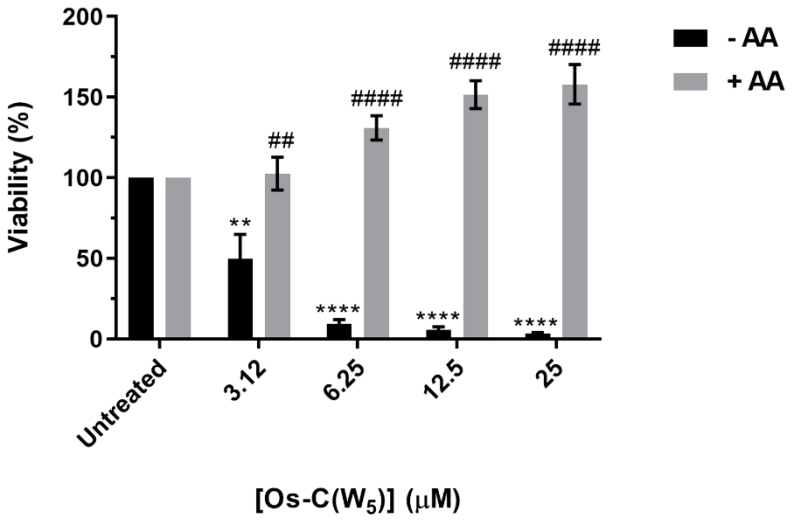

Figure 4.7: Effect of reactive oxygen species production on the antifungal activity of Os-C(W_5). *C. albicans* cells were treated with Os-C(W_5) (3.12 – 25 µM) in the absence (- AA) or presence (+ AA) of 10 mM ascorbic acid for three hours then cell viability was determined using CellTiter Blue. Data represent the mean ± SEM of three independent experiments. A two-way ANOVA was performed followed by a post-hoc Tukey's multiple comparisons test. Asterisks (**$p < 0.01$; ****$p < 0.0001$) represent a significant difference compared with the untreated control and hash symbols ($^{\#\#}p < 0.001$; $^{\#\#\#\#}p < 0.0001$) represent a significant difference in viability between the same concentrations of Os-C(W_5) in the presence and absence of 10 mM ascorbic acid.

Reactive oxygen species are produced as a result of oxidative metabolism by the cell and are crucial for the regulation of cell death, survival, differentiation, signalling and production of factors related to inflammation (32). However, excess and unregulated ROS production is associated with the induction of apoptosis. Madeo *et al*. showed that various stimuli induced

ROS accumulation which subsequently led to apoptotic cell death (33). To date, several AMPs including melittin (34), human lactoferrin (35), cecropin A (34) and coprisin (35) have been shown to induce apoptosis. Treatment with AMPs leads to the generation of ROS that serve as precursors for more potent ROS and contribute to several apoptotic pathways. Electrons that leak from the electron transport chain can react with molecular oxygen to form the superoxide anion. Superoxide dismutase converts superoxide to hydrogen peroxide which is converted to the hydroxyl radical via the Fenton and Haber-Weiss reaction pathways. As a result, the hydroxyl radical can induce apoptosis by disrupting various biological processes (36). Accumulation of ROS leads to several events that are considered hallmarks of apoptosis. The mitochondria are a key site regarding the occurrence of apoptotic events. Ca^{2+} ions play a crucial role in regulating apoptosis in mitochondria and the ER (37). Oxidative stress leads to the release of Ca^{2+} from the ER into the cytoplasm. Subsequently, Ca^{2+} ions enter the mitochondria which results in further ROS production (38). Excess ROS will oxidise sites on the mitochondrial membrane permeability transition pores leading to mitochondrial membrane damage (39).

Lipid peroxidation and mitochondrial membrane depolarisation are consequences of ROS production and lead to mitochondrial membrane disruption and decreased mitochondrial membrane potential, an early event in apoptotic cells (31, 40). Due to the depolarisation of the mitochondrial membrane, cytochrome *c* is released from the mitochondria into the cytoplasm. High cytoplasmic concentrations of cytochrome *c* induce activation of metacaspases, intracellular enzymes that mediate apoptotic processes (26, 41). Consequences of metacaspase activation include disruption of DNA replication, mitochondrial function, and protein and RNA stability (42). Other features that are linked to ROS accumulation and activation of metacaspases include chromatin condensation and DNA fragmentation (43).

4.3.2.3 Changes to cell morphology

Exposure to ROS causes *Candida* species to experience oxidative stress which may lead to cell death by targeting the cell membrane, organelles, lipids, proteins, and nucleic acids (44). Furthermore, ROS production has been linked to morphological changes. Ramirez-Quijas *et al*. treated various *Candida* species with hydrogen peroxide or menadione and observed morphological changes in the cell wall using phase contrast, fluorescence and scanning electron microscopy (45). Therefore, morphological changes following treatment with Os-C(W_5) were investigated using scanning electron microscopy and images are shown in **Figure 4.8**.

Untreated	
6.25 µM Os-C(W_5)	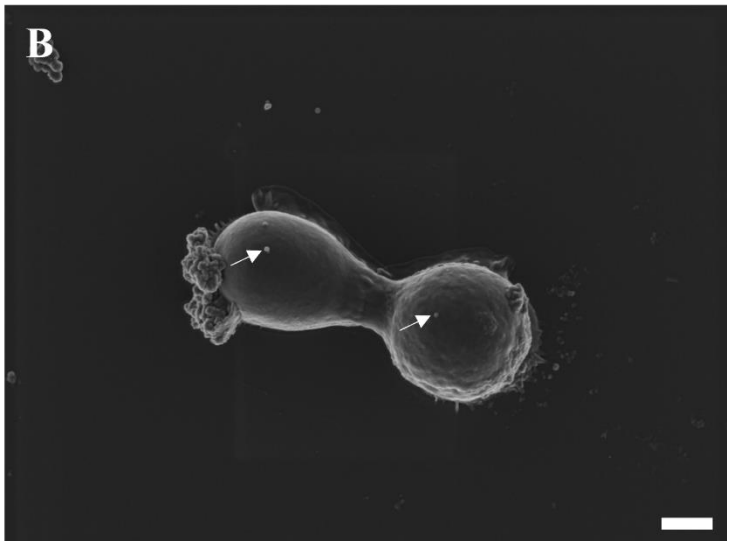
12.5 µM Os-C(W_5)	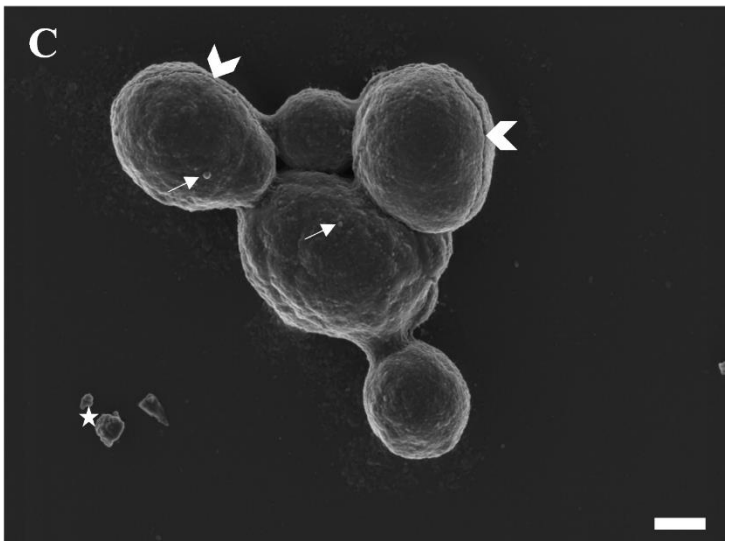

Figure 4.8: Effect of Os-C(W_5) on the morphology of planktonic *C. albicans*. (A) Untreated cells, and cells treated with (B) 6.25 µM or (C) 12.5 µM Os-C(W_5) for three hours. Samples were prepared and viewed using scanning electron microscopy. Effects on cells include cell debris/apoptotic bodies (star), blebs (arrows) and cracking (chevrons). Images were taken at 20000× magnification. Scale bar = 1 µm.

Untreated cells are oval-shaped and have a smooth surface with an intact cell wall and cell membrane. Cell buds and bud scars are also present (**Figure 4.8A**). Treatment with 6.25 µM Os-C(W_5) induces surface roughness and bleb formation (**Figure 4.8B**, arrow heads) (**Figure 4.8B**, thick arrow) which increase following treatment with 12.5 µM Os-C(W_5) (**Figure 4.8C**). Other morphological changes include the presence of cell debris/apoptotic bodies (**Figure 4.8C**, star) and the formation of cracks on the cell surface (**Figure 4.8C**, chevrons). Interestingly, cells treated with Os-C(W_5) are more rounded than the control cells.

Increased surface roughness, blebbing and cell debris/apoptotic bodies are commonly seen after treatment with antifungal agents and are indicators of membrane damage (46-48). Amaral *et al*. observed that the peptide Mo-CBP$_3$-PepIII was active against *C. albicans* and scanning electron microscopy images revealed cracks indicating cell wall damage. A damaged cell wall is detrimental to normal cell function since it affects the osmotic balance with the environment. As a result, there is an efflux of intracellular content which leads to cell death (49). Similarly, AMB binds ergosterol which disrupts the integrity of the cell, leading to the formation of pores, and leakage of intracellular components and consequently also leading to cell death (22). Increased ROS production causes oxidative damage to membranes and important components of membranous organelles, which includes the cell membrane. Consequently, membrane functionality and integrity are lost.

4.4 Conclusion

In double-strength RPMI-1640 medium supplemented with 2% glucose, tryptophan end-tagging of Os-C leads to improved antiplanktonic activity. Os-C is inactive while Os-C(W_5) inhibits planktonic cell growth and cell viability with MIC values of 50 µM and 68.4 ± 13.5 µM, respectively. Although no membrane permeabilisation is observed following Os-C(W_5) exposure, a significant increase in ROS production is observed. Experiments show that ROS production plays a role in the antifungal activity of Os-C(W_5) since ascorbic acid protects cells from the antifungal activity of Os-C(W_5). Finally, Os-C(W_5) induces changes in the morphology of planktonic *C. albicans* such as increased cell surface roughness, apoptotic bodies, and cracks in the cell wall possibly as consequence of excess ROS production.

4.5 References

1. Chu, H. L., Chih, Y. H., Peng, K. L., Wu, C. L., Yu, H. Y., Cheng, D., Chou, Y. T., and Cheng, J. W. (2020) Antimicrobial peptides with enhanced salt resistance and antiendotoxin properties. *International Journal of Molecular Sciences* **21**, 1-18. 10.3390/ijms21186810
2. Ciornei, C. D., Sigurdardottir, T., Schmidtchen, A., and Bodelsson, M. (2005) Antimicrobial and chemoattractant activity, lipopolysaccharide neutralization, cytotoxicity, and inhibition by serum of analogs of human cathelicidin LL-37. *Antimicrobial Agents and Chemotherapy* **49**, 2845-2850. 10.1128/AAC.49.7.2845-2850.2005
3. Kandasamy, S. K., and Larson, R. G. (2006) Effect of salt on the interactions of antimicrobial peptides with zwitterionic lipid bilayers. *Biochimica et Biophysica Acta* **1758**, 1274-1284. 10.1016/j.bbamem.2006.02.030
4. Prinsloo, L., Naidoo, A., Serem, J. C., Taute, H., Sayed, Y., Bester, M. J., Neitz, A. W. H., and Gaspar, A. R. M. (2013) Structural and functional characterization of peptides derived from the carboxy-terminal region of a defensin from the tick *Ornithodoros savignyi*. *Journal of Peptide Science* **19**, 325-332. 10.1002/psc.2505
5. Mbuayama, K. R., Taute, H., Strömstedt, A. A., Bester, M. J., and Gaspar, A. R. M. (2021) Antifungal activity and mode of action of synthetic peptides derived from the tick OsDef2 defensin. *Journal of Peptide Science* **28**, e3383-e3394. 10.1002/psc.3383
6. Yu, H. Y., Tu, C. H., Yip, B. S., Chen, H. L., Cheng, H. T., Huang, K. C., Lo, H. J., and Cheng, J. W. (2011) Easy strategy to increase salt resistance of antimicrobial peptides. *Antimicrobial Agents and Chemotherapy* **55**, 4918-4921. 10.1128/AAC.00202-11
7. Malmsten, M. (2014) Antimicrobial peptides. *Upsala Journal of Medical Sciences* **119**, 199-204. 10.3109/03009734.2014.899278
8. Pasupuleti, M., Schmidtchen, A., Chalupka, A., Ringstad, L., and Malmsten, M. (2009) End-tagging of ultra-short antimicrobial peptides by W/F stretches to facilitate bacterial killing. *PLoS One* **4**, e5285-e5294. 10.1371/journal.pone.0005285
9. Pasupuleti, M., Chalupka, A., Morgelin, M., Schmidtchen, A., and Malmsten, M. (2009) Tryptophan end-tagging of antimicrobial peptides for increased potency against *Pseudomonas aeruginosa*. *Biochimica et Biophysica Acta* **1790**, 800-808. 10.1016/j.bbagen.2009.03.029

10. Schmidtchen, A., Pasupuleti, M., Morgelin, M., Davoudi, M., Alenfall, J., Chalupka, A., and Malmsten, M. (2009) Boosting antimicrobial peptides by hydrophobic oligopeptide end tags. *Journal of Biological Chemistry* **284**, 17584-17594. 10.1074/jbc.M109.011650
11. Schmidtchen, A., Ringstad, L., Kasetty, G., Mizuno, H., Rutland, M. W., and Malmsten, M. (2011) Membrane selectivity by W-tagging of antimicrobial peptides. *Biochimica et Biophysica Acta* **1808**, 1081-1091. 10.1016/j.bbamem.2010.12.020
12. Strömstedt, A. A., Pasupuleti, M., Schmidtchen, A., and Malmsten, M. (2009) Oligotryptophan-tagged antimicrobial peptides and the role of the cationic sequence. *Biochimica et Biophysica Acta (BBA) - Biomembranes* **1788**, 1916-1923. 10.1016/j.bbamem.2009.06.001
13. Sonesson, A., Nordahl, E. A., Malmsten, M., and Schmidtchen, A. (2011) Antifungal activities of peptides derived from domain 5 of high-molecular-weight kininogen. *International Journal of Peptides* **2011**, 761037-761047. 10.1155/2011/761037
14. Schmidtchen, A., Pasupuleti, M., and Malmsten, M. (2014) Effect of hydrophobic modifications in antimicrobial peptides. *Advances in Colloid and Interface Science* **205**, 265-274. 10.1016/j.cis.2013.06.009
15. Rodriguez-Tudela, J. L., Arendrup, M. C., Barchiesi, F., Bille, J., Chryssanthou, E., Cuenca-Estrella, M., Dannaoui, E., Denning, D. W., Donnelly, J. P., Dromer, F., Fegeler, W., Lass-Florl, C., Moore, C., Richardson, M., Sandven, P., Velegraki, A., and Verweij, P. (2008) EUCAST definitive document EDef 7.1: method for the determination of broth dilution MICs of antifungal agents for fermentative yeasts. *Clinical Microbiology and Infection* **14**, 398-405. 10.1111/j.1469-0691.2007.01935.x
16. Promega (2016) CellTiter-Blue® Cell Viability Assay Promega Corporation, Madison, WI, USA
17. Merlino, F., Carotenuto, A., Casciaro, B., Martora, F., Loffredo, M. R., Di Grazia, A., Yousif, A. M., Brancaccio, D., Palomba, L., Novellino, E., Galdiero, M., Iovene, M. R., Mangoni, M. L., and Grieco, P. (2017) Glycine-replaced derivatives of [Pro(3),DLeu(9)]TL, a temporin L analogue: evaluation of antimicrobial, cytotoxic and hemolytic activities. *European Journal of Medicinal Chemistry* **139**, 750-761. 10.1016/j.ejmech.2017.08.040
18. Rossignol, T., Kelly, B., Dobson, C., and d'Enfert, C. (2011) Endocytosis-mediated vacuolar accumulation of the human ApoE apolipoprotein-derived ApoEdpL-W

antimicrobial peptide contributes to its antifungal activity in *Candida albicans*. *Antimicrobial Agents and Chemotherapy* **55**, 4670-4681. 10.1128/AAC.00319-11

19. Lum, K. Y., Tay, S. T., Le, C. F., Lee, V. S., Sabri, N. H., Velayuthan, R. D., Hassan, H., and Sekaran, S. D. (2015) Activity of novel synthetic peptides against *Candida albicans*. *Scientific Reports* **5**, 9657-9658. 10.1038/srep09657
20. Tan, L., Bai, L., Wang, L., He, L., Li, G., Du, W., Shen, T., Xiang, Z., Wu, J., Liu, Z., and Hu, M. (2018) Antifungal activity of spider venom-derived peptide lycosin-I against *Candida tropicalis*. *Microbiological Research* **216**, 120-128. 10.1016/j.micres.2018.08.012
21. D'Auria, F. D., Casciaro, B., De Angelis, M., Marcocci, M. E., Palamara, A. T., Nencioni, L., Mangoni, M. L. (2022) Antifungal activity of the frog skin peptide temporin G and its effect on *Candida albicans* virulence factors. *International Journal of Molecular Sciences* **23**, 1-18. 10.3390/ijms23116345
22. Carolus, H., Pierson, S., Lagrou, K., and Van Dijck, P. (2020) Amphotericin B and other polyenes - discovery, clinical use, mode of action and drug resistance. *Journal of Fungi* **6**, 321-341. 10.3390/jof6040321
23. Golstein, P., Aubry, L., and Levraud, J. (2003) Cell-death alternative model organisms: why and which? *Nature Reviews Molecular Cell Biology* **4**, 798-807. 10.1038/nrm1224.
24. Helmerhorst, E. J., Troxler, R. F., and Oppenheim, F. G. (2001) The human salivary peptide histatin 5 exerts its antifungal activity through the formation of reactive oxygen species. *Proceedings of the National Academy of Science* **98**, 14637-14642. 10.1073/pnas.141366998.
25. Choi, H., and Lee, D. G. (2015) Lycopene induces apoptosis in *Candida albicans* through reactive oxygen species production and mitochondrial dysfunction. *Biochimie* **115**, 108-115. 10.1016/j.biochi.2015.05.009
26. Hwang, B., Hwang, J. S., Lee, J., and Lee, D. G. (2011) The antimicrobial peptide, psacotheasin induces reactive oxygen species and triggers apoptosis in *Candida albicans. Biochemical and Biophysical Research Communications* **405**, 267-271. 10.1016/j.bbrc.2011.01.026
27. Jia, F., Wang, J., Peng, J., Zhao, P., Kong, Z., Wang, K., Yan, W., Wang, R. (2018) The *in vitro*, *in vivo* antifungal activity and the action mode of Jelleine-I against *Candida* species. *Amino Acids* **50**, 229-239. 10.1007/s00726-017-2507-1

28. Peng, C., Liu, Y., Shui, L., Zhao, Z., Mao, X., and Liu, Z. (2022) Mechanisms of action of the antimicrobial peptide cecropin in the killing of *Candida albicans*. *Life (Basel)* **12**, 1-15. 10.3390/life12101581

29. Wang, K., Dang, W., Xie, J., Zhu, R., Sun, M., Jia, F., Zhao, Y., An, X., Qiu, S., Li, X., Ma, Z., Yan, W., and Wang, R. (2015) Antimicrobial peptide protonectin disturbs the membrane integrity and induces ROS production in yeast cells. *Biochimica et Biophysica Acta* **1848**, 2365-2373. 10.1016/j.bbamem.2015.07.008

30. Powers, S. K., and Jackson, M. J. (2008) Exercise-induced oxidative stress: cellular mechanisms and impact on muscle force production. *Physiological Reviews* **88**, 1243-1276. 10.1152/physrev.00031.2007

31. Ma, H., Yang, L., Tian, Z., Zhu, L., Peng, J., Fu, P., Xiu, J., and Guo, G. (2023) Antimicrobial peptide AMP-17 exerts anti-*Candida albicans* effects through ROS-mediated apoptosis and necrosis. *International Microbiology* **26**, 81-90. 10.1007/s10123-022-00274-5

32. Dayem, A. A., Hossain, M. K., Lee, S. B., Kim, K., Saha, S. K., Yang, G. M., Choi, H. Y., and Cho, S. G. (2017) The role of reactive oxygen species (ROS) in the biological activities of metallic nanoparticles. *International Journal of Molecular Sciences* **18**, 1-21. 10.3390/ijms18010120

33. Madeo, F., Fröhlich, E., Ligr, M., Grey, M., Sigrist, S. J., Wolf, D. H., and Fröhlich, K. (1999) Oxygen stress: a regulator of apoptosis in yeast. *Journal of Cell Biology* **145**, 757-767. 10.1083/jcb.145.4.757

34. Park, C., and Lee, D. G. (2010) Melittin induces apoptotic features in *Candida albicans*. *Biochemical and Biophysical Research Communications* **394**, 170-172. 10.1016/j.bbrc.2010.02.138

35. Andres, M. T., Viejo-Diaz, M., and Fierro, J. F. (2008) Human lactoferrin induces apoptosis-like cell death in *Candida albicans*: critical role of K+-channel-mediated K+ efflux. *Antimicrobial Agents and Chemotherapy* **52**, 4081-4088. 10.1128/AAC.01597-07

36. Yun, J., and Lee, D. G. (2016) Cecropin A-induced apoptosis is regulated by ion balance and glutathione antioxidant system in *Candida albicans*. *IUBMB Life* **68**, 652-662. 10.1002/iub.1527

37. Pinton, P., and Rizzuto, R. (2006) Bcl-2 and Ca2+ homeostasis in the endoplasmic reticulum. *Cell Death and Differentiation* **13**, 1409-1418. 10.1038/sj.cdd.4401960

38. Carmona-Gutierrez, D., Eisenberg, T., Buttner, S., Meisinger, C., Kroemer, G., and Madeo, F. (2010) Apoptosis in yeast: triggers, pathways, subroutines. *Cell Death and Differentiation* **17**, 763-773. 10.1038/cdd.2009.219

39. Pereira, C., Silva, R. D., Saraiva, L., Johansson, B., Sousa, M. J., and Corte-Real, M. (2008) Mitochondria-dependent apoptosis in yeast. *Biochimica et Biophysica Acta* **1783**, 1286-1302. 10.1016/j.bbamcr.2008.03.010

40. Curtin, J. F., Donovan, M., and Cotter, T. G. (2002) Regulation and measurement of oxidative stress in apoptosis. *Journal of Immunological Methods* **265**, 49-72. 10.1016/s0022-1759(02)00070-4.

41. Bettiga, M., Calzari, L., Orlandi, I., Alberghina, L., and Vai, M. (2004) Involvement of the yeast metacaspase Yca1 in ubp10-delta-programmed cell death. *FEMS Yeast Research* **5**, 141-147. 10.1016/j.femsyr.2004.07.005

42. Cho, J., and Lee, D. G. (2011) The antimicrobial peptide arenicin-1 promotes generation of reactive oxygen species and induction of apoptosis. *Biochimica et Biophysica Acta* **1810**, 1246-1251. 10.1016/j.bbagen.2011.08.011

43. Ribeiro, G. F., Corte-Real, M., and Johansson, B. (2006) Characterization of DNA damage in yeast apoptosis induced by hydrogen peroxide, acetic acid, and hyperosmotic shock. *Molecular Biology of the Cell* **17**, 4584-4591. 10.1091/mbc.e06-05-0475

44. Maurya, I. K., Pathak, S., Sharma, M., Sanwal, H., Chaudhary, P., Tupe, S., Deshpande, M., Chauhan, V. S., and Prasad, R. (2011) Antifungal activity of novel synthetic peptides by accumulation of reactive oxygen species (ROS) and disruption of cell wall against *Candida albicans*. Peptides **32**, 1732-1740. 10.1016/j.peptides.2011.06.003

45. Ramírez-Quijas, M. D., Zazueta-Sandoval, R., Obregón-Herrera, A., López-Romero, E., and Cuéllar-Cruz, M. (2015) Effect of oxidative stress on cell wall morphology in four pathogenic *Candida* species. *Mycological Progress* **14**, 1-15. 10.1007/s11557-015-1028-0

46. Dananjaya, S. H. S., Udayangani, R. M. C., Oh, C., Nikapitiya, C., Lee, J., and De Zoysa, M. (2017) Green synthesis, physio-chemical characterization and anti-candidal function of a biocompatible chitosan gold nanocomposite as a promising antifungal therapeutic agent. *RSC Advances* **7**, 9182-9193. 10.1039/c6ra26915j

47. Nikapitiya, C., Dananjaya, S. H. S., Chandrarathna, H. P. S. U., De Zoysa, M., and Whang, I. (2020) Octominin: a novel synthetic anticandidal peptide derived from defense protein of *Octopus minor*. *Marine Drugs* **18**, 1-15. 10.3390/md18010056

48. Lyu, Y., Yang, Y., Lyu, X., Dong, N., and Shan, A. (2016) Antimicrobial activity, improved cell selectivity and mode of action of short PMAP-36-derived peptides against bacteria and *Candida*. *Scientific Reports* **6**, 27258-27269. 10.1038/srep27258

49. Amaral, J. L., Souza, P. F. N., Oliveira, J. T. A., Freire, V. N., and Sousa, D. O. B. (2021) Computational approach, scanning electron and fluorescence microscopies revealed insights into the action mechanisms of anticandidal peptide Mo-CBP(3)-PepIII. *Life Sciences* **281**, 119775-119785. 10.1016/j.lfs.2021.119775

Chapter 5: The antibiofilm activity of Os-C(W_5) and its associated mode of action

5.1 Introduction

The National Institutes of Health of the USA estimated that 80% of microbial infections involve pathogenic biofilms which are communities of cells that are attached to a biotic or abiotic surface and are encased in an ECM (1). *Candida* species account for 15% of hospital-acquired cases of sepsis and a mortality rate of 40% with most cases attributed to *C. albicans* (2) which forms difficult to treat biofilms. *C. albicans* biofilms are formed on medical devices such as catheters, contact lenses, dentures and mechanical heart valves and can lead to disseminated bloodstream infections and invasive systemic infections of tissues and organs (3). As a result, the devices need to be removed to treat infections, which can be an expensive and dangerous process.

Biofilms are more resistant to antifungal drugs than planktonic cells meaning that higher doses are required to treat infections. Several cell-based mechanisms such as efflux pumps, mutations of drug targets and the presence of persister cells are involved in resistance to antifungal drugs (4). Furthermore, the ECM plays a key role in conferring resistance to antifungal drugs because of its complex composition. Polysaccharides within the ECM interact with antifungal drugs, forming a complex that prevents drugs from reaching cells and thus rendering them ineffective (5, 6). The presence of the ECM enables cells to evade the host immune response by screening cell wall-associated epitopes that prevent recognition of *Candida* species (7).

Antimicrobial peptides present an alternative to antifungal drugs for the treatment of biofilm-related infections. To date, many AMPs with antibiofilm activity have been discovered. The database of biofilm active AMPs (BaAMPs, https://baamps.it) currently contains 237 peptides that possess antibiofilm activity against a range of microorganisms (8). A biofilm active AMP must be able to either prevent biofilm formation or eradicate preformed biofilms depending on its purpose. Peptides that prevent biofilm formation can be used as coating agents for biomedical devices (9). Conversely, AMPs that eradicate preformed biofilms can be used to treat systemic infections such as candidiasis, cryptococcosis and aspergillosis where the biofilm is fully established (10). Not all AMPs possess both biofilm preventing and eradicating activity; some possess biofilm preventing activity while others possess both activities.

The research presented in Chapter 4 demonstrated that tryptophan end-tagging enhances the antiplanktonic activity of Os-C in physiologically relevant environments. However, as biofilms are clinically relevant, antibiofilm activity is therefore an important property to evaluate. In addition, studies investigating the effect of tryptophan end-tagging on AMP activity have been limited to planktonic cells (11-16).

In this chapter, the effect of tryptophan end-tagging on the biofilm preventing and eradicating activity of Os-C was evaluated. The mode of action was investigated by focusing on three processes involved in biofilm formation: cell adhesion, the yeast-to-hypha transition and ECM production. Finally, antibiofilm activity in the presence of serum containing media was investigated.

5.2 Materials and Methods

5.2.1 Antifungal agents

The peptides used in this chapter were synthesised, prepared, and stored as described in Chapter 3 (Section 3.2.1). Amphotericin B was prepared and stored as described in Chapter 4 (Section 4.2.1).

5.2.2 Preparation of cells for antibiofilm assays

Single colonies were placed in YPD broth and then incubated for 18 hours at 30°C. The overnight culture was centrifuged, the supernatant was discarded, and the pellet was washed and resuspended in RPMI-1640 (a medium that promotes biofilm growth) to a cell density of 2×10^6 CFU/mL for biofilm prevention, adhesion, and ECM analysis assays. For biofilm eradication assays, the cell density was adjusted to 1×10^6 CFU/mL. The final concentration of DMSO in AMB and the untreated growth control for all antibiofilm assays was 0.5%.

5.2.3 Screening for biofilm preventing activity

Biofilm preventing activity was investigated using the method of Troskie *et al*. (17). The cell suspension (50 µL) was added to 50 µL of AMB (0.019 – 5 µM), Os-C or Os-C(W_5) (both 0.78 – 200 µM) in the wells of sterile, 96-well polystyrene plates (Greiner Bio-One; Kremsmünster, Austria). The final concentration range was 0.004 – 2.5 µM for AMB and 0.39 – 100 µM for Os-C and Os-C(W_5). Cells were incubated for either 6 hours or 24 hours at 37°C without shaking, then the medium was removed, and biofilms were washed with 100 µL of phosphate buffered saline (PBS, pH 7.4) which was subsequently removed. Biofilm viability and biomass were determined using the CTB cell viability and crystal violet (CV) staining assays, respectively.

Biofilm viability was determined by adding 100 µL of a 1/10 dilution of CTB to each well, followed by incubation for one hour in the dark. Fluorescence was measured at an excitation wavelength of 535 nm and an emission wavelength of 590 nm using a plate reader.

Biofilm biomass was determined using CV staining (**Figure 5.1**). Crystal violet is a cationic dye that binds to negatively charged cellular components, making the biofilm visible (18). *C. albicans* biofilms were fixed with 100 µL of 20% (v/v) formaldehyde for 15 minutes at room temperature. The fixative was then removed from each well, and the plates were left to dry for a few minutes before 200 µL of 0.1% (w/v) CV was added to each well. After 15 minutes, the CV was removed and 200 µL of dddH_2O was added to wash the plates which were then left to

dry overnight. Qualitative measurements of biofilm biomass were made by viewing cells with an inverted light microscope equipped with a camera (Optika; Ponteranica, Italy).

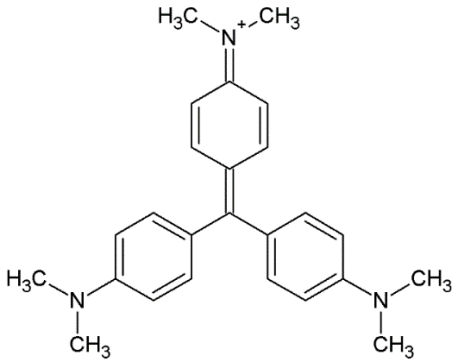

Figure 5.1: Structure of crystal violet. Crystal violet is a cationic stain that interacts with negatively charged cell and extracellular matrix components. The structure of crystal violet was drawn using ChemSketch (ACD/Labs).

Quantitative biomass measurements were made by solubilising CV-stained biofilms with 125 µL of 30% (v/v) acetic acid for 15 minutes. Biomass was quantified by measuring the absorbance of solubilised CV at 550 nm using a plate reader. Biofilm biomass was determined as a percentage relative to untreated cells.

5.2.4 Adhesion assay

The adhesion assay was performed as described by Li *et al*. (19) but crystal violet was used to evaluate the extent of adhesion. The cell suspension (50 µL) was added to 50 µL of 0.019 – 0.312 µM AMB or 1.25 – 20 µM Os-C(W_5) in the wells of a sterile, 96-well polystyrene plate. The final concentration of AMB was 0.009 – 0.156 µM while the final concentration of Os-C(W_5) ranged from 0.625 – 10 µM. After one hour of incubation at 37°C without shaking, non-adherent cells were removed by washing with 100 µL of PBS. Adherent cells were fixed with 100 µL of 20% (v/v) formaldehyde and then stained with 200 µL of 0.1% (m/v) CV. Cell morphology was evaluated with an inverted light microscope equipped with a camera. Adhesion was quantified by extracting the bound CV with 30% (v/v) acetic acid and then measuring the absorbance at 550 nm using a plate reader. The percentage of adherent cells relative to the untreated control was determined.

5.2.5 Morphological transition

The transition from the yeast to hyphal form was investigated as described by Gupta *et al*. (20). An overnight culture of *C. albicans* was resuspended to a cell density of 2×10^6 CFU/mL in

YPD broth supplemented with 20% foetal bovine serum (FBS) and 50 µL of this suspension was added to a polystyrene 96-well plate. An equal volume of AMB (0.019 – 0.312 µM) prepared in YPD broth with 1% DMSO or Os-C(W_5) (1.25 – 20 µM) prepared in YPD broth was added to reduce the final concentration of FBS to 10%. The final concentration ranges of AMB and Os-C(W_5) were 0.009 – 0.156 µM and 0.625 – 10 µM, respectively. Cells were incubated for either 2 hours or 6 hours at 37°C without shaking, washed with 100 µL of PBS to remove any non-adherent cells, and stained with CV as described in Section 5.2.3. Morphological changes were evaluated using an inverted light microscope equipped with a camera.

5.2.6 Biochemical analysis of extracellular material

Changes in ECM composition induced by AMB and Os-C(W_5) were determined by performing biofilm prevention assays for 24 hours. Phosphate buffered saline (200 µL) was added to each well then the biofilms were dislodged from the plate surface with a sterile pipette tip. To further disrupt the biofilm, the plate was vortexed for 30 seconds and then was subjected to a further 15 minutes of sonication using a Bransonic42 water bath sonicator (Branson Ultrasonics; Brookfield, Connecticut, USA) followed by a final vortexing for 30 seconds. The suspensions were transferred to microcentrifuge tubes and then centrifuged for 10 minutes at 13800 × *g* and the collected supernatants were used to determine the carbohydrate, protein, and nucleic acid content.

Carbohydrate content was measured using the phenol-sulfuric acid method described by Masuko *et al.* (21). The supernatant was added to a 96-well plate followed by the addition of 150 µL concentrated sulfuric acid and 30 µL of 5% phenol. After incubation for five minutes at 90°C in a water bath, the samples were cooled to room temperature before the absorbance was measured at 490 nm using a plate reader. The carbohydrate content was calculated using a glucose standard curve. The protein content was measured using the bicinchoninic acid assay (Thermo Fisher Scientific; Waltham, Massachusetts, USA) according to the manufacturer's instructions with bovine serum albumin used to generate a standard curve. Finally, nucleic acid content was determined as described by Hammer *et al.* (22) by measuring the absorbance of the supernatant at 260 nm but the samples were not filtered before measuring the absorbance.

5.2.7 Screening for biofilm eradicating activity

Biofilm eradicating activity was investigated using the method of Troskie *et al*. (17). To determine activity against preformed biofilms, 100 µL of the cell suspension (1×10^6 CFU/mL) was added to the wells of a sterile, 96-well polystyrene plate and then incubated for 24 hours at 37°C without shaking. After 24 hours, the biofilms were washed with 100 µL of PBS which was subsequently removed then 100 µL of AMB (0.009 – 2.5 µM) or Os-C(W_5) (0.39 – 100 µM) was added followed by further incubation for 24 hours at 37°C without shaking. The medium was removed and biofilms were washed with 100 µL of PBS. Biofilm viability and biomass were evaluated using the CTB cell viability and CV staining assays as described in Section 5.2.3.

5.2.8 Activity in serum containing media

The antibiofilm activity of AMB and Os-C(W_5) was determined as described in Section 5.2.3 and Section 5.2.7 in two different FBS containing media. Synthetic wound medium (SWM; 50% peptone water and 50% FBS) was used to mimic a wound environment. RPMI-1640 supplemented with 50% non-heat inactivated FBS (RPMI-1640-50% FBS) was used to represent an extracellular environment. For this initial evaluation of activity in the presence of serum, a single concentration several fold higher than the BIC and the BEC was selected.

For biofilm prevention assays in RPMI-1640-50% FBS, the cell suspension was adjusted to a density of 4×10^6 CFU/mL in RPMI-1640 and an equal volume of 100% FBS was added to reduce the cell density to 2×10^6 CFU/mL. Assays in SWM were performed similarly to assays in RPMI-1640-50% FBS with some changes. Peptone water was used to adjust the cell density to 4×10^6 CFU/mL and an equal volume of 100% FBS was added to reduce the cell density to 2×10^6 CFU/mL. Amphotericin B (5 µM) and Os-C(W_5) (400 µM) were prepared by diluting stocks with either RPMI-1640-50% FBS or SWM and 50 µL was added to the wells of a sterile, 96-well polystyrene plate. The cell suspension (50 µL) was added to AMB and Os-C(W_5) and the final concentrations of AMB and Os-C(W_5) were 2.5 µM and 200 µM, respectively. Cells were incubated for 24 hours at 37°C without shaking. After incubation, the medium was removed, and biofilms were washed with 100 µL of PBS which was subsequently removed. Biofilm viability and biomass were quantified using the CTB cell viability and CV staining assays as described in Section 5.2.3.

For biofilm eradication, the cell suspension was adjusted to a density of 2×10^6 CFU/mL in RPMI-1640 then an equal volume of 100% FBS was added to reduce the cell density to 1 ×

10^6 CFU/mL in RPMI-1640-50% FBS. For experiments with SWM, the cell suspension was adjusted to a density of 2×10^6 CFU/mL using peptone water then an equal volume of 100% FBS was added to reduce the cell density to 1×10^6 CFU/mL. The cell suspension (100 µL) was added to the wells of a 96-well polystyrene plate and cells were incubated for 24 hours at 37°C without shaking. The medium was removed, and biofilms were washed with 100 µL of PBS which was subsequently removed. Amphotericin B (2.5 µM) and Os-C(W_5) (400 µM) were prepared in RPMI-1640-50% FBS or SWM and 100 µL was added to biofilms followed by incubation for another 24 hours at 37°C without shaking. The medium was removed, and biofilms were washed with 100 µL of PBS which was subsequently removed. Biofilm viability and biomass were quantified using the CTB cell viability and CV staining assays as described in Section 5.2.3.

5.2.9 Data analysis

Statistical analysis was performed as described in Section 4.2.8.

Biofilm biomass was determined using the formula:

$$Biofilm\ biomass\ (\%) = 100 \times \frac{Average\ absorbance\ of\ test\ wells}{Average\ absorbance\ of\ untreated\ wells}$$

Three biological repeats were performed in triplicate for all assays and results were expressed as the mean ± SEM. Statistical analysis was performed using GraphPad Prism 7 (San Diego, California, USA). Analysis of variance was performed followed by a post-hoc multiple comparisons test. For biofilm preventing activity, Bonferroni's multiple comparisons test was used to determine whether there was a significant difference in viability and biomass when comparing cells incubated for 6 hours and cells incubated for 24 hours. For assays evaluating prevention of adhesion, ECM production and activity in serum containing media, Dunnett's multiple comparisons test was used to determine whether there was a significant difference between cells treated with AMB or Os-C(W_5) and the untreated control. A p-value of < 0.05 was used to indicate significance: *$p < 0.05$; **$p < 0.01$; ***$p < 0.001$; ****$p < 0.0001$.

5.3 Results and Discussion

5.3.1 Biofilm preventing activity

For biofilms to form, cells must adhere to a surface then undergo a transition from the oval-shaped yeast form to the filamentous hyphal form. Over time, hyphae grow longer, and the protective ECM is also formed. Once the biofilm is fully mature, individual yeast cells will disperse from the biofilm to form new biofilms at different sites. Biofilm formation is especially problematic in clinical settings where biofilms form within the human body or on medical devices (23). To combat biofilm formation, high doses of antifungal drugs are required which could lead to toxic side effects such as kidney and liver toxicity (24). The identification and development of AMPs with antibiofilm activity makes them an attractive alternative to conventional antifungal drugs. Therefore, the biofilm preventing activity of Os-C and Os-C(W_5) was investigated.

The control AMB reduces viability in a dose-dependent manner after 6 hours and 24 hours (**Figure 5.2A**) with BIC values of 0.11 ± 0.02 µM and 0.06 ± 0.01 µM, respectively (**Table 5.1**). No significant difference is observed in terms of viability reduction between both timepoints (**Figure 5.2A**). Biomass reduction is also time- and dose-dependent after exposure to AMB for 6 and 24 hours (**Figure 5.2B**) with BIC values of 0.29 ± 0.02 µM and 0.05 ± 0.02 µM, respectively (**Table 5.1**). A significant difference in biomass reduction between both timepoints is observed from 0.009 – 0.312 µM (**Figure 5.2B**). A significant difference in biomass reduction indicates that the biofilm preventing activity of AMB may be linked to processes of biofilm formation such as adhesion, the yeast-to-hypha transition and ECM production since fewer viable cells are present. Therefore, less biofilm formation takes place.

Table 5.1: Biofilm preventing activity of amphotericin B.

	BIC[a] (µM)	
	Viability	**Biomass**
6 hours	0.11 ± 0.02	0.29 ± 0.02
24 hours	0.06 ± 0.01	0.05 ± 0.02

[a] Lowest concentration of antifungal that caused a 50% reduction in biofilm cell viability or biomass.
All data represents the mean ± SEM of three independent experiments.

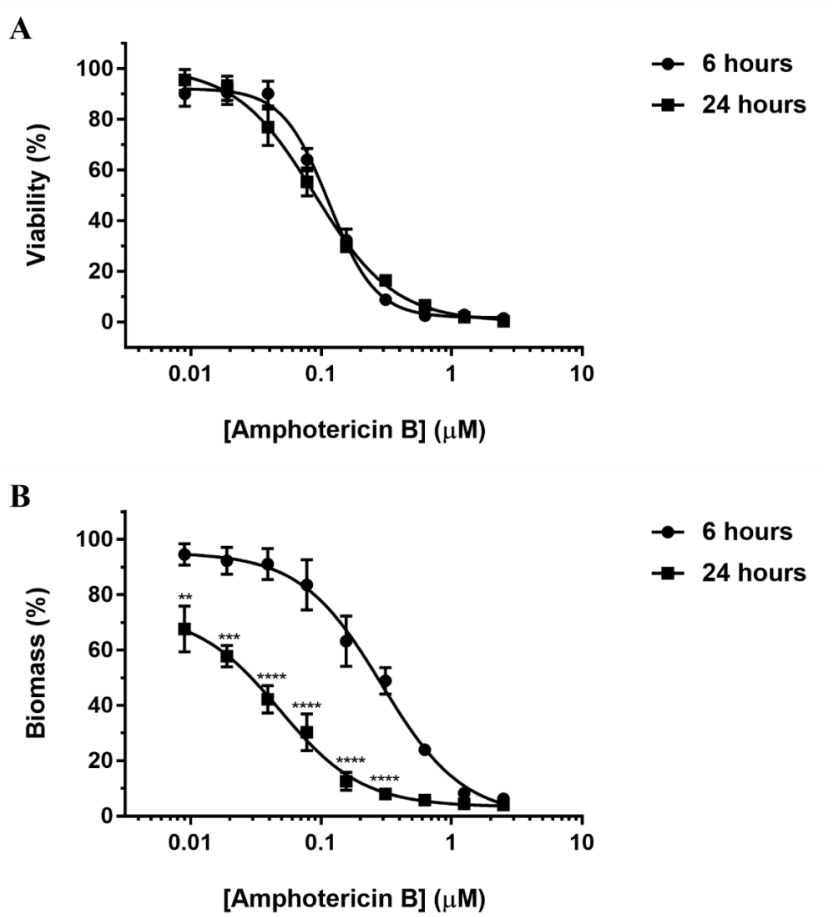

Figure 5.2: Biofilm preventing activity of amphotericin B. *C. albicans* cells were grown in the presence of amphotericin B (0.009 – 2.5 µM) for either 6 hours or 24 hours. (A) Biofilm viability was determined using the CellTiter Blue cell viability assay and (B) biofilm biomass was determined by solubilising crystal violet bound to biofilms with 30% (v/v) acetic acid. Data represents the mean ± SEM of three independent experiments. A two-way ANOVA was performed followed by a post-hoc Bonferroni's multiple comparisons test to compare biomass and viability after 6 hours and 24 hours. Asterisks (**p < 0.01; ***p < 0.001; ****p < 0.0001) represent a significant difference between the same concentrations of amphotericin B after treatment for 6 hours and 24 hours.

Microscopy images reflect the time- and dose-dependent effect on biomass (**Figure 5.3**) following AMB treatment shown in **Figure 5.2B**. After 6 hours, a dense hyphal network is seen after exposure to 0.009 – 0.156 µM AMB. Treatment with 0.625 µM AMB leads to the formation of some cellular aggregates and shorter hyphae. No hyphae are present following treatment with 1.25 µM and 2.5 µM AMB. After 24 hours, a less dense hyphal network is observed after treatment with the lowest concentration of 0.009 µM and the network becomes less dense as the concentration of AMB increases. Shorter hyphae and cellular aggregates are visible after treatment with 0.078 µM AMB and no hyphae are present after exposure to 0.156 – 2.5 µM AMB. Despite a decrease in biomass, the viability of cells exposed to lower concentrations of AMB does not decrease. A likely explanation for this observation is a decrease in the amount of ECM produced following AMB exposure. Therefore, high biofilm viability can be attributed to the presence of hyphal cells.

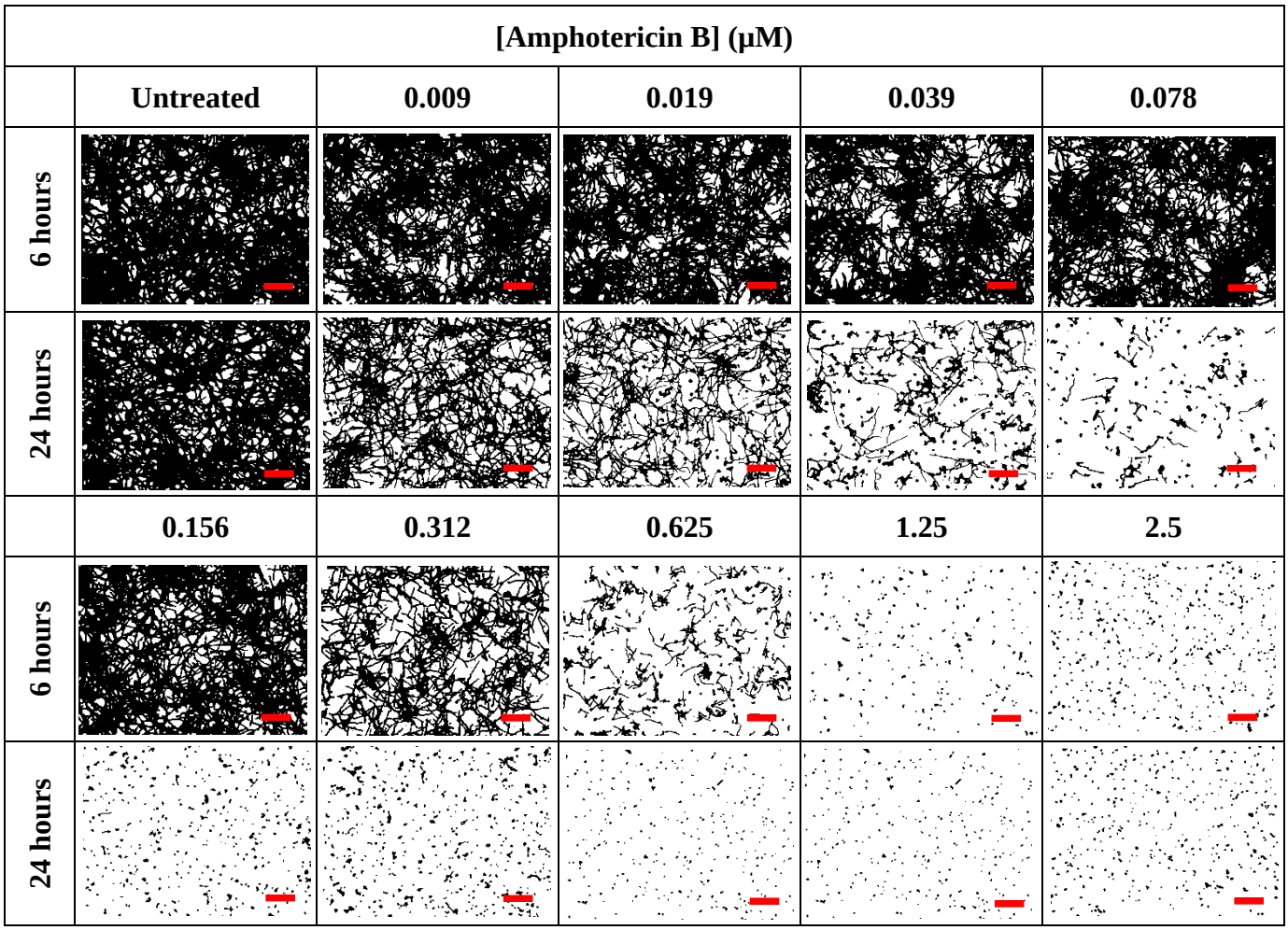

Figure 5.3: Microscopy images of cells exposed to amphotericin B for either 6 hours or 24 hours. *C. albicans* cells were exposed to amphotericin B for either 6 hours (BIC = 0.29 ± 0.02 µM) or 24 hours (BIC = 0.05 ± 0.02 µM), stained with 0.1% (v/v) crystal violet and then images were recorded with an inverted light microscope equipped with a camera. Images were taken at 10× magnification and are representative of three independent experiments. Scale bar = 100 µm.

Os-C does not prevent biofilm formation, but the addition of tryptophan residues leads to improved biofilm preventing activity (**Table 5.2**). Os-C reduces viability by 20% at its highest concentration after 6 hours while treatment after 24 hours leads to an increase in viability as the concentration increases. A significant difference in viability reduction between the two timepoints is observed at 100 µM (**Figure 5.4A**).

Table 5.2: Biofilm preventing activity of Os-C and Os-C(W_5).

	BIC (6 hours, µM)		BIC (24 hours, µM)	
	Viability	**Biomass**	**Viability**	**Biomass**
Os-C	> 100	> 100	> 100	> 100
Os-C(W_5)	4.76 ± 2.81	7.26 ± 1.56	11.2 ± 3.69	10.6 ± 3.77

Data represents the mean ± SEM of three independent experiments.

The highest concentration of Os-C reduces biomass by 24% after 6 hours while lower concentrations reduce biomass by 10% or less. Incubation with Os-C after 24 hours leads to an increase in biofilm biomass (**Figure 5.4B**). Since Os-C partially reduces cell viability after 6 hours, cells may promote regrowth and biofilm formation. This effect was observed with the peptide dendrimer G2OLO-L_2OL_2 where complete killing of *P. aeruginosa* was observed at the MIC (32 µg/mL) after one hour but regrowth was observed after four hours (25).

Os-C(W_5) has a dose-dependent effect on biofilm viability with BIC values of 4.76 ± 2.81 µM and 11.2 ± 3.69 µM after 6 hours and 24 hours, respectively (**Table 5.2**). The increase in the BIC over time could be due to yeast proteases in the medium. Therefore, a higher concentration of peptide is required to prevent biofilm formation (26). A significant reduction in viability between both timepoints is observed between 1.56 – 6.25 µM (**Figure 5.4C**). Os-C(W_5) also has a dose-dependent effect on biofilm biomass. Complete reduction in biomass occurs after treatment with 100 µM and no significant difference in biomass reduction between both timepoints is observed (**Figure 5.4D**).

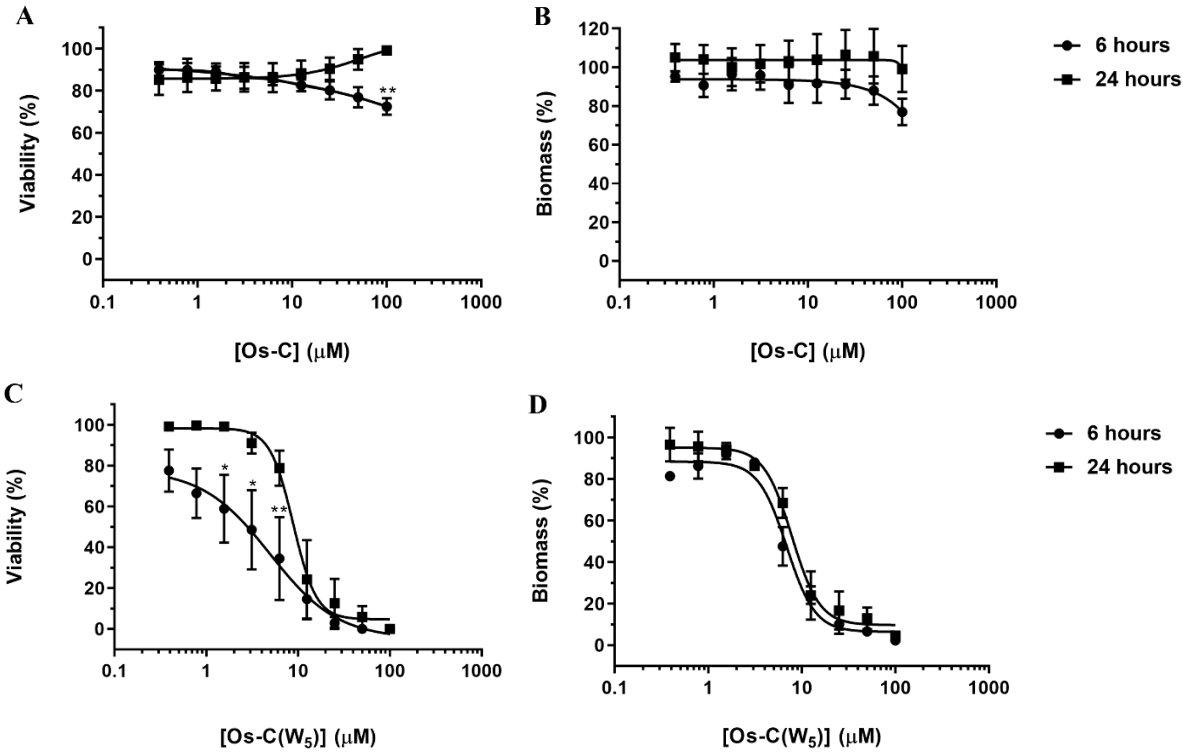

Figure 5.4: Biofilm preventing activity of Os-C and Os-C(W_5) after 6 hours and 24 hours. *C. albicans* cells were grown in the presence of Os-C and Os-C(W_5) (0.39 – 100 µM) for either 6 hours or 24 hours. (A and C) Biofilm viability was determined using the CellTiter Blue cell viability assay. (B and D) Biofilm biomass was determined by solubilising crystal violet bound to biofilms with 30% (v/v) acetic acid. Data represents the mean ± SEM of three independent experiments. A two-way ANOVA was performed followed by a post-hoc Bonferroni's multiple comparisons test. Asterisks (*$p < 0.05$; **$p < 0.01$) represent a significant difference between the same concentrations of Os-C and Os-C(W_5), respectively.

Microscopy images confirm observations from the dose-response curves in **Figure 5.4**. Treatment with 6.25 – 100 µM Os-C does not lead to a change in biofilm formation compared with the untreated control after 6 or 24 hours (**Figure 5.5**). For Os-C(W_5), similar effects are observed after treatment for either 6 hours or 24 hours. Treatment with 6.25 µM Os-C(W_5) leads to a less dense hyphal network while treatment with 12.5 – 100 µM results in shorter hyphae and fewer microcolonies (**Figure 5.5**).

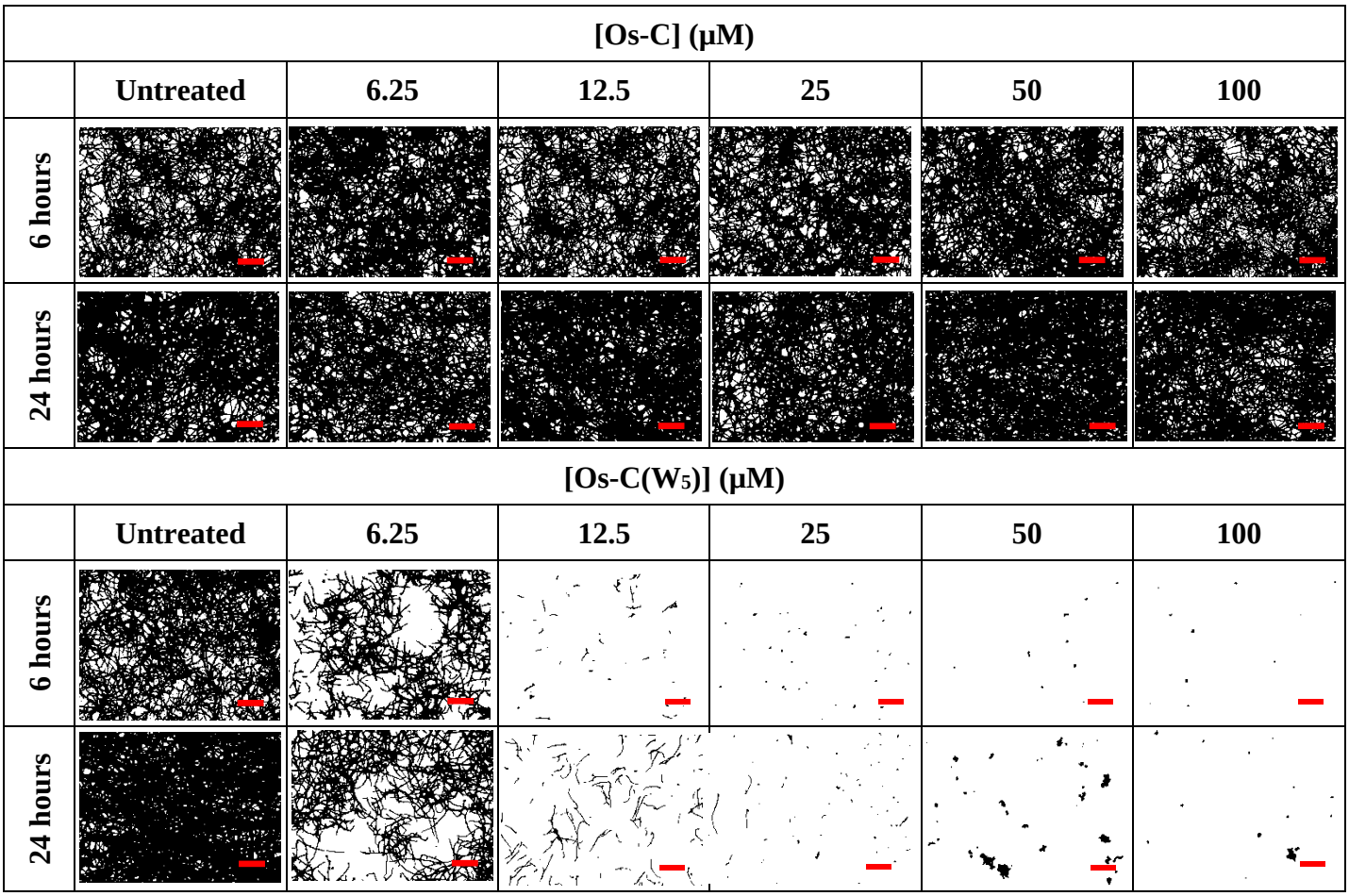

Figure 5.5: Microscopy images of cells exposed to Os-C and Os-C(W_5) for 6 hours and 24 hours. *C. albicans* cells were exposed to Os-C (BIC > 100 µM for 6 hours and 24 hours) and Os-C(W_5) (BIC (6 hours) = 4.76 ± 2.81 µM and BIC (24 hours) = 10.6 ± 3.77 µM) for either 6 hours or 24 hours then stained with 0.1% (v/v) crystal violet. Images were recorded with an inverted light microscope equipped with a camera and are representative of three independent experiments. Images were taken at 10× magnification. Scale bar = 100 µm.

The results demonstrate that tryptophan end-tagging improves the biofilm preventing activity of Os-C in RPMI-1640, a complex medium. To date, studies on the effect of tryptophan end-tagging were focused on the antiplanktonic activity of end-tagged peptides (12-16, 27). However, no study has investigated the effect of this modification on antibiofilm activity.

This study demonstrates that Os-C(W_5) has potent biofilm compared with Os-C. The BIC value obtained after 24 hours (11.2 ± 3.69 µM) is similar to BIC values of 10.8 µM obtained after

exposing *C. albicans* strains B2630 and B63195 to the plant peptide OSIP108 (28). Histatin 5 and its analogue K11R-K17R reduced *C. albicans* biofilm formation at millimolar concentrations with 6 mM histatin 5 reducing cell viability by 81.5% (29). NFAP2, derived from the filamentous fungus *Neosartorya fischeri* was inactive against a fluconazole-resistant strain of *C. albicans* with concentrations as high as 71.8 µM having no effect on cell viability (30). The cathelicidin-related AMP (CRAMP) was identified in the islets of Langerhans of the murine pancreas. One derivative, AS10, possessed strong biofilm preventing activity and had low BIC values ranging from 0.22 µM to 0.67 µM against various *C. albicans* strains (31).

5.3.2 Interference with cell adhesion

The initial step of biofilm formation involves the adhesion of cells to the surface. Therefore, the ideal antifungal agent should be able to prevent cell adhesion. As a result, no biofilm formation will occur. In this assay, AMB and Os-C(W_5) were incubated with *C. albicans*, and **Figure 5.6** shows the effect of both antifungals on *C. albicans* cell adhesion. Images of cells show that AMB and Os-C(W_5) do not prevent adhesion. However, AMB affects the morphology of cells with round microcolonies present following exposure to 0.078 µM and 0.156 µM while exposure to all concentrations of Os-C(W_5) does not affect the morphology of the cells (**Figure 5.6**). Since the images do not indicate whether adhesion is prevented, quantitative data was obtained by solubilising bound CV with 30% (v/v) acetic acid. Adhesion is significantly decreased by 20% following treatment with 0.078 µM AMB and 10 µM Os-C(W_5) (**Figure 5.6**).

Many AMPs were found to prevent the adhesion of *C. albicans* cells to surfaces. Treatment with non-lethal concentrations of 3 µM and 10 µM of the peptide LL-37 for 30 minutes reduced *C. albicans* adhesion to polystyrene and silicone surfaces by 35% and 59%, respectively (32). Another study observed that 64 µM LL-37 reduced the number of adherent *C. albicans* cells by 80% after 30 minutes (33). Psoriasin (1 µM) reduced adhesion of *C. albicans* to polystyrene by 20% within 30 minutes and adhesion studies in the presence of chitin, β-glucan and mannan indicated that adhesion was prevented by interactions with β-glucan (34). Histatin 5 (50 µg/mL) reduced the adherence of *C. albicans* cells to human oral epithelial cells and prevented the yeast-to-hyphae transition (35). Vukosavljevic *et al*. coated polymethylmethacrylate and hydroxyapatite surfaces with 3.41 µM and 3.87 µM histatin 5, respectively, and observed approximately 25% less adhesion to these surfaces within 90 minutes (36).

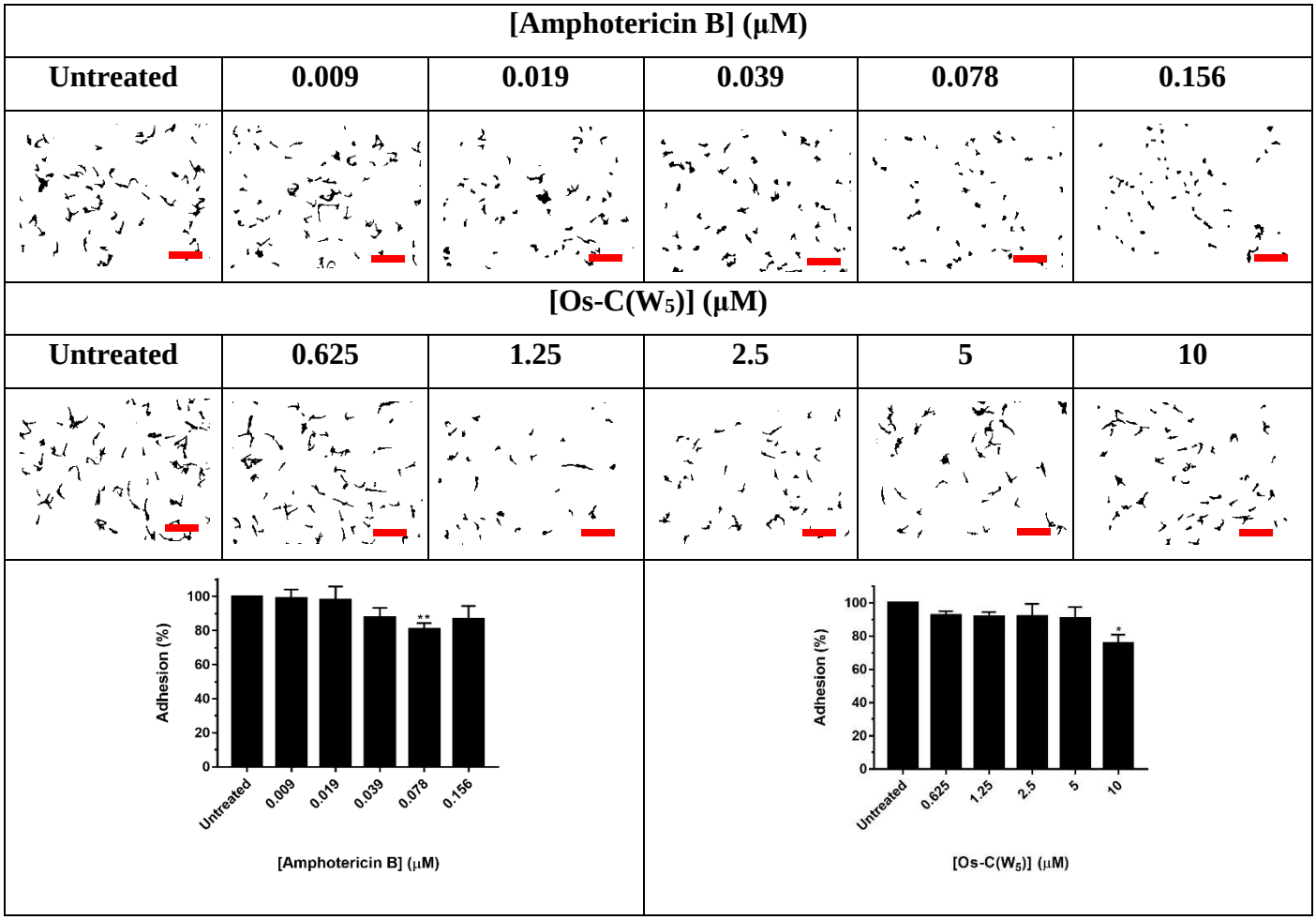

Figure 5.6: Effect of amphotericin B and Os-C(W_5) on *C. albicans* adhesion. *C. albicans* cells were exposed to amphotericin B (0.009 – 0.156 µM) and Os-C(W_5) (0.625 – 10 µM) for 1 hour. Cells were stained with 0.1% (v/v) crystal violet and adhesion was observed using an inverted light microscope equipped with a camera. Images were taken at 20× magnification and are representative of three independent experiments. Scale bar = 50 µm. Bound crystal violet was solubilised with 30% (v/v) acetic acid and quantified by measuring absorbance at 550 nm. Data represents the mean ± SEM of three independent experiments. A one-way ANOVA was performed followed by a post-hoc Dunnett's multiple comparisons test. Asterisks (*p < 0.05; **p < 0.01) represent a significant difference compared with the untreated control.

Based on the observations, prevention of adhesion may contribute to the mode of action of Os-C(W_5) to prevent biofilm formation. This is seen in the microscopy images where a few cells are present after 6 hours and 24 hours (**Figure 5.5**) following exposure to 12.5 – 100 µM of Os-C(W_5). The reduced hyphal network following exposure to 6.25 µM Os-C(W_5) at both timepoints could be linked to reduced cell adhesion which results in a less dense hyphal network.

5.3.3 Morphological transition

The transition from the yeast to the hyphal form aids fungi in evading the host immune response and increases the probability of the fungus entering and damaging host cells (37). Therefore, one approach to treating fungal infections could involve targeting virulence factors which prevents biofilm formation and increases susceptibility to antifungal drugs and components of the innate immune system (38). *Candida* forms hyphae in different environments such as RPMI-1640 medium, serum and N-acetylglucosamine through various pathways (39). Hyphal formation in serum and N-acetylglucosamine takes place via the cyclic adenosine monophosphate-protein kinase A (cAMP-PKA) pathway (39) which plays a role in *C. albicans* energy metabolism, mitochondrial activity, and glycogen synthesis (40, 41).

For the untreated control, hyphal formation activated in YPD broth supplemented with 10% foetal bovine serum, increases with time (**Figure 5.7**). Amphotericin B treatment for 2 hours does not prevent hyphal formation at any concentration. Furthermore, less hyphal formation is observed compared with the untreated control after 6 hours indicating that AMB prevents the yeast-to-hypha transition. Os-C(W_5) does not prevent the yeast-to-hypha transition after 2 hours or 6 hours but aggregates of microcolonies are present after 6 hours (**Figure 5.7**).

Prevention of the yeast-to-hyphal transition depends on the peptide concentration and the exposure time. Subinhibitory concentrations of ToAP2 (3.12 µM and 6.25 µM) and NDBP-5.7 (12.5 µM and 25 µM) did not reduce filamentation or germ tube length of *C. albicans* in RPMI-1640 within 4 hours but 6.25 µM ToAP2 reduced filamentation after 24 hours (42). Although some loss of adhesion is observed for Os-C(W_5) at a concentration close to the BIC (10 µM), the results show that this concentration does not prevent the yeast-to-hypha transition within 6 hours.

Serum inhibits the activity of AMPs due to the interaction of AMPs with serum proteins or degradation of AMPs by serum proteases (43). Therefore, the presence of serum (10% FBS) may inhibit the activity of Os-C(W_5). Since the yeast-to-hypha transition was not prevented in serum, it is possible that Os-C(W_5) may not prevent biofilm formation by targeting any hyphal filamentation-inducing pathways.

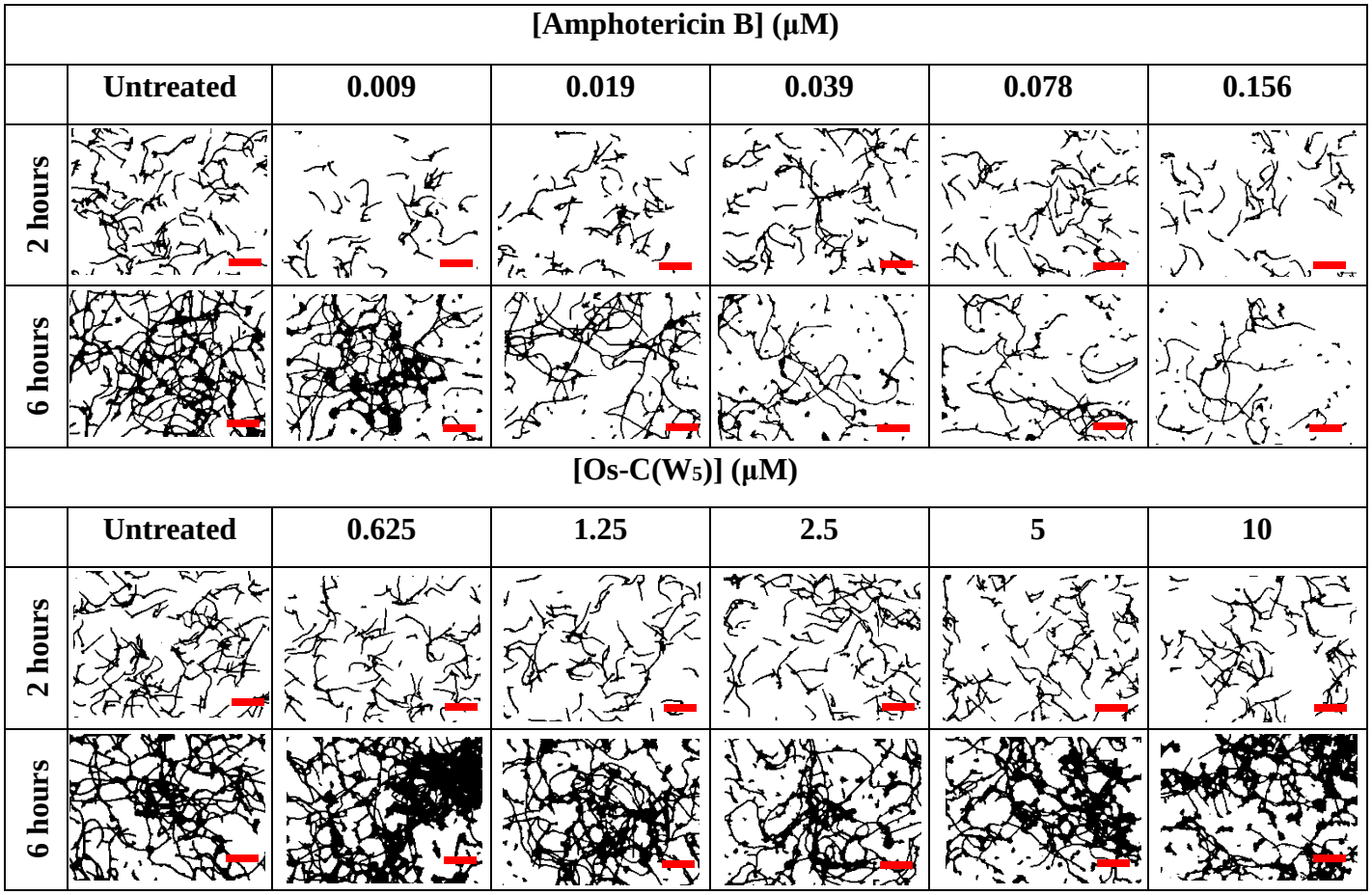

Figure 5.7: Effect of amphotericin B and Os-C(W_5) on the yeast-to-hypha transition. *C. albicans* cells were exposed to amphotericin B (0.009 – 0.156 µM) and Os-C(W_5) (0.625 – 10 µM) for either 2 hours or 6 hours. In the untreated control, hyphal formation is activated in YPD broth supplemented with 10% foetal bovine serum. Cells were stained with 0.1% (v/v) crystal violet and changes in morphology were recorded using an inverted light microscope equipped with a camera. Images were taken at 20× magnification and are representative of three independent experiments. Red arrows indicate aggregates of microcolonies. Scale bar = 50 µm.

5.3.4 Production of extracellular material

The ECM serves as a protective barrier for cells within the biofilm. Therefore, preventing ECM formation could render biofilm-associated cells more susceptible to antifungal drugs. The effect of antifungal molecules on ECM production can be quantified using quantitative reverse transcriptase PCR (44, 45), measurement of the ECM carbohydrate content using the phenol-sulfuric acid assay (46, 47) or by measuring the content of other ECM components (48). In this study, the amount of individual ECM carbohydrates, proteins and nucleic acids was measured (**Figure 5.8**) following exposure to AMB and Os-C(W_5). This approach to quantifying individual *C. albicans* ECM components has previously been applied to phytoactive compounds (49), colloidal nanoparticles (50), conjugated nanoparticles (20) and the antifungal drug fluconazole (51).

	Amphotericin B	Os-C(W_5)
Carbohydrates	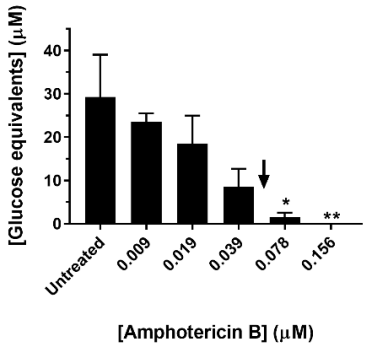	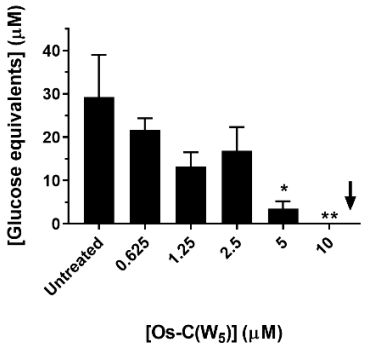
Proteins	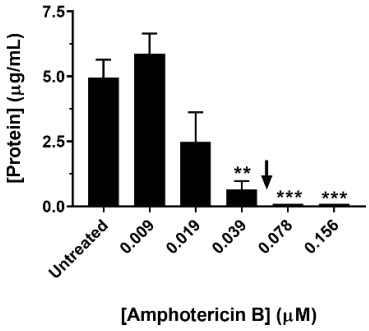	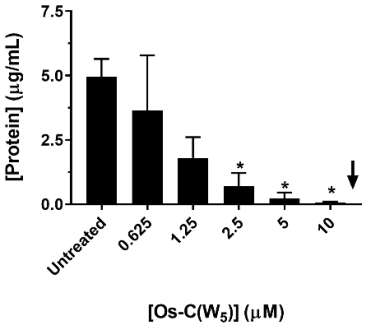
Extracellular nucleic acids	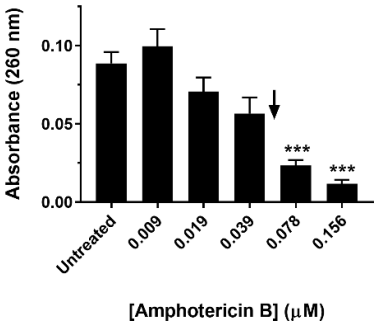	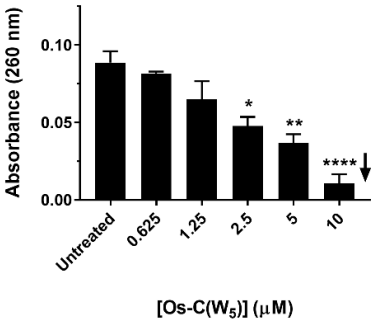

Figure 5.8: Effect of amphotericin B and Os-C(W_5) on the production of the extracellular matrix. *C. albicans* cells were grown in the presence of amphotericin B (0.009 – 0.156 μM) or Os-C(W_5) (0.625 – 10 μM) and soluble ECM was extracted from treated and untreated samples. Carbohydrate content was quantified using the phenol-sulfuric acid assay, protein concentration was measured using the bicinchoninic acid assay and nucleic acid content was quantified by measuring absorbance at 260 nm. Arrows indicate the respective biomass BIC values of amphotericin B (0.05 ± 0.02 μM) and Os-C(W_5) (10.6 ± 3.77 μM) following 24 hours of exposure. Data represents the mean ± SEM of three independent experiments. A one-way ANOVA was performed followed by a post-hoc Dunnett's multiple comparisons test. Asterisks (*p < 0.05; **p < 0.01; ***p < 0.001; ****p < 0.0001) represent a significant difference compared with the untreated control.

Using the phenol-sulfuric acid assay, Zarnowski *et al*. observed that carbohydrates make up approximately 25% of the *C. albicans* ECM and represent the most complex fraction of the

matrix (52). Monosaccharides such as glucose, xylose, mannose, and arabinose are present in the highest quantities (53). A significant reduction in carbohydrate content is observed at the two highest concentrations of AMB and Os-C(W_5) and no carbohydrates are detected following exposure to 10 µM Os-C(W_5) (**Figure 5.8**).

Zarnowski *et al*. identified proteins as the most abundant component of the ECM. The authors observed that proteins account for 55% of the dry weight of *C. albicans* ECM (52). Matrix proteins are thought to serve as linker molecules between extracellular polysaccharides and play a similar role to proteins in the cell wall (54). Exposure to AMB and Os-C(W_5) leads to a decrease in protein content of at least 80% after exposure to 0.039 – 0.156 µM AMB and 2.5 – 10 µM Os-C(W_5) (**Figure 5.8**).

Spectrophotometric measurement of isolated *C. albicans* ECM revealed that extracellular nucleic acids make up 5% of the *C. albicans* ECM (52). Many studies have noted the presence of extracellular DNA (52, 55), but a study by Smolarz *et al*. also noted the presence of extracellular RNA in the ECM of two different *C. albicans* strains (SC5314 and ATCC 10231) (56). The main function of extracellular nucleic acids is to maintain the structural integrity of the biofilm, but another possible feature may involve connecting matrix components (55). Exposure to 0.078 and 0.156 µM AMB leads to a 4- and 8-fold decrease in nucleic acid content, respectively. Os-C(W_5) treatment with 2.5 – 10 µM Os-C(W_5) leads to a 2- to 8-fold decrease in ECM nucleic acids (**Figure 5.8**). Overall, the data show that concentrations of Os-C(W_5) close to the BIC caused a relative reduction in ECM carbohydrates, proteins, and nucleic acids, and this could be due to fewer cells growing after Os-C(W_5) treatment. As a result, less biofilm and ECM formation occurs.

5.3.5 Biofilm eradication activity

The ideal antifungal agent should prevent biofilm formation and eradicate mature biofilms. Indwelling devices such as catheters and prosthetic valves provide the ideal surface for fungal cells to adhere to and eventually form a biofilm. In these situations, high doses of antifungals are used in antifungal lock therapy to eradicate the biofilm (57). To this end, *C. albicans* biofilms were formed over 24 hours and then exposed to several concentrations of AMB or Os-C(W_5). Amphotericin B reduces the viability and biomass of cells in the biofilm in a dose-dependent manner (**Figure 5.9A and 5.9B**) with BEC values of 0.08 ± 0.004 µM and 0.56 ± 0.20 µM, respectively (**Table 5.3**). A similar effect on viability and biomass is observed for

Os-C(W_5) with BEC values of 69.3 ± 11.3 µM and 87.4 ± 11.8 µM, respectively (**Figure 5.9C and 5.9D; Table 5.3**).

Table 5.3: Biofilm eradicating activity of amphotericin B and Os-C(W_5).

	BEC[a] (µM)	
	Viability	**Biomass**
Amphotericin B	0.08 ± 0.004	0.56 ± 0.20
Os-C(W_5)	69.3 ± 11.3	87.4 ± 11.8

[a] Lowest concentration of antifungal that reduced the viability or biomass of cells in a preformed biofilm by 50%. Data represents the mean ± SEM of three independent experiments.

The lowest concentration of AMB (0.009 µM) reduces viability by 26% with all concentrations greater than 0.039 µM reducing viability by over 50% and exposure to 2.5 µM AMB completely reduced cell viability (**Figure 5.9A**). All concentrations of AMB reduce biofilm biomass by at least 40% with 2.5 µM AMB reducing biomass by 79% (**Figure 5.9B**). Exposure to 50 µM and 100 µM Os-C(W_5) reduces cell viability by 30% and 81%, respectively (**Figure 5.9C**). Os-C(W_5) also affects biofilm biomass with notable reductions of 40% and 55% observed at 50 µM and 100 µM, respectively (**Figure 5.9D**). Although some AMPs have biofilm preventing activity, not many AMPs have biofilm eradicating activity. Experiments by Troskie *et al*. revealed that the tyrocidine peptides TrcA, TrcB and TrcC had BEC values of 145 µM, 164 µM and 133 µM, respectively (17). VLL-28, a peptide derived from an archaeal protein, was active against several *C. albicans* clinical isolates and the reference strain ATCC 10231 with a minimum BEC value of 50 µM (58).

Despite partially eradicating preformed biofilms, Os-C(W_5) has a greater effect on the viability of cells within the biofilm. Paulone *et al.* observed a similar outcome with the peptide KP which was active against *C. albicans* (ATCC SC5314) biofilms grown for 48 hours. KP (124 µM) significantly reduced biofilm biomass and viability by approximately 40% and 80%, respectively (45). D'Auria *et al*. saw a similar effect where 128 µM temporin G reduced the viability and biomass of 24-hour-old *C. albicans* (ATCC 10231) biofilms by approximately 75% and 25%, respectively (59).

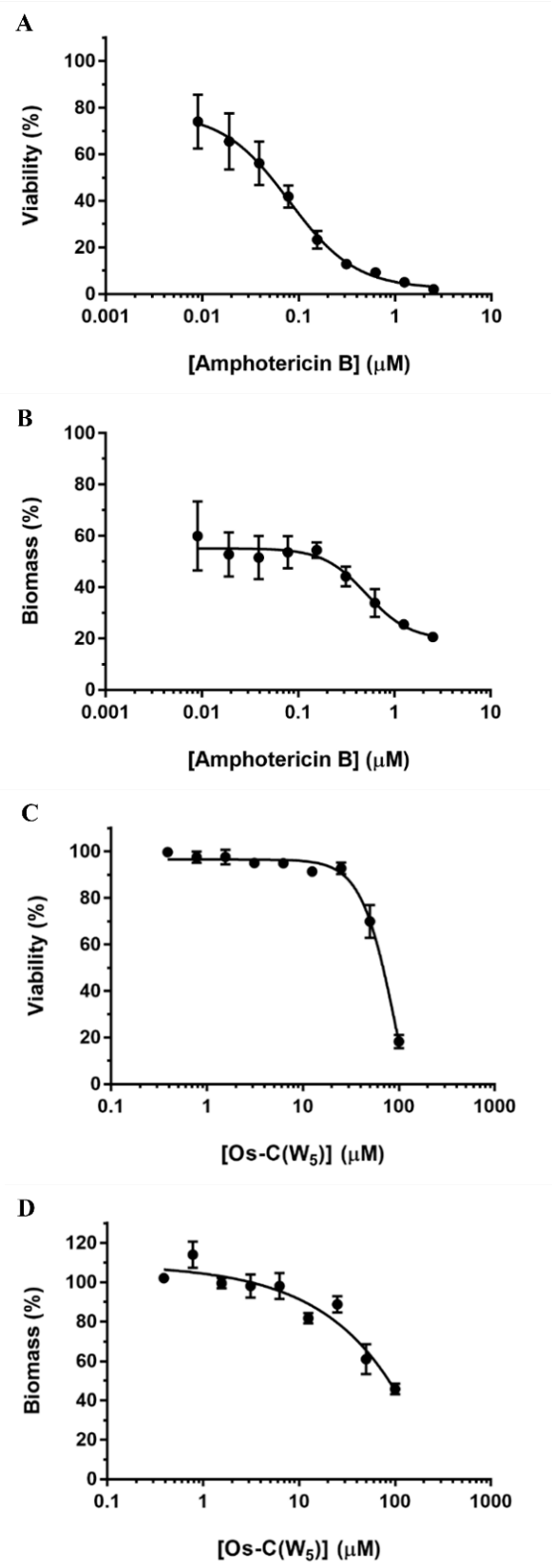

Figure 5.9: Biofilm eradicating activity of amphotericin B and Os-C(W_5). Preformed biofilms were treated with either (A and B) amphotericin B (0.009 – 2.5 μM) or (C and D) Os-C(W_5) (0.39 – 100 μM) for 24 hours then (A and C) viability was measured using CellTiter Blue cell viability assay. (B and D) Biofilm biomass was quantified by solubilising bound crystal violet with 30% acetic acid and measuring the absorbance at 550 nm. Data represent the mean ± SEM of three independent experiments.

Based on these findings, Os-C(W_5) may eradicate biofilms by direct killing of cells embedded within the biofilm. The peptides Seg6D and Seg6L eradicated preformed *P. aeruginosa* biofilms but had different modes of eradication. Confocal microscopy combined with colony count assays indicated that Seg6L detached cells from the biofilm while Seg6D eradicated the biofilm by directly killing cells in the biofilm (60). Further studies are necessary to determine how Os-C(W_5) eradicates preformed biofilms with specific focus on the cellular effects.

5.3.6 Antifungal activity in serum containing environments

An AMP must be active in the presence of serum, for the treatment of systemic infections and infected wounds. Therefore, the biofilm preventing and eradicating activities of AMB and Os-C(W_5) were investigated in two serum containing media. Synthetic wound medium represents a wound environment while RPMI-1640-50% FBS represents the extracellular environment.

Amphotericin B prevents biofilm formation in both environments and significantly reduces the biomass and viability of cells in the presence of RPMI-1640-50% FBS and SWM by almost 100%. Os-C(W_5) inhibits biofilm formation by reducing viability and biomass by 54% and 47% in RPMI-1640-50% FBS, respectively, while viability and biomass are reduced by 61% and 50% in SWM, respectively (**Figure 5.10**).

In the presence of preformed biofilms, AMB and Os-C(W_5) are less active in both media. Amphotericin B significantly reduces viability and biomass in RPMI-1640-50% FBS by 79% and 44%, respectively. In SWM, viability and biomass are reduced by 86% and 74%, respectively. For Os-C(W_5), the viability of preformed biofilms is significantly reduced by 18% in RPMI-1640-50% FBS and 30% in SWM, however, no significant reduction in biomass is observed in either media following treatment with Os-C(W_5) (**Figure 5.11**).

Foetal bovine serum is composed of proteins (serum proteins, transport proteins and enzymes), hormones, growth factors, cytokines, fatty acids, carbohydrates, vitamins, minerals, and inorganic compounds, all components that are necessary for cell growth and maintenance (61). Consequently, FBS is used as a universal growth supplement that is compatible with most human and animal cell types (62). Regarding *C. albicans*, serum enhances cell adherence and biofilm formation on acrylic strips, polystyrene surfaces, and denture lining materials (63). Furthermore, FBS is also known to induce the yeast-to-hypha transition, a key virulence factor of *C. albicans* pathogenesis (64, 65).

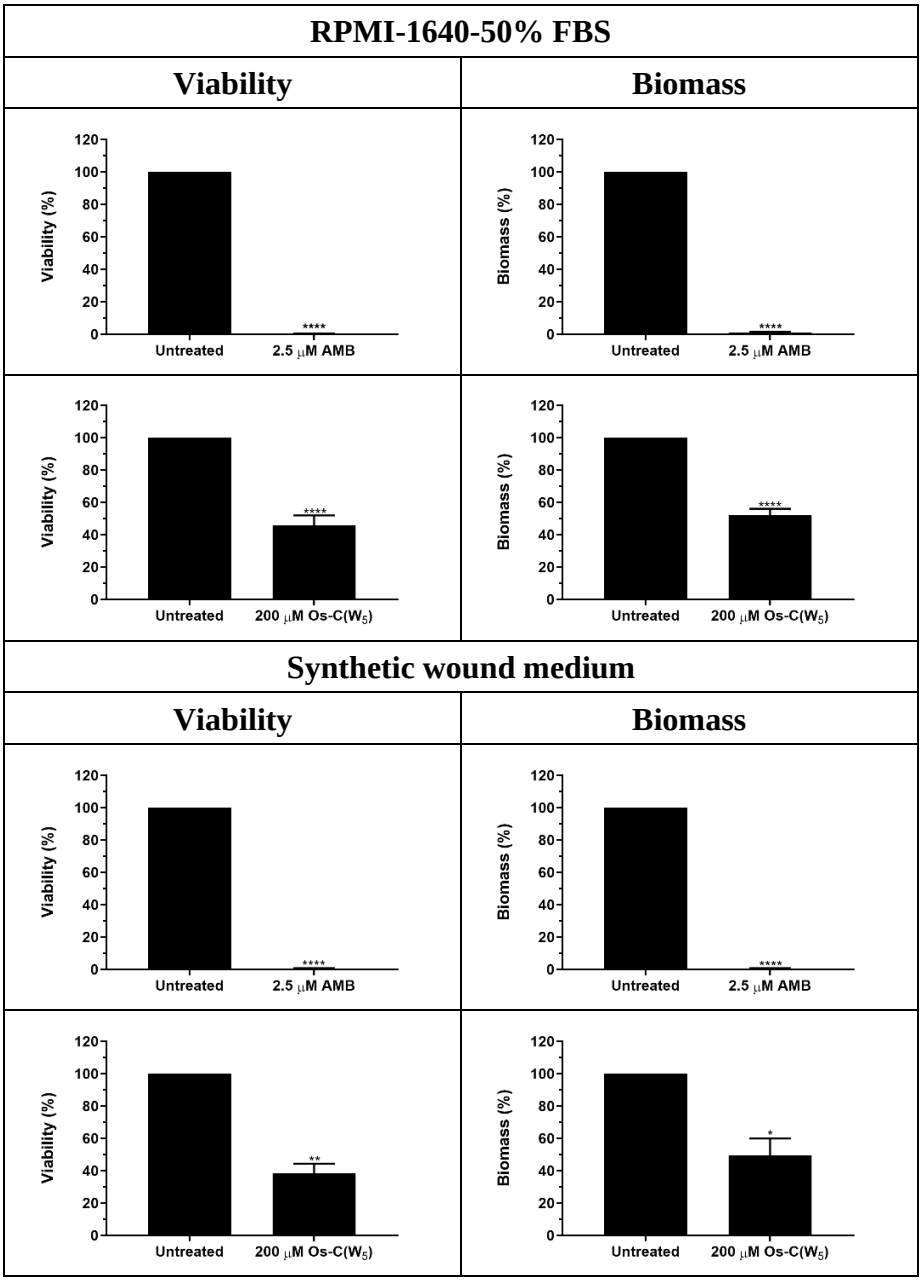

Figure 5.10: Biofilm preventing activity of amphotericin B (AMB) and Os-C(W_5) in serum containing media. *C. albicans* cells were treated with 2.5 µM amphotericin B or 200 µM Os-C(W_5) prepared in either RPMI-1640 supplemented with 50% FBS or synthetic wound medium. Viability was measured using the CellTiter Blue cell viability assay and biomass was measured using crystal violet staining. Data represent the mean ± SEM of three independent experiments. A one-way ANOVA was performed followed by a post-hoc Dunnett's multiple comparisons test. Asterisks (*$p < 0.05$; **$p < 0.01$; ****$p < 0.0001$) represent a significant difference compared with the untreated control.

The presence of serum does not affect the biofilm preventing activity of AMB but a reduction in biofilm eradicating activity is observed. In the absence of serum, 2.5 µM AMB reduces biofilm viability and biomass by 100% and 79%, respectively (**Figures 5.10A and B**). The addition of serum to RPMI-1640 medium leads to a 79% reduction in viability and a 44% reduction in the biomass of preformed biofilms by AMB and a similar biofilm eradicating effect is seen in the presence of SWM (**Figure 5.11**). Derdák *et al*. used fluorescence

polarisation to demonstrate that AMB interacts with human and bovine serum albumin (66). Therefore, reduced antibiofilm activity of AMB may be linked to interactions with serum albumin or other components of FBS.

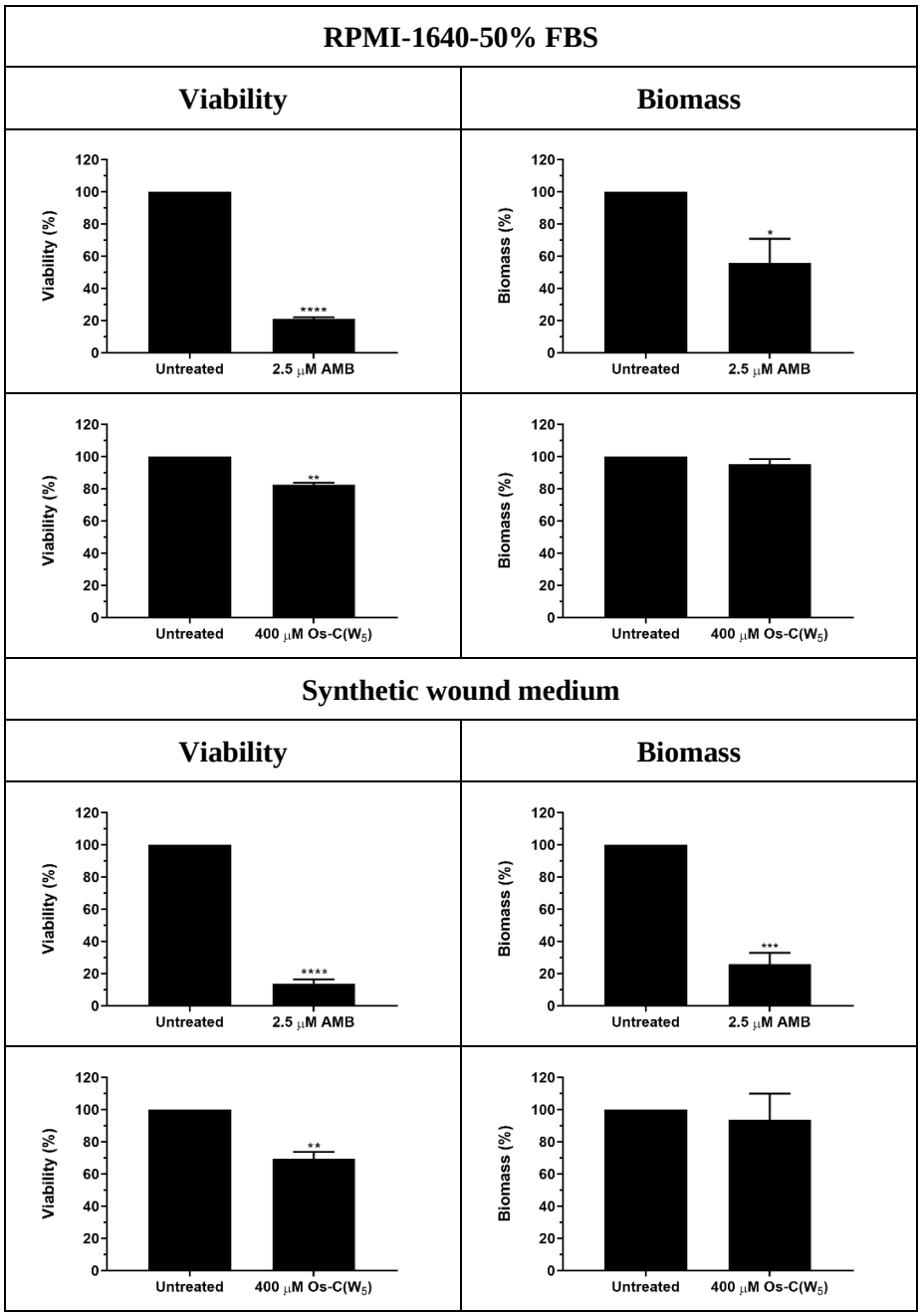

Figure 5.11: Biofilm eradicating activity of amphotericin B (AMB) and Os-C(W_5) in serum containing media. Preformed biofilms were treated with 2.5 μM amphotericin B or 400 μM Os-C(W_5) prepared in media containing either RPMI-1640 supplemented with 50% FBS or synthetic wound medium. Viability was measured using the CellTiter Blue cell viability assay and biomass was measured using crystal violet staining. Data represent the mean ± SEM of three independent experiments. A one-way ANOVA was performed followed by a post-hoc Dunnett's multiple comparisons test. Asterisks (*$p < 0.05$; **$p < 0.01$; ***$p < 0.001$; ****$p < 0.0001$) represent a significant difference compared with the untreated control.

The data reveals that although reduced, Os-C(W_5) retains some antibiofilm activity in a serum containing medium. A concentration approximately 20 times the BIC is required to reduce viability by approximately 50% in both media (**Figure 5.10**) while higher concentrations are required to achieve the same effect against preformed biofilms (**Figure 5.11**).

Similar inhibitory effects of serum were seen by Sonesson *et al*. who tested the activity of 30 µM GHK17WWWWW against planktonic *C. parapsilosis*. In the presence of 50% human serum, the peptide was approximately 50% less active than in physiological salt conditions (15). RI18, a peptide derived from PMAP-36, retained its antibacterial activity against planktonic *E. coli* but lost all antifungal activity against *C. albicans* (CGMCC 2.2086) in the presence of 25% and 50% human serum (67). DJK-5 inhibited *P. aeruginosa* biofilm formation, but activity was almost completely diminished in the presence of 10% FBS (68). The reduced activity of Os-C(W_5) in serum could be due to the interaction of the peptide with serum components such as albumin, proteolytic degradation or the preferential binding of serum components to the fungal membrane which precludes interactions between the peptide and the fungal membrane (69). To reduce these interactions and promote cellular killing in biofilms, drug delivery systems that limit these interactions and delivers Os-C(W_5) to the cell surface should be evaluated in future studies.

5.4 Conclusion

Tryptophan end-tagging enhances the biofilm preventing activity of Os-C. Os-C(W_5) prevents biofilm formation by reducing viability and biomass after treatment for 6 hours and 24 hours. Mode of action studies reveal that Os-C(W_5) reduces cell adhesion and ECM production at concentrations close to the BIC. Furthermore, Os-C(W_5) eradicates preformed biofilms by potentially targeting cells within the biofilm. Decreased production of ECM components by Os-C(W_5) may be linked to reduced cell viability which leads to reduced adhesion. When adhesion is reduced and cells that do attach are targeted, ECM production is reduced, and no biofilm formation is observed. Although reduced, Os-C(W_5) retains some antibiofilm activity in the presence of FBS containing media. Therefore, improving delivery of the peptide may increase activity in the presence of serum and reduce the effect of proteases.

5.5 References

1. Jamal, M., Ahmad, W., Andleeb, S., Jalil, F., Imran, M., Nawaz, M. A., Hussain, T., Ali, M., Rafiq, M., and Kamil, M. A. (2018) Bacterial biofilm and associated infections. *Journal of the Chinese Medical Association* **81**, 7-11. 10.1016/j.jcma.2017.07.012
2. Pfaller, M. A., and Diekema, D. J. (2007) Epidemiology of invasive candidiasis: a persistent public health problem. *Clinical Microbiology Reviews* **20**, 133-163. 10.1128/CMR.00029-06
3. Kojic, E. M., and Darouiche, R. O. (2004) *Candida* infections of medical devices. *Clinical Microbiology Reviews* **17**, 255-267. 10.1128/CMR.17.2.255-267.2004
4. Sanguinetti, M., Posteraro, B., and Lass-Florl, C. (2015) Antifungal drug resistance among *Candida* species: mechanisms and clinical impact. *Mycoses* **58**, 2-13. 10.1111/myc.12330
5. Nett, J. E., Crawford, K., Marchillo, K., and Andes, D. R. (2010) Role of Fks1p and matrix glucan in *Candida albicans* biofilm resistance to an echinocandin, pyrimidine, and polyene. *Antimicrobial Agents and Chemotherapy* **54**, 3505-3508. 10.1128/AAC.00227-10
6. Taff, H. T., Nett, J. E., Zarnowski, R., Ross, K. M., Sanchez, H., Cain, M. T., Hamaker, J., Mitchell, A. P., and Andes, D. R. (2012) A *Candida* biofilm-induced pathway for matrix glucan delivery: implications for drug resistance. *PLoS Pathogens* **8**, e1002848-e1002860. 10.1371/journal.ppat.1002848
7. Johnson, C. J., Cabezas-Olcoz, J., Kernien, J. F., Wang, S. X., Beebe, D. J., Huttenlocher, A., Ansari, H., and Nett, J. E. (2016) The extracellular matrix of *Candida albicans* biofilms impairs formation of neutrophil extracellular traps. *PLoS Pathogens* **12**, e1005884-e1005906. 10.1371/journal.ppat.1005884
8. Di Luca, M., Maccari, G., Maisetta, G., and Batoni, G. (2015) BaAMPs: the database of biofilm-active antimicrobial peptides. *Biofouling* **31**, 193-199. 10.1080/08927014.2015.1021340
9. Chandra, J., Mukherjee, P. K., and Ghannoum, M. A. (2012) *Candida* biofilms associated with CVC and medical devices. *Mycoses* **55**, 46-57. 10.1111/j.1439-0507.2011.02149.x
10. Mushi, M. F., Bader, O., Taverne-Ghadwal, L., Bii, C., Gross, U., and Mshana, S. E. (2017) Oral candidiasis among African human immunodeficiency virus-infected

individuals: 10 years of systematic review and meta-analysis from sub-Saharan Africa. *Journal of Oral Microbiology* **9**, 1317579-1317588. 10.1080/20002297.2017.1317579

11. Pasupuleti, M., Schmidtchen, A., Chalupka, A., Ringstad, L., and Malmsten, M. (2009) End-tagging of ultra-short antimicrobial peptides by W/F stretches to facilitate bacterial killing. *PLoS One* **4**, e5285-e5294. 10.1371/journal.pone.0005285
12. Pasupuleti, M., Chalupka, A., Morgelin, M., Schmidtchen, A., and Malmsten, M. (2009) Tryptophan end-tagging of antimicrobial peptides for increased potency against *Pseudomonas aeruginosa*. *Biochimica et Biophysica Acta* **1790**, 800-808. 10.1016/j.bbagen.2009.03.029
13. Schmidtchen, A., Pasupuleti, M., Morgelin, M., Davoudi, M., Alenfall, J., Chalupka, A., and Malmsten, M. (2009) Boosting antimicrobial peptides by hydrophobic oligopeptide end tags. *Journal of Biological Chemistry* **284**, 17584-17594. 10.1074/jbc.M109.011650
14. Schmidtchen, A., Ringstad, L., Kasetty, G., Mizuno, H., Rutland, M. W., and Malmsten, M. (2011) Membrane selectivity by W-tagging of antimicrobial peptides. *Biochimica et Biophysica Acta* **1808**, 1081-1091. 10.1016/j.bbamem.2010.12.020
15. Sonesson, A., Nordahl, E. A., Malmsten, M., and Schmidtchen, A. (2011) Antifungal activities of peptides derived from domain 5 of high-molecular-weight kininogen. *International Journal of Peptides* **2011**, 761037-761047. 10.1155/2011/761037
16. Strömstedt, A. A., Pasupuleti, M., Schmidtchen, A., and Malmsten, M. (2009) Oligotryptophan-tagged antimicrobial peptides and the role of the cationic sequence. *Biochimica et Biophysica Acta (BBA) - Biomembranes* **1788**, 1916-1923. 10.1016/j.bbamem.2009.06.001
17. Troskie, A. M., Rautenbach, M., Delattin, N., Vosloo, J. A., Dathe, M., Cammue, B. P. A., and Thevissen, K. (2014) Synergistic activity of the tyrocidines, antimicrobial cyclodecapeptides from *Bacillus aneurinolyticus*, with amphotericin B and caspofungin against *Candida albicans* biofilms. *Antimicrobial Agents and Chemotherapy* **58**, 3697-3707. 10.1128/AAC.02381-14
18. Li, X., Yan, Z., and Xu, J. (2003) Quantitative variation of biofilms among strains in natural populations of *Candida albicans*. *Microbiology (Reading)* **149**, 353-362. 10.1099/mic.0.25932-0
19. Li, Y., Chang, W., Zhang, M., Ying, Z., and Lou, H. (2015) Natural product solasodine-3-O-beta-D-glucopyranoside inhibits the virulence factors of *Candida albicans*. *FEMS Yeast Research* **15**, 10.1093/femsyr/fov060

20. Gupta, P., Goel, A., Singh, K. R., Meher, M. K., Gulati, K., and Poluri, K. M. (2021) Dissecting the anti-biofilm potency of kappa-carrageenan capped silver nanoparticles against *Candida* species. *International Journal of Biological Macromolecules* **172**, 30-40. 10.1016/j.ijbiomac.2021.01.035

21. Masuko, T., Minami, A., Iwasaki, N., Majima, T., Nishimura, S., and Lee, Y. C. (2005) Carbohydrate analysis by a phenol-sulfuric acid method in microplate format. *Analytical Biochemistry* **339**, 69-72. 10.1016/j.ab.2004.12.001

22. Hammer, K. A., Carson, C. F., and Riley, T. V. (2004) Antifungal effects of *Melaleuca alternifolia* (tea tree) oil and its components on *Candida albicans*, *Candida glabrata* and *Saccharomyces cerevisiae. Journal of Antimicrobial Chemotherapy* **53**, 1081-1085. 10.1093/jac/dkh243

23. Nobile, C. J., and Johnson, A. D. (2015) *Candida albicans* biofilms and human disease. *Annual Reviews of Microbiology* **69**, 71-92. 10.1146/annurev-micro-091014-104330

24. Nett, J. E., and Andes, D. R. (2016) Antifungal agents: spectrum of activity, pharmacology, and clinical indications. *Infectious Disease Clinics of North America* **30**, 51-83. 10.1016/j.idc.2015.10.012

25. Ramchuran, E. J., Pérez-Guillén, I., Bester, L. A., Khan, R., Albericio, F., Viñas, M., and de la Torre, B. G. (2021) Super-cationic peptide dendrimers-synthesis and evaluation as antimicrobial agents. *Antibiotics (Basel)* **10**, 1-13. 10.3390/antibiotics10060695

26. Lopes, J. L., Nobre, T. M., Siano, A., Humpola, V., Bossolan, N. R., Zaniquelli, M. E., Tonarelli, G., and Beltramini, L. M. (2009) Disruption of *Saccharomyces cerevisiae* by Plantaricin 149 and investigation of its mechanism of action with biomembrane model systems. *Biochimica et Biophysica Acta* **1788**, 2252-2258. 10.1016/j.bbamem.2009.06.026

27. Pasupuleti, M., Schmidtchen, A., and Malmsten, M. (2012) Antimicrobial peptides: key components of the innate immune system. *Critical Reviews in Biotechnology* **32**, 143-171. 10.3109/07388551.2011.594423

28. Delattin, N., De Brucker, K., Craik, D. J., Cheneval, O., Frohlich, M., Veber, M., Girandon, L., Davis, T. R., Weeks, A. E., Kumamoto, C. A., Cos, P., Coenye, T., De Coninck, B., Cammue, B. P. A., and Thevissen, K. (2014) Plant-derived decapeptide OSIP108 interferes with *Candida albicans* biofilm formation without affecting cell viability. *Antimicrobial Agents and Chemotherapy* **58**, 2647-2656. 10.1128/AAC.01274-13

29. Moghaddam-Taaheri, P., Leissa, J. A., Eppler, H. B., Jewell, C. M., and Karlsson, A. J. (2021) Histatin 5 variant reduces *Candida albicans* biofilm viability and inhibits biofilm formation. *Fungal Genetics and Biology* **149**, 103529-103536. 10.1016/j.fgb.2021.103529

30. Kovacs, R., Holzknecht, J., Hargitai, Z., Papp, C., Farkas, A., Borics, A., Toth, L., Varadi, G., Toth, G., Kovacs, I., Dubrac, S., Majoros, L., Marx, F., and Galgoczy, L. (2019) *In vivo* applicability of *Neosartorya fischeri* antifungal protein 2 (NFAP2) in treament of vulvovaginal candididiasis. *Antimicrobial Agents and Chemotherapy* **63**, 1-12. 10.1128/aac

31. De Brucker, K., Delattin, N., Robijns, S., Steenackers, H., Verstraeten, N., Landuyt, B., Luyten, W., Schoofs, L., Dovgan, B., Frohlich, M., Michiels, J., Vanderleyden, J., Cammue, B. P. A., and Thevissen, K. (2014) Derivatives of the mouse cathelicidin-related antimicrobial peptide (CRAMP) inhibit fungal and bacterial biofilm formation. *Antimicrobial Agents and Chemotherapy* **58**, 5395-5404. 10.1128/AAC.03045-14

32. Chang, H. T., Tsai, P. W., Huang, H. H., Liu, Y. S., Chien, T. S., and Lan, C. Y. (2012) LL37 and hBD-3 elevate the beta-1,3-exoglucanase activity of *Candida albicans* Xog1p, resulting in reduced fungal adhesion to plastic. *Biochemistry Journal* **441**, 963-970. 10.1042/BJ20111454

33. Scarsini, M., Tomasinsig, L., Arzese, A., D'Este, F., Oro, D., and Skerlavaj, B. (2015) Antifungal activity of cathelicidin peptides against planktonic and biofilm cultures of *Candida* species isolated from vaginal infections. *Peptides* **71**, 211-221. 10.1016/j.peptides.2015.07.023

34. Brauner, A., Alvendal, C., Chromek, M., Stopsack, K. H., Ehrstrom, S., Schroder, J. M., and Bohm-Starke, N. (2018) Psoriasin, a novel anti-*Candida albicans* adhesin. *Journal of Molecular Medicine* **96**, 537-545. 10.1007/s00109-018-1637-6

35. Moffa, E. B., Mussi, M. C., Xiao, Y., Garrido, S. S., Machado, M. A., Giampaolo, E. T., and Siqueira, W. L. (2015) Histatin 5 inhibits adhesion of *C. albicans* to reconstructed human oral epithelium. *Frontiers in Microbiology* **6**, 1-7. 10.3389/fmicb.2015.00885

36. Vukosavljevic, D., Custodio, W., Del Bel Cury, A. A., and Siqueira, W. L. (2012) The effect of histatin 5, adsorbed on PMMA and hydroxyapatite, on *Candida albicans* colonization. *Yeast* **29**, 459-466. 10.1002/yea.2925

37. Uwamahoro, N., Verma-Gaur, J., Shen, H. H., Qu, Y., Lewis, R., Lu, J., Bambery, K., Masters, S. L., Vince, J. E., Naderer, T., and Traven, A. (2014) The pathogen *Candida*

albicans hijacks pyroptosis for escape from macrophages. *mBio* **5**, e00003-e00014. 10.1128/mBio.00003-14

38. Mayer, F. L., and Kronstad, J. W. (2017) Disarming fungal pathogens: *Bacillus safensis* inhibits virulence factor production and biofilm formation by *Cryptococcus neoformans* and *Candida albicans*. *mBio* **8**, 1-22. 10.1128/mBio.01537-17
39. Chen, H., Zhou, X., Ren, B., and Cheng, L. (2020) The regulation of hyphae growth in *Candida albicans*. *Virulence* **11**, 337-348. 10.1080/21505594.2020.1748930
40. Sun, W., Zhang, L., Lu, X., Feng, L., and Sun, S. (2019) The synergistic antifungal effects of sodium phenylbutyrate combined with azoles against *Candida albicans* via the regulation of the Ras-cAMP-PKA signalling pathway and virulence. *Canadian Journal of Microbiology* **65**, 105-115. 10.1139/cjm-2018-0337
41. Lin, C. J., and Chen, Y. L. (2018) Conserved and divergent functions of the cAMP/PKA signaling pathway in *Candida albicans* and *Candida tropicalis*. *Journal of Fungi (Basel)* **4**, 1-11. 10.3390/jof4020068
42. do Nascimento Dias, J., de Souza Silva, C., de Araujo, A. R., Souza, J. M. T., de Holanda Veloso Junior, P. H., Cabral, W. F., da Gloria da Silva, M., Eaton, P., de Souza de Almeida Leite, J. R., Nicola, A. M., Albuquerque, P., and Silva-Pereira, I. (2020) Mechanisms of action of antimicrobial peptides ToAP2 and NDBP-5.7 against *Candida albicans* planktonic and biofilm cells. *Scientific Reports* **10**, 10327-10340. 10.1038/s41598-020-67041-2
43. Marr, A. K., Gooderham, W. J., and Hancock, R. E. W. (2006) Antibacterial peptides for therapeutic use: obstacles and realistic outlook. *Current Opinion in Pharmacology* **6**, 468-472. 10.1016/j.coph.2006.04.006
44. Morici, P., Fais, R., Rizzato, C., Tavanti, A., and Lupetti, A. (2016) Inhibition of *Candida albicans* biofilm formation by the synthetic lactoferricin derived peptide hLF1-11. *PLoS One* **11**, e0167470-e0167484. 10.1371/journal.pone.0167470
45. Paulone, S., Ardizzoni, A., Tavanti, A., Piccinelli, S., Rizzato, C., Lupetti, A., Colombari, B., Pericolini, E., Polonelli, L., Magliani, W., Conti, S., Posteraro, B., Cermelli, C., Blasi, E., and Peppoloni, S. (2017) The synthetic killer peptide KP impairs *Candida albicans* biofilm *in vitro*. *PLoS One* **12**, e0181278-e0181295. 10.1371/journal.pone.0181278
46. Padmavathi, A. R., Bakkiyaraj, D., Thajuddin, N., and Pandian, S. K. (2015) Effect of 2, 4-di-tert-butylphenol on growth and biofilm formation by an opportunistic fungus *Candida albicans*. *Biofouling* **31**, 565-574. 10.1080/08927014.2015.1077383

47. Yang, L. F., Liu, X., Lv, L. L., Ma, Z. M., Feng, X. C., and Ma, T. H. (2018) Dracorhodin perchlorate inhibits biofilm formation and virulence factors of *Candida albicans*. *Journal of Medical Mycology* **28**, 36-44. 10.1016/j.mycmed.2017.12.011

48. Silva, S., Henriques, M., Martins, A., Oliveira, R., Williams, D., and Azeredo, J. (2009) Biofilms of non-*Candida albicans Candida* species: quantification, structure and matrix composition. *Medical Mycology* **47**, 681-689. 10.3109/13693780802549594

49. Gupta, P., Gupta, S., Sharma, M., Kumar, N., Pruthi, V., and Poluri, K. M. (2018) Effectiveness of phytoactive molecules on transcriptional expression, biofilm matrix, and cell wall components of *Candida glabrata* and its clinical isolates. *ACS Omega* **3**, 12201-12214. 10.1021/acsomega.8b01856

50. Monteiro, D. R., lva, S., Negri, M., Gorup, L. F., de Camargo, E. R., Oliveira, R., Barbosa, D. B., and Henriques, M. (2013) Silver colloidal nanoparticles: effect on matrix composition and structure of *Candida albicans* and *Candida glabrata* biofilms. *Journal of Applied Microbiology* **114**, 1175-1183. 10.1111/jam.12102

51. Fonseca, E., Silva, S., Rodrigues, C. F., Alves, C. T., Azeredo, J., and Henriques, M. (2014) Effects of fluconazole on *Candida glabrata* biofilms and its relationship with ABC transporter gene expression. *Biofouling* **30**, 447-457. 10.1080/08927014.2014.886108

52. Zarnowski, R., Westler, W. M., Lacmbouh, G. A., Marita, J. M., Bothe, J. R., Bernhardt, J., Lounes-Hadj Sahraoui, A., Fontaine, J., Sanchez, H., Hatfield, R. D., Ntambi, J. M., Nett, J. E., Mitchell, A. P., and Andes, D. R. (2014) Novel entries in a fungal biofilm matrix encyclopedia. *mBio* **5**, e01333-01314. 10.1128/mBio.01333-14

53. Zarnowski, R., Sanchez, H., Covelli, A. S., Dominguez, E., Jaromin, A., Bernhardt, J., Mitchell, K. F., Heiss, C., Azadi, P., Mitchell, A., and Andes, D. R. (2018) *Candida albicans* biofilm-induced vesicles confer drug resistance through matrix biogenesis. *PLoS Biology* **16**, e2006872-e2006889. 10.1371/journal.pbio.2006872

54. Chaffin, W. L., Lopez-Ribot, J. L., Casanova, M., Gozalbo, D., and Martinez, J. P. (1998) Cell wall and secreted proteins of *Candida albicans*: identification, function, and expression. *Microbiology and Molecular Biology Reviews* **62**, 130-180. 10.1128/MMBR.62.1.130-180.1998

55. Martins, M., Uppuluri, P., Thomas, D. P., Cleary, I. A., Henriques, M., Lopez-Ribot, J. L., and Oliveira, R. (2010) Presence of extracellular DNA in the *Candida albicans* biofilm matrix and its contribution to biofilms. *Mycopathologia* **169**, 323-331. 10.1007/s11046-009-9264-y

56. Smolarz, M., Zawrotniak, M., Satala, D., and Rapala-Kozik, M. (2021) Extracellular nucleic acids present in the *Candida albicans* biofilm trigger the release of neutrophil extracellular traps. *Frontiers in Cellular and Infection Microbiology* **11**, 681030-681046. 10.3389/fcimb.2021.681030

57. Atriwal, T., Azeem, K., Husain, F. M., Hussain, A., Khan, M. N., Alajmi, M. F., and Abid, M. (2021) Mechanistic understanding of *Candida albicans* biofilm formation and approaches for its inhibition. *Frontiers in Microbiology* **12**, 638609-638642. 10.3389/fmicb.2021.638609

58. Roscetto, E., Contursi, P., Vollaro, A., Fusco, S., Notomista, E., and Catania, M. R. (2018) Antifungal and anti-biofilm activity of the first cryptic antimicrobial peptide from an archaeal protein against *Candida* spp. clinical isolates. *Scientific Reports* **8**, 17570-17580. 10.1038/s41598-018-35530-0

59. D'Auria, F. D., Casciaro, B., De Angelis, M., Marcocci, M. E., Palamara, A. T., Nencioni, L., Mangoni, M. L. (2022) Antifungal activity of the frog skin peptide temporin G and its effect on *Candida albicans* virulence factors. *International Journal of Molecular Sciences* **23**, 1-18. 10.3390/ijms23116345

60. Segev-Zarko, L., Saar-Dover, R., Brumfeld, V., Mangoni, M. L., and Shai, Y. (2015) Mechanisms of biofilm inhibition and degradation by antimicrobial peptides. *Biochemical Journal* **468**, 259-270. 10.1042/BJ20141251

61. Lee, D. Y., Lee, S. Y., Yun, S. H., Jeong, J. W., Kim, J. H., Kim, H. W., Choi, J. S., Kim, G. D., Joo, S. T., Choi, I., and Hur, S. J. (2022) Review of the current research on fetal bovine serum and the development of cultured meat. *Food Science of Animal Resources* **42**, 775-799. 10.5851/kosfa.2022.e46

62. Brunner, D., Frank, J., Appl, H., Schöffl, H., Pfaller, W. and Gstraunthaler, G. (2010) Serum-free cell culture: the serum-free media interactive online database. *ALTEX* **27**, 53-62. 10.14573/altex.2010.1.53

63. Frade, J. P., and Arthington-Skaggs, B. A. (2011) Effect of serum and surface characteristics on *Candida albicans* biofilm formation. *Mycoses* **54**, e154-e162. 10.1111/j.1439-0507.2010.01862.x

64. Yang, L., Liu, X., Sui, Y., Ma, Z., Feng, X., Wang, F., and Ma, T. (2019) Lycorine hydrochloride inhibits the virulence traits of *Candida albicans*. *Biomed Research International* **2019**, 1851740-1851750. 10.1155/2019/1851740

65. Romo, J. A., Pierce, C. G., Chaturvedi, A. K., Lazzell, A. L., McHardy, S. F., Saville, S. P., and Lopez-Ribot, J. L. (2017) Development of anti-virulence approaches for

candidiasis via a novel series of small-molecule inhibitors of *Candida albicans* filamentation. *mBio* **8**, 1-16. 10.1128/mBio.01991-17

66. Derdák, D., Poór, M., Kunsági-Máté, S., and Lemli, B. (2019) Interaction of amphotericin B with human and bovine serum albumins: a fluorescence polarization study. *Chemical Physics Letters* **724**, 13-17. 10.1016/j.cplett.2019.03.049
67. Lyu, Y., Yang, Y., Lyu, X., Dong, N., and Shan, A. (2016) Antimicrobial activity, improved cell selectivity and mode of action of short PMAP-36-derived peptides against bacteria and *Candida. Scientific Reports* **6**, 27258-27269. 10.1038/srep27258
68. Crabbe, A., Liu, Y., Matthijs, N., Rigole, P., De La Fuente-Nunez, C., Davis, R., Ledesma, M. A., Sarker, S., Van Houdt, R., Hancock, R. E., Coenye, T., and Nickerson, C. A. (2017) Antimicrobial efficacy against *Pseudomonas aeruginosa* biofilm formation in a three-dimensional lung epithelial model and the influence of fetal bovine serum. *Scientific Reports* **7**, 43321-43333 10.1038/srep43321
69. Hein-Kristensen, L., Knapp, K. M., Franzyk, H., and Gram, L. (2013) Selectivity in the potentiation of antibacterial activity of α-peptide/β-peptoid peptidomimetics and antimicrobial peptides by human blood plasma. *Research in Microbiology* **164**, 933-940. 10.1016/j.resmic.2013.08.002

Chapter 6: Concluding Discussion

Global reports concerning the impact of fungal infections in clinical settings where there is limited access to antifungal treatments and a low standard of care paints a dire picture of the current state of antifungal development (1). The escalating incidence of fungal infections within clinical settings is on the rise due to increased chronic, systemic, and recurrent fungal infections. Patient populations who are more susceptible to these infections include those with drug-induced immunosuppression or comorbidities such as AIDS and recipients of stem cell and organ transplants (2). The emergence of multidrug-resistant fungi such as *C. auris* (3) coupled with the development of resistance to current antifungal drugs means that there is a need for new antifungal agents and approaches.

Development of new antifungal agents takes many years and requires considerable financial investment. This is further complicated by the similarities shared by mammalian and fungal cells meaning that new antifungal agents must have targets that are specific to fungal cells (4). Previous and current research on antifungal drugs focuses on antifungal agents that target the cell wall, cell membrane and metabolic pathways that are exclusive to fungi (5). Increased knowledge regarding fungal cell genomics and proteomics enables researchers to better understand existing drug targets and identify other potential targets (5, 6). An alternative approach to developing novel antifungal agents is drug repurposing in which new uses are found for old, existing and available drugs that have received regulatory approval (7). This approach expedites the drug development process since the pharmacodynamic, pharmacokinetic and toxicity profiles are already known. Examples of repurposed drugs that show potential as antifungal agents include the anti-inflammatory drug diclofenac (8) and the celecoxib derivative AR-12 (9).

This study sought to demonstrate that AMPs could serve as a source of novel antifungal agents. Antimicrobial peptides are present in eukaryotes and prokaryotes and are potential alternatives or leads for the development of new antifungal drugs due to their role in the innate immune system, protecting the host from bacterial, fungal, viral and protozoan infections (10). Most AMPs are short, cationic, amphipathic, have broad-spectrum activity and possess multiple modes of cell killing (11). In March 2023, the echinocandin lipopeptide rezafungin received approval from the United States Food and Drug Administration for the treatment of

candidaemia and invasive candidiasis (12). Fewer side effects and a longer half-life make rezafungin a more favourable treatment compared with other echinocandins (13).

Os-C displayed potent antimicrobial activity against Gram-negative bacteria, Gram-positive bacteria and the fungus *C. albicans* (ATCC 90028) without toxicity towards human erythrocytes and cell lines (14, 15). Os-C was previously shown to be inactive in the presence of LB broth (15) and this present study shows that Os-C is also inactive in RPMI-1640. Most AMPs are inactive when tested in complex fluids such as serum and under physiological salt conditions (16). Lack of activity in serum is due to proteolytic degradation and proteins that bind to AMPs (17). In salts, inactivity can be caused by the binding of salt-associated cations to the negatively charged components of the cell membrane which prevents electrostatic interactions between AMPs and the membrane and a subsequent loss of activity (18).

Previous studies overcame the inactivity in physiological salt conditions by tagging peptides with hydrophobic stretches of amino acids with tryptophan and phenylalanine proving to be the most potent end-tags (19). Tryptophan and phenylalanine tend to be found in the interfacial region close to the polar lipid headgroups of phospholipids and do not insert deeply into the lipid membrane (20). As a result, tryptophan and phenylalanine residues act as an anchor for the peptide which leads to enhanced salt resistance (21) and antimicrobial activity (22, 23). Another benefit of hydrophobic end-tagging is that the sequence of the peptide is not affected since the end-tags are either on the N- or C-terminus (24).

Hydrophobic end-tagging increases the hydrophobicity of the peptide, making it more likely to be cytotoxic towards eukaryotic cells. Therefore, the number of hydrophobic residues must be optimised if fungal cells are the target. Antifungal activity is made possible due to differences in the cell membrane composition of mammalian membranes which contain cholesterol and fungal membranes which contain ergosterol. Cholesterol condenses the membrane which prevents the insertion of peptides due to the high energetic costs required for membrane insertion (25). On the other hand, ergosterol has a lower membrane condensing effect, meaning that less energy is required for insertion to occur. This was demonstrated by Sonesson *et al.* who observed greater membrane disruption of ergosterol containing liposomes by the peptide GKH17WWW compared with cholesterol containing liposomes indicating that the peptide could be non-cytotoxic (26). Another study showed that Os-C(W_5) is not cytotoxic towards human erythrocytes (R. Chirombo, MSc dissertation, 2023). Therefore, hydrophobic end-tagging is an attractive approach for enhancing the antimicrobial activity of salt-sensitive

peptides without compromising the original peptide sequence and enhancing toxicity towards fungal cells. In this study, the peptide Os-C was modified by adding five tryptophan residues to the C-terminus.

In Chapter 3, the effect of tryptophan end-tagging on the secondary structure of Os-C was investigated using CD spectroscopy and MD simulations. Results indicated that the addition of tryptophan residues alters the secondary structure of Os-C. The presence of a negative band in the CD spectra of Os-C(W_5) between 220 and 230 nm in Tris buffer and SDS is due to the presence of tryptophan residues and has been observed for other peptides tagged with tryptophan (27, 28). Furthermore, interactions with the membrane were investigated using MD simulations which reveal that tryptophan end-tagging does not enhance peptide-membrane interactions but enhances peptide aggregation. Membrane insertion studies show that the tryptophan residues do not insert into the membrane but are located above the membrane. Enhanced aggregation following end-tagging may be beneficial for the formation of higher order structures that may contribute to the antifungal activity of Os-C(W_5) (29).

The addition of tryptophan residues to Os-C leads to changes in peptide-membrane interactions and secondary structure changes which indicate potential differences in the antifungal activity of Os-C and Os-C(W_5). Therefore, the antiplanktonic activity and mode of action of Os-C and Os-C(W_5) was investigated in Chapter 4. Antifungal susceptibility assays show that Os-C is inactive in RPMI-1640, a medium that contains many salts. Conversely, Os-C(W_5) inhibits the growth of planktonic *C. albicans* and reduces cell growth and viability with MIC values of 50 µM and 68.4 ± 13.5 µM, respectively (**Table 6.1**). These findings confirm that tryptophan end-tagging confers antimicrobial activity to a salt-sensitive peptide. Sonesson *et al.* saw similar effects with GKH17 being inactive against *C. parapsilosis* in the presence of 0.15 M sodium chloride. Addition of three to five tryptophan residues to the C-terminus led to a significant decrease in cell survival (26). Enhanced aggregation caused by the addition of tryptophan residues may play a role in the enhanced antifungal activity of Os-C(W_5).

Table 6.1: Antifungal activities of amphotericin B, Os-C and Os-C(W_5).

	MIC[a] (µM)		BIC[b] (µM)		BEC[c] (µM)	
	Growth inhibition	**Cell viability**	**Viability**	**Biomass**	**Viability**	**Biomass**
Amphotericin B	0.625	0.50 ± 0.13	0.06 ± 0.01	0.05 ± 0.02	0.08 ± 0.004	0.56 ± 0.20
Os-C	> 100	ND[d]	> 100	> 100	ND	ND
Os-C(W_5)	50	68.4 ± 13.5	11.2 ± 3.69	10.6 ± 3.77	69.3 ± 11.3	87.4 ± 11.8

[a] Lowest concentration of antifungal that reduced planktonic cell growth or viability by ≥ 90%.
[b] Lowest concentration of antifungal that caused a 50% reduction in biofilm cell viability or biomass.
[c] Lowest concentration of antifungal that reduced the viability or biomass of a preformed biofilm by 50%.
[d] ND, not determined.
All data represents the mean ± SEM of three independent experiments.

Further studies indicate that ROS production and not membrane permeabilisation is the mode of action used by Os-C(W_5) to kill planktonic *C. albicans*. A similar observation was made by Mbuayama *et al*. who observed that in a low salt environment, Os-C induced minimal permeabilisation of *Saccharomyces cerevisiae* liposomes containing 30% ergosterol. Instead, Os-C induced significant ROS production in planktonic cells which was linked to its antiplanktonic activity (30). It is interesting to note that tryptophan end-tagging does not change the mode of action of Os-C.

Although MD simulations provide important information on how AMPs induce pore formation, reduced membrane interaction alludes to alternative mechanisms associated with AMP-mediated growth inhibition or cell death. The cell wall of *C. albicans* contains polysaccharide components along with proteins involved in adhesion, hyphal development, and biofilm formation such as enzymes, morphology-associated proteins, adhesins and binding (receptor) proteins. Disrupting cell wall integrity and/or protein function leads to oxidative stress and associated ROS formation and when in excess inhibits cell wall integrity leading to growth inhibition or cell death (31). Interestingly, for both Os-C and Os-C(W_5), ROS formation was the identified mode of action and although MD simulations clearly show differences in membrane insertion, the production of ROS is associated with residues in the Os-C sequence rather than the presence of terminal tryptophan residues.

Scanning electron microscopy images show changes in morphology following treatment with 6.25 µM and 12.5 µM Os-C(W_5), concentrations that induce ROS production. This suggests that the morphological changes observed could be due to ROS production. Similar observations were made by Ramírez-Quijas *et al.* who treated several *Candida* species with the oxidative

stress inducing compounds menadione and hydrogen peroxide and observed morphological changes such as increased cell roughness (32).

Although activity against planktonic forms of microorganisms is important, activity against biofilms is of greater importance since most recalcitrant infections are caused by biofilms (33). Previous research on tryptophan end-tagging predominantly focused on antibacterial activity (19, 24, 27, 28, 34) with little focus on the effect of this modification on antifungal activity (26). To date, there has been no study on the effect of this modification on the antibiofilm activity. Therefore, Chapter 5 sought to evaluate the antibiofilm activity and discover the mode of action of Os-C(W_5) against *C. albicans* biofilms. Antibiofilm assays indicate that Os-C does not prevent biofilm formation, but tryptophan end-tagging leads to enhanced biofilm preventing activity with BIC values of 4.76 ± 2.81 µM and 11.2 ± 3.69 µM after 6 hours and 24 hours, respectively. An increase in the BIC over time suggests that the peptide could be degraded by proteases that are secreted by *C. albicans* (35, 36). Furthermore, Os-C(W_5) eradicates preformed biofilms with a BEC of 69.3 ± 11.3 µM (**Table 6.1**).

Further investigations into the antibiofilm mode of action show that Os-C(W_5) reduces cell adhesion and the production of ECM components but does not prevent the yeast-to-hyphal transition at concentrations close to the BIC. Based on these results, it is likely that when Os-C(W_5) prevents cell adhesion, fewer cells are available to facilitate biofilm formation which results in minimal ECM production. Some antibiofilm activity is retained in the presence of serum which affects the activity of many AMPs (37). Significant reduction in viability and biomass is seen for biofilm prevention in RPMI-1640-50% FBS and SWM. Furthermore, a significant decrease in viability is seen after preformed biofilms are exposed to Os-C(W_5) in the presence of RPMI-1640-50% FBS and SWM. The reduced activity of Os-C(W_5) is possibly due to degradation by FBS associated proteases or interaction with serum components such as serum albumin (17). The failure of Os-C(W_5) to decrease the biomass of biofilms grown in SWM could be due to the lack of nutrients in this medium. Since SWM is not a nutrient-rich medium, it is likely to promote the formation of more robust biofilms which are more difficult to eradicate (38).

6.1 Limitations and future perspectives

The secondary structures of Os-C and Os-C(W_5) were determined using CD spectroscopy and showed that tryptophan end-tagging alters the CD spectra in the presence of Tris buffer and SDS. Amino acids with aromatic side chains have been found to make significant contributions to CD spectra due to their electric or magnetic dipole transition moments (39). As a result, it is difficult to interpret CD spectra of tryptophan end-tagged peptides (40). To overcome this issue, NMR spectroscopy could be used as an alternative technique. While CD provides a general secondary structure for the whole peptide, NMR provides more detailed information about the secondary structure adopted by each residue within the peptide. Furthermore, three-dimensional structures can be obtained from NMR studies, meaning α-helices and β-sheets are easier to distinguish (41).

The antifungal activity of Os-C(W_5) indicates a potential application in clinical settings. However, dosage-dependent susceptibility to proteases and binding to plasma proteins is a problem (17). Although amino acid modification is an option, the diversity of plasma associated proteases and proteins presents a challenge to identify which specific amino acid(s) to substitute. An alternative approach is the use of DDSs, which ensure that the drug reaches the intended target in the body at therapeutically relevant concentrations while minimising off-target interactions. Several DDSs have been developed to improve the bioavailability of AMPs and prevent inactivation by proteases, physiological temperatures, and changes in pH (42, 43). Examples of DDSs include vesicular, self-emulsifying, microparticle, liposomal and nanoparticle DDSs.

Vesicular DDSs protect peptides from proteolytic degradation. Insulin bound to a vesicular system could be administered orally since the vesicle precluded proteolytic degradation in the upper gastrointestinal tract. Furthermore, this delivery system enabled targeted delivery to hepatocytes (44). Self-emulsifying DDSs are composed of oil, surfactants and co-solvents which protect the drug from enzymatic degradation, decrease first pass metabolism and enhance absorption and permeation of the mucus layer (45). Zupančič *et al*. developed a formulation of the peptide daptomycin containing tricaprylin, medium chain fatty acids (capric and caprylic acid) and PEG-40 hydrogenated castor oil. This delivery system demonstrated greater permeation of the mucus layer, less drug degradation in the presence of α-chymotrypsin and sustained release for six hours when the formulation was emulsified in NaP buffer (46).

Microparticle delivery systems contain particles that are larger than 1 µm and have shown promise as an encapsulation system due to their protective effect which prevents peptide degradation and enhances stability (43). Microparticles also offer a larger surface to volume ratio for gastrointestinal absorption and peptide release (47). An oral delivery system containing polymyxin B was encapsulated into crosslinked alginate and exhibited sustained release and retention of biological activity in simulated gastrointestinal fluids (48). A formulation of the hormonal peptide therapeutic leuprolide in microspheres led to a steady release for up to 6 months (49).

Liposome delivery systems were one of the first systems to reach the market (50). This DDS is composed of vesicles where an aqueous solution is encased in a phospholipid membrane bilayer. As a result, the bioavailability of encapsulated drugs is enhanced because they are protected from enzymatic degradation and are more likely to experience intestinal absorption (51). The glycopeptide vancomycin was loaded into a glycerylcaldityltetraether liposome, and the formulation had greater bioavailability than free vancomycin an hour after oral administration in rats (52).

Nanoparticles include nanospheres and nanocapsules which are nanocarriers composed of either lipids or polymers. Oral administration using nanoparticle delivery protects the peptide from enzymatic degradation. Nanoparticles increase peptide bioavailability, mucus layer diffusion and membrane permeation (53). Attaching AMPs to gold nanoparticles improves antimicrobial activity as described by de Alteriis *et al*. who coated gold nanoparticles with the AMP indolicidin and reported enhanced antibiofilm activity against *C. albicans* (54). Chauhan *et al.* revealed that polymyxin B niosomes (lipid-based nanoparticles) were stable in simulated intestinal and gastric fluids. Further pharmacokinetic studies showed that orally administered polymyxin B niosomes had similar pharmacokinetic parameters to polymyxin B sulfate that was intravenously administered (55).

In addition to having antifungal activity, AMPs must be non-toxic towards host cells (56). Studies have demonstrated that Os-C(W_5) is not toxic towards erythrocytes (R. Chirombo, MSc dissertation, 2023). However, these experiments do not provide insight on how treatment affects an infected host. Therefore, it is necessary to use uninfected *Caenorhabditis elegans* (*C. elegans*) or *Galleria mellonella* (*G. mellonella*) to evaluate toxicity and *C. albicans* infected *C. elegans* or *G. mellonella* to evaluate activity in an infected host (57, 58). The use of *C. elegans* and *G. mellonella* models has several advantages: large numbers of these organisms

can be obtained with little cost and the upkeep of these organisms is cheap, simple and does not require specialised lab equipment. In addition, these organisms can be infected with a wide range of clinically relevant microorganisms (59, 60).

The first interaction between an AMP and a fungal cell is with the cell wall (**Figure 2.8**) which contains polysaccharides such as mannoproteins, β-glucan and chitin (61, 62). Using radial diffusion assays, Mbuayama *et al*. observed that Os-C was inactive after pre-treatment with mannan and partially active following laminarin pre-treatment suggesting that interactions between Os-C and β-1,3-glucan and mannose may be critical for antifungal activity (30). Likewise, as an analogue of Os-C, Os-C(W_5) may also initially interact with these polysaccharides prior to interacting with the cell membrane. Interactions can be investigated by mixing concentrations of Os-C(W_5) with either mannan or laminarin then observing whether antifungal activity is retained.

Prevention of cell wall synthesis is another mode of action used by antifungal agents, especially echinocandins (63). To investigate whether Os-C(W_5) interferes with cell wall synthesis and assembly, antifungal activity can be investigated in the presence of sorbitol, a sugar alcohol that serves as an osmotic protectant for fungal protoplasts. (64, 65). Another potential target of Os-C(W_5) is ergosterol, a component of fungal cell membranes which is targeted by the polyene drugs AMB and nystatin (66). Antifungal susceptibility assays can be conducted in the presence of increasing concentrations of ergosterol to determine whether the peptide binds ergosterol (67).

Molecular dynamics simulations reveal that Os-C(W_5) forms an aggregate on the membrane surface with limited penetration of the cell membrane. Previous research by Remington *et al*. showed that aggregates of tachyplesin I and magainin 2 accumulated on the cell membrane and caused pore formation (68). A novel finding of the present study is that aggregation of Os-C(W_5) on the cell membrane leads to ROS formation, leading to cell wall changes observed with scanning electron microscopy. The mechanism whereby aggregation leads to ROS formation and eventually cell death is unknown. This can be investigated by labelling the N-terminal of Os-C(W_5) with gold (5nm) nanoparticles and then viewing treated cells using transmission electron microscopy (TEM) to determine the localisation of the electron dense Os-C(W_5) within the cell wall and membrane to confirm whether the peptide remains localised on the plasma membrane (69). In addition, ROS mediated damage to membranous organelles such as the mitochondria can be determined using TEM.

Reactive oxygen species accumulation is linked to several events that lead to cell death. Mitochondrial membrane damage is thought to occur by lipid peroxidation due to increased oxidative stress on the cell (70). Higher levels of ROS have been linked to cell necrosis which is cell death due to extreme physical, chemical, or other pathological stimuli (71). Sophorolipid and AMP-17 induced necrotic cell death and permeabilised the cell membrane of *C. albicans* (70, 72). Experiments showed that Os-C(W_5) does not induce membrane permeabilisation, therefore, cell death may not be caused by necrosis.

Apoptosis is a form of programmed cell death that eliminates damaged, mutated, and redundant cells (73). Several ROS such as hydrogen peroxide, superoxide and hydroxyl radicals are thought to play roles in modulating apoptosis in metazoans and yeasts (74). Mitochondrial damage and subsequent changes to the mitochondrial potential are thought to be linked to the early stages of apoptotic cell death (70). Therefore, future experiments should investigate whether Os-C(W_5) treatment affects the mitochondrial membrane potential and whether exposure to Os-C(W_5) induces PS exposure, cytochrome *c* release, metacaspase activation, and DNA fragmentation and condensation which are also considered hallmarks of apoptosis (75).

Various assays can be used to detect hallmarks of apoptosis following treatment. For example, PS exposure, changes in mitochondrial potential, DNA fragmentation, and caspase activation can be evaluated using fluorescence microscopy or flow cytometry. The presence of apoptotic cells can be investigated using Annexin V staining which detects the exposure of PS to the outer leaflet (76). Changes in the mitochondrial membrane potential can be investigated by evaluating the fluorescence of dye Rhodamine-123 using flow cytometry (77). The terminal deoxynucleotidyl transferase dUTP nick end labelling (TUNEL) and 6-diamidino-2-phenylindole (DAPI) staining methods are used to investigate DNA fragmentation (78). Estimation of cytochrome *c* in the mitochondria and cytosol can be determined by measuring the absorbance of the supernatant and resuspended pellet of treated cells, respectively (79). Mitochondrial and cytosolic calcium levels of treated cells can be investigated by measuring the fluorescence of the dyes Rhod-2-AM and Fluo-3-AM, respectively (80). Finally, caspase activation can be evaluated by staining treated cells with CaspACE FITC-VAD-FMK, a fluorescent indicator of apoptosis (77).

Antimicrobial peptides are generally known to target the cell membrane or intracellular targets but not many studies have focused on the effects of AMPs at the protein level. Proteomic analysis of treated cells provides useful information on the protein targets which can provide

further information on the biochemical pathways involved in the induction of ROS by Os-C(W_5). Recent research by Yang *et al*. investigated changes in the proteome of *C. albicans* following exposure to the peptide AMP-17. The research identified differential expression of proteins that were involved in processes such as cell wall synthesis, RNA degradation and oxidative stress (81). Another study by Gbala *et al*. investigated the effect of the peptides actifensin and defensin-d2 on the proteome of multidrug-resistant *P. aeruginosa* and *C. albicans*. Results showed that exposure to the peptides led to differential expression of proteins involved in DNA replication and repair, translation, and membrane transport in *P. aeruginosa*. In *C. albicans*, differentially expressed proteins were involved in oxidative phosphorylation, RNA degradation and energy metabolism (82). Using quantitative proteomic analysis, the mechanism of action of Os-C(W_5) can be further elucidated and could potentially lead to the discovery of novel cell targets.

In addition to developing resistance to antifungal drugs, microorganisms can also develop resistance to AMPs. Although most studies focus on bacterial resistance mechanisms to AMPs (83, 84), some studies found that *C. albicans* develops resistance to several AMPs. The mucin Msb2 is in the cell membrane of *C. albicans* and stabilises the cell wall. A fragment of Msb2 protected *C. albicans* from LL-37 and histatin-5 by binding to the AMPs thus reducing their antifungal effect (85). Furthermore, microscale thermophoresis showed that the Msb2 fragment also protected *S. aureus*, *Enterococcus faecalis* and *Corynebacterium pseudodiphthericum* from the activity of daptomycin indicating a protective effect in polymicrobial settings (86).

Li *et al*. observed that *C. albicans* can resist the toxic effect of histatin 5 by means of Flu1, a polyamine efflux transporter. This finding suggests that AMPs may serve as substrates for fungal efflux transporters (87). In some cases, *C. albicans* secretes proteases in response to AMPs. Histatin 5 was inactivated by the proteases Sap9 and Sap10 which are constitutively expressed during oral infection (88). Therefore, future studies should look at potential mechanisms of resistance development to Os-C(W_5) such as the downregulation of protein transporters, overexpression of efflux pumps, overexpression of proteases, and modifications to the cell wall, cell membrane and intracellular organelles.

Although most *Candida* related infections are attributed to *C. albicans*, the emergence of non-*C. albicans* species is cause for concern as *C. tropicalis*, *C. glabrata*, *C. parapsilosis* and *C. auris* infections have become more prevalent. *C. tropicalis* is recognised as one of the top causative agents of candidaemia in cancer patients (89, 90) and is also responsible for

nosocomial urinary tract infections (91). *C. parapsilosis* is less virulent than other yeast species but is a frequent cause of candidaemia. Outbreaks within hospitals have been linked to the transfer of yeast from the hands of healthcare workers and nosocomial urinary tract infections (92). Despite its inability to form hyphae, *C. glabrata* has emerged as a nosocomial pathogen and is regarded as important due to its resistance to azoles (93, 94). *C. auris* was isolated as early as 1996 in South Korea (95) but became prominent in 2009 after it was isolated from the ear canal of a patient in Japan (96). Further reports of *C. auris* have documented nosocomial infections in Europe, Africa, South America, and North America (97-99). Antifungal susceptibility tests of *C. auris* isolates from hospitals in India, Pakistan, Venezuela, and South Africa indicate that *C. auris* is a greater health threat than *C. albicans*. When tested against antifungal drugs, 93% of isolates were resistant to fluconazole, 35% were resistant to AMB and 7% were resistant to echinocandins. Up to 41% were resistant to two antifungal drug classes and 4% were resistant to three antifungal drug classes (100).

In addition to *C. albicans* and *C. auris*, the WHO also identified *C. neoformans* and *A. fumigatus* as critical priority pathogens. *A. fumigatus* is a major cause of filamentous fungal infections among susceptible patient populations. In some cases, *A. fumigatus* causes invasive aspergillosis which can become chronic, requiring treatment over a prolonged period. A steady increase in invasive aspergillosis has been observed in several parts of the world (101-103). Repeated use of triazoles to treat aspergillosis has led to the proliferation of triazole-resistant *A. fumigatus* which is associated with treatment failure and a mortality range of 30-90% depending on the patient type (104-106). One study reported resistance rates as high as 28% in Europe (107) while another study in the United States reported azole resistance in 3.5-5% of isolates (108).

C. neoformans is the causative agent of cryptococcosis and clinical manifestations of this disease tend to affect the central nervous system (cryptococcal meningitis). The global prevalence of cryptococcal meningitis was 152000 cases and 112000 deaths as recently as 2020, with sub-Saharan Africa accounting for 54% of cases and 63% of deaths (109). *C. neoformans* is susceptible to AMB, flucytosine and azole drugs but resistance to all three drug treatments (110-113) has been reported and relapses are common.

Compared with monomicrobial biofilms, polymicrobial infections are linked to higher mortality rates (114, 115). Polymicrobial biofilms composed of *C. albicans* and bacteria are problematic with a study observing that approximately 27% of hospital-acquired bloodstream

infections caused by *C. albicans* were polymicrobial and the three most commonly isolated bacteria were *S. epidermidis*, *S. aureus* and *Enterococcus* species (116). Interactions between species in a polymicrobial biofilm may lead to enhanced immune evasion, virulence, and drug tolerance. Several studies observed that *C. albicans*-*S. aureus* mixed biofilms enhanced *S. aureus* colonisation and led to enhanced resistance to vancomycin, fluconazole, and miconazole (117-120). Therefore, future studies must evaluate the activity of Os-C(W_5) against other fungal species and bacterial species in monomicrobial and polymicrobial biofilm environments.

Despite growing resistance to antifungal drugs, it is possible to enhance their activity. One approach is the use of antifungal drugs in combination with AMPs which is linked to several advantages. First, toxic side effects associated with the use of antifungal drugs are reduced since a lower dosage of the antifungal drug is administered. Reducing the drug dosage means that the cost of administering the antifungal drug is also reduced. Using multiple drugs in combination means that a wider spectrum of activity is achieved especially if the antifungal agents have different modes of action. As a result, there is a lower likelihood of fungi developing resistance, especially when exposed to multiple antifungal agents at the same time (121).

The peptides RsAFP2 (122), HsAFP1 (123), AS10 (124) and OSIP108 (125) inhibited biofilm formation by *C. albicans*, however, they lacked biofilm eradicating activity. When these peptides were used in combination with caspofungin or AMB, the activity of caspofungin or AMB against preformed biofilms was improved. The cyclic lipopeptide tyrocidine A displayed synergistic activity with AMB against *C. albicans* biofilms. In addition, greater synergism was observed when the tyrocidine A was used in combination with caspofungin *in vitro* and *in vivo* in a *C. elegans* infection model (58). A truncated derivative of the amphibian peptide dermaseptin s3, DsS3(1-16), was used in combination with caspofungin in a murine model of disseminated candidiasis. The DsS3(1-16)-caspofungin combination resulted in greater survival compared to mice that were treated with either DsS3(1-16) or caspofungin on their own (126).

The present study demonstrates the efficacy of tryptophan end-tagging as a simple strategy to boost the antiplanktonic and antibiofilm activity of a salt-sensitive AMP. Compared with Os-C, Os-C(W_5) shows improved antifungal activity. To further develop this AMP for therapeutic application, it is essential to improve stability by identifying and developing an effective DDS,

further elucidating the mode of action, and evaluating activity in more clinically relevant biofilms and polymicrobial infections using relevant *ex vivo* models.

6.2 References

1. Pfavayi, L. T., Denning, D. W., Baker, S., Sibanda, E. N., and Mutapi, F. (2021) Determining the burden of fungal infections in Zimbabwe. *Scientific Reports* **11**, 13240-13252. 10.1038/s41598-021-92605-1
2. Brown, G. D., Denning, D. W., Gow, N. A., Levitz, S. M., Netea, M. G., and White, T. C. (2012) Hidden killers: human fungal infections. *Science Translational Medicine* **4**, 165rv113-165rv116. 10.1126/scitranslmed.3004404
3. Forsberg, K., Woodworth, K., Walters, M., Berkow, E. L., Jackson, B., Chiller, T., and Vallabhaneni, S. (2019) *Candida auris*: the recent emergence of a multidrug-resistant fungal pathogen. *Medical Mycology* **57**, 1-12. 10.1093/mmy/myy054
4. Vassilopoulos, S., and Mylonakis, E. (2022) Avenues for antifungal drug discovery and development: where to now? *Expert Opinion on Drug Discovery* **17**, 667-672. 10.1080/17460441.2022.2098950
5. McCarthy, M. W., Kontoyiannis, D. P., Cornely, O. A., Perfect, J. R., and Walsh, T. J. (2017) Novel agents and drug targets to meet the challenges of resistant fungi. *Journal of Infectious Diseases* **216**, S474-S483. 10.1093/infdis/jix130
6. Abadio, A. K., Kioshima, E. S., Teixeira, M. M., Martins, N. F., Maigret, B., and Felipe, M. S. (2011) Comparative genomics allowed the identification of drug targets against human fungal pathogens. *BMC Genomics* **12**, 75-84. 10.1186/1471-2164-12-75
7. Pushpakom., S., Iorio, F., Eyers, P. A., Escott, K. J., Hopper, S., Wells, A., Doig, A, Guilliams, T., Latimer, J., McNamee, C., Norris, A., Sanseau, P., Cavalla, D., and Pirmohamed, M. (2019) Drug repurposing: progress, challenges and recommendations. *Nature Reviews Drug Discovery* **18**, 41-58. 10.1038/nrd.2018.168
8. Bink, A., Kucharikova, S., Neirinck, B., Vleugels, J., Van Dijck, P., Cammue, B. P. A., and Thevissen, K. (2012) The nonsteroidal antiinflammatory drug diclofenac potentiates the in vivo activity of caspofungin against *Candida albicans* biofilms. *Journal of Infectioous Diseases* **206**, 1790-1797. 10.1093/infdis/jis594
9. Koselny, K., Green, J., DiDone, L., Halterman, J. P., Fothergill, A. W., Wiederhold, N. P., Patterson, T. F., Cushion, M. T., Rappelye, C., Wellington, M., and Krysan, D. J. (2016) The celecoxib derivative AR-12 has broad-spectrum antifungal activity in vitro

and improves the activity of fluconazole in a murine model of cryptococcosis. *Antimicrobial Agents and Chemotherapy* **60**, 7115-7127. 10.1128/AAC.01061-16

10. Bahar, A. A., and Ren, D. (2013) Antimicrobial peptides. *Pharmaceuticals (Basel)* **6**, 1543-1575. 10.3390/ph6121543
11. Brogden, K. A. (2005) Antimicrobial peptides: pore formers or metabolic inhibitors in bacteria? *Nature Reviews Microbiology* **3**, 238-250. 10.1038/nrmicro1098
12. Thompson, G. R., Soriano, A., Skoutelis, A., Vazquez, J. A., Honore, P. M., Horcajada, J. P., Spapen, H., Bassetti, M., Ostrosky-Zeichner, L., Das, A. F., Viani, R. M., Sandison, T., and Pappas, P. G. (2021) Rezafungin versus caspofungin in a phase 2, randomized, double-blind study for the treatment of candidemia and invasive candidiasis: the STRIVE trial. *Clinical Infectious Diseases* **73**, e3647-e3655. 10.1093/cid/ciaa1380
13. Rauseo, A. M., Coler-Reilly, A., Larson, L., and Spec, A. (2020) Hope on the horizon: novel fungal treatments in development. *Open Forum Infectious Diseases* **7**, ofaa016-ofaa034. 10.1093/ofid/ofaa016
14. Malan, M., Serem, J. C., Bester, M. J., Neitz, A. W. H., and Gaspar, A. R. M. (2016) Anti-inflammatory and anti-endotoxin properties of peptides derived from the carboxy-terminal region of a defensin from the tick *Ornithodoros savignyi*. *Journal of Peptide Science* **22**, 43-51. 10.1002/psc.2838
15. Prinsloo, L., Naidoo, A., Serem, J. C., Taute, H., Sayed, Y., Bester, M. J., Neitz, A. W. H., and Gaspar, A. R. M. (2013) Structural and functional characterization of peptides derived from the carboxy-terminal region of a defensin from the tick *Ornithodoros savignyi*. *Journal of Peptide Science* **19**, 325-332. 10.1002/psc.2505
16. Marr, A. K., Gooderham, W. J., and Hancock, R. E. W. (2006) Antibacterial peptides for therapeutic use: obstacles and realistic outlook. *Current Opinion in Pharmacology* **6**, 468-472. 10.1016/j.coph.2006.04.006
17. Hein-Kristensen, L., Knapp, K. M., Franzyk, H., and Gram, L. (2013) Selectivity in the potentiation of antibacterial activity of α-peptide/β-peptoid peptidomimetics and antimicrobial peptides by human blood plasma. *Research in Microbiology* **164**, 933-940. 10.1016/j.resmic.2013.08.002
18. Wu, G., Ding, J., Li, H., Li, L., Zhao, R., Shen, Z., Fan, X., and Xi, T. (2008) Effects of cations and pH on antimicrobial activity of thanatin and s-thanatin against *Escherichia coli* ATCC25922 and *B. subtilis* ATCC 21332. *Current Microbiology* **57**, 552-557. 10.1007/s00284-008-9241-6

19. Pasupuleti, M., Chalupka, A., Morgelin, M., Schmidtchen, A., and Malmsten, M. (2009) Tryptophan end-tagging of antimicrobial peptides for increased potency against *Pseudomonas aeruginosa*. *Biochimica et Biophysica Acta* **1790**, 800-808. 10.1016/j.bbagen.2009.03.029

20. Haney, E. F., Lau, F., and Vogel, H. J. (2007) Solution structures and model membrane interactions of lactoferrampin, an antimicrobial peptide derived from bovine lactoferrin. *Biochimica et Biophysica Acta* **1768**, 2355-2364. 10.1016/j.bbamem.2007.04.018

21. Deslouches, B., Phadke, S. M., Lazarevic, V., Cascio, M., Islam, K., Montelaro, R. C., and Mietzner, T. A. (2005) De novo generation of cationic antimicrobial peptides: influence of length and tryptophan substitution on antimicrobial activity. *Antimicrobial Agents and Chemotherapy* **49**, 316-322. 10.1128/AAC.49.1.316-322.2005

22. McInturff, J. E., Wang, S. J., Machleidt, T., Lin, T. R., Oren, A., Hertz, C. J., Krutzik, S. R., Hart, S., Zeh, K., Anderson, D. H., Gallo, R. L., Modlin, R. L., and Kim, J. (2005) Granulysin-derived peptides demonstrate antimicrobial and anti-inflammatory effects against *Propionibacterium acnes*. *Journal of Investigative Dermatology* **125**, 256-263. 10.1111/j.0022-202X.2005.23805.x

23. Wei, S. Y., Wu, J. M., Kuo, Y. Y., Chen, H. L., Yip, B. S., Tzeng, S. R., and Cheng, J. W. (2006) Solution structure of a novel tryptophan-rich peptide with bidirectional antimicrobial activity. *Journal of Bacteriology* **188**, 328-334. 10.1128/JB.188.1.328-334.2006

24. Schmidtchen, A., Pasupuleti, M., Morgelin, M., Davoudi, M., Alenfall, J., Chalupka, A., and Malmsten, M. (2009) Boosting antimicrobial peptides by hydrophobic oligopeptide end tags. *Journal of Biological Chemistry* **284**, 17584-17594. 10.1074/jbc.M109.011650

25. Mouritsen, O. G., and Zuckermann, M. J. (2004) What's so special about cholesterol? *Lipids* **39**, 1101-1113. 10.1007/s11745-004-1336-x

26. Sonesson, A., Nordahl, E. A., Malmsten, M., and Schmidtchen, A. (2011) Antifungal activities of peptides derived from domain 5 of high-molecular-weight kininogen. *International Journal of Peptides* **2011**, 761037-761047. 10.1155/2011/761037

27. Schmidtchen, A., Ringstad, L., Kasetty, G., Mizuno, H., Rutland, M. W., and Malmsten, M. (2011) Membrane selectivity by W-tagging of antimicrobial peptides. *Biochimica et Biophysica Acta* **1808**, 1081-1091. 10.1016/j.bbamem.2010.12.020

28. Strömstedt, A. A., Pasupuleti, M., Schmidtchen, A., and Malmsten, M. (2009) Oligotryptophan-tagged antimicrobial peptides and the role of the cationic sequence. *Biochimica et Biophysica Acta (BBA) - Biomembranes* **1788**, 1916-1923. 10.1016/j.bbamem.2009.06.001

29. Bhattacharjya, S., and Straus, S. K. (2020) Design, engineering and discovery of novel alpha-helical and beta-boomerang antimicrobial peptides against drug resistant bacteria. *International Journal of Molecular Sciences* **21**, 1-21. 10.3390/ijms21165773

30. Mbuayama, K. R., Taute, H., Strömstedt, A. A., Bester, M. J., and Gaspar, A. R. M. (2021) Antifungal activity and mode of action of synthetic peptides derived from the tick OsDef2 defensin. *Journal of Peptide Science* **28**, e3383-e3394. 10.1002/psc.3383

31. Yu, Q., Zhang, B., Li, J., Zhang, B., Wang, H., and Li, M. (2016) Endoplasmic reticulum-derived reactive oxygen species (ROS) is involved in toxicity of cell wall stress to *Candida albicans*. *Free Radical Biology and Medicine* **99**, 572-583. 10.1016/j.freeradbiomed.2016.09.014

32. Ramírez-Quijas, M. D., Zazueta-Sandoval, R., Obregón-Herrera, A., López-Romero, E., and Cuéllar-Cruz, M. (2015) Effect of oxidative stress on cell wall morphology in four pathogenic *Candida* species. *Mycological Progress* **14**, 1-15. 10.1007/s11557-015-1028-0

33. Jamal, M., Ahmad, W., Andleeb, S., Jalil, F., Imran, M., Nawaz, M. A., Hussain, T., Ali, M., Rafiq, M., and Kamil, M. A. (2018) Bacterial biofilm and associated infections. *Journal of the Chinese Medical Association* **81**, 7-11. 10.1016/j.jcma.2017.07.012

34. Pasupuleti, M., Schmidtchen, A., Chalupka, A., Ringstad, L., and Malmsten, M. (2009) End-tagging of ultra-short antimicrobial peptides by W/F stretches to facilitate bacterial killing. *PLoS One* **4**, e5285-e5294. 10.1371/journal.pone.0005285

35. Lopes, J. L., Nobre, T. M., Siano, A., Humpola, V., Bossolan, N. R., Zaniquelli, M. E., Tonarelli, G., and Beltramini, L. M. (2009) Disruption of *Saccharomyces cerevisiae* by Plantaricin 149 and investigation of its mechanism of action with biomembrane model systems. *Biochimica et Biophysica Acta* **1788**, 2252-2258. 10.1016/j.bbamem.2009.06.026

36. Naglik, J. R., Challacombe, S. J., and Hube, B. (2003) *Candida albicans* secreted aspartyl proteinases in virulence and pathogenesis. *Microbiology and Molecular Biology Reviews* **67**, 400-428. 10.1128/MMBR.67.3.400-428.2003

37. Ciornei, C. D., Sigurdardottir, T., Schmidtchen, A., and Bodelsson, M. (2005) Antimicrobial and chemoattractant activity, lipopolysaccharide neutralization,

cytotoxicity, and inhibition by serum of analogs of human cathelicidin LL-37. *Antimicrobial Agents and Chemotherapy* **49**, 2845-2850. 10.1128/AAC.49.7.2845-2850.2005

38. Price, B. L., Lovering, A. M., Bowling, F. L., and Dobson, C. B. (2016) Development of a novel collagen wound model to simulate the activity and distribution of antimicrobials in soft tissue during diabetic foot infection. *Antimicrobial Agents and Chemotherapy* **60**, 6880-6889. 10.1128/AAC.01064-16
39. Woody, R. W. (1994) Contributions of tryptophan side chains to the far-ultraviolet circular dichroism of proteins. *European Biophysics Journal* **23**, 253-262. 10.1007/BF00213575
40. Freskgard, P. O., Martensson, L. G., Jonasson, P., Jonsson, B. H., and Carlsson, U. (1994) Assignment of the contribution of the tryptophan residues to the circular dichroism spectrum of human carbonic anhydrase II. *Biochemistry* **33**, 14281-14288. 10.1021/bi00251a041
41. Bhattacharjya, S., and Ramamoorthy, A. (2009) Multifunctional host defense peptides: functional and mechanistic insights from NMR structures of potent antimicrobial peptides. *FEBS Journal* **276**, 6465-6473. 10.1111/j.1742-4658.2009.07357.x
42. Vargason, A. M., Anselmo, A. C., and Mitragotri, S. (2021) The evolution of commercial drug delivery technologies. *Nature Biomedical Engineering* **5**, 951-967. 10.1038/s41551-021-00698-w
43. Deshayes, C., Arafath, M. N., Apaire-Marchais, V., Roger, E. (2021) Drug delivery systems for the oral administration of antimicrobial peptides: promising tools to treat infectious diseases. *Frontiers in Medical Technology* **3**, 778645-778657. 10.3389/fmedt.2021.778645
44. Geho, W. B., Geho, H. C., and Gana, T. J. (2009) Hepatic-directed vesicle insulin: a review of formulation development and preclinical evaluation. *Journal of Diabetes Science and Techniology* **3**, 1451-1459. 10.1177/193229680900300627.
45. Mahmood, A., and Bernkop-Schnurch, A. (2019) SEDDS: a game changing approach for the oral administration of hydrophilic macromolecular drugs. *Advanced Drug Delivery Reviews* **142**, 91-101. 10.1016/j.addr.2018.07.001
46. Zupančič, O., Partenhauser, A., Lam, H. T., Rohrer, J., and Bernkop-Schnürch, A. (2016) Development and *in vitro* characterisation of an oral self-emulsifying delivery system for daptomycin. *European Journal of Pharmaceutical Sciences* **81**, 129-136. 10.1016/j.ejps.2015.10.005

47. Singh, M. N., Hemant, K. S. Y., Ram, M., and Shivakumar, H. G. (2010) Microencapsulation: a promising technique for controlled drug delivery. *Research in Pharmaceutical Sciences* **5**, 65-77.,

48. Coppi, G., Sala, N., Bondi, M., Sergi, S., and Iannuccelli, V. (2006) *Ex-vivo* evaluation of alginate microparticles for polymyxin B oral administration. *Journal of Drug Targets* **14**, 599-606. 10.1080/10611860600864182.

49. Schwendeman, S. P., Shah, R. B., Bailey, B. A., and Schwendeman, A. S. (2014) Injectable controlled release depots for large molecules. *Journal of Controlled Release* **190**, 240-253. 10.1016/j.jconrel.2014.05.057

50. Barenholz, Y. (2012) Doxil -- the first FDA-approved nano-drug: lessons learned. *Journal of Controlled Release* **160**, 117-134. 10.1016/j.jconrel.2012.03.020

51. Nguyen, T. X., Huang, L., Gauthier, M., Yang, G., and Wang, Q. (2016) Recent advances in liposome surface modification for oral drug delivery. *Nanomedicine* **11**, 1169-1185. 10.2217/nnm.16.9.

52. Uhl, P., Pantze, S., Storck, P., Parmentier, J., Witzigmann, D., Hofhaus, G., Huwyler, J., Mier, W., and Fricker, G. (2017) Oral delivery of vancomycin by tetraether lipid liposomes. *European Journal of Pharmaceutical Sciences* **108**, 111-118. 10.1016/j.ejps.2017.07.013

53. Aguirre, T. A., Teijeiro-Osorio, D., Rosa, M., Coulter, I. S., Alonso, M. J., and Brayden, D. J. (2016) Current status of selected oral peptide technologies in advanced preclinical development and in clinical trials. *Advanced Drug Delivery Reviews* **106**, 223-241. 10.1016/j.addr.2016.02.004

54. de Alteriis, E., Maselli, V., Falanga, A., Galdiero, S., Di Lella, F. M., Gesuele, R., Guida, M., and Galdiero, E. (2018) Efficiency of gold nanoparticles coated with the antimicrobial peptide indolicidin against biofilm formation and development of *Candida* spp. clinical isolates. *Infection and Drug Resistance* **11**, 915-925. 10.2147/IDR.S164262

55. Chauhan, M. K., and Bhatt, N. (2019) Bioavailability enhancement of polymyxin B with novel drug delivery: development and optimization using quality-by-design approach. *Journal of Pharmaceutical Sciences* **108**, 1521-1528. 10.1016/j.xphs.2018.11.032.

56. Ebenhan, T., Gheysens, O., Kruger, H. G., Zeevaart, J. R., and Sathekge, M. M. (2014) Antimicrobial peptides: their role as infection-selective tracers for molecular imaging. *Biomed Research International* **2014**, 867381-867396. 10.1155/2014/867381

57. Li, R., Chen, C., Zhang, B., Jing, H., Wang, Z., Wu, C., Hao, P., Kuang, Y., and Yang, M. (2019) The chromogranin A-derived antifungal peptide CGA-N9 induces apoptosis in *Candida tropicalis*. *Biochemical Journal* **476**, 3069-3080. 10.1042/BCJ20190483

58. Troskie, A. M., Rautenbach, M., Delattin, N., Vosloo, J. A., Dathe, M., Cammue, B. P. A., and Thevissen, K. (2014) Synergistic activity of the tyrocidines, antimicrobial cyclodecapeptides from *Bacillus aneurinolyticus*, with amphotericin B and caspofungin against *Candida albicans* biofilms. *Antimicrobial Agents and Chemotherapy* **58**, 3697-3707. 10.1128/AAC.02381-14

59. Ewbank, J. J., and Zugasti, O. (2011) *C. elegans*: model host and tool for antimicrobial drug discovery. *Disease Models and Mechanisms* **4**, 300-304. 10.1242/dmm.006684

60. Pereira, T. C., de Barros, P. P., Fugisaki, L. R. O., Rossoni, R. D., Ribeiro, F. C., de Menezes, R. T., Junqueira, J. C., and Scorzoni, L. (2018) Recent advances in the use of *Galleria mellonella* model to study immune responses against human pathogens. *Journal of Fungi (Basel)* **4**, 1-19. 10.3390/jof4040128

61. Cabib, E., and Arroyo, J. (2013) How carbohydrates sculpt cells: chemical control of morphogenesis in the yeast cell wall. *Nature Reviews Microbiology* **11**, 648-655. 10.1038/nrmicro3090

62. Wang, K., Dang, W., Xie, J., Zhu, R., Sun, M., Jia, F., Zhao, Y., An, X., Qiu, S., Li, X., Ma, Z., Yan, W., and Wang, R. (2015) Antimicrobial peptide protonectin disturbs the membrane integrity and induces ROS production in yeast cells. *Biochimica et Biophysica Acta* **1848**, 2365-2373. 10.1016/j.bbamem.2015.07.008

63. Frost, D. J., Brandt, K. D., Cugier, D., and Goldman, R. (1995) A whole-cell *Candida albicans* assay for the detection of inhibitors towards fungal cell wall synthesis and assembly. *The Journal of Antibiotics* **48**, 306-310. 10.7164/antibiotics.48.306.

64. Carrasco, H., Raimondi, M., Svetaz, L., Di Liberto, M., Rodriguez, M. V., Espinoza, L., Madrid, A., and Zacchino, S. (2012) Antifungal activity of eugenol analogues. Influence of different substituents and studies on mechanism of action. *Molecules* **17**, 1002-1024. 10.3390/molecules17011002

65. Gucwa, K., Milewski, S., Dymerski, T., and Szweda, P. (2018) Investigation of the antifungal activity and mode of action of *Thymus vulgaris*, *Citrus limonum*, *Pelargonium graveolens*, *Cinnamomum cassia*, *Ocimum basilicum*, and *Eugenia caryophyllus* essential oils. *Molecules* **23**, 1-18. 10.3390/molecules23051116

66. Kathiravan, M. K., Salake, A. B., Chothe, A. S., Dudhe, P. B., Watode, R. P., Mukta, M. S., and Gadhwe, S. (2012) The biology and chemistry of antifungal agents: a review. *Bioorganic and Medicinal Chemistry* **20**, 5678-5698. 10.1016/j.bmc.2012.04.045

67. D'Auria, F. D., Casciaro, B., De Angelis, M., Marcocci, M. E., Palamara, A. T., Nencioni, L., Mangoni, M. L. (2022) Antifungal activity of the frog skin peptide temporin G and its effect on *Candida albicans* virulence factors. *International Journal of Molecular Sciences* **23**, 1-18. 10.3390/ijms23116345

68. Remington, J. M., Liao, C., Sharafi, M., Ste Marie, E. J., Ferrell, J. B., Hondal, R. J., Wargo, M. J., Schneebeli, S. T., and Li, J. (2020) Aggregation state of synergistic antimicrobial peptides. *The Journal of Physical Chemistry Letters* **11**, 9501-9506. 10.1021/acs.jpclett.0c02094

69. Chitrani, B. D., Ghazani, A. A., and Chan, W. C. W. (2006) Determining the size and shape dependence of gold nanoparticle uptake into mammalian cells. *Nano Letters* **6**, 662-668. 10.1021/nl052396o

70. Ma, H., Yang, L., Tian, Z., Zhu, L., Peng, J., Fu, P., Xiu, J., and Guo, G. (2023) Antimicrobial peptide AMP-17 exerts anti-*Candida albicans* effects through ROS-mediated apoptosis and necrosis. *International Microbiology* **26**, 81-90. 10.1007/s10123-022-00274-5

71. Chang, W. Q., Wu, X. Z., Cheng, A. X., Zhang, L., Ji, M., and Lou, H. X. (2011) Retigeric acid B exerts antifungal effect through enhanced reactive oxygen species and decreased cAMP. *Biochimica et Biophysica Acta* **1810**, 569-576. 10.1016/j.bbagen.2011.02.001

72. Haque, F., Verma, N. K., Alfatah, M., Bijlani, S., and Bhattacharyya, M. S. (2019) Sophorolipid exhibits antifungal activity by ROS mediated endoplasmic reticulum stress and mitochondrial dysfunction pathways in *Candida albicans*. *RSC Advances* **9**, 41639-41648. 10.1039/c9ra07599b

73. Rockenfeller, P., and Madeo, F. (2008) Apoptotic death of ageing yeast. *Experimental Gerontology* **43**, 876-881. 10.1016/j.exger.2008.08.044

74. Benaroudj, N., Lee, D. H., and Goldberg, A. L. (2001) Trehalose accumulation during cellular stress protects cells and cellular proteins from damage by oxygen radicals. *Journal of Biological Chemistry* **276**, 24261-24267. 10.1074/jbc.M101487200

75. Lee, H., Hwang, J. S., and Lee, D. G. (2017) Scolopendin, an antimicrobial peptide from centipede, attenuates mitochondrial functions and triggers apoptosis in *Candida albicans*. *Biochemical Journal* **474**, 635-645. 10.1042/BCJ20161039

76. Sasidharan, S., Nishanth, K. S., and Nair, H. J. (2022) Ethanolic extract of *Caesalpinia bonduc* seeds triggers yeast metacaspase-dependent apoptotic pathway mediated by mitochondrial dysfunction through enhanced production of calcium and reactive oxygen species (ROS) in *Candida albicans*. *Frontiers in Cellular and Infection Microbiology* **12**, 970688-970709. 10.3389/fcimb.2022.970688

77. Li, Y., Shan, M., Zhu, Y., Yao, H., Li, H., Gu, B., and Zhu, Z. (2020) Kalopanaxsaponin A induces reactive oxygen species mediated mitochondrial dysfunction and cell membrane destruction in *Candida albicans*. *PLoS One* **15**, e0243066-e0243080. 10.1371/journal.pone.0243066

78. Hwang, J. H., Choi, H., Kim, A. R., Yun, J. W., Yu, R., Woo, E. R., and Lee, D. G. (2014) Hibicuslide C-induced cell death in *Candida albicans* involves apoptosis mechanism. *Journal of Applied Microbiology* **117**, 1400-1411. 10.1111/jam.12633

79. Wani, M. Y., Ahmad, A., Aqlan, F. M., and Al-Bogami, A. S. (2021) Citral derivative activates cell cycle arrest and apoptosis signaling pathways in *Candida albicans* by generating oxidative stress. *Bioorganic Chemistry* **115**, 105260-105269. 10.1016/j.bioorg.2021.105260

80. Tian, J., Lu, Z., Wang, Y., Zhang, M., Wang, X., Tang, X., Peng, X., and Zeng, H. (2017) Nerol triggers mitochondrial dysfunction and disruption via elevation of Ca^{2+} and ROS in *Candida albicans*. *The International Journal of Biochemistry & Cell Biology* **85**, 114-122. 10.1016/j.biocel.2017.02.006

81. Yang, L. B., Guo, G., Tian, Z. Q., Zhou, L. X., Zhu, L. J., Peng, J., Sun, C. Q., and Huang, M. J. (2022) TMT-based quantitative proteomic analysis of the effects of novel antimicrobial peptide AMP-17 against *Candida albicans*. *Journal of Proteomics* **250**, 104385-104395. 10.1016/j.jprot.2021.104385

82. Gbala, I. D., Macharia, R. W., and Magoma, G. (2022) Recombinant actifensin and defensin-d2 induce critical changes in the proteomes of multidrug-resistant *Pseudomonas aeruginosa* and *Candida albicans*. *Microbiology Spectrum* **10**, 1-15. 10.1128/spectrum.02062-22

83. El Shazely, B., Yu, G., Johnston, P. R., and Rolff, J. (2020) Resistance evolution against antimicrobial peptides in *Staphylococcus aureus* alters pharmacodynamics beyond the MIC. *Frontiers in Microbiology* **11**, 103-113. 10.3389/fmicb.2020.00103

84. Assoni, L., Milani, B., Carvalho, M. R., Nepomuceno, L. N., Waz, N. T., Guerra, M. E. S., Converso, T. R., and Darrieux, M. (2020) Resistance mechanisms to

antimicrobial peptides in Gram-positive bacteria. *Frontiers in Microbiology* **11**, 593215-593234. 10.3389/fmicb.2020.593215

85. Szafranski-Schneider, E., Swidergall, M., Cottier, F., Tielker, D., Roman, E., Pla, J., and Ernst, J. F. (2012) Msb2 shedding protects *Candida albicans* against antimicrobial peptides. *PLoS Pathogens* **8**, e1002501-e1002514. 10.1371/journal.ppat.1002501
86. Swidergall, M., Ernst, A. M., and Ernst, J. F. (2013) *Candida albicans* mucin Msb2 is a broad-range protectant against antimicrobial peptides. *Antimicrobial Agents and Chemotherapy* **57**, 3917-3922. 10.1128/AAC.00862-13
87. Li, R., Kumar, R., Tati, S., Puri, S., and Edgerton, M. (2013) *Candida albicans* flu1-mediated efflux of salivary histatin 5 reduces its cytosolic concentration and fungicidal activity. *Antimicrobial Agents and Chemotherapy* **57**, 1832-1839. 10.1128/AAC.02295-12
88. Meiller, T. F., Hube, B., Schild, L., Shirtliff, M. E., Scheper, M. A., Winkler, R., Ton, A., and Jabra-Rizk, M. A. (2009) A novel immune evasion strategy of *Candida albicans*: proteolytic cleavage of a salivary antimicrobial peptide. *PLoS One* **4**, e5039-e5047. 10.1371/journal.pone.0005039
89. Nucci, M., and Colombo, A. L. (2007) Candidemia due to *Candida tropicalis:* clinical, epidemiologic, and microbiologic characteristics of 188 episodes occurring in tertiary care hospitals. *Diagnostic Microbiology and Infectious Disease* **58**, 77-82. 10.1016/j.diagmicrobio.2006.11.009
90. Weinberger, M., Perez, S., Samra, Z., Ostfeld, L., Bash, E., Turner, D., Goldschmeid-Reouven, A., Regev-Yochay, G., Pitlik, S. D., and Keller, N. (2005) Characteristics of candidaemia with *Candida albicans* compared with non-albicans *Candida* species and predictors of mortality. *The Journal of Hospital Infection* **61**, 146-154. 10.1016/j.jhin.2005.02.009
91. Rho, J., Shin, J. H., Song, J. W., Park, M., Kee, S. J., Jang, S. J, Park, Y. Y., Suh, S. P, and Ryang, D. W. (2004) Molecular investigation of two consecutive nosocomial clusters of *Candida tropicalis* candiduria using pulsed-field gel electrophoresis. *The Journal of Microbiology* **42**, 80-86.,
92. Bonassoli, L. A., Bertoli, M., and Svidzinski, T. I. E., (2005) High frequency of *Candida parapsilosis* on the hands of healthy hosts. *The Journal of Hospital Infection* **59**, 159-162. 10.1016/j.jhin.2004.06.033
93. Tsai, H., and Bobek, L. A. (1997) Studies of the mechanism of human salivary histatin-5 candidacidal activity with histatin-5 variants and azole-sensitive and -resistant

Candida species. *Antimicrobial Agents and Chemotherapy* **41**, 2224-2228. 10.1128/AAC.41.10.2224

94. Thein, Z. M., Samaranayake, Y. H., and Samaranayake, L. P. (2007) *In vitro* biofilm formation of *Candida albicans* and non-albicans *Candida* species under dynamic and anaerobic conditions. *Archives of Oral Biology* **52**, 761-767. 10.1016/j.archoralbio.2007.01.009

95. Lee, W. G., Shin, J. H., Uh, Y., Kang, M. G., Kim, S. H., Park, K. H., and Jang, H. C. (2011) First three reported cases of nosocomial fungemia caused by *Candida auris*. *Journal of Clinical Microbiology* **49**, 3139-3142. 10.1128/JCM.00319-11

96. Satoh, K., Makimura, K., Hasumi, Y., Nishiyama, Y., Uchida, K., and Yamaguchi, H. (2009) *Candida auris* sp. nov., a novel ascomycetous yeast isolated from the external ear canal of an inpatient in a Japanese hospital. *Microbiology and Immunology* **53**, 41-44. 10.1111/j.1348-0421.2008.00083.x

97. Borman, A. M., Szekely, A., and Johnson, E. M. (2016) Comparative pathogenicity of United Kingdom isolates of the emerging pathogen *Candida auris* and other key pathogenic *Candida* species. *mSphere* **1**, 1-8. 10.1128/mSphere.00189-16

98. Calvo, B., Melo, A. S., Perozo-Mena, A., Hernandez, M., Francisco, E. C., Hagen, F., Meis, J. F., and Colombo, A. L. (2016) First report of *Candida auris* in America: clinical and microbiological aspects of 18 episodes of candidemia. *Journal of Infection* **73**, 369-374. 10.1016/j.jinf.2016.07.008

99. Magobo, R. E., Corcoran, C., Seetharam, S., and Govender, N. P. (2014) *Candida auris*–associated candidemia, South Africa. *Emerging Infectious Diseases* **20**, 1248-1250. 10.3201/eid2007.131765

100. Lockhart, S. R., Etienne, K. A., Vallabhaneni, S., Farooqi, J., Chowdhary, A., Govender, N. P., Colombo, A. L., Calvo, B., Cuomo, C. A., Desjardins, C. A., Berkow, E. L., Castanheira, M., Magobo, R. E., Jabeen, K., Asghar, R. J., Meis, J. F., Jackson, B., Chiller, T., and Litvintseva, A. P. (2017) Simultaneous emergence of multidrug-resistant *Candida auris* on 3 continents confirmed by whole-genome sequencing and epidemiological analyses. *Clinical Infectious Diseases* **64**, 134-140. 10.1093/cid/ciw691

101. Brissaud, O., Guichoux, J., Harambat, J., Tandonnet, O., and Zaoutis, T. (2012) Invasive fungal disease in PICU: epidemiology and risk factors. *Annals of Intensive Care* **2**, 6-13. 10.1186/2110-5820-2-6

102. Lass-Florl, C., and Cuenca-Estrella, M. (2017) Changes in the epidemiological landscape of invasive mould infections and disease. *Journal of Antimicrobial Chemotherapy* **72**, i5-i11. 10.1093/jac/dkx028

103. Verweij, P. E., Chowdhary, A., Melchers, W. J., and Meis, J. F. (2016) Azole resistance in *Aspergillus fumigatus*: can we retain the clinical use of mold-active antifungal azoles? *Clinical Infectious Diseases* **62**, 362-368. 10.1093/cid/civ885

104. Falcone, M., Massetti, A. P., Russo, A., Vullo, V., and Venditti, M. (2011) Invasive aspergillosis in patients with liver disease. *Medical Mycology* **49**, 406-413. 10.3109/13693786.2010.535030

105. Lestrade, P. P., Bentvelsen, R. G., Schauwvlieghe, A. F. A. D., Schalekamp, S., van der Velden, W. J. F. M., Kuiper, E. J., van Paassen, J., van der Hoven, B., van der Lee, H. A., Melchers, W. J. G., de Haan, A. F., van der Hoeven, H. L., Rijnders, B. J. A., van der Beek, M. T., and Verweij, P. E. (2019) Voriconazole resistance and mortality in invasive aspergillosis: a multicenter retrospective cohort study. *Clinical Infectious Diseases* **68**, 1463-1471. 10.1093/cid/ciy859

106. van der Linden, J. W., Arendrup, M. C., Warris, A., Lagrou, K., Pelloux, H., Hauser, P. M., Chryssanthou, E., Mellado, E., Kidd, S. E., Tortorano, A. M., Dannaoui, E., Gaustad, P., Baddley, J. W., Uekotter, A., Lass-Florl, C., Klimko, N., Moore, C. B., Denning, D. W., Pasqualotto, A. C., Kibbler, C., Arikan-Akdagli, S., Andes, D., Meletiadis, J., Naumiuk, L., Nucci, M., Melchers, W. J., and Verweij, P. E. (2015) Prospective multicenter international surveillance of azole resistance in *Aspergillus fumigatus*. *Emerging Infectious Diseases* **21**, 1041-1044. 10.3201/eid2106.140717

107. Bueid, A., Howard, S. J., Moore, C. B., Richardson, M. D., Harrison, E., Bowyer, P., and Denning, D. W. (2010) Azole antifungal resistance in *Aspergillus fumigatus*: 2008 and 2009. *Journal of Antimicrobial Chemotherapy* **65**, 2116-2118. 10.1093/jac/dkq279

108. Wiederhold, N. P., Badali, H., McCarthy D., Patterson H., Sanders S., Mele J., Fan, H, and Gibas, C. (2020) Susceptibility patterns of contemporary *Aspergillus fumigatus* isolates from the United States to azole antifungals., https://aaam2020.org/wp-content/uploads/2020/03/Poster-12.pdf

109. Zhao, Y., Ye, L., Zhao, F., Zhang, L., Lu, Z., Chu, T., Wang, S., Liu, Z., Sun, Y., Chen, M., Liao, G., Ding, C., Xu, Y., Liao, W., and Wang, L. (2023) *Cryptococcus neoformans*, a global threat to human health. *Infectious Diseases of Poverty* **12**, 20-37. 10.1186/s40249-023-01073-4

110. Kelly, S. L., Lamb, D. C., Taylor, M., Corran, A. J., Baldwin, B. C., and Powderly, W. G. (1994) Resistance to amphotericin B associated with defective sterol delta 8-->7 isomerase in a *Cryptococcus neoformans* strain from an AIDS patient. *FEMS Microbiology Lettters* **122**, 39-42. 10.1111/j.1574-6968.1994.tb07140.x.

111. Lozano-Chiu, M., Paetznick, V. L., Ghannoum, M. A., and Rex, J. H. (1998) Detection of resistance to amphotericin B among *Cryptococcus neoformans* clinical isolates: performances of three different media assessed by using E-Test and National Committee for Clinical Laboratory Standards M27-A methodologies. *Journal of Clinical Microbiology* **36**, 2817-2822. 10.1128/JCM.36.10.2817-2822.1998.

112. Sionov, E., Chang, Y. C., Garraffo, H. M., and Kwon-Chung, K. J. (2009) Heteroresistance to fluconazole in *Cryptococcus neoformans* is intrinsic and associated with virulence. *Antimicrobial Agents and Chemotherapy* **53**, 2804-2815. 10.1128/AAC.00295-09

113. Stone, N. R., Rhodes, J., Fisher, M. C., Mfinanga, S., Kivuyo, S., Rugemalila, J., Segal, E. S., Needleman, L., Molloy, S. F., Kwon-Chung, J., Harrison, T. S., Hope, W., Berman, J., and Bicanic, T. (2019) Dynamic ploidy changes drive fluconazole resistance in human cryptococcal meningitis. *Journal of Clinical Investigation* **129**, 999-1014. 10.1172/JCI124516

114. Pavlaki, M., Poulakou, G., Drimousis, P., Adamis, G., Apostolidou, E., Gatselis, N. K., Kritselis, I., Mega, A., Mylona, V., Papatsoris, A., Pappas, A., Prekates, A., Raftogiannis, M., Rigaki, K., Sereti, K., Sinapidis, D., Tsangaris, I., Tzanetakou, V., Veldekis, D., Mandragos, K., Giamarellou, H., and Dimopoulos, G. (2013) Polymicrobial bloodstream infections: epidemiology and impact on mortality. *Journal of Global Antimicrobial Resistance* **1**, 207-212. 10.1016/j.jgar.2013.06.005

115. Pittet, D., Li, N., Woolson, R. F., and Wenzel, R. P. (1997) Microbiological factors influencing the outcome of nosocomial bloodstream infections: a 6-year validated, population-based model. *Clinical Infectious Diseases* **24**, 1068-1078. 10.1086/513640.

116. Klotz, S. A., Chasin, B. S., Powell, B., Gaur, N. K., and Lipke, P. N. (2007) Polymicrobial bloodstream infections involving *Candida* species: analysis of patients and review of the literature. *Diagnostic Microbiology and Infectious Disease* **59**, 401-406. 10.1016/j.diagmicrobio.2007.07.001

117. Adam, B., Baillie, G. S., and Douglas, L. J. (2002) Mixed species biofilms of *Candida albicans* and *Staphylococcus epidermidis*. *Journal of Medical Microbiology* **51**, 344-349. 10.1099/0022-1317-51-4-344

118. Harriott, M. M., and Noverr, M. C. (2010) Ability of *Candida albicans* mutants to induce *Staphylococcus aureus* vancomycin resistance during polymicrobial biofilm formation. *Antimicrobial Agents and Chemotherapy* **54**, 3746-3755. 10.1128/AAC.00573-10

119. Kean, R., Rajendran, R., Haggarty, J., Townsend, E. M., Short, B., Burgess, K. E., Lang, S., Millington, O., Mackay, W. G., Williams, C., and Ramage, G. (2017) *Candida albicans* mycofilms support *Staphylococcus aureus* colonization and enhances miconazole resistance in dual-species interactions. *Frontiers in Microbiology* **8**, 258-268. 10.3389/fmicb.2017.00258

120. Kong, E. F., Tsui, C., Kucharikova, S., Andes, D., Van Dijck, P., and Jabra-Rizk, M. A. (2016) Commensal protection of *Staphylococcus aureus* against antimicrobials by *Candida albicans* biofilm matrix. *mBio* **7**, 1-12. 10.1128/mBio.01365-16

121. Harris, M. R., and Coote, P. J. (2010) Combination of caspofungin or anidulafungin with antimicrobial peptides results in potent synergistic killing of *Candida albicans* and *Candida glabrata in vitro*. *International Journal of Antimicrobial Agents* **35**, 347-356. 10.1016/j.ijantimicag.2009.11.021

122. Vriens, K., Cools, T. L., Harvey, P. J., Craik, D. J., Braem, A., Vleugels, J., De Coninck, B., Cammue, B. P. A., and Thevissen, K. (2016) The radish defensins RsAFP1 and RsAFP2 act synergistically with caspofungin against *Candida albicans* biofilms. *Peptides* **75**, 71-79. 10.1016/j.peptides.2015.11.001

123. Vriens, K., Cools, T. L., Harvey, P. J., Craik, D. J., Spincemaille, P., Cassiman, D., Braem, A., Vleugels, J., Nibbering, P. H., Drijfhout, J. W., De Coninck, B., Cammue, B. P. A, and Thevissen, K. (2015) Synergistic activity of the plant defensin HsAFP1 and caspofungin against *Candida albicans* biofilms and planktonic cultures. *PLoS One* **10**, e0132701-e0132722 10.1371/journal.pone.0132701

124. De Brucker, K., Delattin, N., Robijns, S., Steenackers, H., Verstraeten, N., Landuyt, B., Luyten, W., Schoofs, L., Dovgan, B., Frohlich, M., Michiels, J., Vanderleyden, J., Cammue, B. P. A., and Thevissen, K. (2014) Derivatives of the mouse cathelicidin-related antimicrobial peptide (CRAMP) inhibit fungal and bacterial biofilm formation. *Antimicrobial Agents and Chemotherapy* **58**, 5395-5404. 10.1128/AAC.03045-14

125. Delattin, N., De Brucker, K., Craik, D. J., Cheneval, O., Frohlich, M., Veber, M., Girandon, L., Davis, T. R., Weeks, A. E., Kumamoto, C. A., Cos, P., Coenye, T., De Coninck, B., Cammue, B. P. A., and Thevissen, K. (2014) Plant-derived decapeptide OSIP108 interferes with *Candida albicans* biofilm formation without affecting cell

viability. *Antimicrobial Agents and Chemotherapy* **58**, 2647-2656. 10.1128/AAC.01274-13

126. MacCallum, D. M., Desbois, A. P., and Coote, P. J. (2013) Enhanced efficacy of synergistic combinations of antimicrobial peptides with caspofungin versus *Candida albicans* in insect and murine models of systemic infection. *European Journal of Clinical Microbiology & Infectious Diseases* **32**, 1055-1062. 10.1007/s10096-013-1850-8

Appendix A: Reverse-phase high performance liquid chromatography data for Os-C and Os-C(W_5)

Sample Name :Os-C
Sample ID :U7284ED080-3
Time Processed :16:55:01
Month-Day-Year Processed :04/23/2019

Pump A : 0.065% trifluoroacetic in 100% water (v/v)
Pump B : 0.05% trifluoroacetic in 100% acetonitrile (v/v)
Total Flow:1 ml/min
Wavelength:220 nm
<<LC Time Program>>

Time	Module	Command	Value
0.01	Pumps	Pump A B.Conc	5
25.00	Pumps	Pump A B.Conc	65
25.01	Pumps	Pump A B.Conc	95
32.00	Pumps	Pump A B.Conc	95
32.01	Pumps	Pump A B.Conc	5
40.00	Pumps	Pump A B.Conc	5
40.00	Controller	Stop	

<<Column Performance>>
<Detector A>
Column : AlltimaTM C18 4.6 x 250 mm
Equipment:ZJ17010508

<Chromatogram>

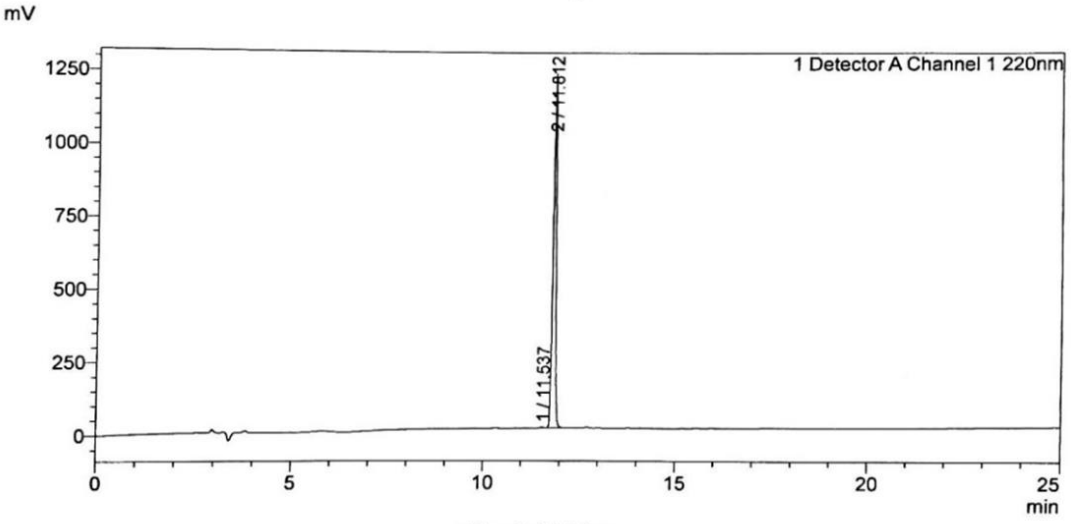

<Peak Table>

Detector A Channel 1 220nm

Peak#	Ret. Time	Area	Height	Area%
1	11.537	15935	3440	0.243
2	11.812	6554556	1226601	99.757
Total		6570491	1230041	100.000

Sample Name :Os-C(W5)
Sample ID :U732ZHI190-1
Time Processed :15:38:55
Month-Day-Year Processed :12/03/2022

Pump A : 0.065% trifluoroacetic in 100% water (v/v)
Pump B : 0.05% trifluoroacetic in 100% acetonitrile (v/v)
Total Flow:1 ml/min
Wavelength:220 nm
<<LC Time Program>>

Time	Module	Command	Value
0.01	Pumps	B.Conc	5
25.00	Pumps	B.Conc	65
25.01	Pumps	B.Conc	95
27.00	Pumps	B.Conc	95
27.01	Pumps	B.Conc	5
35.00	Pumps	B.Conc	5
35.01	Controller	Stop	

<<Column Performance>>
<Detector A>
Column :Inertsil ODS-SP 4.6 x 250 mm
Equipment: GR11010440

<Chromatogram>

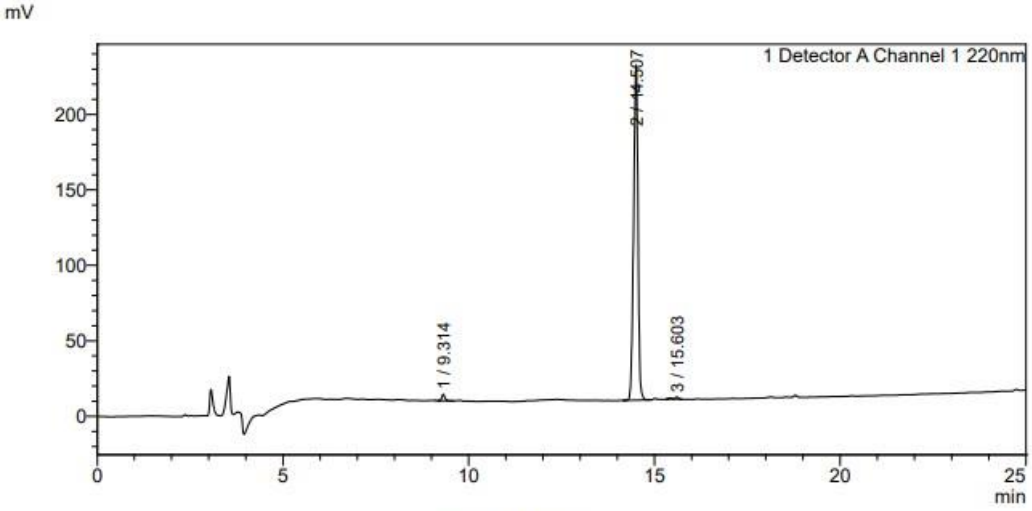

<Peak Table>

Detector A Channel 1 220nm

Peak#	Ret. Time	Area	Height	Area%
1	9.314	23880	4323	1.284
2	14.507	1823444	222154	98.013
3	15.603	13085	1481	0.703
Total		1860410	227957	100.000

Appendix B: Mass spectrometry data for Os-C and Os-C(W_5)

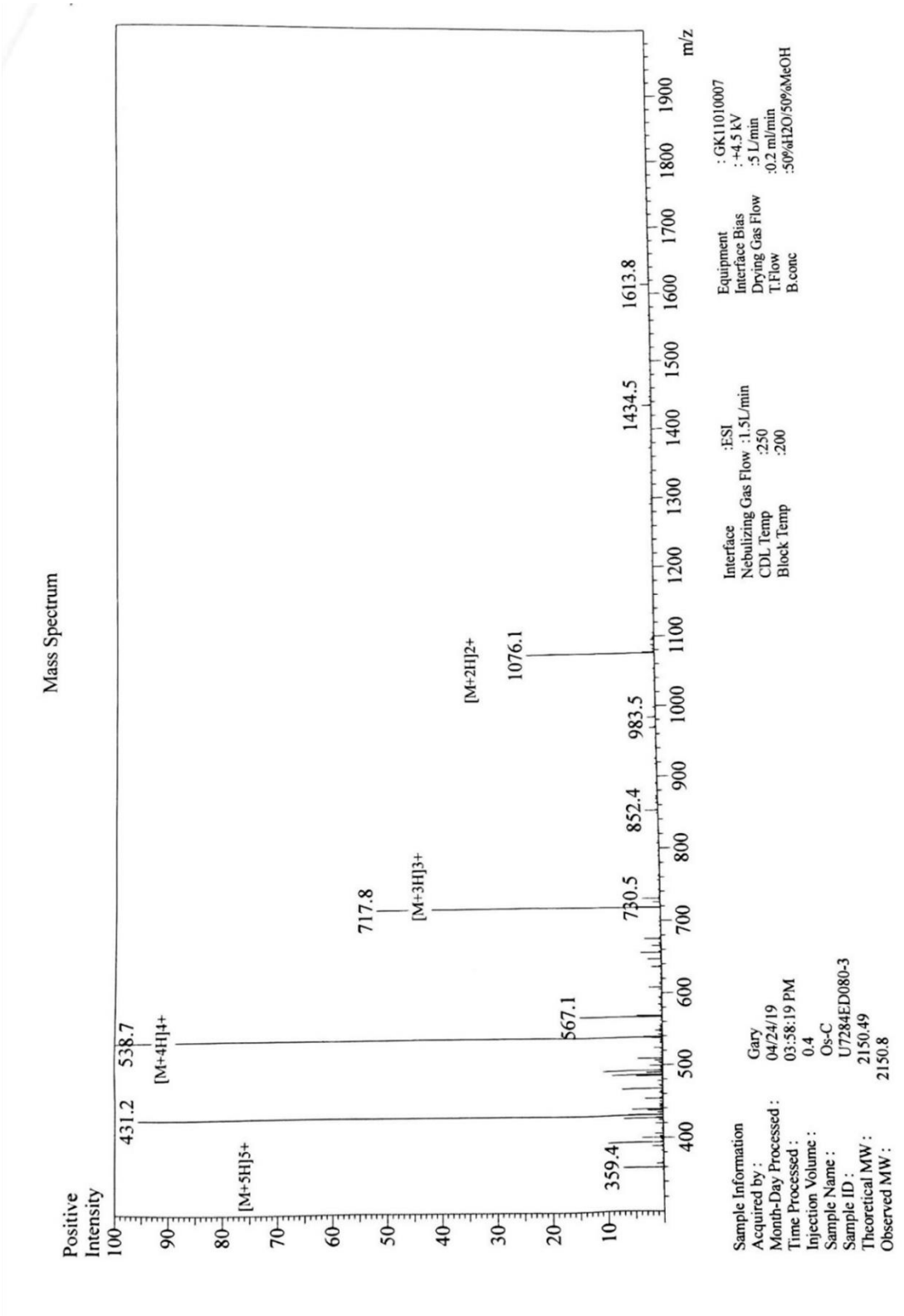

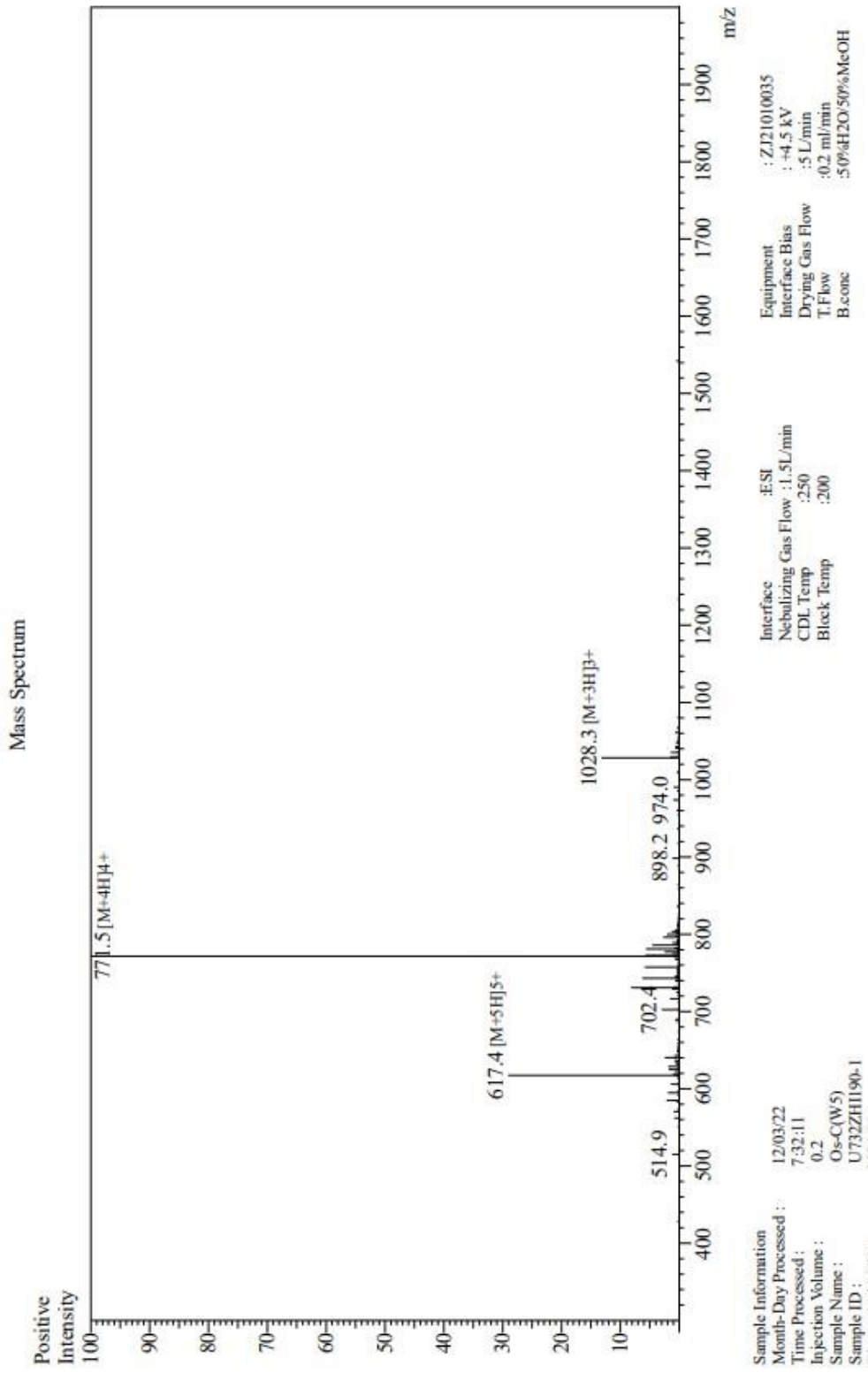
Mass Spectrum
Positive
Intensity
m/z
771.5 [M+4H]4+
617.4 [M+5H]5+
1028.3 [M+3H]3+
514.9
702.4
898.2
974.0
Sample Information
Month-Day Processed : 12/03/22
Time Processed : 7:32:11
Injection Volume : 0.2
Sample Name : Os-C(W5)
Sample ID : U732ZHI190-1
Theoretical MW : 3081.55
Observed MW : 3082.0
Interface :ESI
Nebulizing Gas Flow : 1.5L/min
CDL Temp :250
Block Temp :200
Equipment : ZJ21010035
Interface Bias : +4.5 kV
Drying Gas Flow :5 L/min
T.Flow :0.2 ml/min
B.conc :50%H2O/50%MeOH